

**Deciphering acclimation strategies to
combined abiotic stresses in
Arabidopsis thaliana: a functional
genomics approach**

Zhang Jiang

**Deciphering acclimation strategies to combined abiotic stresses in
Arabidopsis thaliana: a functional genomics approach**

**Ontcijferen van gecombineerde abiotische stress
acclimatisatiestrategieën in *Arabidopsis thaliana*: een *functional
genomics* benadering**

(met een samenvatting in het Nederlands)

Proefschrift

ter verkrijging van de graad van doctor aan de
Universiteit Utrecht
op gezag van de
rector magnificus, prof. dr. H.R.B.M. Kummeling,
ingevolge het besluit van het college voor promoties
in het openbaar te verdedigen op

maandag 12 feburari 2024 des middags te 2.15 uur

door

Zhang Jiang

geboren op 27 augustus 1992
te Jilin, China

Author: Zhang Jiang
Provided by thesis specialist Ridderprint, ridderprint.nl
Printing: Ridderprint
Layout and design: Jacolijn de Krom, persoonlijkproefschrift.nl
ISBN: 978-94-6483-706-3

© Copyright 2024: Zhang Jiang, Utrecht, The Netherlands
All rights reserved. No part of this thesis may be reproduced, stored in a retrieval
system, or transmitted in any form or by any means without prior written permission
by the author.

Promotor:

Prof. dr. R. Sasidharan

Copromotor:

Dr. M. van Zanten

Beoordelingscommissie:

Prof. dr. C. Delker

Dr. C.M.M. Gommers

Prof. dr. I. Rieu

Prof. dr. K.H.W.J. ten Tusscher

Prof. dr. A.C.M. van Wees

Contents

Chapter 1	General introduction	7
Chapter 2	Effects of simultaneous and sequential abiotic stresses on Arabidopsis growth, development, and physiology	29
Chapter 3	Characterization of the Arabidopsis transcriptome response to simultaneous and sequential abiotic stresses	71
Chapter 4	Molecular components mediating multi-stress resilience in Arabidopsis	119
Chapter 5	The transcription factor GOLDEN2-LIKE 2 regulates thermomorphogenesis in Arabidopsis in a complex manner that may involve PIF4 and auxin	167
Chapter 6	Summarizing discussion	195
References		204
Layman summary		244
Samenvatting		246
摘要		248
Acknowledgments		250
Curriculum Vitae		253
List of publications		254

This thesis was accomplished with financial support from the China Scholarship Council (201806170025)



General Introduction

Zhang Jiang, Rashmi Sasidharan*, Martijn van Zanten*
* Shared senior authors

Plant stress resilience, Utrecht University

Plant responses to abiotic stresses

Climate change has increased the incidence of weather extremes, posing a serious challenge for global food security (Stott, 2016; Schiermeier, 2018). According to a recent report published by the Intergovernmental Panel on Climate Change (IPCC), climate change-associated heat waves, episodes of droughts, floods and storms caused massive loss of crop productivity in 2022 (Intergovernmental Panel On Climate Change (Ipcc), 2023). Therefore, it is of major interest to enhance plant tolerance to abiotic stresses to ensure sufficient crop output.

Plants grown in either natural, or agro- environments, frequently encounter and respond to different environmental stimuli. In recent years, studies on plant tolerance to various environmental signals have received increasing attention (Wu et al., 2007; Suzuki et al., 2014; Zhu, 2016; Lamers et al., 2020; Zhang et al., 2022a). Such studies provided indispensable insights into the molecular machinery underlying functional response strategies to diverse environmental stresses. Climate change-associated increases in average temperatures are a major threat to crop growth and yield (Hatfield & Prueger, 2015; Yu et al., 2019). Warmer temperatures in turn increase the incidence of precipitation extremes of drought and flooding (Garner et al., 2015; Fahad et al., 2017; Marchin et al., 2022; Intergovernmental Panel On Climate Change (Ipcc), 2023).

When threatened by heat stress, a variety of physiological processes are adversely affected, including photosynthesis, cell membrane thermostability and osmotic regulation (Kotak et al., 2007; Hemantaranjan, 2014; Zhao et al., 2020b). The expression of heat shock transcription factors (HSFs) and heat shock proteins (HSPs) are rapidly induced, to safeguard cells and allow the resumption of normal cellular and physiological activities (Albertos et al., 2022). However, temperature increases in natural or agri -settings are sometimes gradual and mild, involving only a few degrees of ambient temperature elevation (Lee et al., 2020). Even such mild changes, when imposed on plants that are susceptible (*i.e.*, Arabidopsis), can result in a suite of morphological alterations including, for example, leaf elongation and hyponasty (increase in leaf angle). These traits can enhance plant cooling capacity during their growth in warm temperatures (Crawford et al., 2012; Van Zanten et al., 2013; Praat et al., 2021) and are collectively termed ‘thermomorphogenesis’. This is a whole-plant acclimation strategy (or a ‘trait syndrome’) typically governed by a complex signal transduction network consisting of diverse regulatory modules (Quint et al., 2016; Casal & Balasubramanian, 2019; Perrella et al., 2022). A well-characterized signal mediator involved in thermomorphogenesis, is PHYTOCHROME INTERACTING FACTOR 4 (PIF4), which acts as a master transcription factor (TF) hub regulating downstream responses

(Proveniers & Van Zanten, 2013; Quint et al., 2016; Park et al., 2021b). Under warm temperatures, PIF4 transcriptionally activates the auxin biosynthetic gene *YUCCA8* (*YUC8*) (Sun et al., 2012), to eventually promote thermomorphogenic growth.

Both salt and drought can commonly arise in natural environments and impose turgor loss (Krasensky & Jonak, 2012). The early responses to salt are closely related and mechanically overlap with drought responses as they both elicit osmotic stress (Zhu, 2002). However, prolonged exposure to salt leads to toxicity and nutrient imbalance in addition to water limitation (Zhang et al., 2006; Chaves et al., 2009). Stomatal closure is a typical physiological response of shoots under both salt and drought conditions to prevent transport-mediated water loss, despite photosynthesis being disrupted due to the impaired gas exchange (Song & Matsuoka, 2009; Dos Santos et al., 2022). The regulation of stomatal closure during salt or drought is primarily controlled by abscisic acid (ABA) through a series of signaling components in guard cells such as reactive oxygen species (ROS), reactive carbonyl species (RCS), nitric oxide (NO) and calcium ion (Ca^{2+}) (Bharath et al., 2021; Zhao et al., 2021a; Muhammad Aslam et al., 2022). Additionally, ABA has also been demonstrated to have a prominent role in regulating root growth and architecture under salt and drought conditions (Fernando & Schroeder, 2016). When Arabidopsis plants encounter moderate to high salt concentrations (75-150 mM NaCl), the elevation of endogenous ABA results in a quiescent period in post-emergent lateral roots, forming Casparian strips (a ring-like, specialized cell-wall modification) that function as a barrier to the diffusion of sodium ion (Na^+) through the endodermis (Naseer et al., 2012; Duan et al., 2013; Fernando & Schroeder, 2016; Zou et al., 2022). ABA-mediated root response during drought involves the elongation of primary roots. Upon moderate drought, ABA promotes auxin transport in the root tip of Arabidopsis and rice (*Oryza sativa*), enhancing the release of protons by activating H^+ -ATPase to maintain primary root elongation, which enables subsoil foraging for water and nutrient that ultimately enables an increased hydraulic conductivity (Pagès, 2011; Xu et al., 2013; Muhammad Aslam et al., 2022).

In contrast to drought where water-uptake is considerably hampered, flooding (waterlogging or submergence) creates an excess water supply, disrupting normal gas exchange and light availability (when shoots are submerged in turbid waters). This leads to a carbon and energy crisis and ultimately cell death (Mommer & Visser, 2005; Sasidharan et al., 2018). When plants are flooded, the limitation in gas diffusion induces rapid accumulation of the volatile hormone ethylene. Ethylene is a key player mediating a series of flood-adaptive morphological and physiological changes in both shoot and roots (Sasidharan & Voeselek, 2015; Jia et al., 2021). Typical underwater responses triggered by ethylene accumulation, for example, include accelerated

petiole (*Rumex palustris*) or internode (*Oryza sativa*) elongation upon complete submergence (Kende et al., 1998; Peeters et al., 2002; Voeselek, 2003; Chen et al., 2011), or the development of aerenchyma during waterlogging. Both these traits facilitate enhanced internal aeration permitting gas exchange from aerial non-flooded parts to the hypoxic regions of the plant (Kawase & Whitmoyer, 1980; Jackson & Armstrong, 1999; Yamauchi et al., 2013; Langan et al., 2022). In Arabidopsis, ethylene accumulation due to flooding triggers the stabilization of the essential low-oxygen TFs, group VII ETHYLENE RESPONSE FACTORS (ERFVIIs), through NO depletion and consequently leads to hypoxia acclimation (Gibbs et al., 2011; Hartman et al., 2019). Furthermore, constitutive expression of SUBMERGENCE-1A (SUB1A), a rice ERF VII TF, confers tolerance to multiple stresses including drought, submergence and dehydration stress experienced upon de-submergence (Fukao et al., 2011; Yeung et al., 2018). In addition to tissue dehydration, plants recovering from complete dark-submergence also encounter challenges such as reoxygenation stress, reillumination stress and tissue senescence (Yeung et al., 2019; Yuan et al., 2023a).

Abiotic stresses can occur simultaneously or sequentially

Abiotic stresses rarely occur in a fully isolated manner. Co-occurring abiotic stresses often cause distinct effects on plants and elicit different acclimation responses, compared to individual stresses (Choudhury et al., 2017; Zhang & Sonnewald, 2017; Nadeem et al., 2022; Zandalinas & Mittler, 2022). For example, in wheat (*Triticum aestivum*), episodes of prolonged drought in combination with heat waves exacerbate biomass reduction and loss of grain yield, when compared to individually applied drought or heat (Pradhan et al., 2012; Perdomo et al., 2015; Tricker et al., 2018). This inhibition in crop growth under combined stress is attributed to the negative interactions between heat and drought, with the effects becoming additive when combined (Suzuki et al., 2014). Additionally, a recent meta-analysis (Cohen et al., 2021) using >120 published cases studying crop responses to combined heat and drought stress, revealed that it caused on average twice the decrease in relative yield (to control) compared to exposure to heat stress alone.

For plants grown in natural or field conditions, the encountered (combined) abiotic stresses are often at a gradual or sublethal severity, and hence relatively mild, compared to those reported in experimental laboratory studies (Zhang et al., 2020a; Morales et al., 2022). Sublethal stresses, compared to lethal stresses or stresses at a moderate severity, cause typically less damage to plant growth, but can evoke distinct acclimation responses (Clauw et al., 2015; Mohanty, 2003; Zhu et al., 2021). Acclimation responses are governed by coordinated complex molecular networks, especially when

multiple stressors coexist (Suzuki et al., 2014; Zandalinas et al., 2020). Therefore, a comprehensive understanding of plant acclimations - and the underlying signaling and response mechanisms - to sublethal combinatorial stresses and the corresponding individual stresses, typically at developmental, morphological, physiological, and molecular levels, is urgent and necessary. Such understanding will facilitate the production and informed breeding of next-generation multi-stress tolerant crops capable of maintaining high productivity and quality in a changing climate.

Mechanisms of acclimation to combinatorial abiotic stresses

Despite the typical reduction in growth and yield caused by combinatorial stresses (Jumrani & Bhatia, 2018; Cohen et al., 2021; Sareen et al., 2023), plants are not passive and have evolved a series of adaptive responses at the morpho-physiological level to counteract these unfavorable stress conditions (Nadeem et al., 2022; Zhang et al., 2022a). The exact nature of the morphological and physiological responses to a given combinatorial stress condition can differ from those elicited by the corresponding individual stressors, as plants perceive the stress combination as a new state of stress (Pandey et al., 2015). Therefore, the physiological and molecular effects of combinatorial stress cannot be deduced by simply summing up the effects of the corresponding single stresses. A well-documented example of this is the stomatal responses of Arabidopsis to combined heat and drought stress (Rizhsky et al., 2004). When confronted with heat stress, Arabidopsis plants open their stomata to enable leaf cooling through transpiration, while under drought they reduce the stomatal conductance to prevent water loss. Upon the simultaneous application of both heat and drought, the stomatal conductance remained at a low level. Similar results of the leaf stomatal response under combined heat and drought stress conditions were observed in other plant species such as tobacco (*Nicotiana tabacum*) (Rizhsky et al., 2002), citrus plants (*Citrus*) (Zandalinas et al., 2016b), broadleaf evergreen species (Marchin et al., 2022) and soybean (*Glycine max*, hereafter soybean) (Sinha et al., 2023b), suggesting that the stomatal responses under combined heat and drought are conserved across different species. However, recent studies (Sinha et al., 2022; Zandalinas & Mittler, 2022) have unveiled a deviant stomatal regulation in soybean flowers subjected to a heat and drought combination. In this intriguing case, plants prioritized transpiration through flowers over transpiration through leaves to ensure a lower innate temperature of the floral structures to maintain the proper functioning of reproductive processes. Consequently, when heat and drought coexisted, leaf stomata remained closed while flower stomata were open (termed as 'different transpiration'). The differences in stomatal regulation within the same individual highlight a tissue-dependent responses to combinatorial stress conditions. Of note,

the age or developmental stage at which plants are exposed to combinatorial stress also determines the outcome of plant growth and morpho-physiological responses. For instance, the negative impact of combined heat and drought on plant yield is more pronounced if the stress combination happens during the reproductive stage than when it occurs during vegetative growth (Cohen et al., 2021).

Stomatal aperture regulation plays a crucial role in determining plant CO₂ uptake. Together with the stabilization of ribulose biphosphate carboxylase oxygenase (Rubisco) and the functional integrity of Photosystem II (PSII), they jointly affect photosynthetic activity during combinatorial stress conditions (Nishiyama & Murata, 2014; Castro et al., 2019; Peng et al., 2022). Combined heat and drought stress, for example, caused exacerbated impediment of photosynthesis in both C3 and C4 plants, compared to either heat or drought stress in isolation (Zhu et al., 2021a; Netshimbupfe et al., 2022). In cotton (*Gossypium arboreum*) cultivars, combined heat and drought stress caused a decrease in net photosynthetic rate and plant damage (Carmo-Silva et al., 2012; Zandalinas et al., 2018), although this inhibition in photosynthesis, reflected by a low Rubisco activity, was more pronounced in a drought-sensitive cultivar compared to a drought-tolerant cultivar. Similarly, a significant decrease in photosynthetic activity was observed in two heat-tolerant tomato (*Solanum lycopersicum*, hereafter tomato) cultivars, but not in a heat-sensitive cultivar, during simultaneous exposure to combined heat and drought stress. This suggests that photosynthetic responses to combined stresses may not align with the tolerance to individual stresses (Zhou et al., 2017). These studies imply that the maintenance of photosynthetic activity is important for acclimation to combinatorial stresses (Zandalinas et al., 2018) and is genotype-dependent.

Chloroplasts play a central role in sensing environmental fluctuations (Dogra & Kim, 2019). The chloroplast is a major source of ROS production, during native photosynthesis, and especially under stress conditions (Foyer & Shigeoka, 2011; Maruta et al., 2012). Disrupted photosynthetic capacity accompanied by limited CO₂ availability, can induce ROS overproduction and eventually cause damage to lipid membranes and cellular organelles (Suzuki et al., 2012; Zandalinas et al., 2017a; Castro et al., 2019). However, ROS overproduction can be ameliorated by the accumulation of ROS detoxification proteins such as superoxide dismutase (SOD), ascorbate peroxidase (APX), peroxiredoxin and glutathione peroxidase (GPX), or antioxidants such as glutathione (GSH) and ascorbic acid (Mittler, 2002; Mittler et al., 2004). These ROS-scavenging components display a unique pattern (in terms of types of enzymes and levels of antioxidant accumulation) under combined stress conditions compared to the relative individual stresses in plants (Choudhury et al., 2017). High antioxidant

capacity under stress conditions is considered beneficial for stress tolerance, as it limits damage (Caverzan et al., 2016; Hasanuzzaman et al., 2020; Qamer et al., 2021), and is typically genotype-dependent (Shabbir et al., 2022). Differences in antioxidant capacity, for instance, explain the differences in drought and high-temperature stress tolerance between two citrus genotypes, Carrizo citrange and Cleopatra mandarin, where Carrizo plants more efficiently coordinated the antioxidants involved in ROS detoxification and displayed a better performance and yield under combined stress compared to Cleopatra plants (Zandalinas et al., 2017a).

Stress exposure can have dramatic effects not only on chloroplast structures, but also on resident proteins, such as Rubisco and Filamentous temperature sensitive H (FtsHs) (Das et al., 2016; Zhao et al., 2016a; Balfagón et al., 2019a; Mamaeva et al., 2020). The combined ROS production from the chloroplast and other cellular compartments (e.g., mitochondria, apoplast, peroxisome, nuclei) constitutes an overall 'ROS signature' (Choudhury et al., 2017) which can vary between single and combined stresses (Choudhury et al., 2017). For example, in poplar (*Populus yunnanensis*, hereafter poplar) plantlets, different ROS levels caused by individually applied heat, drought and the combination resulted in varying levels of antioxidant enzyme productions (Li et al., 2014).

ROS also has a signaling role in regulating stress acclimation, especially during simultaneously occurring stresses (Suzuki et al., 2012; Mittler, 2017; Zandalinas et al., 2018). Zandalinas *et al.* showed that Arabidopsis plants with impaired ROS signaling (*rbohD* mutant) or scavenging (*apx1* mutant) exhibited poor survival rates under multifactorial stress combinations (up to a combination of six stressors at the same time), compared to wild-type plants (Zandalinas et al., 2021b). Furthermore, ROS waves have been identified as essential drivers of plant systemic signaling pathways in response to combinatorial stresses such as combined high light and heat stress or sequentially applied waterlogging followed by completely submergence (Peláez-Vico et al., 2023; Zandalinas et al., 2020). Another indispensable role of ROS in plant stress acclimation is the modulation of signal communications between chloroplast and nucleus (retrograde signaling) (Foyer & Hanke, 2022; Li & Kim, 2022). For instance, chloroplast-localized protein ETHYLENE-DEPENDENT GRAVITROPISM-DEFICIENT AND YELLOW-GREEN 3 (EGY3) interacts with Cu/Zn-SOD2 (CSD2) to promote H₂O₂-mediated retrograde signaling, enhancing the tolerance of Arabidopsis plants to salt stress (Zhuang et al., 2021). However, ROS-mediated chloroplast-to-nuclear retrograde signaling in the context of combinatorial-stress tolerance has been poorly studied.

Concepts of stress interactions

Unlike the additive effects elicited by stress combinations (Vile et al., 2012; Ahmed et al., 2015b), the co-occurrence of two different environmental stressors can sometimes lead to antagonistic effects (Suzuki et al., 2014). For example, drought-induced reduction in stomatal conductance can enhance the tolerance to ozone (O₃) stress, when the two stresses co-occur, as the closed stomata prevent O₃ from entering plants (Paakkonen et al., 1998; Löw et al., 2006). In 2006, Mittler and colleagues introduced the concept of 'The Stress Matrix' to describe the interactions of (two) co-existing stressors in stress combinations that have significant impacts on agricultural production (Mittler, 2006a). However, other researchers have pointed out that this matrix oversimplifies the complexity of combined stress scenarios (Mahalingam, 2015). In recent years, the stress matrix has been adapted and expanded to include more stress interactions (Mittler & Blumwald, 2010; Anwar et al., 2021a) and different physiological factors (Zandalinas & Mittler, 2022). Suzuki and coworkers (Suzuki et al., 2014) further refined the stress matrix by considering, for example, the dual interactions (both positive and negative) of combined heat and salinity stress on plant growth. They demonstrated that in tomato plants, combined heat and salinity stress promoted the accumulation of glycine betaine and trehalose, which helped maintain a high K⁺ concentration (thus a lower ratio of Na⁺ and K⁺) to improve cell water status and photosynthesis compared to salinity alone (Rivero et al., 2014). However, the same combined stress scenario evoked enhanced negative effects on tissue development in wheat seedlings (Keleş & Öncel, 2002) or photosynthetic growth in *Arabidopsis* (Suzuki et al., 2016a).

In general, the physiological (and molecular) responses to a combinatorial stress are predominantly determined by the (relative) most severe stressor (Pandey et al., 2015). Accordingly, the stress magnitude, order and duration play crucial roles in determining the morpho-physiological outcomes of combinatorial stresses (Mittler, 2006a; Anwar et al., 2021a; Nadeem et al., 2022). Stress magnitude refers to the relative or absolute intensity of individual stressors, such as the absolute temperature during heat or cold stress (Praat et al., 2021; Zhu et al., 2022a), the soil water content during drought stress (Ma et al., 2014), light availability during submergence (Mohanty, 2003; Vashisht et al., 2011; Sasidharan et al., 2018), or the days post infection (dpi) during pathogenesis (Pal et al., 2022). Additionally, the number of co-existing stressors during a combinatorial stress scenario is also an important factor in determining the outcome for the plant. A recent study by Zandalinas *et al.* presented a new concept termed 'multifactorial stress combination' to describe how the combination of many co-occurring environmental stresses (up to six) affects plant growth, survival, physiological and molecular responses (Zandalinas et al., 2021b). This study suggested that while

individually applied stresses sometimes have minimal effects on plant growth and survival, the accumulated impacts of multifactorial stress combination are detrimental. This highlights the synergistic interactions between individual stressors during their simultaneous occurrences.

Building upon these findings and some other pioneering work discussing how global-change factors impact the ecosystem processes (Rillig et al., 2019; Zandalinas et al., 2021a), a 'multifactorial stress principle' was proposed to depict the synergistic effects of stapled stressors and how they affect plants and ecosystems (Zandalinas & Mittler, 2022). With an increase in the number and complexity of stressors (simultaneously) affecting a plant or an ecosystem, plant functioning or ecosystem processes will drastically decline, even if the level of the individual stressors involved in the multifactorial stress combination is low enough to not significantly affect plant growth and survival if applied in isolation. Overall, these studies have emphasized the importance of considering the relevance and impact of subtle (or sublethal) stresses when studying plant acclimations to combinatorial stresses.

When plants are confronted with a sequential stress combination, the first stress exposure, even if mild, may induce priming or memory effects, altering the responses to future challenges (Hilker et al., 2016; Zhang & Sonnewald, 2017). Therefore, the order in which the two stresses are encountered can be crucial in determining the effect size of the response of the plant (Ahmed et al., 2015b; Zandalinas et al., 2021b). For instance, poplar plants that were pre-exposed to drought exhibited a reduction in stomatal conductance, which alleviated the harsh effect of a subsequent O₃ stress. Conversely, when O₃ stress was applied prior to drought, the slow stomatal responses induced by O₃ accelerated plant water loss during a subsequent drought exposure (Pollastrini et al., 2014; Mahalingam, 2015).

Molecular mechanisms underlying acclimation to combinatorial stresses

Morpho-physiological responses to sequential and combined stresses involve changes at transcriptional, translational and metabolic levels, coordinated by complex molecular signal transduction networks (Zhang & Sonnewald, 2017; Anwar et al., 2021a). Combinatorial stresses can elicit unique molecular signatures that are different from those induced by either of the corresponding individual stresses, as has been shown by many ~omics studies (Rizhsky et al., 2004; Mittler, 2006a; Zhao et al., 2016a; Zandalinas et al., 2018; Nadeem et al., 2022; Shabbir et al., 2022; Zandalinas & Mittler, 2022). However, Pandey *et al.* proposed that plant responses to a given stress

combination are majorly determined by the more severe (dominant) stressor, as the transcriptome response to combined stress resemble those observed under the more severe individual stress (Pandey et al., 2015). These similarities at the molecular level are reflected by a substantial proportion of shared transcripts.

Recently, the adoption of integrated systems biology approaches (the integration of more than one omics approach), commonly referred to as 'Multi-Omics Approach', has emerged as a tool to comprehensively decipher molecular acclimation strategies of plants under combinatorial stresses (Anwar et al., 2021a; Kolb et al., 2022; Shabbir et al., 2022; Da Ros et al., 2023). Anwar *et al.* have summarized previously identified responsive characteristics of Arabidopsis and maize plants under heat, drought and their combination at the transcriptomic, proteomic and metabolic levels (Rizhsky et al., 2004; Zhao et al., 2016a; Anwar et al., 2021a). This study revealed a considerable portion of differentially regulated transcripts, proteins and metabolites under the combined stress condition that were not apparently regulated if only the corresponding single stresses were applied. This again suggests that combined stress exerts unique and significant reconfigurations at different molecular levels. Importantly, by integrating the approaches of genetic enrichment analysis such as Gene Ontology (GO) (Ashburner et al., 2000) and Kyoto Encyclopedia of Genes and Genomes (KEGG) (Kanehisa, 2000), the identified transcript, proteins and metabolites that are uniquely regulated under combined stresses are annotated for the relevant molecular functions, which can help provide insights into the typical generic processes and master regulators guarding plants against combinatorial stresses (Rejeb et al., 2014; Pandey et al., 2015; Zandalinas et al., 2020b).

Transcriptional and post-transcriptional regulation

Plant TFs are essential for controlling growth and developmental processes that shape acclimation to environmental stimuli and mediate responses to combinatorial stresses (Liu et al., 1999; Yoon et al., 2020; Strader et al., 2022). An early study by Suzuki *et al.* highlighted a transcriptional coactivator Multiprotein Bridging Factor 1c (MBF1c) and its function in conferring tolerance to osmotic stress, heat stress and their combination, by perturbing or partially activating the ethylene-response signal transduction pathway (Suzuki et al., 2005). Furthermore, the functional characterization of MBF1c revealed that its accumulation in Arabidopsis plants under combined water deficit and heat stress is ABA-dependent (Zandalinas et al., 2016a).

Investigations into plant TFs and their functions in combinatorial-stress acclimation often take the entire TF family into account. For example, by examining the Arabidopsis transcriptome under combined heat and drought stress and the corresponding

individual stresses (Rizhsky et al., 2004), a considerable number of transcripts encoding HSFs were enriched during stress combination and shown to be differentially regulated compared to the corresponding individual stresses. The differences mainly involved the degree of expression of *HsfC1* and the presence of *HsfA6a*, *HsfA2* and *HsfA3* (Rizhsky et al., 2004). A meta-analysis (Zandalinas et al., 2020) identified 340 transcripts that were commonly upregulated during Arabidopsis subjection to combined drought and heat (Rizhsky et al., 2004), salinity and heat (Suzuki et al., 2016b), and high light and heat (Balfagón et al., 2019a). Among these transcripts, TFs belonging to the HSF, myeloblastosis (MYB) and ethylene response factor (ERF) families were significantly overrepresented. Moreover, different expression patterns of these TFs under combined stress conditions, compared to the corresponding individual stresses, indicated that transcriptomic responses of plants to different stress combinations could be regulated by unique TFs that are dedicated to each of the different stress combinations. This can be by additive, subtractive or combinatorial effects of expression patterns of different groups of TFs, generating a novel overall TF expression pattern that is unique to the stress combination (Zandalinas et al., 2020). Although some studies demonstrated that WRKY transcription factors (WRKYs) play a role in acclimation to combined abiotic and biotic stresses (Bai et al., 2018), none of these WRKY TFs were present in the identified 340 transcripts (Zandalinas et al., 2020). However, recent studies on plant responses to multifactorial stress combinations have drawn attention to the role of WRKYs in conferring plant responses to four- to six- factor stress combinations (Zandalinas et al., 2021b; Pascual et al., 2022).

Given the magnitude of the impact of plant TFs on mediating stress adaptations, other TFs and their family members, are likely involved in regulating acclimation to combinatorial stresses. For example, the NAC transcription factor family (NACs), one of the largest plant TF families, has been implicated in regulating multi-stress tolerance in various plant species (Jensen et al., 2010; Shao et al., 2015; Li et al., 2018c), and might also be taken into account as potential combinatorial-stress responsive TFs in future studies.

In addition to the study of TF families, a recent study by Azodi *et al.* proposed the use of *cis*-regulatory codes (Zou et al., 2011) to improve the understanding of transcriptional regulation under combinatorial stress (Azodi et al., 2020). By integrating information on putative/known combined-stress *cis*-regulatory elements and ~omics data (including sequence conservation, chromatin accessibility and histone modification profiles), important *cis*-regulatory promoter elements mediating tolerance to combined heat and drought stress were predicted. While most of the *cis*-regulatory elements found in the model are similar to known TF binding motifs involved in heat and/

or drought stress responses, some point to TFs with no established association to either stress condition (Azodi et al., 2020). Likewise, another study (Sewelam et al., 2020) on transcriptional and metabolic responses to drought, heat, salinity and their combinations, demonstrated that plant exposure to combinatorial stress conditions triggers transcription of several genes with yet uncharacterized functions. Overall, these findings highlight the complexity of transcriptional regulations in plants under combinatorial stress conditions and that current knowledge on this important subject still needs to be expanded.

Although transcriptional regulation is essential for plant acclimation to environmental stresses, post-transcriptional regulation, particularly at the microRNA (miRNA) level, has emerged as a key factor in the modulation of stress signaling pathways (Zhang & Sonnewald, 2017; Xu et al., 2019). In recent years, a growing body of evidence on the role of plant miRNAs as (a)biotic stress regulators, has added new conceptual insight into the molecular understanding of plant stress resilience (Sunkar et al., 2012; Shriram et al., 2016). However, research investigating the regulatory roles of miRNAs during combinatorial stress is still relatively scarce (Xu et al., 2019; Villalba-Bermell et al., 2021). Nonetheless, some researchers have taken the initiative to explore this field. For example, by using a deep-sequencing approach, unique miRNAs and their targets were unveiled under combinatorial stress conditions compared to the corresponding isolated stresses in different plant species such as tomato (Zhou et al., 2020), soybean (Ning et al., 2019), and melon (Villalba-Bermell et al., 2021). Moreover, miRNAs were also shown to be closely associated with the regulation of specific biological processes under combinatorial stresses. For instance, an Arabidopsis loss-of-function mutant of miRNA *ath-miR164c* exhibited an accumulation of proline to counteract harsh effects caused by combined drought and bacterial infection stress (Gupta et al., 2020). This is because *ATH-miR164C* can negatively regulate the expression of *1-PYRROLINE-5-CARBOXYLATE SYNTHASE 1 (P5CS1)*, a gene that controls proline metabolism, at the post-transcriptional level. In addition, Liu *et al.* recently constructed a comprehensive regulatory network that illustrated the molecular responses to combined heat and drought in durum wheat (*Triticum turgidum durum*), by integrating multiple omics analysis, including small RNAome (sRNAome), mRNA transcriptome and degradome (Liu et al., 2020). This study provided novel and fundamental insight at the whole-genome level into transcriptional and post-transcriptional regulation of combinatorial stress. Given the essential role of miRNAs in mitigating combinatorial environmental stresses, they can be considered as novel targets for engineering combinatorial-stress resilient crops in the future.

Translational and post-translational regulation

Abiotic stresses can have significant impact on the plant proteome, especially when more than one stress coincide (Kosová et al., 2018). This is evidenced by numerous differentially regulated proteins under combinatorial stresses compared to the relative individual stresses (Rizhsky et al., 2004; Li et al., 2014; Das et al., 2016; Habibpourmehraban et al., 2022). Of note, HSPs are among the most prominent proteins regulating plant tolerance to various combinatorial stresses (Li et al., 2014; Rizhsky et al., 2004; Sewelam et al., 2020; Zandalinas et al., 2020; Zhao et al., 2016). A recent study (Balfagón et al., 2023) investigating proteome and transcriptome signatures of two citrus genotypes, Carrizo citrange (*Citrus sinensis* × *Poncirus trifoliata*) and Cleopatra mandarin (*Citrus reshni*), under the triple combination of heat stress, high irradiance and drought, revealed the importance of maintaining HSPs, typically small HSPs and HSP70s, for combined stress tolerance. This is because HSPs chaperone stress-denatured proteins, to prevent their irreversible aggregation, and translocate unfolded or misfolded proteins out of the endoplasmic reticulum (ER) (Balfagón et al., 2023). Moreover, Zhao *et al.* found that in addition to HSPs, LATE EMBRYOGENESIS ABUNDANT Proteins (LEAs) are also highly present when maize (*Zea mays*) were subjected to combined heat and drought stress (Zhao et al., 2016a). Furthermore, this study investigated the changes in receptor proteins, protein kinases and phosphatases during combined stress conditions. When maize plants were exposed to combined heat and drought stress, the expression of three membrane receptor proteins was significantly regulated, including two downregulated receptors; brassinosteroid LRR receptor kinase and gibberellin receptor GIDIL2, and the upregulated receptor; mitochondrial import receptor subunit TOM22, which points to the involvement of hormonal perception and regulation in response to the combined stress. Moreover, glycogen synthase kinase family proteins, together with protein kinase Kelch repeat/Kelch were implicated in the regulation of heat and drought combined in maize (Zhao et al., 2016a).

Receptor-like kinases (RLKs) are a family of membrane receptors responsible for perceiving different environmental stimuli and balancing plant growth and stress responses (Soltabayeva et al., 2022; Zhu et al., 2023) and with roles in combinatorial-stress responses. For instance, the pathogenesis-related 5 (PR5) RLK 2 (PR5K2) has been shown to modulate plant responses to drought by phosphorylating protein Phosphatase 2Cs (PP2Cs) in Arabidopsis (Baek et al., 2019). PP2Cs are important protein phosphatases in the ABA signaling pathway (Singh et al., 2016) and mediate ROS (Rahikainen et al., 2016) signaling. Because both ABA and ROS signaling regulate the tolerance to various types of stresses (Suzuki et al., 2016b; Zandalinas et al., 2016a;

Choudhury et al., 2017), including combinatorial stresses, RLKs are promising targets for investigations into combinatorial-stresses acclimation.

Several protein kinases are involved in combined stress acclimation (Rejeb et al., 2014; Zhang & Sonnewald, 2017), such as mitogen-activated protein kinases (MAPKs) and calcium-dependent protein kinases (CDPKs). Noticeably, MAPK3, 4, and 6 have been found to phosphorylate the heat stress factor HSFA4A and activate the expression of the downstream targets to counteract combined heat and salinity stress in Arabidopsis (Andrási et al., 2019). Additionally, MAPK3 and 6 in Arabidopsis are also reported to be essential for the regulation of cross acclimation (Beckers et al., 2009), which refers to the phenomenon in which pre-exposure to one stress modifies the responses to a different subsequent (Foyer et al., 2016; Llorens et al., 2020). Collectively, MAPKs might be of much value for future combinatorial-stress studies.

Epigenetic regulation

Epigenetic processes involving DNA methylation and histone modifications, play a crucial role in modulating the expression of stress-responsive genes at both the transcriptional and post-transcriptional levels by, changing the chromatin status of these genes (Luo & He, 2020; Miryeganeh, 2021). In response to sequentially combinatorial stresses, cross-acclimation is closely associated with epigenetic regulation (Munné-Bosch & Alegre, 2013; Walter et al., 2013). After being primed by the initial stress, plants establish a cross-stress memory through epigenomic (including sRNA-mediated regulation, DNA methylation and chromatin changes), transcriptomic, proteomic, and metabolic regulations (Liu et al., 2022a). Consequently, when confronted with a second stress, the established shared signaling pathways between the two stresses facilitate the responses to the subsequent stress (Liu et al., 2022a). Importantly, the imprinted stress memory by epigenetic modifications may be inherited over generations (trans-generational memory) (Hirayama & Shinozaki, 2010a; Sun et al., 2021; Ramakrishnan et al., 2022), which could provide leads for training of crops to enhance tolerance to multiple (sequential) environmental stimuli.

Extensive studies have been conducted on epigenetic and epigenomic responses to single abiotic stress (Crisp et al., 2016; Begcy & Dresselhaus, 2018; Miryeganeh, 2021). However, studies focusing on epigenetic regulation under stress combinations remain limited. It can be hypothesized that epigenomic changes induced by either of the two stressors during their co-occurrence can influence the responses to another stressor. For example, mildly elevated ambient temperature enables tri-methylation of histone H3 at lysine 4 (H3K4me3) methylation and therefore promotes the expression of auxin-related genes in Arabidopsis (Perrella et al., 2022). When combined with another stress

(e.g., drought, salinity), the promoted expression of the auxin-related genes may exert an additive effect on the responses of the second stressor. Nevertheless, as molecular responses to combinatorial stress are frequently distinct from those induced by the corresponding single stresses (Mittler, 2006a; Pandey et al., 2015; Zhang & Sonnewald, 2017; Zandalinas et al., 2020a; Anwar et al., 2021a), it is equally likely that the co-existence of two stressors may induce – and be regulated by – a unique epigenomic signature that is distinct from the one evoked by the respective single stresses.

Metabolic regulation

Plant responses to combinatorial stresses often directly or indirectly involve changes in plant metabolism (Zandalinas et al., 2018). Metabolic profiling studies have revealed additive metabolic reconfigurations in response to combinatorial stresses compared to corresponding individual stresses (Rizhsky et al., 2004; Sewelam et al., 2020; Guo et al., 2021; Li et al., 2021a). Several studies have uncovered the roles of such compounds in modulating diverse types of combinatorial stress acclimations using multi-omics approaches (Rizhsky et al., 2004; Sewelam et al., 2020; Guo et al., 2021; Patel et al., 2022).

Zandalinas *et al.* summarized the changes in primary metabolites in Arabidopsis plants exposed to multiple individual stresses and their combinations, including changes in sugars, amino acids, tricarboxylic acid (TCA) cycle metabolites and other molecules such as L-ascorbate and lactate (Zandalinas et al., 2022a). When encountering environmental stresses, sugar levels in plants can be drastically influenced due to the changes in photosynthesis and carbohydrate consumption (Sami et al., 2016). However, sugars are also key players in stress perception as a signaling molecule, as an osmoprotectant and in ROS scavenging (Dong & Beckles, 2019; Saddhe et al., 2021). For example, Arabidopsis plants exposed to combined heat and drought stress, accumulated high levels of sugars like sucrose, maltose and glucose (Rizhsky et al., 2004) and acted as a major osmoprotectant under the combined stress condition. Similarly, maize plants exposed to combined cold and drought stress, increased raffinose levels facilitated osmotic adjustment and protection of the photosynthetic apparatus from oxidative damage (Guo et al., 2021).

Protein degradation during stress leads to the accumulation of free amino acids (Batista-Silva et al., 2019). This also contributes to osmotic adjustment and ROS scavenging (Hildebrandt, 2018; Batista-Silva et al., 2019; Zandalinas et al., 2022b). Especially proline, a crucial amino acid, is well known for its role in protecting cellular osmosis during stress and recovery (Hayat et al., 2012). Proline accumulated in peanut (*Arachis hypogaea*) under stress combinations that included salt (e.g., heat and salt, drought and salt, heat and salt and mannitol (an osmoticum)) (Patel et al., 2022). Despite

its osmoprotectant role during osmotic stresses such as salt and drought (Chun et al., 2018), proline was replaced by sucrose as a major osmoprotectant, when drought co-existed with heat in *Arabidopsis*, because proline might be too toxic to cells during the combined stress condition (Rizhsky et al., 2004). Also when drought was combined with Turnip mosaic virus (TuMV) infection, proline content in *Arabidopsis* plants increased (Prasch & Sonnewald, 2013). Such dynamic changes in proline accumulation indicate the complexity of metabolic responses to different stress combinations. Additionally, a study by Balfagón *et al.* highlighted the importance of another amino acid, γ -Aminobutyric acid (GABA) in response to combined heat and high light stress in *Arabidopsis*, as GABA might promote autophagy during such combinatorial stresses (Balfagón et al., 2022). Furthermore, levels of TCA cycle metabolites decreased in plants exposed to combinatorial stresses such as water deficit in combination with salt and high light combined with heat (Li et al., 2021a; Balfagón et al., 2022), as these detrimental stress combinations can compromise plant respiration. In field-grown maize plants, the levels of TCA cycle metabolites negatively correlated with grain yield under combined heat and drought stress (Obata et al., 2015).

Flavonoids are a group of phenolic compounds that belong to one of the three secondary metabolite groups (*i.e.*, phenolic compounds, terpenes/isoprenoids, nitrogen or sulfur containing compounds (Aharoni & Galili, 2011)). Flavonoids have an antioxidant role when plants encounter abiotic stresses such as salinity (Zhang et al., 2021b; Gourlay et al., 2022), drought (Hernandez et al., 2004; Rao et al., 2020), or UV-B stress (Nascimento et al., 2015; Gao et al., 2019). When confronted with cold combined with salt, pepper plants (*Capsicum*) accumulated more flavonoids compared to the relative individual stresses (Genzel et al., 2021). Moreover, some studies (Ahmed et al., 2015a; Zandalinas et al., 2017b; Ibrahim et al., 2019; Schulz et al., 2021; Jan et al., 2022b) have proposed a correlation between combinatorial stress tolerance and high levels of plant flavonoid accumulation. This provides opportunities for selecting tolerant cultivars for specific combinatorial stresses.

Hormonal regulation- ABA in the spotlight

Phytohormone biosynthesis and signaling precisely regulate plant growth, development and responses to different types of abiotic and biotic stresses (Suzuki, 2016; Verma et al., 2016; Rasool, 2023). ABA is particularly important for regulating tolerance to multiple abiotic stresses, especially osmotic stresses (Tuteja, 2007a; Fujita et al., 2011). For instance, *Nine-cis-epoxycarotenoid Dioxygenase 3* (*OsNCED3*), a gene controlling ABA biosynthesis in rice, is responsible for conferring plant tolerance to salt, polyethylene glycol (PEG) and H_2O_2 (Huang et al., 2018). Overexpression of *OsNCED3* also enhances salinity and water stress tolerance (Huang et al., 2018; Ye et al., 2023).

ABA has a role in mediating plant tolerance to combinatorial stress, particularly when an osmotic stress (imposed by drought or salinity) is one of the co-occurring stresses. For example, *Arabidopsis* ABA signaling or biosynthesis mutants exhibit impaired acclimation to combined heat and drought (Zandalinas et al., 2016a) or heat and salt stress (Suzuki et al., 2016b), reflected by reduced growth and survival compared to wildtype plants (Suzuki et al., 2016b; Zandalinas et al., 2016a). However, given the complexity of hormonal regulations under combinatorial stresses, the alterations of applied stressors or the plant species/genotype can lead to distinct hormonal responses (Suzuki, 2016; Zandalinas et al., 2022b). For example, in contrast to ABA being crucial in regulating heat and drought response (Zandalinas et al., 2016a), jasmonic acid (JA) is required for *Arabidopsis* acclimation to combined heat and high light stress (Balfagón et al., 2019a). Citrus plants subjected to combined heat and drought stress, accumulated high levels of salicylic acid (SA) compared to the corresponding individual stresses and controls, while ABA levels surprisingly decreased (Zandalinas et al., 2016b). Seemingly, this phenomenon is due to the interactions between different hormones under a specific (combinatorial) stress condition (Suzuki, 2016; Zhang & Sonnewald, 2017). For example, *Arabidopsis* plants employ SA/JA- dependent signaling during the sequential stress event of drought followed by pathogen infection, which antagonizes ABA biosynthesis and signaling pathways during early stages of this stress (Gupta et al., 2017). Therefore, when considering phytohormones as targets for improving combinatorial stress tolerance, the interactive effects among different hormones must also be considered. Furthermore, *Arabidopsis* mutants deficient in glutathione exhibit increased susceptibility to combined cold and osmotic stress, with a differential regulation of transcripts responsive to ABA, ethylene, auxin and brassinosteroids (BRs) (Kumar et al., 2015). These findings indicate potential crosstalk between hormonal regulation and antioxidative response in combinatorial- stress acclimation. Notably, studies investigating the functions of specific hormones, such as ethylene, auxin, or gibberellic acid, in plant response to combinatorial stresses remain scarce and warrant further exploration.

Thesis outline

In this thesis, we followed an integrated experimental approach to uncover physiological and molecular mechanisms underlying *Arabidopsis* responses to simultaneously or sequentially applied sublethal combinatorial stresses (Figure 1.1). We focus on i) combined high temperature and drought and ii) flooding followed by drought, both of which are relevant in nature and in an agricultural context and have already - and will further - increase in frequency due to climate change.

In **Chapter 2**, we characterized and compared the effects of these combined and sequential stresses, and the corresponding individual stresses, on a suite of morphological, developmental, and physiological traits. Our results show that combinatorial stresses mostly elicited additive effects on plant growth, development and physiological responses compared to the (corresponding) isolated stresses. Moreover, based on the most responsive traits (*i.e.*, chlorophyll change, leaf initiation, and days to wilting) of the plant under combinatorial stress conditions, we established a suitable multi-stress experimental setup as a basis for investigating the molecular mechanisms underlying the observed phenotypic changes in the subsequent chapters.

To probe the molecular basis of plant resilience to combinatorial abiotic stresses, a comparative mRNA sequencing (RNA-seq) approach was employed in **Chapter 3**. This allowed us to characterize and compare the transcriptome responses of young Arabidopsis leaves during the subjection to combined or sequential stresses and their corresponding individual stresses. Surprisingly, the analysis of the RNA-seq experiments uncovered the presence of an uncharacterized comovirus in our plants that we named Arabidopsis Latent Virus 1 (ArLV1) (Verhoeven et al., 2023). The presence of this virus did not affect the Arabidopsis transcriptome and did not trigger obvious phenotypes under control or under our mild stress conditions.

The transcriptomic profiling of the remaining Arabidopsis-specific reads revealed that combinatorial stresses triggered a profound transcriptome reconfiguration that was distinct from either of the stresses applied individually. Furthermore, the RNA-seq analyses identified several key molecular processes, including plastid-to-nucleus communication (retrograde signaling) and ABA signaling, and potential candidate genes that likely contribute to the acclimation of Arabidopsis to combined and sequential abiotic stresses.

Using a genetic approach by testing mutants, in **Chapter 4** we uncovered and confirmed effects of several identified candidate genes (chapter 3) on plant growth, development and wilting under combined or sequential stresses. We were able to identify and confirm both positive and negative modulators of the typical phenotypic traits contributing to whole-plant responsiveness to sublethal combinatorial stresses. Of note, EARLY FLOWERING 6 (ELF6) and ARABIDOPSIS/DOPSIS TOXICOS EN LEVADURA 80 (ATL80), together with the phytohormone ABA, were identified as master regulators contributing to the acclimation of combined and/or sequential abiotic stresses.

The transcriptome analysis also pointed towards a potential involvement of chloroplast-associated genes in mediating responsiveness to high temperature stresses imposed

in isolation or in combination with drought. In **Chapter 5**, we deciphered in detail the role of GOLDEN2-LIKE 2 (GLK2), a transcription factor responsible for the expression of photosynthesis-associated nuclear genes (*PhANGs*) and chloroplast development, in thermal responses. We show that GLK2 is stabilized under high temperature conditions and suppresses typical Arabidopsis thermomorphogenic responses such as petiole and hypocotyl elongation. This occurred independent of the well-characterized GENOMES UNCOUPLED 1 (GUN1)-mediated retrograde signaling pathway. Although not fully understood, the findings connect chloroplast function to thermomorphogenesis add a new layer to the current understanding of plant high temperature responsiveness.

Altogether, the results of the integrated approach described in this thesis (Figure 1.1) provide a comprehensive understanding of plant response to sublethal combinatorial stresses at the developmental, morphological, physiological and molecular genetic levels. In **Chapter 6**, the main findings are discussed together with the limitations of this study, and we provide an outlook on future research on combinatorial stress resilience.

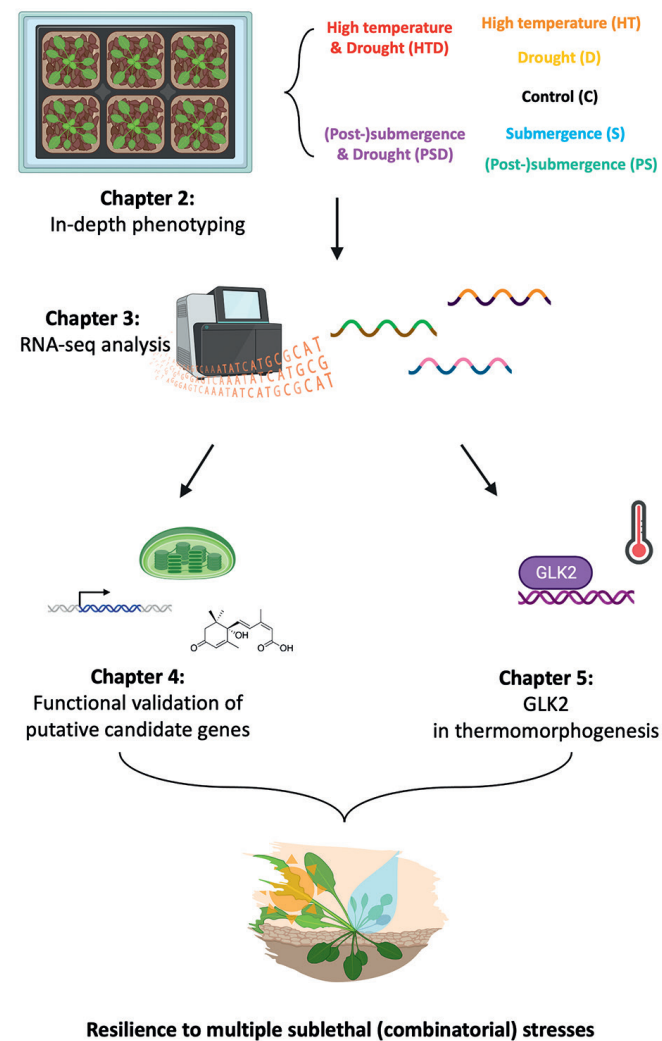


Figure 1.1 Schematic representation of the experimental approach described in this thesis. *Arabidopsis thaliana* Col-0 wild-type plants were treated with two types of sublethal combinatorial stresses; i) combined high temperature and drought (HTD) and ii) submergence followed by drought (PSD), as well as with their corresponding individual stresses (drought (D), high temperature (HT), submergence (S), (post-)submergence (PS) and control conditions (C). In-depth phenotyping was performed at different time-points to characterize and compare the effects of individual and combinatorial abiotic stresses on plant growth, development, and physiology (**Chapter 2**). This was informative for the subsequent mRNA-sequencing (RNA-seq) approach employed to identify key molecular processes and potential candidate genes involved in the acclimation to combinatorial stresses (**Chapter 3**). The putative candidate genes were further validated for their phenotypic effects during the subjection to combinatorial stresses by testing mutants in these genes (**Chapter 4**). The outcomes of the RNA-seq analysis hinted at the involvement of chloroplasts in thermal responsiveness. Therefore, the role of

GOLDEN-LIKE 2 (GLK2), a transcription factor mastering the expression of photosynthesis-associated nuclear genes (*PhANGs*) and chloroplast development, in thermomorphogenesis, was investigated (**Chapter 5**). This comprehensive study at both phenotypic and molecular levels provides insight into plant resilience to combined or sequential abiotic stresses at a sublethal severity.



2

Effects of simultaneous and sequential abiotic stresses on Arabidopsis growth, development and physiology

Zhang Jiang, Yihong Li, Ava Verhoeven, Martijn van Zanten*,
Rashmi Sasidharan*

* Shared senior authors

Plant Stress Resilience, Utrecht University, The Netherlands

Abstract

Plants grown in natural or agricultural environments are frequently exposed to abiotic stress combinations occurring either simultaneously or sequentially. Even though these stresses rarely occur in isolation, most research on plant stress tolerance has focused on single environmental stressors imposed at a lethal severity. Plant responses to sublethal abiotic stress combinations, at both the phenotypic and molecular levels, can be distinct from the responses to the corresponding single stresses. It is thus crucial to characterize the mechanisms underlying plant acclimation to combinatorial sublethal stresses. Here, we carried out a comprehensive phenotypic characterization at the morphological, developmental, and physiological levels on *Arabidopsis thaliana* plants exposed to two distinct combinatorial sublethal abiotic stresses; i) high ambient temperature in combination with drought and ii) submergence followed by drought, as well as the corresponding individual stresses.

Our results revealed distinct plant responses under combined stresses. Individually applied drought stress had very subtle effects. However, when drought was combined with either prior submergence or high temperature, additive effects were elicited as reflected by significantly enhanced reductions in plant growth and leaf lengthening, respectively. Combined or sequential stresses also resulted in distinct physiological responses compared to the relative single stresses, typically in the context of changes in chlorophyll content and stomatal conductance. Overall, our work i) highlights the unique responsiveness elicited by combinatorial stresses at morphological and physiological levels in comparison with the corresponding individual stresses and ii) presents a suitable multi-stress experimental system as basis for investigating the relevant molecular mechanisms underlying the observed phenotypic responses in Chapter 3-4.

Introduction

Climate change has become a significant problem for earth's inhabitants, increasing the occurrence of diverse detrimental abiotic stresses such as heat waves, droughts and flooding (IPCC, 2021; Kreibich et al., 2022; Schiermeier, 2018; Stott, 2016). These adversities negatively impact the natural environment and crop productivity and therefore are a threat to food security (Raymond et al., 2020; Zandalinas et al., 2021a). As sessile organisms, plants in both natural and agro- environments constantly encounter and respond to all kinds of environmental signals.

In the past decades, acclimation to various abiotic stress signals has been thoroughly studied in multiple plant species (Wu et al., 2007; Zhu, 2016; Fahad et al., 2017; Lamers et al., 2020; Zandalinas et al., 2022a). These studies have provided invaluable insight into the molecular pathways mediating various stress acclimation responses and their functional significance. However, these studies often mainly focused on single abiotic stresses that are applied to severe levels and for a short term, with often lethal consequences for the plant. Abiotic stresses, however, rarely occur in isolation (Mittler, 2006b; Zandalinas & Mittler, 2022) and occurrences of unfavorable 'stressful' conditions often coincide, either simultaneously or sequentially. For example, progressive drought resulting in soil drying, is frequently accompanied by elevated ambient temperatures (Lamaoui et al., 2018). Similarly, persistent rainfall often alternates with dry periods, resulting in a sequential combination of flooding and drought (Miao et al., 2009). Some studies have highlighted how different scenarios of combinatorial stresses can have more destructive effects on crop yields than individual stresses (Prasad et al., 2011; Pandey et al., 2017; Cohen et al., 2021).

In nature, abiotic stresses are often milder (at a sublethal severity) than in experimental laboratory studies (Bailey-Serres & Colmer, 2014; Van Dooren et al., 2020; Zhang et al., 2020a; De Smet et al., 2021). Some plant species, such as *Arabidopsis thaliana* can be sensitive to even mild environmental changes in the laboratory. Such changes, for instance, evoked by a small increase in ambient temperature or a shift in light quality (reduced red and far-red ratio), often affect a multitude of phenotypic traits simultaneously, resulting for example in leaf elongation, an increase of leaf angle (hyponasty) and accelerated flowering time (Quint et al., 2016; Pantazopoulou et al., 2017). These so-called whole-plant acclimation strategies, or 'trait syndromes' are typically regulated by complex molecular networks, especially when multiple stresses are involved. Importantly, the stresses can have synergistic or antagonistic interactions during the combinatorial occurrence, and thus the responsiveness cannot be simply deduced by counting the sum of the responses evoked by the two individual stresses

(Balfagón et al., 2019; Mittler, 2006; Rivero et al., 2022; Rizhsky et al., 2004; Suzuki et al., 2014; Zandalinas et al., 2020). A typical example highlighting this is the opposing stomatal responses of plants under high temperature and drought. High temperature induces stomatal opening to allow leaf cooling through transpiration, while drought causes plants to reduce the stomatal conductance to prevent unnecessary water loss. When high temperature and drought occur concurrently, however, the stomata remain closed (Rizhsky et al., 2004; Mittler & Blumwald, 2010; Zandalinas et al., 2016a, 2016b).

The acclimation strategy fitting a given concurrent stress combination is determined by various (sometimes limiting) factors, such as plant genotype, developmental age, and the relative and absolute severity of the two stresses (Zandalinas et al., 2016b; Zhou et al., 2017; Sinha et al., 2021b; Rivero et al., 2022; Zandalinas & Mittler, 2022). In conclusion, the acclimation strategy adopted by the plant in response to a concurrent or simultaneous stress combination can possibly be a blend or additional effect of either of the acclimation strategies to individual stresses, or a unique response, not matching either of the individual stress outputs (Prasch & Sonnewald, 2015; Choudhury et al., 2017; Zhang & Sonnewald, 2017).

Several factors are considered crucial in determining the effect size of a given sequential stress, such as the severity and duration of stresses (Zandalinas et al., 2021a). Additionally, the sequence in which the two stressors are applied plays a pivotal role in determining the responsiveness to a sequential stress (Banti et al., 2008; Kong & Henry, 2016). When confronted with a sequential combinatorial stress, the exposure to the first stress (if non-lethal) can in some cases enhance the acclimation to the second stress, which is termed 'cross acclimation' (Bowler & Fluhr, 2000; Çakırlar et al., 2008; Kong & Henry, 2019). This phenomenon often involves many coordinated signal transduction pathways and hormonal changes triggered by both stressors (Hossain et al., 2018; Anwar et al., 2021a; Rossatto et al., 2023). For example, soil salinity pretreatment can alleviate the subsequent low-temperature damage in tomato plants, as salt stress-triggered signal cascades can activate downstream overlapping transduction pathways (e.g., reactive oxygen species (ROS), abscisic acid (ABA) and low-temperature signaling) that enhance photosynthetic acclimation under low-temperatures (Liu & Li, 2022).

In another example, the growth ratio and biomass accumulation of three tree species (*Annona glabra*, *Acer rubrum* and *Bursera simaruba*) at the seedling stage under sequentially applied flooding and drought, appear to differ depending on the order in which the two stresses are applied. If the stress sequence of flooding and drought was reversed, the response changed as well (Miao et al., 2009).

Despite the highlighted importance of understanding multi-stress acclimation mechanisms, the topic remains relatively poorly studied (Rivero et al., 2022; Zandalinas et al., 2020; Zandalinas and Mittler, 2022). Thus, a comprehensive investigation of plant acclimation to combinatorial sublethal abiotic stresses at the morphological, physiological, functional, and molecular levels is needed. This will be essential for meeting the long-term goal of breeding broad-spectrum stress resilience in crops suffering from climate change.

Here, to identify and characterize phenotypic traits underlying plant responses to simultaneous and sequential sublethal abiotic stresses, we exposed *Arabidopsis* plants to i) combined high ambient temperature and drought (HTD) and ii) prolonged submergence (in the light) followed by drought (PSD), and the corresponding individual stresses. Both of these combinatorial stresses are relevant and occur frequently in natural and agro- environments (Mittler, 2006b; Miao et al., 2009). For a series of timepoints that correlated to the soil water loss and physiological changes under individual and combinatorial stresses, plant growth, development and physiological responses were assessed at both the whole-plant and leaf levels.

Our data demonstrated that *Arabidopsis* plants subjected to combined and sequential sublethal stresses elicit distinct responses at the morphological and physiological levels compared to corresponding isolated stresses in a leaf age-dependent manner. Furthermore, these unique responses caused by combinatorial stresses are likely due to the negative interactions between the two stressors during the combination scenarios. In this chapter we establish the 'optimal' time-points, based on the physiological responses of plants under multiple sublethal abiotic stresses, for the in-depth transcriptomic analysis in Chapter 3, where we characterize and compare the molecular changes underlying the observed responses to single and combinatorial stresses.

Results

Combined abiotic stress impedes new leaf formation and accelerates wilting

To study the effect of single and combined abiotic stresses on plant growth, *Arabidopsis* Columbia-0 (Col-0) plants were subjected to two different stress combinations when they reached the 10-leaf stage (LS10; *i.e.*, having 10 true leaves): i) high ambient temperature (27 °C day and night) + progressive drought (HTD) and ii) submergence, followed by progressive drought (PSD) after de-submergence (post-submergence phase) at 21 °C (Figure 2.1). Plants were also subjected to control conditions (C; at 21 °C

day and night) and corresponding single stresses: high temperature (HT; 27 °C day and night), submergence (S) in the light (submergence during day and night), whereafter plants were well-watered during the post-submergence phase (PS). Drought (D) was imposed in a progressive manner by withholding watering. After 5 days, the average soil water content (%SWC) dropped to 50–65%, of field water capacity (= 100% saturation), and thereafter to 30–40% after 10 days (Figures S2.1A and S2.1B). Long-term progressive drought eventually results in wilting (Harb et al., 2010; Zhao et al., 2016c; Malefo et al., 2020). In our experimental system, plants subjected to HTD and PSD displayed earlier wilting than in D alone (Figures 2.2A-C).

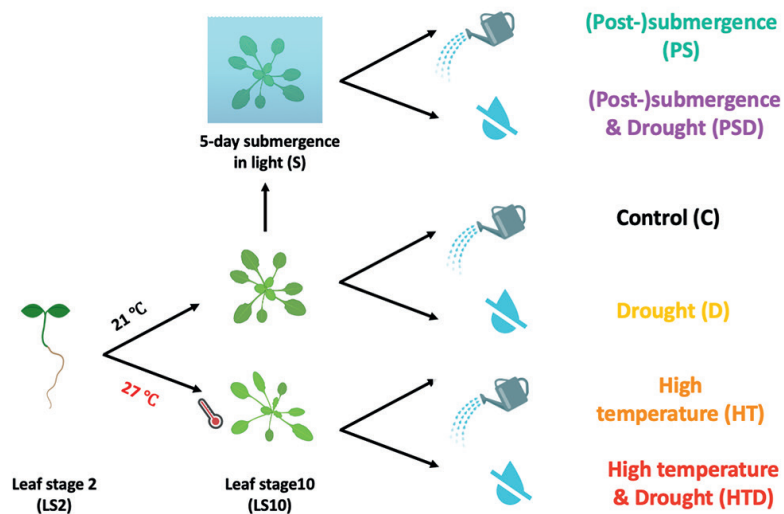


Figure 2.1: Overview of the experimental setup for imposing combined and sequential sublethal abiotic stresses, their single applications, and controls.

2-leaf stage (LS2) *Arabidopsis Col-0* plants were pre-grown at 21 °C or 27 °C (day and night) until they reached the 10-leaf stage (LS10). Subsequently, the plants were subjected to either high ambient temperature in well-watered conditions (27 °C; HT), to progressive drought at 21 °C (D), or progressive drought at high ambient temperature (27 °C; HTD). For the submergence treatment, 10-leaf stage plants were subjected to complete submergence at 21 °C for 5 days in the light and thereafter experienced post-submergence recovery under either well-watered conditions (PS), or under progressive drought (PSD). Control plants are indicated with a C and were well watered and kept at 21 °C. Note that the colour codes used to depict each of the treatments are also used in subsequent figures in this chapter and rest of the thesis.

The daily change in leaf number (*i.e.*, daily leaf initiation) was recorded throughout the experiments until drought-treated plants (D, HTD and PSD) showed symptoms of wilting (Figure 2.2D-E). This parameter indicates the ability of the shoot apical

meristem to generate new leaves and is a marker for plant viability (Cleland, 2001). Plants exposed to HT showed initially a comparable leaf initiation rate as plants in C conditions, but leaf formation was steadily delayed ~9 days after the treatment started, while during submergence (S) plants had 2-3 leaves less compared to plants grown at C already after 5 days. During PS, plant leaf initiation resumed to rates comparable to plants grown at C. D had a relatively subtle effect on new leaf formation, especially during the first 10 days. However, plants subjected to combined stresses (HTD and PSD) produced fewer new leaves than those subjected to the corresponding single stresses. Overall, these results suggest that stresses, and especially when combined, hinder leaf formation and accelerate wilting.

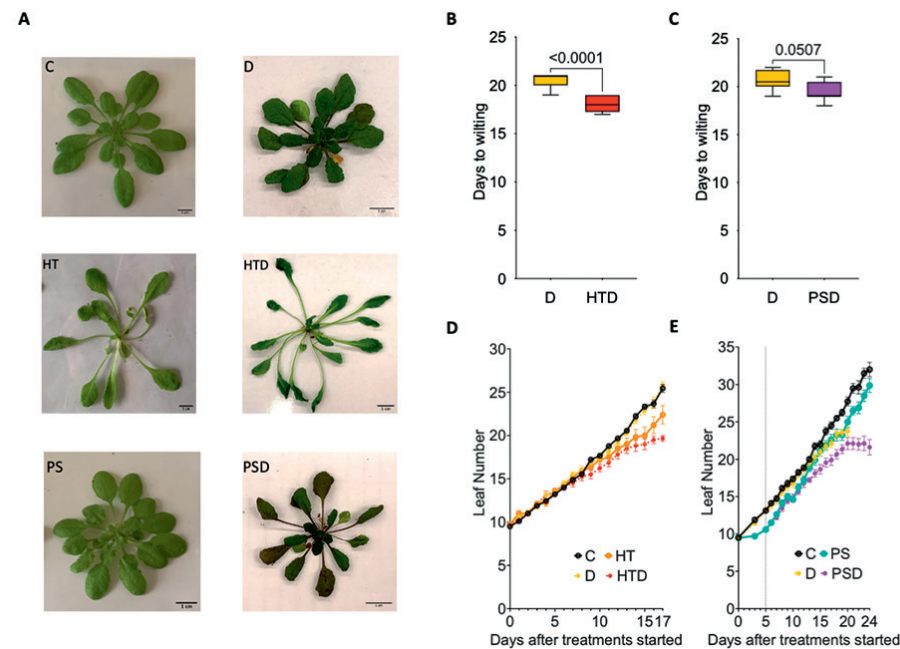


Figure 2.2: Effect of combined and sequential sublethal stresses on leaf initiation and wilting.

(A) Representative images showing *Arabidopsis Col-0* rosettes at the wilting stage (right column; non-turgid) after individually applied progressive drought and the relative controls (left column; turgid non-wilted plants) at control temperature (21 °C, C and D, upper row), high temperature (27 °C) combined with drought (HT and HTD, middle row) and post submergence followed by drought (PS and PSD, bottom row). (B, C) Number of days until wilting was observed in plants subjected to (B) drought at control temperature (21 °C; D) and at high ambient temperature (27 °C; HTD) and (C) drought at control temperature (21°C; D) and post-submergence followed by drought (PSD). Days were counted after water was withdrawn. (B) $n = 8-10$. (C) $n = 8-9$. Boxes indicate boundaries of the second and third quartiles (Q) of the data distribution. Black horizontal bars indicate median and whiskers Q1 and Q4 values within 1.5 times the interquartile range. Numbers above the bars indicate p values (unpaired t-test). (D, E) Leaf number of plants exposed to combined high temperature and drought (D) (HTD; pink) or post-submergence followed by drought (E) (PSD; blue), and the associated single stresses (HT, HTD, D, PS, PSD) and controls (C). Error bars indicate means \pm SEM, (D) $n = 6-18$. (E) $n = 5-33$. The dashed vertical line in panel (D) indicates the moment plants were de-submerged. For color codes and abbreviations see legend figure 2.1.

Increase in leaf chlorophyll content imposed by drought is age-dependent

Chlorophyll content is considered a marker of early stress responses as it is often affected by adverse environmental conditions (Mecey et al., 2011; Neelam; Yang, 2013,

2013; Qi et al., 2021; Suzuki et al., 2016). Previous studies suggested that chlorophyll changes in leaves caused by abiotic stresses are age-dependent (Yeung et al., 2018; Kanojia et al., 2021; Rankenberg et al., 2021). To investigate the chlorophyll dynamics under single and combined stresses, and especially to detect effects of early drought responsiveness, we first classified all true leaves (thus excluding cotyledons) of 10 leaf-stage (LS10) plants into three categories based on their developmental stages: the three oldest leaves (old; 1-3), three intermediate leaves (4-6) and the most recently formed four leaves (young; 7-10) (Figure 2.3A).

Chlorophyll content was measured daily throughout the experiment of the three differentially aged groups until the leaves started to wilt. We observed that plants subjected to HT, S and PS had reduced chlorophyll content compared to those subjected to C conditions independent of leaf age (Figures 2.3B-C). However, drought-treated plants at control temperature (D) or during de-submergence (PSD) showed increased chlorophyll content compared to the relative controls (C and PS). This increase in chlorophyll content in drought-treated plants was confirmed by separate experiments where chlorophyll content of the same young leaves was measured using two different methods: a chlorophyll meter-based non-destructive measurement and a destructive biochemical assay (Figures S2.2A and 2.2B). Of note, the drought-induced chlorophyll accumulation was detectable at ~5 days (measured by the chlorophyll-meter assay, but the induction was not significant when measured by the biochemical assay), except for HTD, where the increase was only visible after day 9. We then decided to take 0, 5, 10 and 15 (only for C and D in comparison with PS and PSD) days after the stress initiations as the sampling timepoints for the following experiments in this chapter (Figure 2.4).

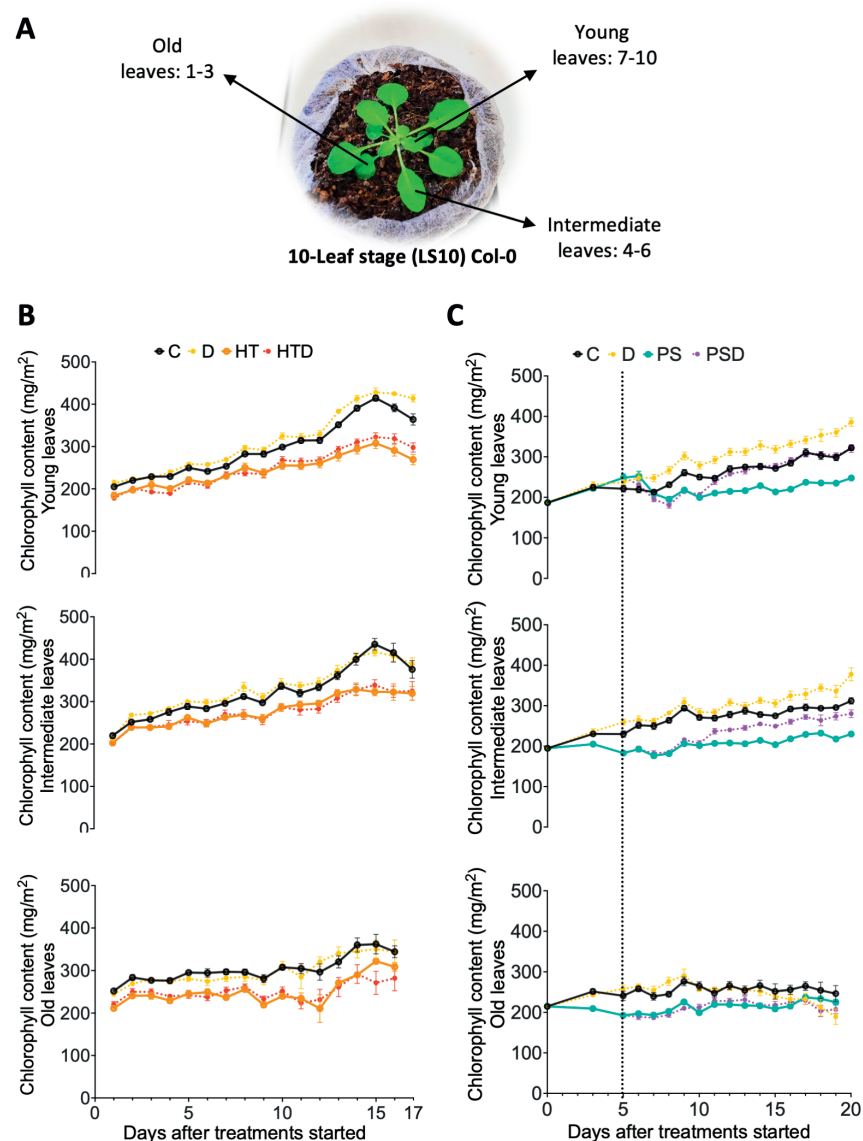


Figure 2.3: Chlorophyll dynamics in response to stresses are leaf-age dependent.

(A) Representative image of a 10-leaf stage (LS10) Col-0 plant on Jiffy coco pellet growth substrate, with young, intermediate, and old leaves indicated. Associated leaf numbers are counted starting from the first true leaves (thus excluding the cotyledons). (B, C) Chlorophyll content of young (upper row), intermediate (middle row), and old leaves (lower row) exposed to high temperature & drought (HTD) (B) or post-submergence & drought (PSD) (C), as well as the associated single stresses (HT, PS, D). Error bars indicate means \pm SEM, (A) $n=4-9$. (B) $n=5-33$. The dashed vertical line in panel (C) indicates the moment plants were de-submerged. For color codes and abbreviations see legend figure 2.1.

During this project a required renewal of our Utrecht University phytotron growth facility and accompanying switch from fluorescence tube lighting to LEDs took place. All follow-up experiments in this chapter, and those in chapters 3, 4 and 5, were performed in renovated LED climate rooms. Although conditions remained in theory identical (except for a change in the light spectrum and intensity), we revalidated our experimental system. We repeated the following experiments: i) quantification of progressive soil water loss; ii) wilting timepoint; and iii) chlorophyll measurements on young leaves and compared the data with those generated in the old fluorescent light growth chambers.

In the new LED-growth chambers, the rate of soil water loss under drought was similar to that measured in the old phytotron chambers (compare Figure S2.3A with S2.1A and S2.1B). Despite this, regardless of the combination with HT or S, drought-treated plants (D, HTD and PSD) wilted several days earlier than those in the old fluorescent light chambers (Figure S2.3B compared to 2.2B and 2.2C). However, the differences between D, HTD and PSD remained significant. Accordingly, the %SWC at the point of wilting was significantly higher under PSD than under D and HTD, but there were no significant differences in terms of wilting point %SWC between D and HTD (Figure S2.3C). Possibly, this early wilting can be attributed to changes in air circulation rates inside the chambers.

Finally, we validated if the observed increase in chlorophyll content in drought-treated plants (Figure 2.3B-C) was consistent in the new chambers. Indeed, after a 5-day drought (D) treatment, chlorophyll content of young leaves was higher compared with control (well-watered) plants (Figure S2.3D-E), confirming our earlier findings. Additionally, the average chlorophyll content measured in the new chambers positively correlated (Figure S2.3, tables) with the data obtained in the growth chambers equipped with fluorescent tubes. Thus, we conclude that in general our data was reproducible regardless of whether fluorescent tubes or LEDs chambers were used.

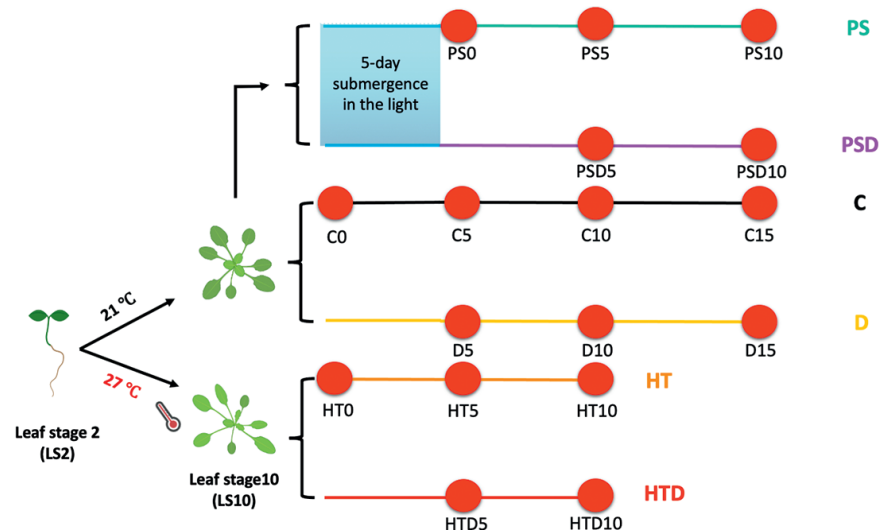


Figure 2.4: Experimental scheme for phenotypic effect studies.

Harvest moments and measurements were typically conducted at 0, 5, 10 and 15 (C and D) days after the drought (D, HTD and PSD) started (indicated by red dots), with average %SWC of 100%, 50–65%, 30–40% and ~20% respectively (Figures S2.1 and 2.3A). For C, HT and PS the %SWC were maintained at the saturated level (95%–100%) across all timepoints. Comparisons were carried out within the same timepoints (as indicated by the numbers). For color codes and abbreviations see legend figure 2.1.

High temperature and drought combination elicits distinct effects on plant growth, development, and physiology than when applied in isolation.

To further characterize the responses to HT, D and their combination (HTD), various phenotypic and physiological traits were measured on LS10 rosette plants at 0, 5, and 10 days (Figures 2.5, 2.6 and S2.4). Under control conditions (C), rosette growth was reflected in an increase in total leaf area, petiole and blade length, biomass (dry weight) and below ground by root growth (Figure 2.5A–G). D did not hamper the increase in total leaf area and petiole length, but it did have a small, but significant, effect on blade length increase after 10 days (Figures 2.5B–D and S2.4C). Plants grown in HT showed a typical ‘open-architecture’ phenotype referred to as “thermomorphogenesis” (Quint et al., 2016). This included a larger total leaf area, and more elongated and hyponastic leaves compared to plants grown at 21 °C (Figure 2.5A–E). When plants were subjected to HTD, the hyponastic growth was similar to HT, whereas hyponastic growth at C was similar to D, indicating that drought does not affect the leaf angle (Figure 2.5E). Moreover, plants treated with the HTD formed smaller rosettes and shorter petioles

and leaf blades in comparison with plants exposed to single HT stress, but rosette sizes, petiole length and leaf blade length under HTD exceeded the values observed under D (Figures 2.5B–D, S2.4). Together, this indicates that during the subjection to HTD, the single D and HT stresses interact resulting in intermediate trait values. Plants grown in HT or D did not differ in dry weight compared to plants in C (Figure 2.5F). However, the HTD combination caused significant dry-weight reduction after 10 days compared to HT, but not to C.

Under water-limiting conditions, plants can elongate their roots to enhance water uptake (Waidmann et al., 2020; Kang et al., 2022; Yang et al., 2022b). This was confirmed by our results, as our drought-treated plants (D and HTD) generated longer primary roots than non-droughted plants (C and HT) (Figure 2.5G). Interestingly, HT caused an increase in primary root length 5 days after treatment began, but not after 10 days (Figure 2.5G). HT in combination with D (HTD) elicited the strongest increase in primary root length, suggesting D and HT are additive in the context of root growth.

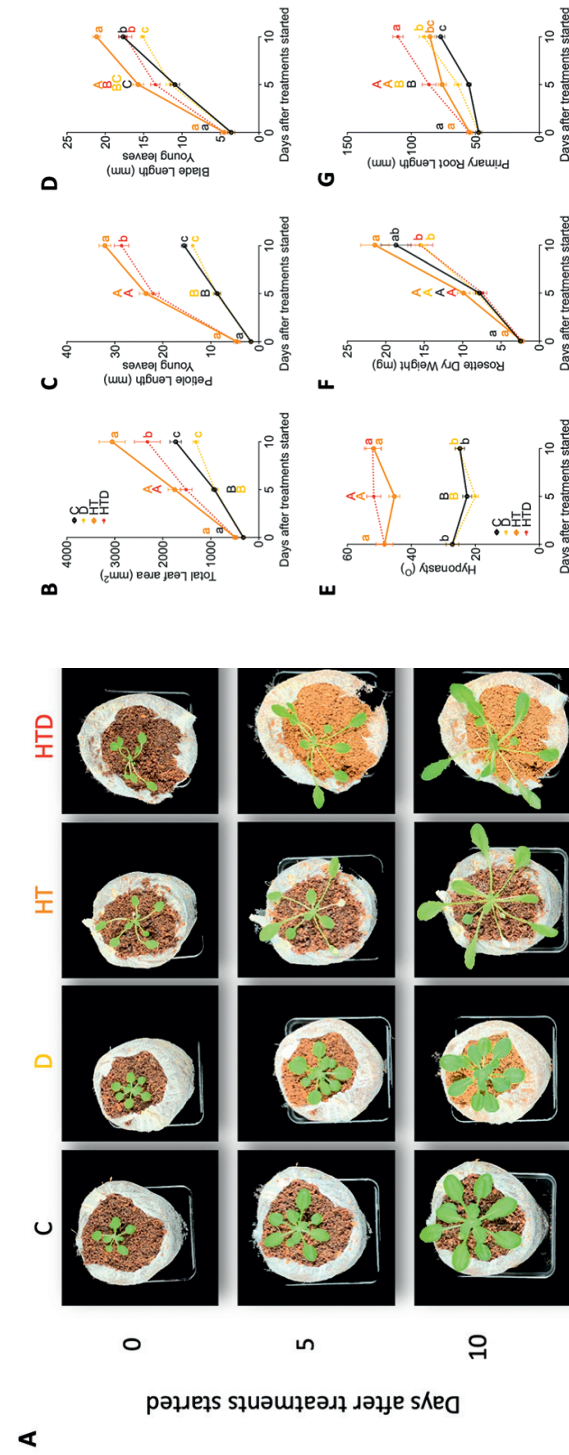


Figure 2.5: Effects of combined sublethal stresses; high ambient temperature and drought and the corresponding single stresses on various phenotypic traits.

(A) Representative images of whole rosettes on Jiffy coco pellet growth substrate, subjected to single and combined stresses at 0, 5, and 10 days, counted from the moment that the treatments started. (B) Total leaf area of the whole rosette. (C, D) Average length of petiole (C) and blade (D) of young leaves. (E) Average angles of the 2 most hyponastic leaves of individual plants, relative to the horizontal. (F) Rosette dry weight. (G) Primary root length. (B-G) Error bars indicate means \pm SEM. Letters denote significant differences between different treatments at the same time points ($p < 0.05$, 2-way ANOVA with Tukey's Post-hoc test). For color codes and abbreviations see legend figure 2.1.

Plants encounter cellular water stress when soil water declines during drought and this is closely linked with regulation of stomatal opening (Lu et al., 2009; Wahab et al., 2022). We observed that plants contained relatively more water under high temperature conditions (HT and HTD) than at control temperatures (C and D) (Figure 2.6A). However, stomatal conductance of plants in C and HT was not significantly different, whereas C and HTD did differ significantly, with HTD having lower stomatal conductance (Figure 2.6B). D caused, as expected, a reduction in relative water content corresponding with a significant decline in stomatal conductance compared to C (Figure 2.6B).

It is well-documented that leaf surface temperature increases as a consequence of stomatal closure (Crawford et al., 2012; Violet-Chabrand & Lawson, 2020). The imaging of plants with a high-resolution thermal imaging camera revealed that under D, leaf temperature significantly increased approximately 10 days after the treatment started (Figure 2.6C and 2.6D, both left). When treated with HTD, the elevation of leaf surface temperature happened earlier: from day 8 onwards (Figure 2.6C and 2.6D, both right). Moreover, temperature discrepancy between control and drought treated plants at 27 °C (HT and HTD) was greater than those at 21 °C (C and D), indicating that the drought effect on leaf temperature was more pronounced when combined with high temperature.

Malondialdehyde (MDA) content reflects the extent of lipid peroxidation caused by ROS production (Morales & Munné-Bosch, 2019). Together with electrolyte (ion) leakage, they are considered general indicators for cell damage (Nielsen et al., 1997; Sharma et al., 2012). In general, MDA values declined over development (time), but values were comparable among the applied stresses and control, except for day 0, in which plants pre-grown in HT showed significantly lower MDA content than at C (and D) (Figure 2.6E). This might be because plants were pre-grown in HT, leading to acclimation to HT, which is reflected by a reduced level of lipid peroxidation and hence a lower MDA content compared to C. However, the pre-growth at HT caused enhanced level of ion leakage (Figure 2.6F), suggesting the occurrence of membrane damage by HT. Furthermore, increased ion leakage in plants grown at high ambient temperatures (HT and HTD) was strongly tempered by a combination with 10-day drought (10 days of HTD), while it had no effect when D was applied in isolation, at least up to 10 days of treatment (Figure 2.6F).

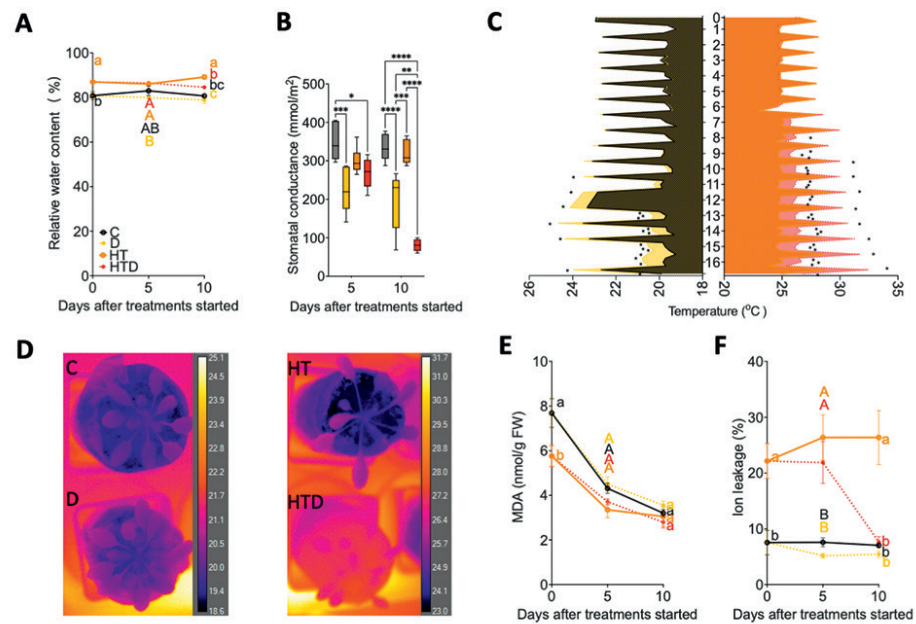


Figure 2.6: Effects of combined high temperature and drought, the corresponding single stresses and control conditions on various physiological traits.

(A) Rosette water content relative to the maximal water content that the leaves can hold (100%, turgid water - dry weight). $n=8-11$. (B) Stomatal conductance of young leaves at 5 and 10 days after treatments started. $n=5-6$. Boxes indicate boundaries of the second and third quartiles (Q) of the data distribution. Black horizontal bars indicate median and whiskers Q1 and Q4 values within 1.5 times the interquartile range. Asterisks represent significant differences ($*p < 0.05$, $**p < 0.01$, $***p < 0.001$, $****p < 0.0001$, 2-way ANOVA with Tukey's Post-hoc test). (C) Dynamic change in leaf surface temperature at 21 °C (C and D, left) and 27 °C (HT and HTD, right). Lines represent the average leaf temperature as measured every 6 hours (ZT = 0, 6, 12, and 18 h). $n = 3$. Asterisks represent significant differences between measured leaf temperature within the same timepoints ($p < 0.05$, One-way ANOVA with Tukey's Post-hoc test). Note that temperature fluctuates between the photoperiod (peak) and dark period. Data from three time points (ZT = 18 h on day 11 and ZT = 0 and 6 h on day 12 in 21 °C) were not recorded due to camera failure. (D) Representative thermal images of plants at 21 °C (C and D-treated, left) and 27 °C (HT-treated and HTD-treated, right) 10 days after the treatments started. (E) Rosette Malondialdehyde (MDA) content. $n = 5-10$. (F) Rosette ion leakage relative to the maximal electrolyte conductivity (100%). $n=6$. (A, E, F) Error bars indicate means \pm SEM. Letters denote significant differences between different treatments within the same time points ($p < 0.05$, 2-way ANOVA with Tukey's Post-hoc test). For color codes and abbreviations see legend figure 2.1.

Effects of submergence on plant growth, development and physiology are exaggerated when followed by drought

To unravel the effects of sequential flooding and drought stress (PSD) compared to D and PS applied in isolation, as well as C, we examined the phenotypic and physiological traits of plants subjected to these stress treatments for 0, 5, 10, and 15 days (Figures 2.7, 2.8, S2.5, S2.6 and S2.7). Five days of complete submergence in the light (S) was already sufficient to severely inhibit rosette growth, indicated by a smaller total leaf area and shorter leaves (both petiole and blade length) compared to non-submerged plants (C and D) (Figures 2.7A-D, S2.5). During the post-submergence phase (PS and PSD), plants could recover if irrigation was applied (PS), as indicated by the similarity between slopes of the curves over time between PS and C when the time window of 5 days (moments plants were taken out of the water) up to 15 days is considered (Figures 2.7, S2.6).

Drought had a significant impact on young leaf expansion (inhibiting length of the petiole and blade) if it lasted for 10 or 15 days (Figures 2.7B-D, S2.6A-C). Under PSD, this inhibition was enhanced. As expected, leaf angle strongly increased during submergence (hyponastic growth) but was restored to pre-submergence levels a few days after submergence (Figure 2.7E). Like in the HT experiments, D had again no influence on plant hyponasty even if the drought period was either extended to 15 days or in combination with prior submergence (Figures 2.7E and S2.6D).

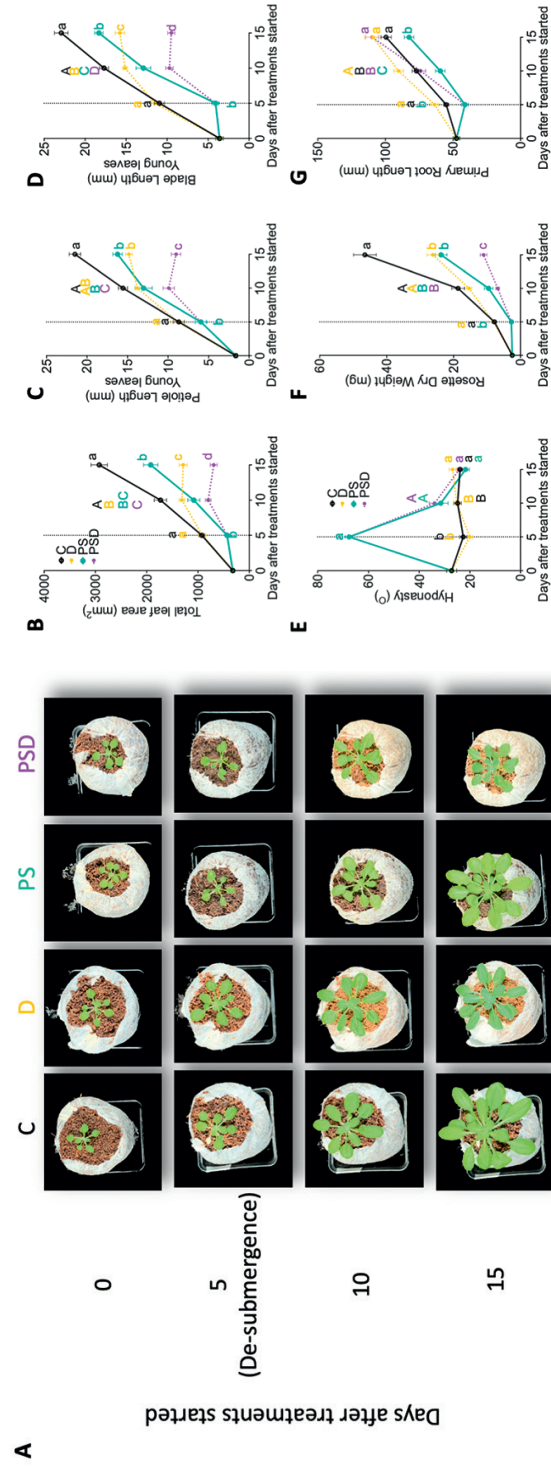


Figure 2.7: Effects of sequential submergence and drought stress on various phenotypic traits.

(A) Representative images of whole rosettes on Jiffy coco pellet growth substrate subjected to single and sequential stresses at 0, 5, 10 and 15 days, after the treatments started. **(B)** Total leaf area of the whole rosette. $n=15-20$. **(C, D)** Average length of the petiole **(C)** and blade **(D)** of young leaves. $n=15-21$. **(E)** Average angles of the 2 most hyponastic leaves of individual plants, relative to the horizontal. $n=14-21$. **(F)** Rosette dry weight. $n=15-18$. **(G)** Primary root length. $n=14-21$. **(B-G)** Error bars indicate means \pm SEM. Letters denote significant differences between different treatments at the same time points ($p < 0.05$, 2-way ANOVA with Tukey's Post-hoc test). The dashed vertical lines indicate the moment plants were de-submerged. For color codes and abbreviations see legend figure 2.1.

Corresponding to the leaf traits mentioned above, submerged plants had a considerably decreased rosette dry weight compared to non-submerged plants (Figures 2.7F and S2.6E). Five days of D treatment barely affected dry weight accumulation, but a 10- and 15-day D treatment did have a significant negative effect on dry weight, compared to the control. PSD resulted in the lowest dry weight accumulation compared to submergence alone (Figures 2.7F and S2.6E).

Submergence and drought can have a contrasting effect on primary root elongation (Takenaka et al., 2018; Kang et al., 2022). Our results showed that submergence significantly restricted the lengthening of primary roots, whereas drought could promote root elongation (Figures 2.7G and S2.6F). Interestingly, root elongation was enhanced under PSD.

Drought had a significant negative effect on the relative water content after 15 days, but not 10 days, compared to the control (C) (Figure 2.8A). However, if prior submerged, 10-day drought treatment (PSD) already elicited a significant decrease in relative water content (Figure S2.7A). This is consistent with the results of leaf stomatal conductance, where the conductance under D and PSD were relatively low and comparable after 15 days (Figures 2.8B, S2.7B), while after submergence rosette relative water content was restored to a level similar to non-submerged plants, if well-watered during the de-submergence phase (PS).

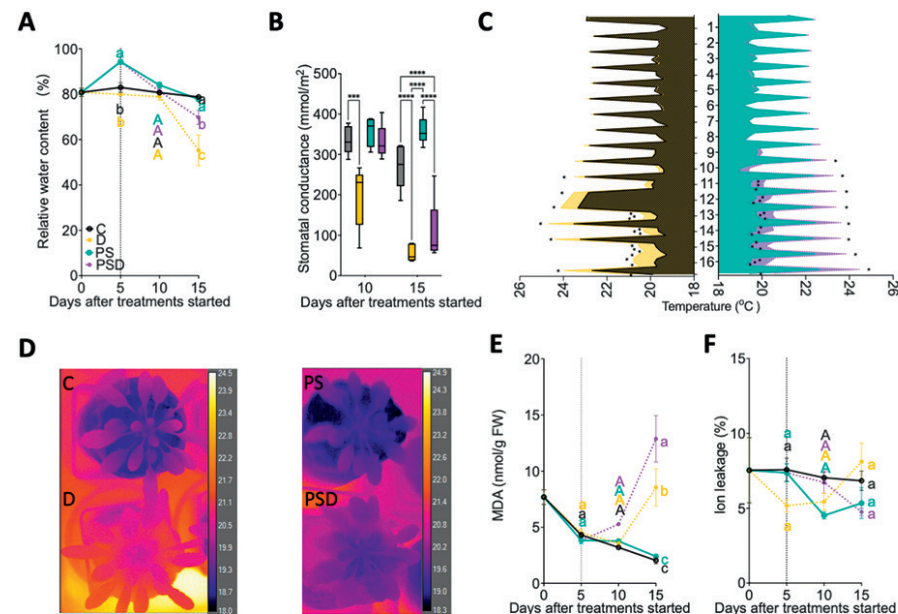


Figure 2.8: Effects of submergence followed by recovery under drought or well-watered conditions, drought in isolation and control conditions on various physiological traits. (A) Rosette water content relative to the maximal water content that the leaves can hold (100%, turgid water - dry weight). $n=15-16$. (B) Stomatal conductance of young leaves at 5 and 10 days after treatments started. $n=5-6$. Boxes indicate boundaries of the second and third quartiles (Q) of the data distribution. Black horizontal bars indicate median and whiskers Q1 and Q4 values within 1.5 times the interquartile range. Asterisks represent significant differences between measured leaves within the same timepoints ($*p < 0.05$, $**p < 0.01$, $***p < 0.001$, $****p < 0.001$, 2-way ANOVA with Tukey's Post-hoc test). (C) Dynamic changes in leaf surface temperature of plants with (PS & PSD, right) and without (C & D, left) pre-submergence treatment. Lines represent the average leaf temperature measured every 6 hours (ZT = 0, 6, 12, and 18 h). $n = 3$. Asterisks represent significant differences between measured leaf temperature within the same timepoints ($p < 0.05$, One-way ANOVA with Tukey's Post-hoc test). Note that temperature fluctuates between the photoperiod (peak) and dark period. Data from three time points (ZT = 18 h on day 11 and ZT = 0 h and 6 on day 12 in 21 °C) were not recorded due to the camera failure. (D) Representative thermal images of plants in absence of prior submergence subjected to control and drought treatments for 15 days (C and D, left), or in present of prior submergence followed by either well-watered condition or drought for 10 days (PS and PSD, right). (E) Rosette malondialdehyde (MDA) content. $n = 5-10$. (F) Rosette ion leakage relative to the maximal electrolyte conductivity (100%). $n=6$. (A, E, F) Error bars indicate means \pm SEM. Letters denote significant differences between different treatments within the same time points ($p < 0.05$, 2-way ANOVA with Tukey's Post-hoc test). For color codes and abbreviations see legend figure 2.1. The dashed vertical lines indicate the moment plants were de-submerged.

We next investigated if submergence treatment affected the drought-induced temperature increase of the leaf surface (Figures 2.8C-D). We observed that leaf

temperature significantly increased after a 9-day drought treatment in the de-submergence phase (PSD), which is 1 day earlier compared with the lack of prior submergence (D) (Figure 2.8C). Furthermore, temperature differences between submerged groups (PS and PSD) were similar to those between non-submerged groups (C and D).

Finally, we assessed MDA content and ion leakage. Drought significantly increased MDA accumulation, especially when it was combined with prior submergence (PSD) (Figures 2.8E, S2.7C). While 5- or 10- day D triggered no significant changes in MDA accumulation, the MDA content was significantly higher under D compared to C or PS if the drought treatment (D) lasted for 15 days (Figures 2.8E, S2.7C). However, no clear effect of PSD, D or PS was observed on ion leakage (Figures 2.8F, S2.7D).

Discussion

Plants are frequently subjected to combinations of sublethal abiotic stresses in both natural environments and agricultural fields. These stress combinations often elicit unique responses at the developmental, morphological, phenological, physiological and molecular levels, when compared to the stress occurring in isolation (Mittler, 2006b; Suzuki et al., 2014). Here, we performed a comprehensive characterization of *Arabidopsis* responses to combinatorial sublethal abiotic stresses of high temperature, drought (HT, D, HTD) and submergence and drought (S, PS, D, PSD).

It is known that the co-occurrence of abiotic stresses can cause synergistic, antagonistic, or additive effects, depending on the interactions between individual stressors (Zandalinas & Mittler, 2022). In our study, plants exposed to HTD or PSD had, for instance, lower leaf initiation rates than plants exposed to the respective single stresses (Figures 2.2D-E), implying that combined stresses had additive negative impact on plant growth. Our findings showed that the average time to wilting was approximately 20 days after the withdrawal of water (Figures 2.2B-C). However, both a 5-day prior submergence (PSD) treatment or the presence of elevated temperature (HTD) significantly accelerated wilting time. These findings thus suggest that under combined stress conditions (HTD and PSD), HT and D, as well as PS and D, interacted additively rather than synergistically or antagonistically (meaning combined effects of multiple stressors are respectively equal or less than the summation of individual stressors) in the context of rosette plant growth.

By assessing the changes in chlorophyll content of differently aged leaves under multiple abiotic stresses (Figures 2.3B-C), we uncovered distinct physiological

responses provoked by combined stresses compared to the individual stresses, which appeared to be leaf-age dependent. In line with previous studies (Winkel et al., 2014; Hussain et al., 2019; Kim et al., 2020; Zhuang et al., 2020), where plants experienced chlorophyll deprivation under abiotic stresses such as high temperature, drought, or submergence, we here showed chlorophyll deprivation caused by HT and S in all leaf stages compared to controls (Figures 2.3 B-C). Drought-induced chlorophyll changes were more pronounced in young and intermediate leaves compared to old leaves (Figures 2.3, S2.2 and S2.3). This is consistent with previous findings (Berens et al., 2019; Bui et al., 2020) showing that juvenile tissues are in general more responsive to environmental stresses than mature tissues.

Interestingly, drought promoted rather than impeded chlorophyll accumulation in young and intermediate leaves in our experiments (Figures 2.3 B-C), contrasting with some previously reported findings (Zhang et al., 2020; Zhuang et al., 2020), in which chlorophyll content of drought-exposed plants drastically declined. This drought-induced chlorophyll increase is most likely a synchronistic genotype- and age-dependent response, which has been previously demonstrated (Zhou et al., 2017). Zhou *et al.* showed that under drought treatment, the chlorophyll content of drought-tolerant tomato cultivars kept increasing. In another study, drought-treated tobacco plants displayed a high chlorophyll content in the upper (young) leaves but not in the lower (old) leaves (Macková et al., 2013). The maintained high chlorophyll content under a given stress is considered a protection mechanism to protect leaves from harsh stresses (Macková et al., 2013; Nankishore & Farrell, 2016). The increased chlorophyll content in young leaves could be an acclimation strategy to cope with drought. Additionally, drought in combination with high temperature, but not when combined with prior submergence, drastically delayed drought-induced chlorophyll increase, suggesting a more predominant role of HT under HTD than PS has under PSD in affecting the physiological responses to drought.

High temperature has a predominant effect on plant development and physiological responses over drought when occurring simultaneously.

In general, the responsiveness to a given (combinatorial) stress is highly dependent on the severity and duration of individual stresses and the order of events (Anwar et al., 2021a). The in-depth morphological characterization of plants subjected to D, HT and HTD demonstrated that under HTD conditions the effect of HT on plant rosette growth and leaf development (*i.e.*, leaf elongation and hyponasty), prevails over that of D (*i.e.*, reduced leaf size and shoot biomass) (Figures 2.5B- F S2.4B-D). Interestingly, despite the mild effect imposed by D on these phenotypic traits, a significantly enhanced drought effect was observed under HTD relative to HT, confirming that HT adds to

the negative effect of D on plant growth and development when the two stressors are combined. This prevailing effect of HT over D under HTD may be due to the pre-exposure of HT before D was applied, as one prior applied stress is able to ameliorate the impact of the subsequent one during the combination treatment (Guo et al., 2021). In contrast to our findings, some researchers highlighted the predominant effect of drought over heat on plant growth and development when these two stressors are applied concurrently (Zhou et al., 2017). However, high ambient temperature used in our study was merely 27 °C (See; Chapter 2, Materials and Methods), which is not considered heat stress (Praat et al., 2021; Zhu et al., 2022a).

In contrast to the negative effect of HTD on plant shoot growth, primary root lengthening was significantly enhanced under HTD compared to that under HT or D (Figure 2.5G). This reveals the existence of additive interactions between HT and D in affecting plant belowground development during HTD. In response to high temperature, the primary root growth of *Arabidopsis* is largely promoted by increasing cell division rates in the root apical meristem through the *de novo* auxin biosynthesis and polar auxin transport (Ai et al., 2023). When drought occurs, plants stimulate root elongation to improve water capture in deeper soil (Markhart, 1985), which is accomplished by re-allocating resources from shoot to root (Reinelt et al., 2023). This resource allocation is likely stress-dose dependent (Agathokleous et al., 2019) and governed by ABA (Chen et al., 2021b). In this case, HTD-promoted primary root lengthening may indicate an additional effect caused by both auxin and ABA, eventually leading to more dry mass allocation from shoot to root, which could be partially reflected by the reduced shoot dry weight under HTD compared to individual HT. However, to better elucidate the shoot-to-root resource allocation, including its hormonal regulations, additional measurements such as root biomass, root/shoot ratio and/or endogenous ABA concentration, should be performed in future work.

By induction of thermomorphogenic phenotypes, as described in this chapter (Figures 2.5 and S2.4), the plant is thought to enhance leaf cooling capacity through transpiration, which thus should reasonably result in increased water loss compared to control temperature-grown plants (Crawford et al., 2012; Bueno et al., 2019). However, we found on the contrary that plants under HT maintained a higher relative water content and comparable stomatal conductance compared to C (Figure 2.6A-B). One possible explanation for this apparent discrepancy is that water was not limiting in our HT conditions or that plant developmental adaptations to high ambient temperature promote water conservation by generating lower stomatal densities than at normal temperatures (Crawford et al., 2012). Since measurements of stomatal index were not included in our present study, future work should elucidate whether stomatal density

is indeed affected by our mild high temperature conditions. However, drought (D) led, as expected, to stomatal closure already at 5 days after stopping watering (Figure 2.6B). This suggests an early drought response by – or that affects the stomata, which is in accordance with the notion that stomatal closure is among the first responses to occur under drought (Bechtold et al., 2016; Pirasteh-Anosheh et al., 2016). It is also in line with our previous finding that 5-days of D is sufficient to trigger some early physiological responses such as changes in chlorophyll content (Figure 2.3B). Furthermore, in comparison to the respective individual-stress controls, plants exposed to HTD displayed stronger decreases in stomatal conductance and relative water content, as well as accelerated leaf temperature increase (Figure 2.6 A-D), implying a distinct physiological response elicited by the combined stress compared to the relative single stresses. Because the stomatal density and the closure under drought are fine-tuned by multiple signal molecules such as reactive oxygen species (ROS), calcium (Ca⁺) and ABA (Liu et al., 2022b), plants under HTD might employ unique response signatures at the molecular level.

Sublethal abiotic stresses as used in this study barely caused lipid peroxidation, as indicated by MDA levels in D, HT and HTD compared to C (Figure 2.6E). HT, on the other hand, resulted in a significant increase in ion leakage, which was later tempered by D (Figure 2.6F). Similar findings were described in a study on drought and heat responses in *Eucalyptus globulus* (Correia et al., 2018), although in this paper a prolonged drought was applied prior to heat, resulting in enhanced osmoprotection during the stress combination period. We therefore hypothesize that in our study the prolonged exposure of plants to HT prior to D might elicit osmotic protections to minimize membrane damage during HTD.

Prior submergence in the light alters the subsequential drought effect on plant growth, development, and physiology.

When submerged, plant survival is, in general, higher if there is no light limitation (Mohanty, 2003; Vashisht et al., 2011). However, submergence under sufficient illumination can cause hyperoxia (Lee et al., 2011; Vashisht et al., 2011; Pedersen et al., 2017), which when coupled with CO₂ limitation, can eventually cause photorespiration that impedes plant development (Sasidharan et al., 2018). Our results revealed that submergence in the light caused a significant negative impact on plant growth, including impeded leaf expansion and dry weight accumulation in comparison to non-submerged plants (C and D) (Figures 2.7B-D, 2.7F and S2.5B-D). However, despite shoot growth and leaf development being significantly hampered, submergence in the light (in our study) did not cause lethal phenotypes as reported by previous studies for submergence in the darkness (Vashisht et al., 2011; Van Veen et al., 2013). This is

mainly due to the fact that during submergence in light, plant photosynthesis is not damaged as much as submergence in the darkness (Sasidharan et al., 2018). After water recedes, dark-submerged plants suffer additional damage from re-exposure to light and excess oxygen, which triggers the production of excessive reactive oxygen species (ROS) and delayed recovery of plant growth (Yeung et al., 2018; Yuan et al., 2023b). Light-submerged plants were able to steadily recover if optimal irrigation was applied following de-submergence (Figures 2.7B-D, 2.7F). However, when plants recovering from submergence experienced progressive drought (PSD), leaf lengthening, rosette area increase and dry mass accumulation were significantly inhibited compared to plants experiencing only drought (Figures 2.7B-D, 2.7F), implying that PSD has a more stressful effect on plant growth and rosette development than the individual stresses. Earlier work (Luo et al., 2009) already highlighted the essential role of photosynthetic acclimation during submergence recovery. Drought, on the other hand, can be a major impediment to photosynthesis (Cornic, 2000; Chaves et al., 2009). The enhanced inhibition of growth and development of plants under PSD can thus likely be explained by hampered photosynthetic acclimation by successively imposed drought during the post-submergence phase. Additionally, the inhibition of plant shoot growth caused by PSD aligns well with the notion that a combinatorial stress might elicit a more drastic impact on plant growth and development than any of the individually-applied stresses (Shabbir et al., 2022). Furthermore, by comparing the drought effect in the presence or absence of prior submergence on shoot development traits (Figure S2.6A-E, Table S2.1), we unraveled that the differences between PS and PSD were greater than those between C and D after 10 days. This implies that PS exerted a negative and synergic effect on D in regulating plant growth and development under PSD.

In contrast to drought, which induces continuous primary-root elongation (Markhart, 1985) (Figures 2.5G and 2.7G), prolonged submergence usually arrests root elongation due to the energy deprivation caused by the dampened respiration (Takenaka et al., 2018; Mignolli et al., 2021). However, prior light-submergence strikingly promoted drought-induced primary root elongation (Figure S2.6F) in our experiments, suggesting an additive interaction between PS and D during PSD in regulating root growth. Similar to the effect imposed by HTD on root lengthening (Figure 2.5G), plants might adopt an enhanced shoot-to-root resource allocation strategy when confronted with PSD. Likely, these enhanced root responses can be due to cross acclimation between PS and D. Previous research has shown that in response to a given sequential stress, the prior stressor is able to trigger common signal transducing molecules to improve the tolerance to the subsequent stressor (Pastori & Foyer, 2002; Mittler, 2006b; Foyer et al., 2016; Hossain et al., 2016). In our work, a possible regulator of cross acclimation under PSD is the phytohormone ABA, which has previously been shown to be a key player

in both submergence and drought responses (Sharp & LeNoble, 2002; Benschop et al., 2005), particularly in regulating root lengthening under drought (Zhang et al., 2022c).

10 days of drought caused a decline in water content that was significantly enhanced when preceded by a 5-day submergence (PSD) (Figure S2.7A). However, the effect of the sequential stress (PSD) on relative water content is less strong than 15-day drought (much closer to the drought-triggered wilting time) (Figure 2.8A). Under PSD, plants exhibited a stronger decrease in stomatal conductance than in PS and D, possibly to counteract the water loss (Figures 2.8B and S2.7B). These distinct physiological responses adopted by plants under PSD again suggest that the combinatorial stress is able to provoke a unique response signature compared to the corresponding individual stresses, which is consistent with previous studies (Suzuki et al., 2014; Balfagón et al., 2019a) and the findings we reported of plant responses to combined high temperature and drought (HTD).

Although both HT and PS interact with D and consequently elicit distinct effects on plant physiology under the combined stress conditions, HT and PS seemingly affect the physiological responsiveness to HTD and PSD to different degrees. For example, when combined with HT, drought-promoted leaf temperature increase occurred substantially earlier than under individual drought conditions (Figure 2.6C). In contrast, a submergence pre-treatment (S) did not accelerate the drought-induced leaf temperature elevation (Figure 2.8C). Furthermore, stomatal conductance decreased drastically 5 days after HTD (Figure 2.6B) but not during 5-day PSD (Figures 2.8B and S2.7B). One possible explanation is that stomata are more susceptible to high temperature than (post-)submergence, resulting in a more pronounced stomatal response when combined with drought.

We also demonstrated that the levels of rosette ion leakage were not significantly affected by individual or sequential stresses (Figures 2.8F and S2.7D), whereas MDA level in PSD-treated plants was significantly higher compared to relative controls, including D, at day 15 (Figure 2.8E). MDA level in general reflects the degree of lipid peroxidation (Sharma et al., 2012). Similar as electrolyte leakage (ion leakage), MDA is considered a biomarker of plant cell damage (Nielsen et al., 1997; Zhang et al., 2021c). Here, despite the ion leakage under both individual and sequential stresses being barely affected (Figure 2.8F), the increased accumulation of MDA under PSD thus suggests that the sequential stress caused greater damage to the plant than individual applied stress. This is in accordance with a previous study where alfalfa seedlings experienced more cell-membrane damage when exposed to combined abiotic stresses compared to the individual stresses (Bao et al., 2020). Furthermore,

when compared to plants subjected to 10-day D, the greater MDA abundance of plants subjected to 10-day PSD also implies that the prior submergence likely exacerbates the detrimental impact imposed by drought (Figure S2.6C). Of note, the MDA level, in general, was not as abundant as previously reported when confronted with lethal stresses (Ahmed et al., 2013), which underlines the sublethal nature of our stress treatments.

In conclusion, the results presented in this chapter document the unique acclimation responses to sublethal combinatorial stresses in *Arabidopsis*. Our work establishes an experimental system for further exploration of molecular mechanisms underlying characterized phenotypic and physiological responses (See; Chapter 3). Furthermore, our study can contribute to the establishment of mechanistic models for predicting trait responsiveness of crops under the given stress conditions. Such investigations of plant responses to combined sublethal abiotic stresses in the context of plant growth, development, and physiology, are critical considering the increased co-occurrence of these stresses in the context of climate change. Collectively, this work has therefore the potential to contribute to the development of multi-stress resilient crops that maintain optimal yields in future climate conditions.

Acknowledgements

This work is supported by the Netherlands Organization for Scientific Research (NWO) (project no. 867.15.031 to AV) and the China Scholarship Council (CSC) (project no. 20186170025 to ZJ). We thank Alejandro Morales (Wageningen University & Research, The Netherlands) for the advice on the experimental design and for the discussion of the results, and Yorrit van de Kaa for helping with seed harvesting.

Materials and Methods

Plant materials and growth conditions

Arabidopsis thaliana Col-0 (Col-0; NASC stock center ID: N1092) seeds were sown on moist potting soil (Primasta BV, Asten, The Netherlands) and stratified at 4 °C in darkness for 4 days. After stratification, seeds were transferred to a growing chamber (MD1400; Snijders, The Netherlands) for germination with the following conditions: 8h photoperiod / 16h darkness, 21 °C, 120-150 $\mu\text{mol m}^{-2} \text{s}^{-1}$ photosynthetically active radiation (PAR) with fluorescence tube lightening, and 70% relative humidity. After switching to the LED's lighting system (see result text), the light intensity was increased to 130-150 $\mu\text{mol m}^{-2} \text{s}^{-1}$ PAR, with other conditions unchanged.

When plants reached the 2 true-leaf stage (LS2), they were individually transplanted to Jiffy 7c coconut pellet growth substrate (Jiffy Products International BV, Zwijndrecht, The Netherlands) that were pre-soaked in deionized water and 50 mL Hoagland solution (Millenaar et al., 2005) to the final saturated weight of 250 ± 20 g. The pellets with transplanted plants were then contained in 9 x 9 cm square pots, to prevent tumbling over, and placed in trays that were covered by transparent lids. Trays with plants were kept in the growing chamber with the above-mentioned conditions, or in another chamber with identical conditions except for a temperature of 27 °C. One day after the transplantation the lids were removed. Plants were supplied with additional Hoagland solution on the 2nd, 5th, and 7th day after transplantation. Irrigation was accomplished by adding water to the trays every 2 days and randomization of pellets was performed every time plants were watered, to ensure homogeneousness and correct for confounding positional effects.

Stress treatment

Plants subjected to high-temperature treatments (HT and HTD) were grown at 27 °C starting from LS2, while plants for all other treatments and controls (C) remained in the chamber at 21 °C, including during subjection to the stress condition. When the majority of plants reached the 10 true-leaf stage (LS10), they were divided into two groups, based on the developmental stages: i) plants with 9 or 10 true leaves and ii) plants at early 11 true-leaf stage. Plants that did not belong to either of the two groups were discarded. Plants from each group were equally mixed and randomized and progressive drought was imposed by withholding watering (D) at 21 °C and combined high ambient temperature and drought (HTD) in 27 °C. The well-watered counterparts in the two temperature conditions were control (C) and individual high temperature treatments (HT). All stress treatments were initiated two hours after the photoperiod started.

Plants subjected to submergence (PS and PSD) and their non-submerged controls (C) were pre-grown and treated at 21 °C. One day before the treatments started, plastic tubs (54 x 27 x 37 cm) were disinfected with a chlorine tablet (Diversey Lnc., Racine, USA) for at least two hours and thereafter thoroughly rinsed. Then the tubs were filled with deionized water and left in the growing chamber overnight to equilibrate the water temperature to the room temperature. Plants were then completely submerged (S) 2 hours after the photoperiod started for a total of 5 days. After 5 days the submerged plants were removed from the water and the pellets were covered from below and the side by absorbent papers for the removal of excess water (not touching the plants). When the weight of these pellets reached a comparable level as the weight of well-watered control plants (250 ± 20 g), they were subjected to either

a regime of regular irrigation, or to progressive drought conditions by withholding watering. These groups were referred to as post-submergence and recovery (PS) and post-submergence in combination with drought (PSD), respectively. Non-submerged control groups (C) and (D) were as treated as indicated above.

Quantification of drought

The percentage of soil water content (%SWC) was used as a proxy for drought (*i.e.*, an indication of soil drying). %SWC was calculated by the ratio of measured pellet weight (W_p) and the saturated pellet weight at field capacity (W_s , approximately 250 ± 20 mg):

$$\%SWC = \frac{W_p}{W_s} \times 100\%.$$

In general, after 5-day drought treatment, average %SWC dropped to approximately 50%, whereas after 10 days %SWC reached ~30% (See; Figures S2.1A and S2.1B).

Scoring of leaf number

Leaf number was scored to assess leaf initiation (rate). In short, the number of all visible leaves, excluding cotyledons, was scored daily after the stress treatments started.

Chlorophyll content measurements

Chlorophyll content was determined both non-destructively and by a destructive biochemical assay. For the non-destructive assay, a CM-300 Chlorophyll Meter (Opti-Sciences Inc., Hudson, USA) with a fluorescent detector was used. After calibration, the detector was placed at 5 mm distance from the leaf for 3 seconds and chlorophyll content per square meter (mg / m^2) was automatically calculated based on the fluorescent intensity.

For biochemical detection of chlorophyll content, leaves were detached and placed in a 1.5 mL Eppendorf tube. 1mL 96% DMSO was added for the extraction of chlorophyll. Tubes were then incubated in the dark on a shaking incubator at 65 °C for 30 minutes and cooled down for 30 minutes in the dark to room temperature. For each sample, 250 μL of the extracts was pipetted into a 96-well microplate and the absorption at the wavelengths of 664 nm, 647 nm, and 750 nm was determined by a spectrophotometer plate reader (Synergy HT Multi-Detection Microplate Reader; BioTek Instruments Inc., USA). The remaining plant tissue (deprived of chlorophyll) was dried in an oven set at 80 °C for 3 days and subsequently weighed on an analytic balance (Sartorius BP221S, Göttingen, Germany) to determine the dry weight. Chlorophyll a, b, and total chlorophyll content were calculated based on the following formulas and normalized by dry weight:

$$\text{Chl}_a = 12.25 \times (A_{664} - A_{750}) - 2.55 \times (A_{647} - A_{750})$$

$$\text{Chl}_b = 20.31 \times (A_{647} - A_{750}) - 4.91 \times (A_{664} - A_{750})$$

$$\text{Chl}_{\text{total}} = \text{Chl}_a + \text{Chl}_b$$

Measurements of rosette traits and dry weight

To characterize rosette traits, plants subjected to different stress treatments were selected and side pictures were first taken for the measurement of leaf angle (hyponasty) with a regular camera, of the two most hyponastic opposing intermediate-aged leaves, placed perpendicular to the camera. Plant shoots were subsequently detached from the roots and flattened by pressing them using a transparent paper on a blank paper, fit with a scale. Top pictures were taken with a regular camera. ImageJ software (National Institutes of Health, USA) was used to determine the leaf traits, including the total leaf area, petiole, and blade length of young, intermediary, and old leaves. For the determination of hyponasty, leaf angle relative to the horizontal was measured by taking the average angle of the capture opposing leaves that were most hyponastic. Dry weight was measured in a similar manner as described above for the plants used for chlorophyll content assays.

Root length measurement

To measure root length, the cover of the pellet was gently removed, and the soil was carefully rinsed away with tap water to recover the root system. The primary root length, starting from the junction of hypocotyl and root, was then measured with a ruler.

Measurement of rosette relative water content

Excised rosettes were first weighed on an analytic balance (Sartorius BP221S, Göttingen, Germany) to determine the fresh weight and then immediately allowed to saturate with water in 9 cm plastic petri dishes for 24 hours in the dark. After removing the excess water from the leaf surface with a tissue, the turgor weight of plants was measured. Plants were then dried in the oven at 80°C for 3 days and eventually the dry weight was recorded. The relative water content was calculated based on the following formula: $((\text{Fresh weight} - \text{dry weight}) / (\text{turgor weight} - \text{dry weight})) \times 100\%$

Stomatal conductance measurements

Stomatal conductance was measured using an SC-1 Leaf Porometer (Decagon Devices, Inc., Pullman, USA) of young leaves. The porometer was initially equilibrated to the ambient temperature and then calibrated at least 3 times to get stable readouts. The measurements were conducted on the adaxial side of the leaf and the porometer was always re-equilibrated to ambient temperature and humidity between readings.

Leaf temperature measurements

The measurements of leaf surface temperatures was performed using LS10 Arabidopsis plants. A FLIR A655sc High-Resolution LWIR thermal imaging (IR) (Teledyne FLIR, USA) camera, equipped with a 13.1 mm FoV 45° x 33.7° Hawkeye IR lens, was mounted on top of the plants for recording of the leaf surface temperatures. Thermal images were captured every 15 minutes using FLIR ResearchIR Max 4 software (Teledyne FLIR, USA) from the start of the stress treatments till wilting occurred. Obtained thermal pictures were then used to determine leaf temperature: 6 leaves per plant were selected and leaf surface temperatures were measured 'every day' at ZT = 0, 6, 12, 18 h. For every 4th image, equaling every 24 hours, the regions of interest were manually adjusted for correcting the leaf growth and movement, which ensured that the same region was always tracked throughout the entire experiment.

Malondialdehyde (MDA) measurements

To determine the Malondialdehyde (MDA) content, the entire rosette was first weighed to obtain fresh weight and then grinded in presence 1 mL 80% (w/v) ethanol in a pre-cooled mortar with a pestle. Samples were then transferred to a 1.5 mL Eppendorf tube and centrifuged at 16000 rpm for 20 minutes at 4 °C. 0.5 mL supernatant was mixed with the same amount of TCA/TBA solution made by 0.65% (w/v) thiobarbituric acid in 20% (w/v) trichloroacetic acid. The mixture was incubated on a shaking incubator for 30 minutes at 95 °C and thereafter cooled-down for 5 minutes in an ice bath. After centrifugation at 10000 rpm for 10 minutes at 4 °C, the samples were measured by a spectrophotometer plate reader (Synergy HT Multi-Detection Microplate Reader; BioTek Instruments Inc., USA) at absorbances of 532 nm and 600 nm. The MDA concentration was calculated based on the following formula, normalized by fresh weight: $\text{MDA (nmol/mL)} = ((A_{532} - A_{600}) / 155000) \times 1000000$

Ion leakage measurements

Rosettes were detached from the roots and were immediately transferred to a 50 mL falcon tube containing 30 mL deionized water (*i.e.*, the solution) and shaken on a roller for 1 hour at room temperature. After rolling, 100 µL solution was pipetted onto the pre-calibrated EC-33 conductivity meter (HORIBA, Japan) to determine the initial conductivity. Samples in the remaining solution were then incubated in a water bath at 95 °C for 30 minutes to destroy all membranes. After cooling down to room temperature, 100 µL solution was taken to quantify the final conductivity. Ion leakage was calculated based on the formula: $\text{Ion leakage} = (\text{Initial conductivity} / \text{final conductivity}) \times 100\%$

Statistical analysis

Figures in this chapter were generated using GraphPad Prism 9 (GraphPad Software, La Jolla, USA) and Biorender.com. Unpaired t-test, one-way or two-way ANOVA followed by Tukey's multiple test were performed by GraphPad Prism 9. The significance was considered as $p < 0.05$.

Supplemental Data

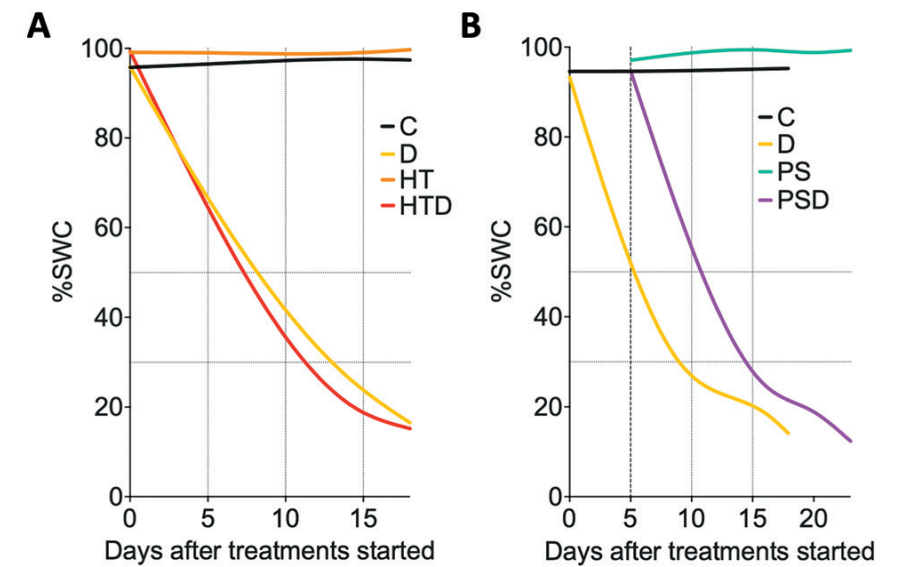
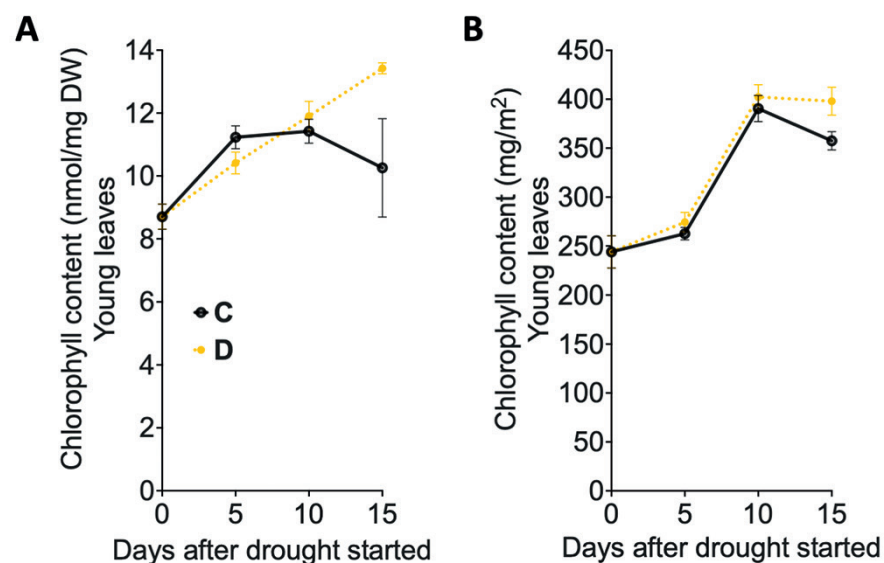
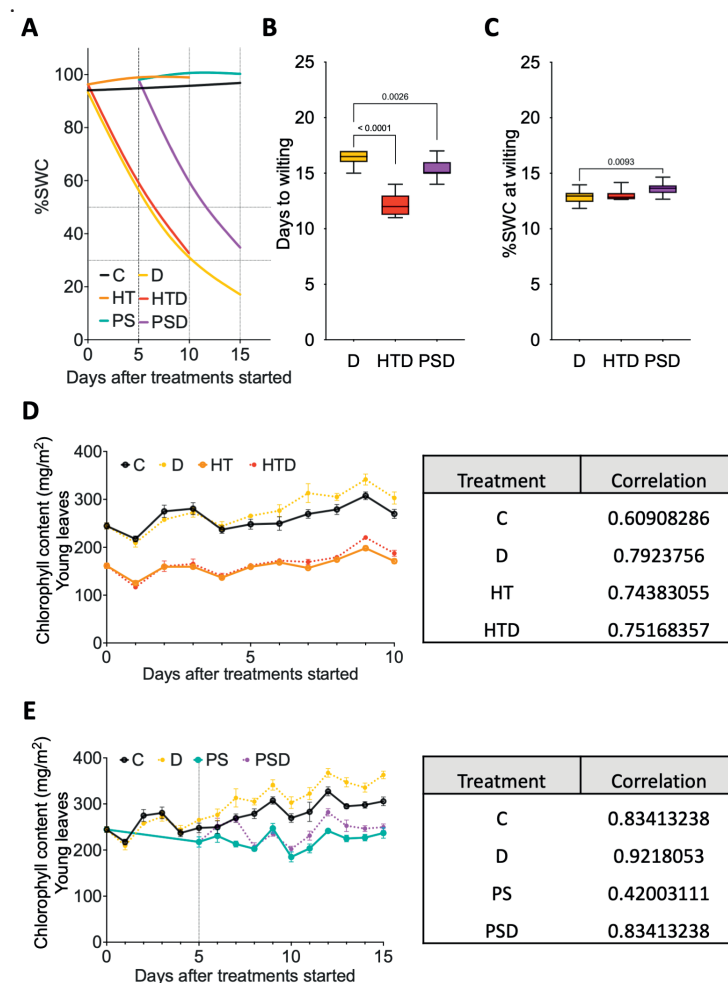


Figure S2.1:

Progressive decline in soil water content (%SWC) during combined high temperature and drought (**A**) and post submergence followed by drought (**B**) and the related single stress experiments and control. (**A**) $n=3-18$. (**B**) $n=8-34$. For color codes and abbreviations see legend figure 2.1.

**Figure S2.2:**

Chlorophyll content of young leaves in control (C) and drought (D) conditions, obtained by destructive biochemical assay (A) and by using a chlorophyll-meter (B). Harvests and measurements were conducted at 0, 5, 10, and 15 days after drought started. Error bars indicate means \pm SEM. $n=4-5$. For color codes and abbreviations see legend figure 2.1

**Figure S2.3: Validation of soil drying, point of wilting and chlorophyll measurements in the renovated LED-growth chambers. (A)**

Percentage of soil water content (%SWC) under different stress treatments in the renovated LED-growth chamber. $n=4-20$. (B, C) Number of days (B), and percentage of soil water content (C), at the moment that plants began to wilt, when subjected to single drought (D), high temperature + drought (HTD), or post-submergence + drought (PSD). Days were counted after water was withdrawn. Boxes indicate boundaries of the second and third quartiles of the data distribution. Black horizontal bars indicate median and whiskers Q1 and Q4 values within 1.5 times the interquartile range. Numbers indicate p values (unpaired t-test). (B) and (C) $n=10-12$. (D, E) Chlorophyll content of young leaves of plants subjected to combined (D) and sequential (E) stress and the relevant single stresses and controls. The tables indicate Pearson correlation coefficients of corresponding (averaged) chlorophyll content under different stress treatments between the 'old' fluorescent tube-lid growth chambers and the 'new' renovated LED-chambers. Error bars indicate means \pm SEM, $n=4-20$. The dashed vertical line indicates the moment plants were de-submerged. For color codes and abbreviations see legend figure 2.1.

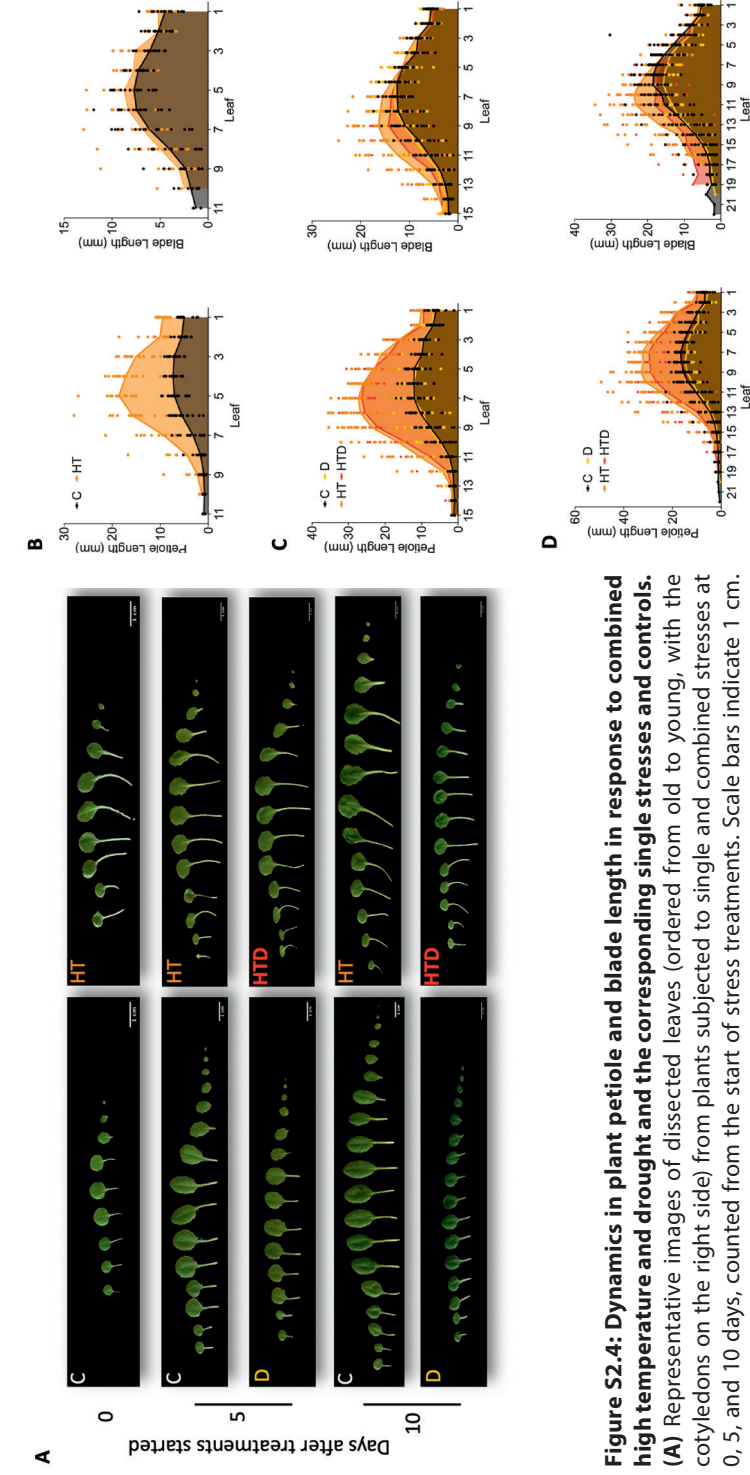


Figure S2.4: Dynamics in plant petiole and blade length in response to combined high temperature and drought and the corresponding single stresses and controls.

(A) Representative images of dissected leaves (ordered from old to young, with the cotyledons on the right side) from plants subjected to single and combined stresses at 0, 5, and 10 days, counted from the start of stress treatments. Scale bars indicate 1 cm. **(B, C, D)** Petiole (left) and blade (right) lengths of all leaves from plants subjected to high temperature combined with drought and related single stresses and control at 0 **(B)**, 5 **(C)** and 10 **(D)** days after the start of stress treatments. Dots and lines indicate individual plants and averaged data, respectively. $n = 15-21$. For color codes and abbreviations see legend figure 2.1.

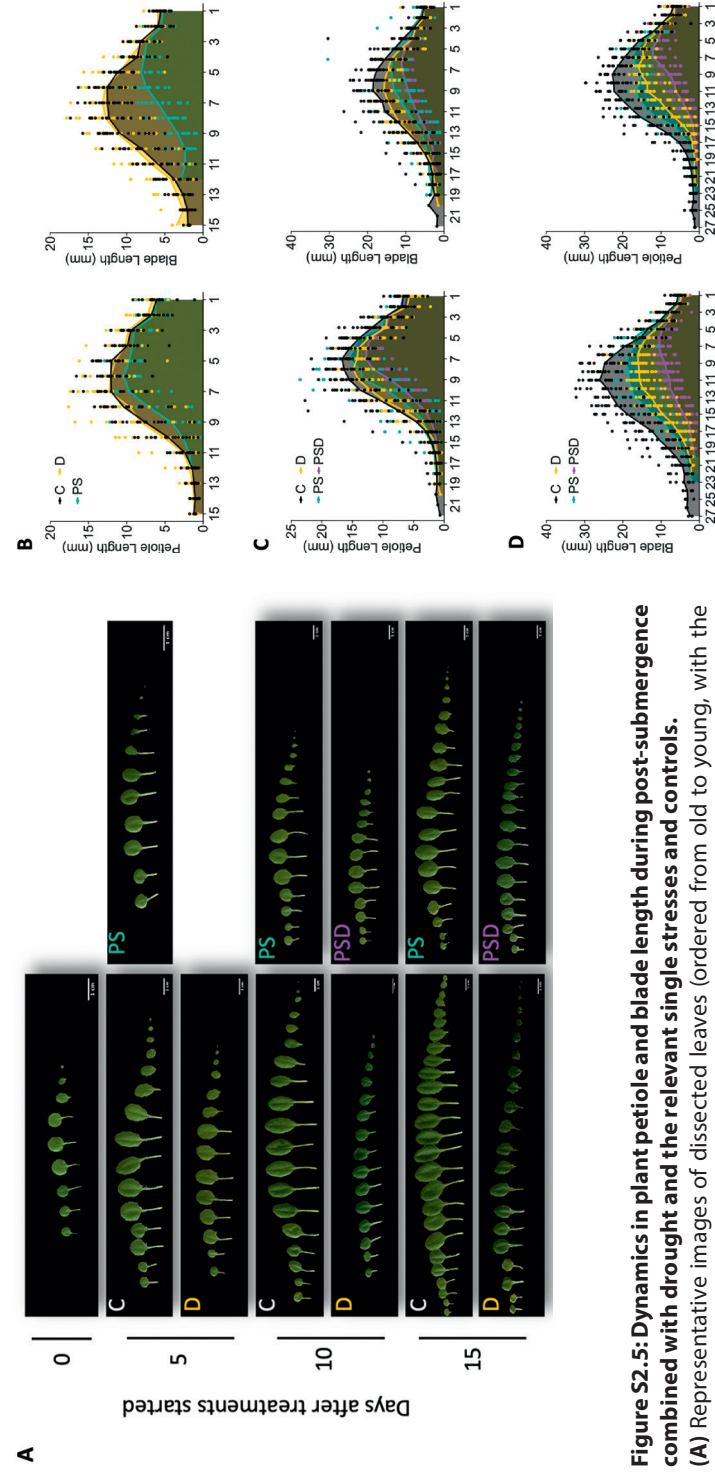


Figure S2.5: Dynamics in plant petiole and blade length during post-submergence combined with drought and the relevant single stresses and controls.

(A) Representative images of dissected leaves (ordered from old to young, with the cotyledons on the right side) from plants subjected to single and sequential stresses at 0, 5, 10 and 15 **(C and D)** days, counted from the start of the stress treatments. Scale bars indicate 1 cm. **(B, C, D)** Petiole (left) and blade (right) lengths of all leaves from plants subjected to post-submergence followed by drought and related single stresses and control at 0 **(B)**, 5 **(C)** and 10 **(D)** days after the start of de-submergence phase. Dots and lines indicate individual plants and averaged data, respectively. $n = 15-21$. For color codes and abbreviations see legend figure 2.1.

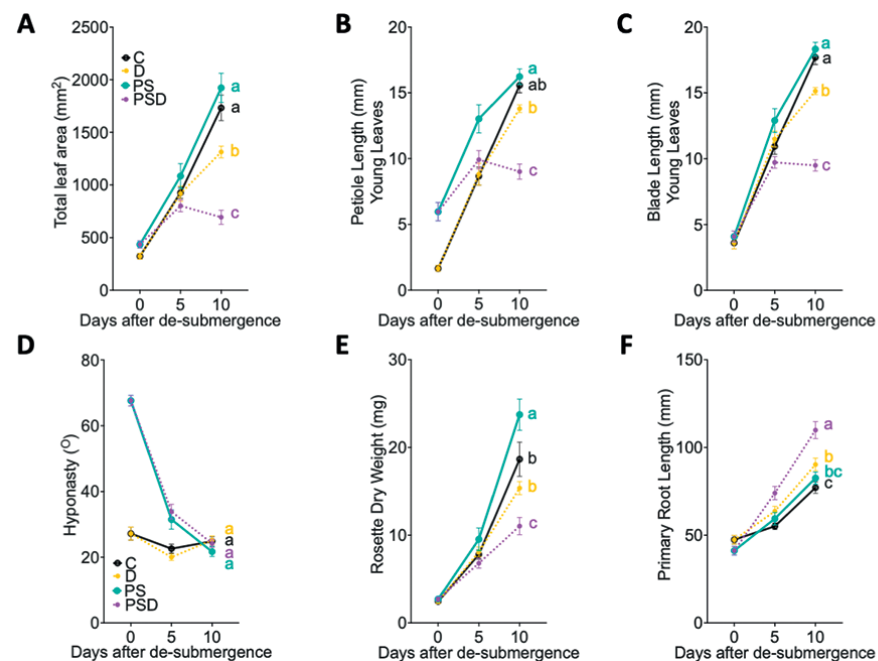


Figure S2.6: Phenotypic trait levels as an effect of drought in presence or absence of prior submergence.

(A) Total leaf area of the whole rosette. n= 15-20. (B, C) Averaged length of the petiole (B) and blade (C) of the young leaves. n= 15-21. (D) Averaged angles of the 2 most hyponastic leaves of individual plants, relative to the horizontal. n= 14-21. (E) Rosette dry weight. n= 15-18. (F) Primary root length n=14-21. Error bars indicate means \pm SEM. Letters denote significant differences between different treatments the stress treatments ($p < 0.05$, 2-way ANOVA with Tukey's Post-hoc test). For color codes and abbreviations see legend figure 2.1.

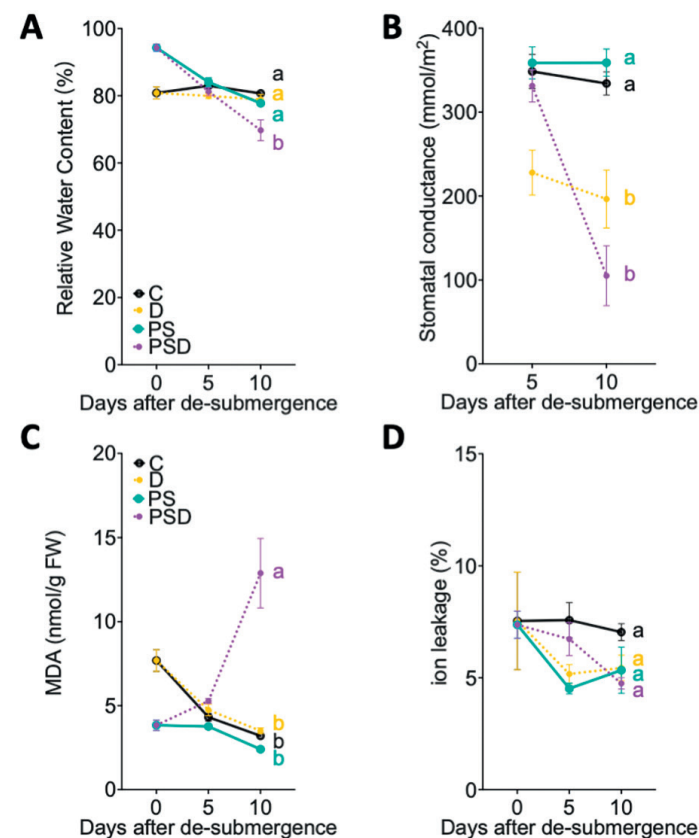


Figure S2.7: Physiological trait levels as effect of drought in present or absent of prior submergence.

(A) Rosette water content relative to the maximal water content that the leaves can hold (100%, turgid water - dry weight). n= 15-16. (B) Stomatal conductance of young leaves. n= 5-6. (C) Rosette Malondialdehyde (MDA) content. n= 5-10. (D) Rosette ion leakage relative to the maximal electrolyte conductivity (100%). n= 6. Error bars indicate means \pm SEM. Letters denote significant differences between different treatments at the last timepoint of the stress treatments ($p < 0.05$, 2-way ANOVA with Tukey's Post-hoc test). For color codes and abbreviations see legend figure 2.1.

Table S2.1: Statistical analysis of phenotypic trait level comparisons between applied stresses and control as indicated by p values of phenotypic and physiological effects in Figure S2.6 and S2.7.

Indicated are the p values of the multiple comparisons (2-way ANOVA) of measured factors carried out between droughted and non-droughted groups at 0, 5 and 10 days during de-submergence phase.

Factors	0		5		10	
	C vs D	PS vs PSD	C vs D	PS vs PSD	C vs D	PS vs PSD
Whole rosette area	>0.9999	>0.9999	0.9998	0.0726	0.0003	<0.0001
Hyponasty	>0.9999	>0.9999	0.6884	0.7707	0.9985	0.7469
Petiole length (young leaves)	>0.9999	>0.9999	0.9983	0.0054	0.1178	<0.0001
Blade length (young leaves)	>0.9999	>0.9999	0.8737	0.0003	0.0008	<0.0001
Dry weight	>0.9999	>0.9999	0.995	0.1958	0.0624	<0.0001
Primary root length	>0.9999	>0.9999	0.2089	0.0131	0.0074	<0.0001
Stomatal conductance	-	-	0.005	0.8768	0.0012	<0.0001
Relative water content	>0.9999	>0.9999	0.548	0.6126	0.8553	0.0027
MDA	>0.9999	>0.9999	0.9283	0.3739	0.9754	<0.0001
Ion leakage	>0.9999	>0.9999	0.3717	0.4488	0.703	0.9784



3

Characterization of the Arabidopsis transcriptome response to simultaneous and sequential abiotic stresses

Zhang Jiang, Ava Verhoeven, Rashmi Sasidharan*, Martijn van Zanten*

* Shared senior authors

Plant Stress Resilience, Utrecht University

Part of this work is published in:

Verhoeven, A., Kloth, K.J., Kupczok, A., Oymans, G.H., Damen, J., Rijnsburger, K., Jiang, Z., Deelen, C., Sasidharan, R., van Zanten, M. and van der Vlugt, R.A.A. (2023), Arabidopsis latent virus 1, a comovirus widely spread in Arabidopsis thaliana collections. New Phytol, 237: 1146-1153.

Abstract

Plants either in a natural or agricultural environment, often encounter stresses in combination. Yet studies on resilience mechanisms have focused mainly on plant responses to single environmental stresses. Investigating molecular mechanisms mediating relevant stress combinations is therefore essential. In chapter 2 we demonstrated that in comparison with the corresponding individual abiotic stresses, combinations of sublethal stresses that are simultaneously or sequentially imposed on plants can elicit distinct physiological responses in *Arabidopsis thaliana*. Here we used our established multi-stress experimental system to probe the molecular mechanisms underlying resilience to combinatorial abiotic stresses. For this, a comparative mRNA sequencing approach (RNA-seq) was used to characterize the transcriptome responses of young *Arabidopsis* leaves to two combinatorial sublethal stresses; i) combined high temperature and drought and ii) submergence (in the light) followed by drought, as well the corresponding individual stresses.

Unexpectedly, the analysis of RNA-seq data revealed the presence of a previously uncharacterized comovirus. Our analyses indicated that the existence of this virus (named *Arabidopsis* Latent Virus 1 (ArLV1)) does not cause significant effects on the *Arabidopsis* transcriptome or the phenotype under control or stress conditions. The current dataset was therefore deemed suitable for the original goal of characterizing molecular responses to multi-stresses. It provides a platform for delving for candidate genes and processes that putatively control the responses to individual, combined, and sequential sublethal stresses.

Our data revealed that for high temperature and drought, simultaneous stress exposure caused a more profound transcriptome reconfiguration than either stress alone, with high temperature dominating the response. In contrast, submergence still triggered a more significant reconfiguration of the transcriptome compared to drought alone. Although drought had a mild effect in both stress combinations, a unique and more significant transcriptome signature was detected when it was combined with high temperature simultaneously, or submergence sequentially. Our dataset permitted the identification of molecular processes and candidate regulatory genes (including transcription factors (TFs) and phytohormones that contribute to the timely acclimation of *Arabidopsis* to combined and sequential sublethal abiotic stresses. Overall, our data i) highlights the unique transcriptomic signatures imposed by combined and sequential sublethal stresses compared to the corresponding single stresses, which require the coordination of multiple molecular regulators and integrated signaling pathways and ii) identifies candidate regulators of multi-stress tolerance for further validation.

Introduction

The unpredictable effects of climate change on weather patterns is negatively impacting crop productivity (Shabbir et al., 2022; Kopecká et al., 2023) and threatening food security (Masson-Delmotte et al., 2021; Cushman et al., 2022; Kumar et al., 2022). The occurrence of abiotic stresses such as heat, drought and flooding have dramatically increased and there has been extensive research on underlying research mechanisms (Larkindale et al., 2005; Harb et al., 2010; Van Veen et al., 2016). However, the focus has been predominantly on single stresses, often involving abrupt transfer of plants into severe stress conditions. In natural or agricultural settings, these abiotic stresses seldom happen in isolation (Mittler, 2006b; Suzuki et al., 2014). It is now known that co-occurring stresses elicit greater and distinct effects on plant growth, development and physiology compared to the corresponding (isolated) stresses (Zandalinas et al., 2021a; Rivero et al., 2022).

Additionally, stress onset is often gradual and sublethal. When faced with suboptimal environments, plants need to sense and acclimate by for instance adapting their morphology and diverse physiological processes, such as developing differently shaped leaves or adjusting antioxidant levels when confronted a slight change in ambient temperature (Leipner et al., 1997; Praat et al., 2021). One example is thermomorphogenesis, which is characterized by an open rosette architecture (*i.e.*, hyponastic leaf movement, induced lengthening of petioles, primary root elongation and hypocotyl elongation), evoked by an increase in ambient temperature of just a few degrees (Quint et al., 2016; Casal & Balasubramanian, 2019). At the molecular level, thermomorphogenesis is governed by a complex signaling network involving diverse regulators such as phytohormones and transcription factors (Castroverde & Dina, 2021; De Smet et al., 2021). Of note, PHYTOCHROME INTERACTING FACTOR 4 (PIF4) is a central transcription factor regulating above-ground thermomorphogenesis in *Arabidopsis* (Van Zanten et al., 2013; Lee et al., 2021a), while the below-ground (root) response to high temperature is regulated by ELONGATED HYPOCOTYL 5 (HY5) (Gaillochet et al., 2020; Lee et al., 2021a). Some studies have also highlighted the emerging importance of epigenetic processes in thermomorphogenesis responses (Zioutopoulou et al., 2021). For example, the dynamic positioning and removal of histone H3 lysine K4 (H3K4) methylation, is proposed as a signaling hub in temperature signaling networks participating in coordinating diverse high-temperature responses (Perrella et al., 2022).

Like elevated ambient temperatures, sublethal water stresses, such as drought or prolonged submergence, can provoke a multitude of changes at the morphological, physiological and molecular levels in cereal crops (Toulotte et al., 2022). In rice (*Oryza*

sativa), constitutively expressing an ethylene responsive TF (ERF), SUBMERGENCE-1A (SUB1A), confers tolerance to more than one water stress including drought, submergence and dehydration stress upon de-submergence (Fukao et al., 2011). This multi-stress tolerance through *SUB1* depends on the coordination of various phytohormones such as abscisic acid (ABA), ethylene and gibberellic acid (GA) (Fukao et al., 2011; Sasidharan & Voeselek, 2015; Bin Rahman & Zhang, 2016).

Despite the existence of dedicated signal transduction pathways mediating acclimation to a certain stressor, a simultaneous or sequential combination of another stressor can drastically affect the regulatory network at the molecular level (Rasmussen et al., 2013; Coolen et al., 2016a; Anwar et al., 2021a). A well-studied abiotic stress combination is combined severe heat stress and drought stress, which elicits unique transcriptomic and metabolic effects on plants compared to either of the two stresses applied in isolation (Rizhsky et al., 2004). These unique effects correspond to the physiological alterations adopted by plants under the combined stress condition, such as the enhanced reduction of stomatal conductance and the accumulation of sucrose as a major osmoprotectant. Furthermore, it has also been demonstrated that increasing the number of co-occurring stressors, or applying the stress(es) at different developmental stages, can drastically alter the transcriptomic responses to a given combinatorial stress (Zandalinas et al., 2021b; Sinha et al., 2023a). This suggests that the impact of a stress combination is determined by multiple factors and underlines its complex nature (Zandalinas & Mittler, 2022).

One crucial factor influencing the molecular responses to combinatorial stresses, particularly during sequential stresses, is the order in which the two successive stresses occur. For example, transcriptome profiles of *Arabidopsis* subjected to six sequential double stress combinations between *Botrytis cinerea* infestation, *Pieris rapae* infestation and drought application, were shown to be more similar to that of the second stress, despite that the first-stress triggered transcriptome signature is always detectable in the sequential stress profile (Coolen et al., 2016b). While these studies have uncovered some of the molecular features involved in response to combinatorial stresses, the knowledge of central biological processes and molecules mediating long-term sublethal combined or sequential stresses is still lacking.

In Chapter 2, we characterized the effects of two combinatorial sublethal stresses; i) combined high temperature and drought and ii) submergence followed by drought, on a selection of *Arabidopsis* growth and development traits. We showed that the effects of combined or sequential stress on several phenotypes are different and in general additive compared to those of the corresponding individual stresses.

Additionally, combined and sequential stresses elicited unique physiological responses compared to the corresponding individual stresses, in a leaf age-dependent manner.

In this chapter, we investigated the effect of these same single and combinatorial sublethal stresses on plant transcriptome, with the aim of characterizing key underlying molecular processes and identifying candidate genes that can be functionally studied. By using an RNA-seq approach, we uncovered unique transcriptomic signatures imposed by combined or sequential stresses in comparison with isolated stresses. Furthermore, our data revealed that acclimation to combinatorial sublethal stresses in young leaves involves synchronous regulation of multiple generic processes such as plastid-nucleus communication (retrograde signaling), ABA signaling and photo-acclimation. We also identified several potential regulators of the observed stress acclimation processes for further functional validation (Chapter 4).

Results and Discussion

Transcriptomic responses elicited by combined and sequential sublethal stresses are time- and treatment- dependent

To characterize the transcriptomic changes triggered by sublethal abiotic stresses, we used a comparative RNA-seq approach on *Arabidopsis* Columbia-0 (Col-0) plants exposed to i) combined high temperature and drought (HTD) and ii) submergence in the light, followed by drought (PSD), and the relevant individual stresses (D, HT, PS) as well as the control (C). We observed that physiological responses to drought-associated treatments were leaf age- and timepoint-dependent (See; Chapter 2). We therefore sampled only young leaves (7th-10th leaves counted from the earliest emerged true leaves at LS10) under individual and combinatorial stresses at the pre-defined timepoints of 0 (moment of stress application), 5, and 10 days after stress treatment initiation (Figure 3.1). In total RNA-seq (Illumina) was performed on 58 samples, distributed among 15 different harvesting timepoints, resulting in a total of 3,628,334,664 detected reads (Figure S3.1, Table S3.2). Subsequently, the reads of each sample were mapped to the *Arabidopsis thaliana* reference transcriptome (TAIR). 72% of the mapped reads across individual samples aligned to the *Arabidopsis* transcriptome, ranging from a minimum of 5.4 million reads to a maximum of 61.8 million per sample (Figure S3.1).

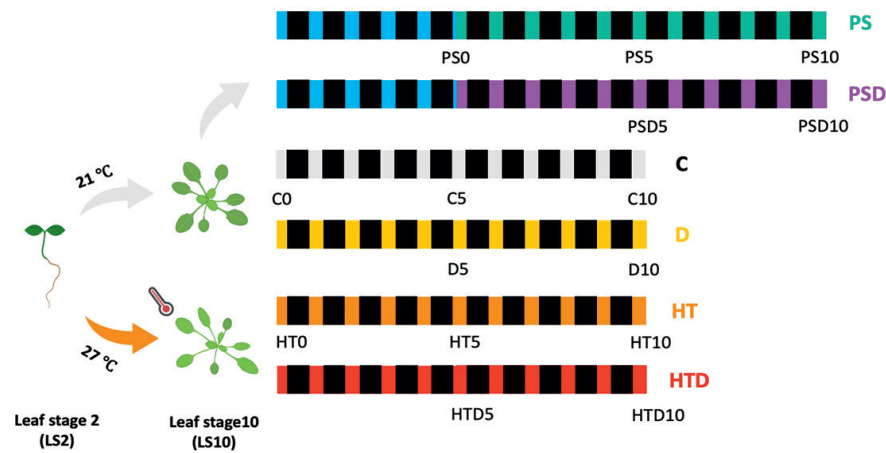


Figure 3.1: Experimental setup and sampling timepoints for transcriptomic profiling.

Arabidopsis Col-0 plants were pre-grown at 21°C or 27°C (day and night) until 10-leaf stage (LS10) and were subsequently exposed to individual or combinatorial stresses, respectively: C; control (black), D; drought (yellow), S; 5-day submergence in the light (blue), PS; (post-) submergence (green), PSD; (post-)submergence & drought (purple), HT; high temperature (orange), HTD; high temperature & drought (red). Sample harvesting was carried out at 0, 5 and 10 days after the treatments started, as indicated with the combination of treatment abbreviations and numbers. Color areas represent the 8-hour light period supplemented with multiple stress treatments, black areas represent the 16-hour darkness at night. All samples were harvested at the same time during the photoperiod, at ZT = 2 hours. Note that the color codes and abbreviations used to depict each of the treatments are also used in subsequent figures.

For approximately one third of sequenced samples, less than 50% of the reads mapped to the Arabidopsis transcriptome (Figure S3.1). This suggested the presence of a contaminant in the plant materials used for the sequencing. An initial BLASTN search for the unknown sequences identified Arabidopsis Latent Virus 1 (ArLV1), as a possible contaminant. To confirm the nature of the reads that were not mapping to the Arabidopsis genome, we extracted the unmapped reads from each sample and mapped these to the two different RNA segments of ArLV1 (RNA1 and RNA2; GenBank accessions MH899120.1 and MH899121.1, respectively). On average, only 1.77% of the reads per sample did not map to either Arabidopsis or ArLV1, which led us to conclude that ArLV1 was the only contaminant present in the samples. To assess if ArLV1 infections caused any visible symptoms on plants, we re-analyzed the rosette pictures of harvested plants for RNA-seq and compared the phenotypic effects (*i.e.*, total leaf area and leaf numbers of plants exposed to 5-day C after LS10 and scanned for any visual phenotypes) of plants that contained high viral load (average reads

mapping to ArLV1 = 81.6%), to those with an apparent low virus load (average = 4.18% of the reads mapping to ArLV1) in control (C) conditions. We did not observe any significant differences between highly infected and relatively healthy plants (Figure S3.2A-C), suggesting no significant impact of the viral infection on plant growth (hence the name; latent virus).

Viral infections can have substantial impact on the host transcriptome and affect the output of the -omics analyses, even in the absence of apparent phenotypic effects on the plant (Shates et al., 2019). To investigate whether the dataset(s) contaminated by ArLV1 caused any significant effects on Arabidopsis transcriptome, we compared the samples mapping above and below 50% to the Arabidopsis transcriptome on day 5 of the control (C) treatment (Figure S3.2D). We did not detect any differentially expressed genes between both fractions (linear model with a *Benjamini Hochberg* correction, FDR < 0.05), implying that ArLV1 does not evoke significant effects on the plant transcriptome.

Comparing the transcriptome from the various sampled timepoints during multiple stress treatments by PCA analysis revealed significant changes in time (PCO1, explaining 29,88% of the observed variation), in addition to stress-associated effects (separated over PCO1 and PCO2) (Figure 3.2A). As expected, individual biological replicates of the same timepoint and stress treatment clustered together (Figures 3.2A and S3.3). Notably, transcriptomes of drought-exposed plants (D) were not so different from controls (C) as evidenced by the close clustering of these samples across different timepoints. Superimposing the fraction of reads mapping to the Arabidopsis genome per sample on the PCA (Figure 3.2B) revealed no clear pattern, showing that (the level of) ArLV1 contamination did not significantly affect the stress-mediated transcriptomic changes in our dataset. We therefore decided to continue processing our data using all the samples except two samples (day 5 control) of which the mapping percentages to Arabidopsis transcriptome were below 10%.

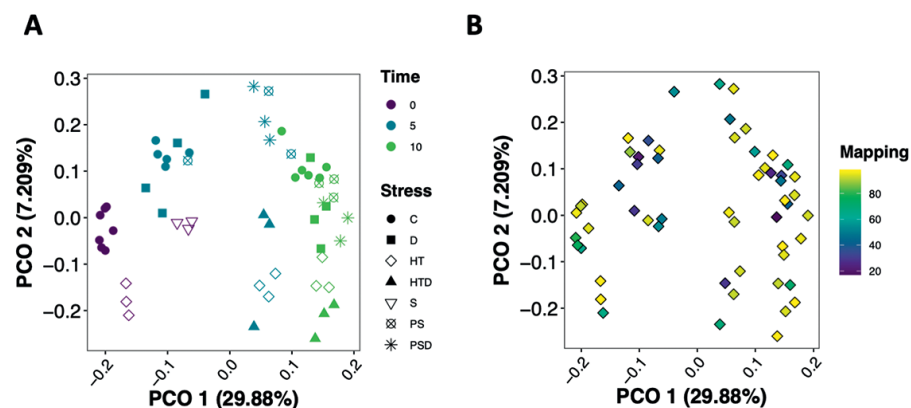


Figure 3.2: Principal component analysis (PCA) of transcriptomes of young leaves exposed to different stress conditions.

(A, B) PCA analysis visualizing distributions of samples categorized by time (0 = purple, 5 days = blue and 10 days = green) and the different stresses, indicated by symbols (A) and the fraction of reads per sample mapping to the Arabidopsis transcriptome (B). Fraction of reads mapping to the Arabidopsis reference transcriptome is presented by a color scale. For abbreviations see legend figure 3.1.

Combined high temperature and drought elicit a major reconfiguration of the transcriptome with a dominant high-temperature effect

To estimate the effects of D, HT and HTD on the transcriptome, we identified the number of differentially expressed genes (DEGs) ($|\text{Log}_2\text{FC}| > 0$, $\text{FDR} < 0.05$) by comparing the fold changes of different samples (D, HT and PSD) to the corresponding controls (C), at the same harvesting timepoint (Figure 3.3A). At timepoint 0 days (LS10), we identified 548 DEGs, including 321 upregulated and 227 downregulated genes in the high temperature (HT) samples. When the HT treatment was prolonged, the number of DEGs increased after 5 days but decreased after 10 days (Figure 3.3A), suggesting a potential acclimation strategy employed by the long-term exposure to high temperature (Van Zanten et al., 2013).

The drought treatment (D) did not elicit significant transcriptomic changes. We detected only 3 DEGs, *GUARD-CELL-ENRICHED GDSL LIPASE 3 (GGL3)*, *PHOSPHOFRUCTOKINASE 1 (PFK1)* and *AT5G16990* (not functionally annotated), during the entire drought treatment period (day 5 and 10 after subjection to D conditions). This aligns with the relative mild drought effects on, for example, rosette biomass accumulation and leaf lengthening especially during the early stage (5 day) of drought (D) application (See; Chapter 2, Figures 2.5 and 2.7). Some studies have shown that severe drought exposure can have a major impact on the Arabidopsis transcriptome (Bouzid et al.,

2019; Chen et al., 2021a). Our experiments, however, imposed mild progressive drought, which could explain why the effects on the plant transcriptome are not as profound as observed under severe drought (Clauw et al., 2015). Plants in our treatment did experience drought as evidenced typical physiological responses (Yasir et al., 2019; Hura et al., 2022), which were measured following the same timepoints as the RNA-seq experiments (See; Chapter 2 Figures 2.5-2.8), such as the elongated primary root, the reduced (young leaf) stomatal conductance along with decreased rosette water content during D compared to C.

Indeed, the relative mild transcriptome changes under progressive drought are consistent with a earlier study in which only 41 DEGs were identified after Arabidopsis plants were subjected to a 5-day progressive drought treatment, despite drought causing a significant inhibition of plant growth (Prasch & Sonnewald, 2013). Furthermore, it is possible that the young leaves that were sampled in our work are less sensitive to environmental stresses than older leaves or roots, as plants might evoke protective mechanisms to secure developing tissues from adversities (Verelst et al., 2013).

Interestingly, when high temperature and drought treatments were combined (HTD), the effect of drought is more apparent. Many more DEGs (1680 in total after 5 + 10 days of HTD) were observed in HTD than under either individually applied stress (HT or D) (Figure 3.3A). This suggests that the combined stress has a greater impact on plant transcriptome than the corresponding individual stresses in isolation. This also aligns with previous study on soybean (*Glycine max*) responses to combined heat and water defect (Sinha et al., 2023a), in which a more pronounced transcriptome reconfiguration was observed during the exposure to the combined stress compared to individual stresses. By comparing the identities of DEGs (D, HT and HTD at 5 and 10 days after the treatments started), it was shown that HTD resulted in many unique DEGs (955) that were not affected by D or HT applied in isolation (Figure 3.3B). This implies that combined stress evokes a unique response relative to the single stresses. The conclusion also corroborates other work showing that combinatorial stresses usually impose a distinct transcriptomic signature, when compared to the corresponding individual stresses (Rasmussen et al., 2013; Shaar-Moshe et al., 2017; Balfagón et al., 2019b). Furthermore, HT and HTD appear to share a substantial number (469) of overlapping DEGs, suggesting that HT has a more dominant effect on plant transcriptome than D in the responses to combined stress (HTD) (Figure 3.3B). This is also in accordance with our previous observations that HT overrides D in affecting plant growth and leaf lengthening under HTD (See; Chapter 2 Figure 2.5). Moreover, only 2 DEGs were found to be commonly regulated by D, HT and HTD (Figure 3.3B);

PFK1 and *AT5G16990*. *PFK1* is important for sugar homeostasis in leaf metabolism and in source-sink relationships in Arabidopsis (Perby et al., 2022), while *AT5G16990* participates in the responses to oxidative stresses (Mano et al., 2005). Both of the two DEGs were upregulated after 5-day D, HT and HTD treatments, suggesting that these triple-stress responsive genes might be involved in early responses to individual (D and HT) and combined stresses (HTD) in young leaves.

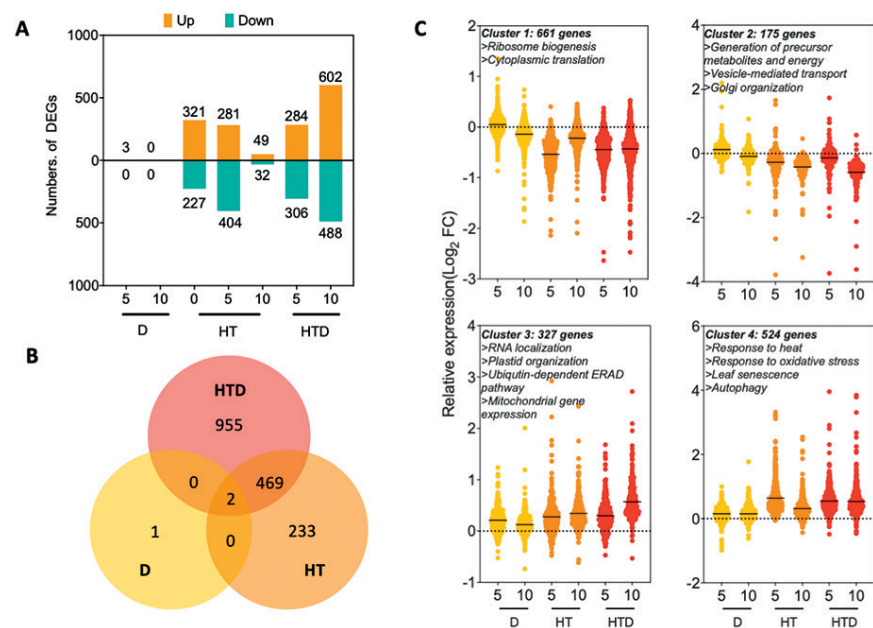


Figure 3.3: Effect of combined high temperature and drought (HTD) stress and the corresponding single stresses (D, HT) on the Arabidopsis transcriptome.

(A) The number of up- (orange) or down- (green) regulated DEGs ($|\text{Log}_2\text{FC}| > 0$, $p < 0.05$) at day 0 (the pre-growth effect of HT before the drought treatment started), 5, and 10 days after the treatments (D) started (note HT was prolonged), compared to control (C) conditions. (B) Venn diagram showing the number of DEGs commonly or differently detected in the combined (HTD) and single (D, HT) stresses. (C) *k-means* clustering presenting expression patterns of identified DEGs (Table S3.9) at timepoints 5 and 10 days during combined and individual stress treatments. Violin plots indicate the distributions of relative expression (Log_2FC) of identified DEGs. Mean values of each violin plot are indicated by a solid black line. Dashed horizontal lines indicate $\text{Log}_2\text{FC} = 0$. Key enriched biological processes identified by Gene Ontology analysis are listed above the clusters. For color coding and abbreviations see figure 3.1 legend.

We employed a *k-means* clustering approach to identify gene clusters with similar expression patterns across different timepoints and treatments (Figure 3.3C). We used all the 1687 detected DEGs at day 5 and 10, across individual and combined stress

treatments. Gene Ontology (GO) annotation was used to identify the most significant (adjusted P value < 0.01) biological processes in each cluster (Figure 3.3C and Table S3.3). The 1687 DEGs clustered into 4 groups: Cluster 1 and Cluster 2 consisted of DEGs that were downregulated under HT as well as in HTD conditions but were almost unchanged under D. Cluster 1 was the largest cluster, containing 661 DEGs. This cluster was dominated by genes associated with ribosome activities and translation (*i.e.*, GO:0042254, GO:0042273, GO:0002181, GO:0042255 and GO:0042274). Cluster 2 included 175 DEGs, with multiple biological processes affecting such as generation of precursor metabolites and energy (GO:0006091), vesicle-mediated transport (GO:0016192) and Golgi organization (GO:0007030). These GO terms imply that HTD, in general, affects ribosome and protein processing, which is highly relevant to plant growth and development under stress conditions (Ohbayashi & Sugiyama, 2018).

DEGs that were upregulated in HT and HTD were in Cluster 3 (327 DEGs) and Cluster 4 (524 DEGs) (Figure 3.3C and Table S3.3). Cluster 3 was dominated by DEGs associated with RNA mobility and processing (*i.e.*, GO:0006403, GO:0000375, GO:0000373 and GO0034660), which is in line with previous findings that RNA processing, particularly alternative RNA splicing (GO:0000375 and GO:0000373), enables plant acclimation to environmental stresses (Calixto et al., 2018; Nardeli et al., 2023). Furthermore, several organelle-associated GO terms, such as plastid organization (GO:00096575), ubiquitin-dependent endoplasmic-reticulum-associated protein degradation (ERAD) pathway (GO:0030433), and terms related to mitochondrial activities (GO:0000959 and GO:0140053), were highly enriched in this cluster. The mitochondrial respiratory electron transport chain (mETC) functions to form ATP through oxidative phosphorylation and eventually integrates into metabolic reactions for energy provision via the connection with tricarboxylic acid (TCA) cycle. mECT is also responsible for the production of antioxidants to benefit plants stress resilience (Welchen et al., 2021). Recent studies have highlighted the links between mitochondria and hormonal responses (Berkowitz et al., 2016; Bittner et al., 2022). For example, the accumulation of mitochondrial reactive oxygen species (ROS) influences ABA-dependent stomatal closure (Postiglione & Muday, 2023). The indication that mitochondrial activities are affected in the HTD treatment, thus could explain the significantly reduced stomatal conductance under HTD, compared to controls (See; Chapter 2 Figure 2.6B).

The DEGs in cluster 4 were linked with stress responsiveness, such as response to heat (GO:0009480), response to oxidative stress (GO:0006979), leaf senescence (GO:0010150) and response to starvation (GO:0042594). The heat response GO term in the HTD-upregulated cluster corresponds with the predominant effect of high temperature, relative to drought. This is in accordance with previous studies where temperature

stress (usually severe heat stress) was combined with another stressor such as drought, salt, or high light. Typically, in these situations the temperature cue, more than the other stressor, defines the transcriptomic signature when the two stressors occur simultaneously (Balfagón et al., 2019b; Sewelam et al., 2020). It should be noted, however, that heat stress elicits different responses at the molecular level than high ambient temperature, as used here (Li et al., 2018a; Fonseca De Lima et al., 2021; Praat et al., 2021). As an example, heat shock proteins (HSPs) and heat shock factors (HSFs) are both essential players mediating heat stress responses (Scharf et al., 2012; Tian et al., 2021). These factors participate in regulating acclimation to combined heat and drought stress (Sewelam et al., 2020; Sinha et al., 2022, 2023a). However, in our RNA-seq dataset, HSFs and HSPs were not highly overrepresented among the DEGs in the HTD-upregulated clusters, with only two HSFs (HEAT SHOCK TRANSCRIPTION FACTOR B2B (HSFB2B) and 4 (HSF4)) and four HSPs (DNA J PROTEIN A69 (DJC69), HEAT SHOCK PROTEIN 70-6 (HSP70-6) and 70 (HSP70), AT5G05750) present in the dataset (of 24 HSPs and 156 HSPs annotated in Arabidopsis). Furthermore, the upregulation of genes associated with oxidative stress responses under HTD suggests excessive ROS production (Mittler, 2017; Mittler et al., 2022), even though HT and HTD can both promote ROS production, the triggered ROS signatures can differ between the individual and combined stresses (Choudhury et al., 2017).

Interestingly, genes associated with chloroplast organization (GO:0009657) were not only significantly enriched in the HTD-upregulated gene clusters (cluster 3), but also in the dataset obtained by applying HT in isolation (timepoint 0 days, before D started) (Figure 3.3C and Table S3.4). This hints at a role for chloroplasts in mediating responses to both HT and HTD. Although chloroplasts are believed to be involved in the perception of - and acclimation to - temperature stresses such as heat or chilling stresses (Gan et al., 2019; Hu et al., 2020), little is known about their function in response to mildly elevated temperature as used (HT) in our study. Chloroplasts communicate with the nucleus at the interorganelle level through retrograde signaling (RS). This enables the modulation of nuclear gene expression, based on the chloroplast status (Veciana et al., 2022a). One of the best studied mediators of plastid-to-nuclear retrograde signaling is GENOMES UNCOUPLED 1 (GUN1), which coordinates signal relay from chloroplast to regulate the expression of photosynthesis-associated nuclear genes (*PhANGs*) during the de-etiolation process in seedlings (Hernández-Verdeja et al., 2022). PHYTOCHROME INTERACTING FACTORS (PIFs) act antagonistically with GUN1-mediated retrograde signaling pathways to control *PhANGs* (Martín et al., 2016). Because PIFs play a central role in thermomorphogenic responses (Lee et al., 2021a; Burko et al., 2022; Delker et al., 2022), it is possible that GUN1-mediated retrograde

signaling pathways might also be involved in plant responses to high ambient temperature.

Prior submergence alters the transcriptome response to drought

To characterize the effect of the sequential stress of submergence followed by drought on the plant transcriptome, several comparisons (of Log_2FC in gene expression) were made; i) To determine the effects of submergence (S), plants subjected to 5-day submergence were compared to those of pre-submergence at LS10. ii) To determine the effects of submergence followed by well-watered (PS) or drought (PSD), plants subjected to 5- or 10- day PS or PSD were compared to those grown at C for 5 or 10 days (after reaching the LS10 stage), respectively. This approach ensures that comparisons are carried out between samples at equivalent developmental stages. iii) Drought effects were assessed by comparing plants harvested at 5 or 10 days after D started to those grown under C at the same timepoints.

DEGs were calculated based on the same criteria as used for the HT/HTD datasets described above ($|\text{Log}_2\text{FC}| > 0$, $\text{FDR} < 0.05$). In total, 5-day submergence resulted in 3390 DEGs (2469 upregulated and 921 downregulated DEGs) (Figure 3.4A), reflecting a considerable reconfiguration of the transcriptome by submergence. Plants confronted with submergence adopt a series of metabolic and cellular adjustments, mediated by multiple phytohormones (ethylene entrapment, gibberellin acid (GA) and ABA), to overcome the adversities imposed by flooding. This includes either a conservative use of carbohydrate and ATP reserves to enable quick recovery following de-submergence or investment in rapid shoot elongation to escape from floods (Bailey-Serres & Voesenek, 2008; Voesenek & Bailey-Serres, 2015). Oxygen sensing and signaling via the Group-VII Ethylene Response Factor (ERF7), in response to flooding-induced hypoxia (Gibbs et al., 2011; Licausi et al., 2011; Giuntoli & Perata, 2018; Hartman et al., 2019), triggers downstream acclimation responses and promotes hypoxia survival.

Despite the pronounced effects on plant transcriptome caused by submergence mentioned above, following de-submergence (PS) only a limited number of DEGs were detected at day 5 (2 DEGs) and 10 (51 DEGs) (Figure 3.4A), suggesting the comparability of plant transcriptome under PS and C. This correlates with our previous finding that plants that are well-irrigated in the post-submergence phase displayed comparable leaf development rate compared to those in control conditions (C) (See; Chapter 2, Figures 2.7 and S2.6). To better elucidate the restored transcriptomic effects by PS compared to S, we examined the expression patterns (indicated as transcripts per million (TPM)) of 49 core-hypoxia responsive genes under PSD related stress conditions (S, PS, PSD and D) and the control (C) in our RNA-seq dataset (Figure S3.4). These

genes have been previously shown to be induced in their expressions by hypoxic treatments (*i.e.*, submergence) regardless of plant organs and cell types (Mustroph et al., 2009). Here we observed that the expression of several hypoxia genes was markedly increased during submergence, but their expression was tempered during all de-submergence treatments and timepoints (PS and PSD at day 5 and 10), regardless of the presence of drought, which hints to alleviation of hypoxia effects during de-submergence. However, even though both of D and PS applied in isolation did not impose drastic transcriptomic changes, when the two stressors were combined during the de-submergence phase (PSD), more DEGs were observed (897 DEGs in total at 5 and 10 days after PSD) (Figure 3.4A). Like HTD, PSD also led to a unique transcriptomic signature, as the majority of DEGs identified after PSD treatment were not affected by PS nor D (Figure 3.4B). This unique reconfiguration of the transcriptome under sequential and combined stress is consistent with the concept that the prior exposure to one stress can have profound consequences on the outcome of the second stress (Rejeb et al., 2014), which is referred to as cross-acclimation. Despite the transcriptome differences between plants subjected to PSD and PS, these two stressors elicited 33 shared DEGs. These DEGs are shown to be functionally associated with Arabidopsis ribosome in the KEGG analysis with the classes of genetic information processing and translation (Figure S3.5) and could be general stress-responsive factors. According to a previous study (Coolen et al., 2016a), in which Arabidopsis plants were exposed to six sequential double stresses, the transcriptome profiles of plants are most similar to that of the second stressor. This is despite the fact that the first stressor also evokes a marked transcriptome signature when applied in isolation and could trigger adaptative responses. In our study, it is difficult to draw a similar conclusion, as a complete elucidation of the commonalities between PSD and individual D application is hampered by the limited number of DEGs found under D.

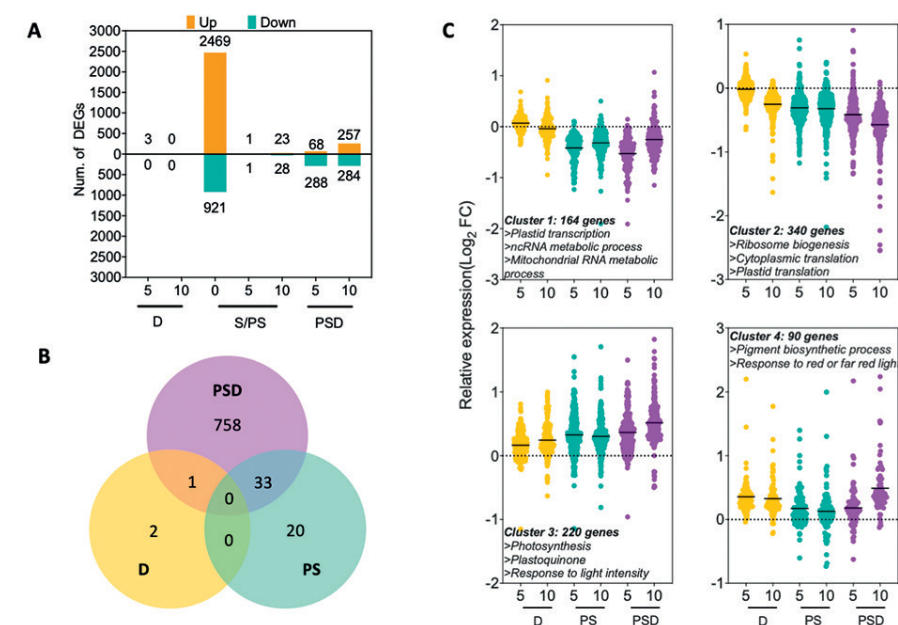


Figure 3.4: Effect of submergence followed by drought (PSD), or well-watered conditions (PS), and drought (D) alone on the Arabidopsis transcriptome.

(A) The number of up- (orange) or down- (green) regulated DEGs ($|\text{Log}_2\text{FC}| > 0$, $p < 0.05$) at day 0 (the start of post-submergence period), 5 and 10 days after the treatments started, compared to control (C) conditions. (B) Venn diagram showing the number of DEGs commonly or differentially expressed in the sequential (PSD) and single (D, PSD) stresses. (C) *k-means* clustering presenting expression patterns of identified DEGs (Table S3.9) at timepoints 5 and 10 days during combined and individual stress treatments. Violin plots indicate the distributions of relative expression (Log_2FC) of identified DEGs, mean values of each violin plot are indicated by a solid black line. Dashed horizontal lines indicate $\text{Log}_2\text{FC} = 0$. Key enriched biological processes (BPs) by Gene Ontology analysis are listed along with clusters. For color coding and abbreviations see figure 3.1 legend.

To characterize the expression patterns of identified DEGs during exposure to D, PS and PSD, we performed *k-means* clustering on all 814 DEGs from day 5 and day 10 across all the three stress treatments. This led to the identification of four clusters, of which two contain PS- and PSD-downregulated genes (Cluster 1 and Cluster 2) and two contain upregulated genes in these conditions (Cluster 3 and Cluster 4) (Figure 3.4C, Table S3.5). GO term analysis revealed that Cluster 1 and 2 were dominated by genes associated with nucleic acid (GO:0034660, GO:0006281, GO:0006334), ribosome (GO:0042254, GO:0042255, GO:0042274) and translation-related processes (GO:0002181, GO:0006417, GO:0032544, GO:1901259). This enrichment likely implies an considerable effect of PS and PSD on plant ribosome and translation, which are

important players for plant stress resilience (Son & Park, 2023). Additionally, several of the downregulated GO terms in clusters 1 and 2 are associated with plastid functions (GO:0042793, GO:0015995, GO:0032544, GO:0009657, GO:0045036, GO:1901259), indicating impeded chloroplast activities during post-submergence (PS and PSD).

In Cluster 3 photosynthesis-related GO terms were significantly enriched (GO:0015979, GO:0010258, GO:0006778) (Figure 3.4C, Table S3.5). Of these three upregulated GO term categories, at least NADH dehydrogenase complex (plastoquinone) assembly (GO:0010258) is relevant to abiotic stress responses (Pshybytko et al., 2008; Dopp et al., 2021). Plastoquinone (PQ) functions as an electron transporter in the electron transport chain of oxygenic photosynthesis (Swiezewska, 2004), acting as antioxidants to scavenge free radicals and participating in the biosynthesis of phytohormones such as GA and ABA (Liu & Lu, 2016). Additionally, PQ is also responsible for regulating cell signal transduction in plant photo-acclimation processes (Yang et al., 2001). Furthermore, under the GO term of porphyrin-containing compound metabolic process (GO:0006778), *GENOMES UNCOUPLED 4 (GUN4)* is interesting for further investigation in the context of post-submergence recovery, as it is an essential mediator of retrograde signaling between chloroplast and nucleus (Tarahi Tabrizi et al., 2016; Li et al., 2023). Collectively, these identified GO terms might point to a putative PSD-acclimation strategy that involves the coordination of signal transduction pathways associated with PQ-mediated photo-acclimation and chloroplast-to-nuclear retrograde signaling.

In Cluster 4, only two GO categories (GO:0046148, GO:0009639) were enriched (Figure 3.4C, Table S3.5). Of note, one of them, *CYTOKININ-RESPONSIVE GATA FACTOR 1 (CGA1/GNL)* is commonly shared by these two GO groups. Interestingly, this gene was originally identified as controlling chloroplast development (Jeong & Shih, 2003; Reyes et al., 2004; Hudson et al., 2011), but has recently been associated with post-(dark)submergence recovery (Yeung, 2018) and stomatal differentiation (Klermund et al., 2016). Given the high expression level of *CGA1* compared to the rest of PSD-upregulated genes and its prominent role in stress acclimation (Table S3.7), further investigation of the physiological function of *CGA1* in PSD tolerance is warranted.

Identification of putative regulatory factors mediating acclimation to combined and sequential stresses

Plant TFs play essential roles in regulating plant development and stress responses (Jin et al., 2015). In our RNA-seq dataset, the differentially regulated TFs, especially those being upregulated under either HTD or PSD, are of particular interest to investigate as the transcriptional upregulation of these (positive) regulators hints at their involvement

in combinatorial stress acclimation. Thus, to identify these positively regulated TFs under combined or sequential stresses, we searched for differentially expressed TFs enriched in HTD- and PSD- upregulated clusters (Cluster 3 and 4 in both HTD and PSD datasets). A DEG was considered a TF if it was annotated as member of one of 50 Arabidopsis TF families in the AtTFDB database (<https://agris-knowledgebase.org/AtTFDB>) (Figure 3.5A-B).

In total, 48 different TFs from 23 TF families were identified as being upregulated by HTD (35) or PSD (21), with 8 TFs overlapping between the two groups (Figure S3.6). Notably, 5 TFs including ARABIDOPSIS TOXICOS EN LEVADURA 66 (ATL66), DREB AND EAR MOTIF PROTEIN 3 (DEAR3), HSF2B, HSF4 and WHIRLY2 displayed relatively strong differential expression ($\text{Log}_2\text{FC} > 1$) in HTD either at day 5 or at day 10 (Figure 3.5A and Table S3.6). HSF2B and HSF4 are known to mediate responsiveness to heat (Baniwal et al., 2004; Scharf et al., 2012; Lin et al., 2018) or heat-predominated combinatorial stresses (Balfagón et al., 2019a; Sewelam et al., 2020). WHIRLY2 can be localized to mitochondria, plastids and the nucleus, and is able to regulate leaf senescence and carbon allocation from maternal tissues to filial tissues, as a potential retrograde signaling modulator (Huang et al., 2020). The significant upregulation of WHIRLY2 thus may point to a role for a retrograde signaling-mediated carbon allocation strategy in responses to HTD stress. Specific studies elucidating a role for DEAR3 and ATL66 in stress responses are still lacking. However, TFs from the same transcription factor family (ERF/AP2 and ATL) hint that these TFs might also be corresponding to abiotic stress acclimation (Guzmán, 2012; Sazegari et al., 2015).

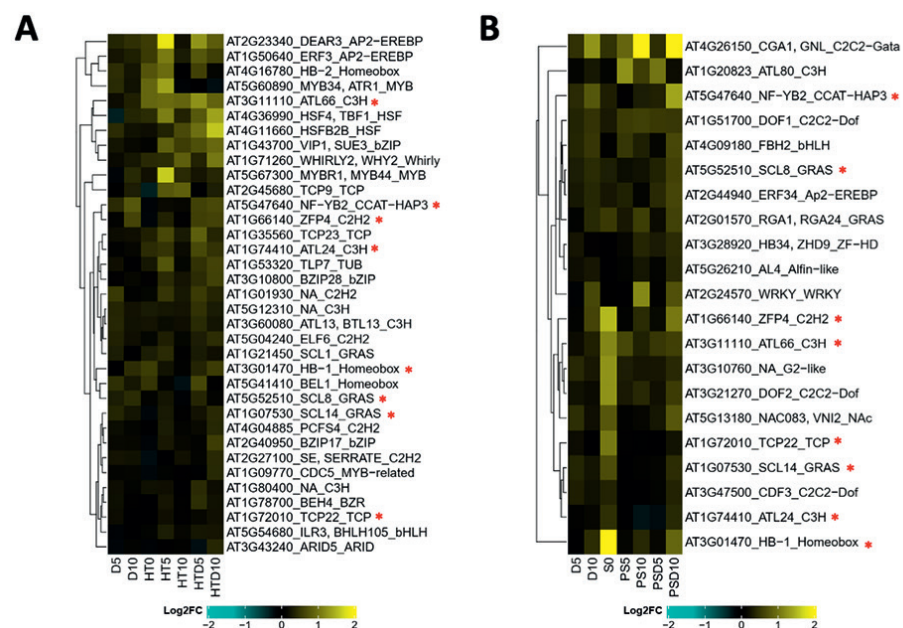


Figure 3.5: Transcription factors (TFs) identified among the upregulated DEGs in the PSD and HTD datasets.

(A, B) Heatmaps showing relative expression of TFs identified in the upregulated clusters of combined (HTD) along with the individual applied stresses HT and D (A) and sequential (PSD) along with individually applied stresses D and PS (B). For each identified TF, the AGI gene locus ID, the commonly used abbreviation (if available) and TF family the factor belonged to, are listed. Color scales indicate Log_2FC values (relative to control (C) conditions). Asterisks indicate overlapping TFs between (A) and (B). For abbreviations of stress treatments see figure 3.1 legend.

In addition to the profoundly upregulated TFs ($\text{Log}_2\text{FC} > 0$), BASIC LEUCINE ZIPPER 28 (bZIP28) and 17 (bZIP17) were also induced during HTD (Table S3.6). These two TFs have previously been characterized as key players in modulating endoplasmic reticulum-mediated unfolded protein responses (ER-mediated UPR) and were shown to synergistically regulate cell elongation to promote root lengthening during plant vegetative growth (Kim et al., 2018). This may point to involvement of ER-stress responses during HTD acclimation. Of note, only 7 out of all 35 HTD-upregulated TFs displayed similar upregulation trends under individual HT (thus in the absence of drought) (Table S3.6), underlining the unique response that is evoked by combined stress application, relative to the application of single stresses.

Apart from the above-highlighted TF CAG1, ARABIDOPSIS TOXICOS EN LEVADURA 80 (ATL80), ZINC FINGER PROTEIN 4 (ZFP4) and NUCLEAR FACTOR Y, SUBUNIT B2 (NF-YB2/HAP3b) were also upregulated in response to PSD ($\text{Log}_2\text{FC} > 1$) (Figure 3.5B, Table S3.7). NF-YB2 regulates several biological processes including flowering-time (Zhao et al., 2017) and ABA-mediated seed germination (Kumimoto et al., 2013). Previous research has documented that the overexpression of NF-YB2 confers Arabidopsis with dehydration tolerance as NF-YB2 is able to bind to the promoters of dehydration-inducible genes (Sato et al., 2019). Moreover, even though the molecular functions of ATL80 or ZFP4 have not been thoroughly characterized at this moment, some studies made the putative connections between these TFs and abiotic stress adaptations (Joseph et al., 2014; Suh & Kim, 2015).

Of note, only 3 out of a total of 21 PSD-upregulated TFs identified, were significantly induced under 5 or 10 days of PS (Table S3.7). Thus, 18 TFs were uniquely induced by the sequential stress, highlighting that PSD-elicited a transcriptomic signature that differs from single stress application. However, 12 of them were significantly upregulated by 5-day submergence (S) (Table S3.7), suggesting that the effect of the prior submergence event, part of the PSD treatment, persisted to affect the sequential-stress transcriptome signature. This corresponds with the previous notions from other studies (Coolen et al., 2016a; Davila Olivas et al., 2016).

In addition to the identification of TFs, we constructed gene regulatory networks (GRNs) to identify putative upstream regulators and co-expressors associated with the upregulation of DEGs under HTD and PSD (Figure 3.6). Here, DEGs from the upregulated HTD or PSD clusters (Clusters 3 and 4) were inputted respectively and the GRNs were built using TF2network tool (Kulkarni et al., 2018). This tool integrates the information of both of protein-DNA interactions and co-expression that are experimentally confirmed or computationally predicted in Arabidopsis.

In total, the obtained HTD network consisted of 12913 interactions between 847 regulators (nodes), while only 4169 interactions between 340 regulators were formed in PSD network (Figure 3.6). To identify putative master regulators in the GRNs, we selected the top 11 nodes with the highest number of connections with the others within the same GRN. Of the selected regulators, four genes were shared by both the HTD- and PSD- networks; *G-BOX BINDING FACTOR 3 (GBF3)*, *ABSCISIC ACID RESPONSIVE ELEMENT-BINDING FACTOR 1 (ABF1)*, *ABA INSENSITIVE 5 (ABI5)* and *NF-YB2* (Figure 3.6, table). All four genes have already been identified as key players mediating the tolerance to a wide range of abiotic stresses (Ramegowda et al., 2017; Fernando et al., 2018; Ren et al., 2022). NF-YB2 has an important role in plant stress acclimations

as discussed above. *GBF3*, has previously demonstrated to be a TF targeting specific stress responsive genes when plants experience combined drought and *Pseudomonas syringae* infection (Dixit et al., 2019). Both *ABF1* and *ABI5* are previously characterized to be involved in ABA signaling (Linden et al., 2021). Of note, it is evidence that in Arabidopsis *ABF3* can activate *ABI5* and thus confers salt tolerance (Chang et al., 2019).

The central modulator of thermomorphogenic responses, PHYTOCHROME INTERACTING FACTOR 4 (*PIF4*) (Proveniers & Van Zanten, 2013; Quint et al., 2016), was identified as one of the 11 nodes with the highest number of connections with the others in the HTD network (Figure 3.6). This may point to a novel role in mediating the acclimation to HTD despite the high-temperature response being partially restrained by the combination with drought (See; Chapter 2).

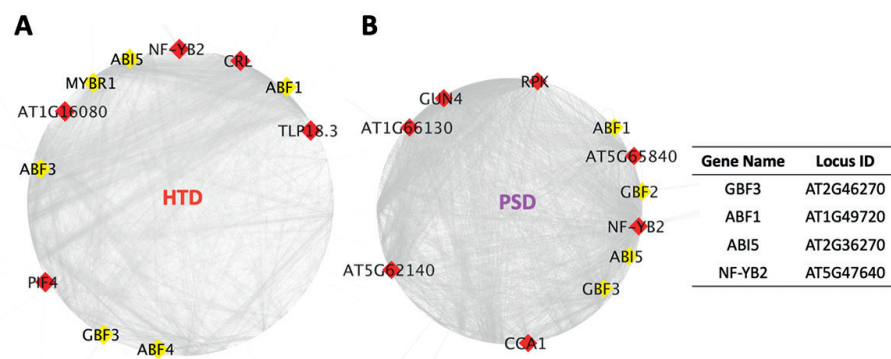


Figure 3.6: Gene regulatory network (GRN) analysis for upregulated DEGs in combined and sequential sublethal stresses.

(A, B) GRNs for DEGs from the upregulated gene clusters in combined high temperature and drought (HTD) (A) and submergence followed by drought (PSD) (B). For each GRN, the putative upstream regulators (11) with the greatest number of connections with the others in the same network were indicated. The genes associated with ABA responses were highlighted with yellow nodes and the common highlighted regulators shared by the two GRNs are indicated in the table.

In addition to the overlapping regulators between the two GRNs, another five genes (*PHOSPHORIBULOKINASE (PRK)*, *AT5G65840*, *AT5G62140*, *AT1G66130* and *GUN4*) in the PSD network (note *GUN4* and *AT1G66130* had the same number of nodes in GRN, therefore in totally 11 overrepresented genes are shown in Figure 3.6 instead of 10). These five genes were shown to be relevant for photosynthesis or chloroplast activities (Larkin et al., 2003; Bosco et al., 2004; Ascencio-Ibáñez et al., 2008; Tarahi Tabrizi et al., 2016; Gurrieri et al., 2019, 2023). This strengthens our previous notion that photo-acclimation or plastid-to-nucleus signaling might play a role in PSD acclimation. Moreover, quite a

large proportion of the highlighted regulators from the HTD- and PSD- networks are associated with ABA signaling (*GBF2*, *GBF3*, *ABF1*, *ABF3*, *ABF4*, *ABI5* and *MYBR1*) (Choi et al., 2000; Kim et al., 2017; Ramegowda et al., 2017), suggesting that the responsiveness to HTD and PSD may involve ABA regulation. This is not surprising, as ABA is a central regulator of various abiotic stress responses (Wani, 2015; Sah et al., 2016; Tuteja, 2007).

Hormonal regulations under combined and sequential sublethal stresses

Because our data hinted that ABA may play a role in responsiveness to HTD and PSD, we performed a hormone-specific-signature analysis using the HORMONOMETER tool (Volodarsky et al., 2009) (Figure 3.7A). The HORMONOMETER tool correlates transcriptomic signatures of the imported dataset to that with datasets obtained after exogenous hormone application at different timepoints (Volodarsky et al., 2009). Indeed, a clear ABA signature was observed under both HTD and PSD treatment, further supporting that ABA may have a role in regulating combined (HTD) or sequential (PSD) stress responses. This result was experimentally validated using an ABA reporter GUS line *6xABRE_RD29A:GUS* to visualize ABA signaling under multiple stress conditions at the same sampling timepoints (Figure 3.7B). Results indicate that both HT and HTD stimulate ABA signaling, in agreement with the observed hormonal signatures in our transcriptome data. Individually applied D, however, did not trigger any visible staining, even though the drought period lasted for 10 days (Figure 3.7B). This is in line with our finding that D only imposed a very subtle effect on plant physiology/development (See; Chapter 2) and on the transcriptome. However, when combined with submergence (PSD), ABA signaling was markedly enhanced, which complied with observed ABA signatures by the HORMONOMETER tool (Figure 3.7B). Collectively, ABA signaling thus seemingly plays a role in mediating plant responses to combinatorial stresses (HTD and PSD), which is in line with previous studies that ABA is involved in plant responses to stress combinations (Suzuki et al., 2016a; Berens et al., 2019; Zandalinas & Mittler, 2022).

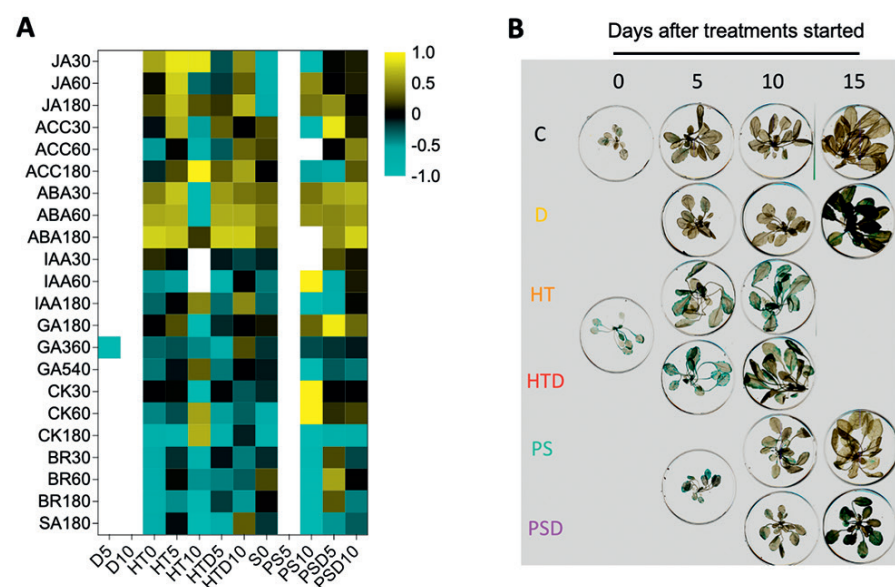


Figure 3.7: Hormonal signatures for DEGs associated with combined or sequential sublethal stresses.

(A) HORMONOMETER identified correlations between the transcriptomic signatures of Arabidopsis exposed to individual and combinatorial stresses at different timepoints (X-axis), and hormone signatures triggered by exogenous hormone applications in different time courses (Y-axis). For the abbreviations of hormones: JA; jasmonic acid, ACC; 1-Aminocyclopropane-1-carboxylic acid, ABA; abscisic acid, IAA; Indole-3-acetic acid, GA; gibberellic acid, CK; cytokinins, BR; brassinosteroids, SA; salicylic acid. Numbers following the hormones indicate minutes after the hormone applications. Colors scales indicate the levels of correlation, with yellow representing a positive correlation, cyan a negative correlation, black for no correlation and white for blank (lack of the correlation information due to the limited number of inputted DEGs). **(B)** Representative images of *6xABRE_RD29A:GUS* stained rosettes, subjected to individual, combined and sequential stresses at 0, 5, 10 and 15 days after the treatments started. For colors and abbreviations of stress treatments see figure 3.1 legend.

The HORMONOMETER profile (Figure 3.7A) also suggested the potential involvement of other hormones in regulating combinatorial stress responses. For example, the hormonal signature of 5-day PSD-treated plants displayed high correlations with those treated by ACC (an ethylene precursor) and GA. However, the enhanced correlations were tempered if PSD treatment lasted for 10 days, possibly due to the crosstalk between different hormones (Murphy, 2015), as both ethylene and GA are antagonistically regulated by ABA (Sharp & LeNoble, 2002; Liu & Hou, 2018). On the other hand, ABA has also been found to antagonistically interact with brassinosteroids (BR) in regulating plant thermotolerance (Divi et al., 2010), which may explain the negative correlation between the BR profile and the HT- / HTD-triggered transcriptome

signatures. Furthermore, the salicylic acid (SA) signature in general negatively correlated with the PSD- induced transcriptome signature (Figure 3.7A). One possible explanation is that abiotic stresses can blunt SA-mediated plant immune responses, and this suppression is most likely mediated by ABA (Yasuda et al., 2008; Berens et al., 2019). Notably, a highly induced cytokinin (CK) and auxin/IAA signature appeared after PS treatment (Figure 3.7A), which can be correlated to the steady recovery of plant growth under a well-watered de-submergence phase (See; Chapter 2), as both CK and IAA positively affect growth and leaf development of Arabidopsis (Dreher et al., 2006; Park et al., 2021a).

Identification of multi-stress tolerant factors

One of the goals of our study is to identify general stress regulators mediating tolerance to multiple abiotic stresses including drought, post-submergence and high temperature. We therefore searched for all DEGs associated with these stress treatments in our dataset (D, HT and PS, neglecting HTD and PSD in this case). However, because we only identified a limited number of DEGs, especially under D and PS conditions, we calculated the effects of each of the three stress treatments within the entire dataset, regardless of whether they were individually applied or combined with another stress. By overlapping each of the single-stress triggered DEGs, we eventually identified 31 genes showing changes in expression in response to all the three stresses. These genes can thus be considered 'multi-stress-associated genes' (Figure 3.8A).

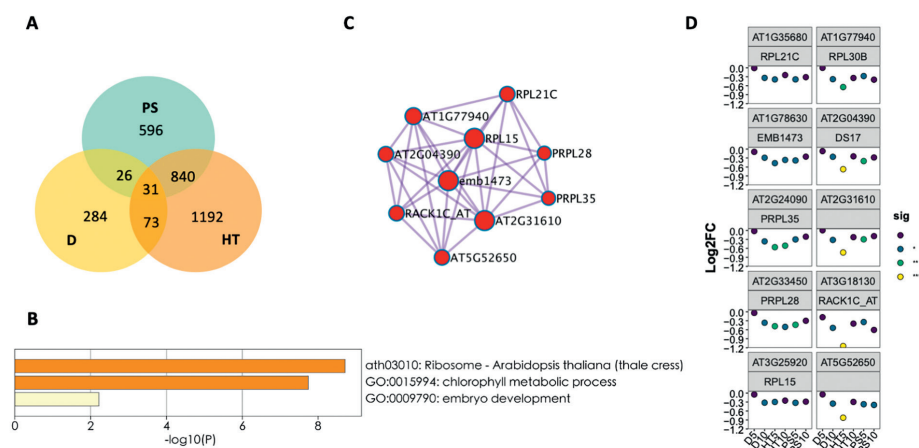


Figure 3.8: Identification of multi-stress responsive genes from the RNA-seq dataset

(A) Venn diagram presenting the overlap (and uniqueness) in DEGs elicited by the transcriptomic effects of 5- and 10- day drought (D), post-submergence (PS) and high temperature (HT) treatments in the entire RNA-seq dataset. (B) Gene ontology enrichment analysis for the 31 multi-stress responsive genes shared by all three stresses (center of the VENN diagram). The most significantly ($p < 0.01$) enriched GO terms of KEGG pathways and biological processes were listed with the significances indicated by $-\log_{10}(p)$ values. (C) MCODE network presenting a cluster of 10 densely connected genes, predicted based on protein-protein interactions (PPIs) of the 31 multi-stress genes. (D) Relative expression levels, indicated as Log_2FC , under individual stress treatments (D, PS and HT) of the 10 genes of the MCODE network. Colors represent the statistical significances of expression values, relative to control (C) conditions. Gene locus AGI IDs were indicated along with the most commonly used gene names. For abbreviations see figure 3.1 legend.

Next, we performed Gene Ontology (GO) enrichment analysis to investigate the biological functions of these highlighted 31 multi-stress-associated genes (Figure S3.8). The enrichment identified ribosome (ath03010) protoporphyrinogen IX biosynthetic process (GO:0006782) and regulation of translation (GO:0006417) (Figure 3.8B). Indeed, several of the 31 genes encode ribosomal proteins (RPs) involved in translation, such as *RIBOSOMAL PROTEIN BL21C* (*RPL21C*), *RIBOSOMAL PROTEIN EL30Y* (*RPL30B*), *RIBOSOMAL PROTEIN BL28C* (*PRPL28*), and *RIBOSOMAL PROTEIN UL15C* (*RPL15*). However, as ribosomal protein gene expression can be largely influenced by adverse growth conditions (Liu et al., 2014), these factors may just be the general stress-downregulated genes. By using the MCODE tool (Bader & Hogue, 2003), 10 ribosomal genes densely connected with each other in the protein-protein interaction (PPI) network were identified from the 31 genes (Figure 3.8C). These 10 genes were all downregulated during each of the individual stress treatments (Figure 3.8D), suggesting that these genes are likely general stress responsive genes. In contrast to these ribosomal genes, three genes

(of the 31) exhibited consistent upregulation trends across D, HT and PS: *AT1G04350*, *GAMMA-VPE* and *AT4G16190* (Figure S3.7). Both *GAMMA-VPE* and *AT4G16190* are members of cysteine proteinases (Van Wyk et al., 2014; Hatsugai et al., 2015) and have previously been characterized as important stress modulators (Kinoshita et al., 1999; Bernoux et al., 2008). We therefore conclude that *GAMMA-VPE* and *AT4G16190* are potential multi-stress responsive genes of D, PS and HT.

Conclusions

Taken together, our transcriptome analyses revealed unique response signatures imposed by sublethal combinatorial abiotic stresses, which might account for the unique phenotypic or physiological traits characterized before (See; Chapter 2). The RNA-seq data analysis enabled the identification of genetic processes, candidate genes (including TFs and overrepresented genes in GRNs) and hormonal regulators that may contribute to the acclimation to combined and sequential sublethal stresses as well as multi-(single)stress modulators. Given that these identified stress regulators may be essential for the tolerance to combinatorial stresses, it is necessary to further verify the physiological functions of these candidates (Table S3.8, also see; Chapter 4).

Acknowledgements

This work is supported by the Netherlands Organization for Scientific Research (NWO) (project no. 867.15.031 to AV) and the China Scholarship Council (CSC) (project no. 20186170025 to ZJ). We thank Hans van Veen (University of Groningen, The Netherlands) for providing help with data analysis. We also thank Basten Snoek, Rene van der Vlugt (Wageningen University & Research, The Netherlands) and Charlotte Gommers (Wageningen University & Research, The Netherlands) for the discussion of the results.

Material and methods

Plant materials and growth conditions

Arabidopsis thaliana Columbia-0 (Col-0; NASC stock center ID: N1092) plants were grown as described in Chapter 2. In brief, seeds were stratified and thereafter grown in a climate-controlled growth chamber (8 h photoperiod / 16 h darkness, 21 °C, 120-150 $\mu\text{mol m}^{-2} \text{s}^{-1}$ PAR with fluorescence tube lightening, 70% relative humidity) until they reached 2 true leaf stage (LS2). Plants were then individually transferred to Jiffy 7c coconut pellets (Jiffy Products International BV, Zwijndrecht, The Netherlands) that were presoaked in 50 mL Hoagland solution (Millenaar et al., 2005) and thereafter saturated with deionized water to a final weight of 250 ± 20 g per pellet. Plants

subjected to high temperature (HT and HTD) were transferred to a growth chamber set at 27 °C, with otherwise similar conditions as used for C, D, PS and PSD treatments. Nutrition supplementation and randomization were performed as described in Chapter 2 (See; Chapter 2, Materials and Methods).

Stress treatments and sample harvesting

Plants were subjected to individual (PS, D, HT) or combined stresses (HTD, PSD) or kept at control conditions (C), at the day they reached 10-true-leaf stage (LS10). The stress treatments for the transcriptomic analyses were applied as described in Chapter 2. Sample harvesting was performed 2 hours after the photoperiod began (ZT = 2 hours) at 0, 5 and 10 days after treatments started, which aligns with the timepoints of the phenotypic characterizations described in Chapter 2, except for the 15-day C and D treatment and control, which was not used for the transcriptomic analysis described in this chapter. For the plant tissue sampling at each timepoint, 5-6 plants were chosen and 2 of the young leaves (leaf 7 to 10, counting from the earliest emerged true leaves (See; Chapter 2, Figure 2.3A) from individual plants (including petioles) were dissected and pooled together. Samples were immediately snap-frozen in liquid nitrogen and stored at -80 °C until further processing. In total, 58 samples were collected consisting of 3-7 independent biological replicates (leaf pools) across all harvesting timepoints. The percentage of soil water content (%SWC) at the moment of harvesting of samples are indicated in Table S3.1.

RNA isolation and sequencing sample preparation

Frozen samples from -80 °C were grinded using a cryogenic grinding mill (Retsch, Haan, Germany) to a fine powder and plant total RNA was extracted using the RNeasy kit (Qiagen, Germany) following the manufacturers protocol. Samples were diluted to 25 µg RNA / µL in a total volume of 60 µL using DEPC-treated water.

RNA quality control, library construction and Illumina sequencing

RNA quality control, library construction and Illumina sequencing was done commercially by Macrogen (Macrogen, Amsterdam, The Netherlands). Total RNA integrity and purity were checked using an Agilent Technologies 2100 Bioanalyzer (Agilent Technologies, Palo Alto, USA) and only samples with RNA Integrity Number of 7 or above were used for library construction. Library preparation was performed based on the TruSeq stranded mRNA protocol (Illumina, USA). The constructed libraries were sequenced by Illumina Novaseq6000 sequencer (Illumina, USA) with 150 bp pair-end reading, providing FASTQ files output.

Data processing and sequence alignment

Data processing, including adaptor trimming and reads filtering, was conducted using *CUTADAPT* (Martin, 2011). The Truseq adaptor sequences 'AGATCGGAAGAGCACACGTCTGAACTCCAGTCA' and 'AGATCGGAAGAGCGTCGTGTAGGGAAAGAGTGT' were trimmed with a maximum error rate of 0.07. Reads filtering was based on the criterion of the minimum cutoff length of 30 bp and quality score of 20. This yielded at least 61 million clean pair-end reads per sample. The trimmed and filtered reads were then assembled and mapped to the *A. thaliana* transcriptome (Araport10) using *KALLISTO* (Bray et al., 2016).

Normalization and calculation of differential expression

Before analysis, the transcripts per (kilobase) million (TPM) values were filtered and transformed in R software (RStudio, Inc). Next, Arabidopsis gene-expression was filtered for read detection of \log_2 TPM > 2 in all the samples. We also removed two samples with a total mapped Arabidopsis read count below 7 million due to the ArLV1 infection. This filtering step resulted in 6087 detected genes (out of 27655 protein coding genes in the assembly). Subsequently, the TPM values were transformed by:

$$TPM_{\log,i,j} = \log_2(TPM_{i,j} + 1)$$

where TPM_{\log} was the \log_2 -normalized TPM value of gene *i* (one out of 6087) and sample *j* (one out of 56 samples).

For the principal component analysis (PCA) and correlation analysis, a ratio was also calculated with the mean of the TPM, by

$$TPM_{ratio,i,j} = \log_2\left(\frac{TPM_{i,j}}{TPM_i}\right)$$

where TPM_{ratio} was the \log_2 of the TPM value of gene *i* (one out of 6087) and sample *j* (one out of 56 samples), divided by the average TPM value over all samples for gene *i*. To understand the sources of variance in the expression data, principal component analyses were performed with the *prcomp* function in R with the parameter *scale = TRUE* on the TPM_{ratio} -transformed expression data. Likewise, correlation matrices were made on the TPM_{ratio} -transformed expression data with *cor* and the *heatmap* function in R.

For the determination of ArLV1 effects on plant transcriptome, Control samples at timepoint 5 days (no applied abiotic stress) were selected, as three of these samples contained relatively few reads mapping to ArLV1 (0.01-9.56%) and four samples

contained high amounts of ArLV1 (78.94- 90.08%). Only for this analysis, the complete dataset including the two low-quality samples was used.

Statistical analysis was done in R using the \log_2 -normalized TPM values in linear models ran for 5 and 10 days timepoints separately, with the different stress treatments as variables when compared to the control treatment (C) at the same timepoint. The obtained significances were corrected using a Benjamini-Hochberg adjustment for multiple testing (provided by the *prcomp* function). Visualization of the significantly expressed genes was done with the *ggplot2* package (Wickham, 2009).

Gene clustering, Gene Ontology (GO) enrichment and Protein network analysis

To visualize gene expression differences, *k-means* clustering was used to arrange the significantly regulated genes in clusters with similar expression patterns. The optimal number of clusters was determined visually by plotting the within-cluster sums of squares and the average silhouette with the *fviz_nbclust* function from the *factoextra* package in R (Lê et al., 2008). Groups with a high variation in expression between the stress treatments were chosen for additional enrichment analysis.

For the GO enrichment analysis, Metascape (Metascape, <http://Metascape.org/>) (Zhou et al., 2019) was used to characterize the biological processes and the enriched pathways by Kyoto Encyclopedia of Genes and Genomes (KEGG) of the inputted candidates. The process enrichment was carried out following the settings of p value cutoff = 0.01, minimal number of overlapping genes = 3 and a minimal enrichment value = 1.5.

For the protein network analysis, the list of protein IDs were inputted into Metascape which incorporated the dataset of physical protein-protein interactions (PPIs) from BioGrid (Chatr-aryamontri et al., 2017) and protein interaction networks were extracted and formed by the candidates. The integrated algorithm MCODE was subsequently utilized to identify the densely connected network complexes from the PPI network.

Transcription factor (TF) analysis

The locus IDs of Arabidopsis were inputted into Arabidopsis transcription factor database (AtTFDB, <https://agris-knowledgebase.org/AtTFDB/>) and TFs were automatically identified by annotating the candidates to TFs from 50 different TF families. The \log_2 FC and significances of the identified TFs were then plotted as heatmap figures using R.

Construction of gene regulatory networks (GRNs)

Candidate gene IDs were first imported into TF2Network (Kulkarni et al., 2018) to search for the information of their promoter binding sites and thereafter the putative upstream TFs were identified. These TFs were then analyzed for the co-expressions and protein-DNA interactions with the predicted targets and the networks thereafter generated using Cytoscape (Shannon et al., 2003).

Hormonal signature analysis

HORMONOMETER (Volodarsky et al., 2009) was used to characterize the hormonal signature of the RNA-seq dataset. Locus IDs, \log_2 FC and statistical significances of the candidates were together imported into HORMONOMETER and the correlations between the input RNA-seq dataset and known transcriptome responses triggered by exogenous hormone applications (Goda et al., 2008) were then calculated. The output of the analysis was plotted as heatmaps using GraphPad Prism 9 (GraphPad Software, La Jolla, USA).

Histochemical GUS assay

Entire rosettes of *6xABRE_RD29A:GUS* were harvested at 0, 5, 10 and 15 (only for C and D) days after the treatment started and immediately fixed in 90% acetone (v/v) at -20 °C for 20 min and then washed by washing solution (0.1 M phosphate buffer pH=7, 10 mM EDTA, 2 mM $K_3Fe(CN)_6$) under vacuum for 10 min in darkness. Plants were subsequently transferred to the staining solution (0.1 M phosphate buffer pH=7, 10 mM EDTA, 1 mM $K_3Fe(CN)_6$, 1mM $K_4Fe(CN)_6 \cdot H_2O$) and vacuumed for 10 min in darkness, followed by an overnight incubation at 37 °C. To stop the staining, samples were soaked in 3:1 acetic acid: ethanol solution for 1 hour at 37 °C and were cleared with 70% ethanol (v/v) for 10 minutes. The stained plant tissues were scanned by an Epson V800 scanner (EPSON, Japan).

Supplemental Data

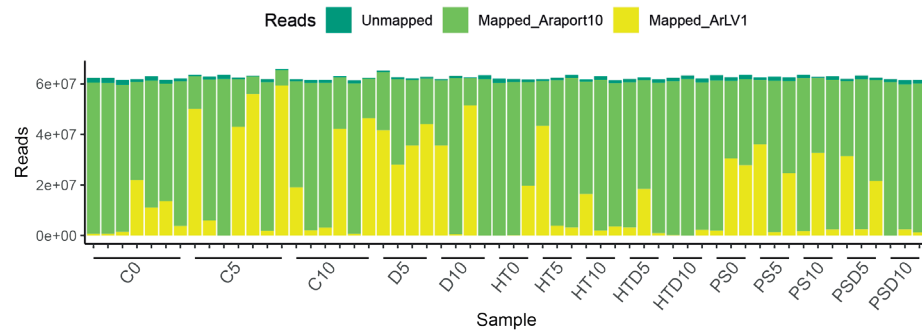


Figure S3.1: Sequence coverage of RNA-seq dataset.

Number of sequenced reads mapping to known Arabidopsis genes part of the transcriptome (Mapped_Araport10, green), RNA1 and RNA2 of the ArLV1 virus (Mapped_ArLV1, yellow) or neither of the two (Unmapped, dark green). For abbreviations see figure 3.1 legend.

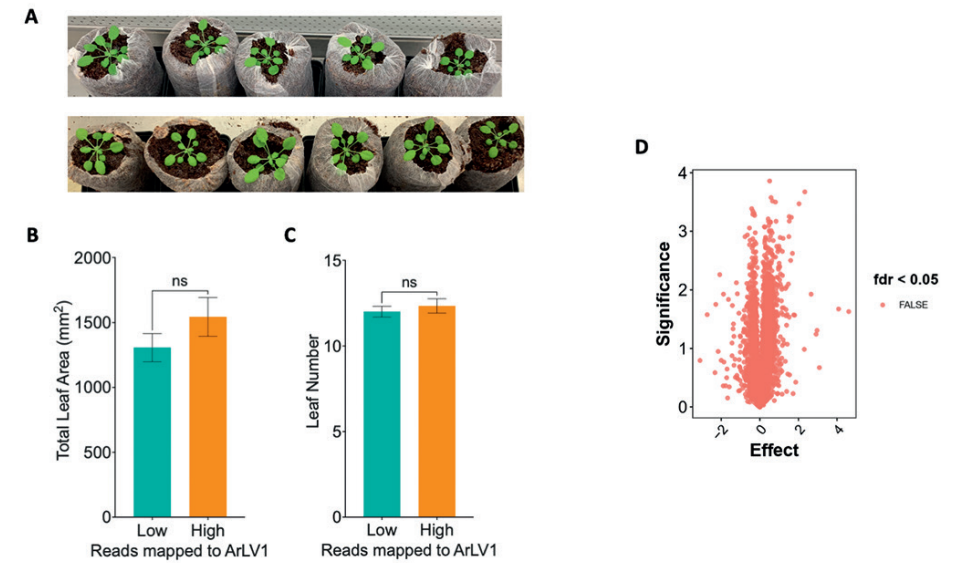


Figure S3.2: Effects of ArLV1 infections on Arabidopsis growth, development and transcriptome.

(A) Representative images showing each of the pooled plants containing either low (upper row, average percentage of sequence mapping to ArLV1 is 4.18%) or high (bottom row, average percentage of sequence mapping to ArLV1 is 81.6 %) levels ArLV1 sequence reads. The two groups of Arabidopsis plants were grown under control conditions for 5 days after which the (B, C) total leaf area (B) and number of leaves (C) were measured. Error bars indicate means ± SEM, n = 5-6. ns indicates a non-significant difference. (D) Volcano plot showing transcriptomic differences between samples mapping above and below 50% to the *A. thaliana* transcriptome in Control (C) plants at timepoint 5 days. Genes with FDR (false detection rate) < 0.05 are considered significant.

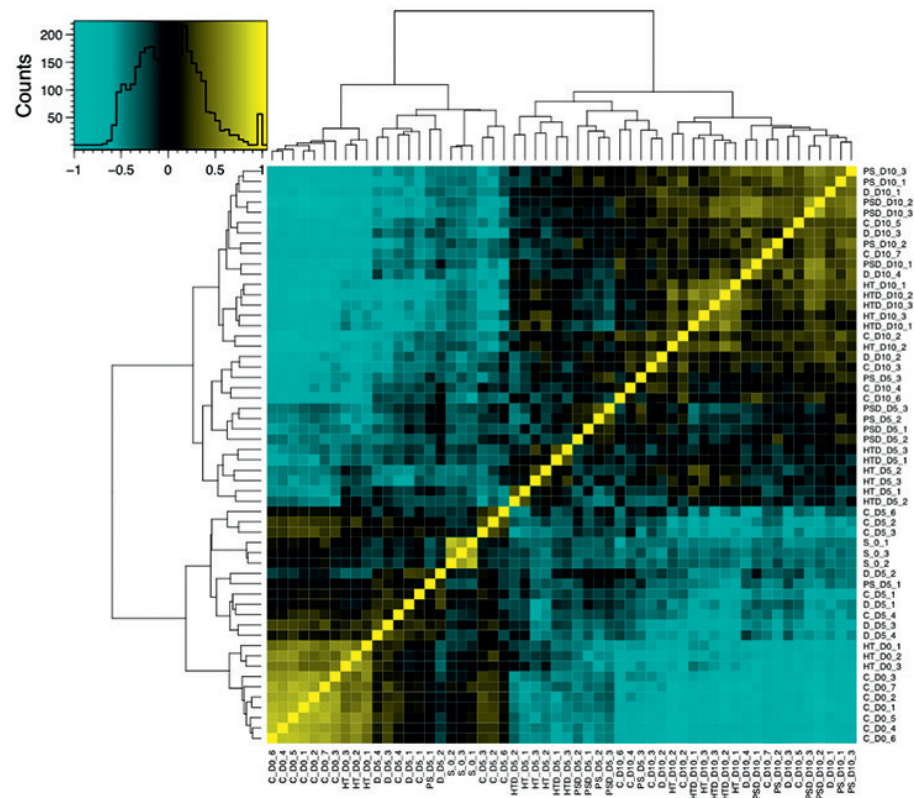


Figure S3.3:

Correlation matrix of all samples in the RNA-seq dataset visualizing the distribution of transcripts of all 56 samples that passed the quality control. The color scale indicates the strength of the correlation (negative: blue, positive: yellow) and the distribution of the matrix values. The relatednesses of individual samples are indicated by the hierarchal clustering trees. Samples are named as; abbreviation_timepoint_biological replicate. For abbreviations see figure 3.1 legend.

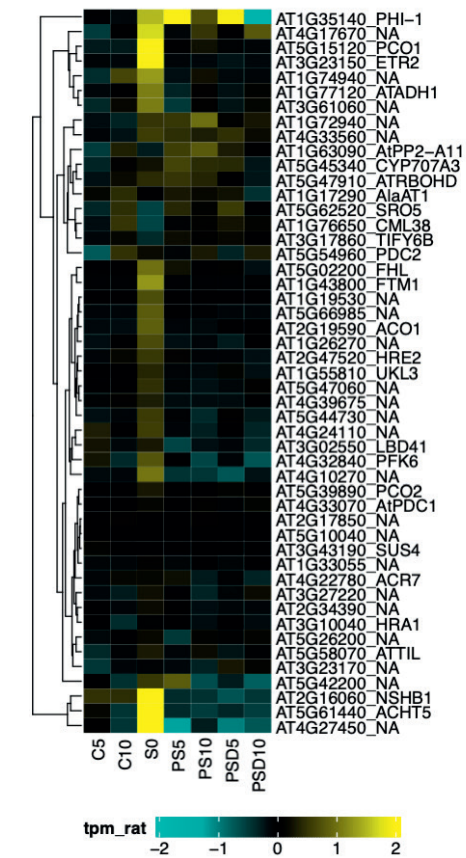


Figure S3.4: Expression of 49 core-hypoxia responsive genes

Heatmap showing the expression ratio in transcripts per million (TPM) of hypoxia responsive genes under submergence (S) followed by drought (PSD) and the relevant individual (D and PS) stresses and control (C). Indicated are the AGI gene locus ID and the commonly used abbreviation. The color scale indicates the expression levels, yellow represents up- and blue represents down-regulation. For abbreviations see figure 3.1 legend.

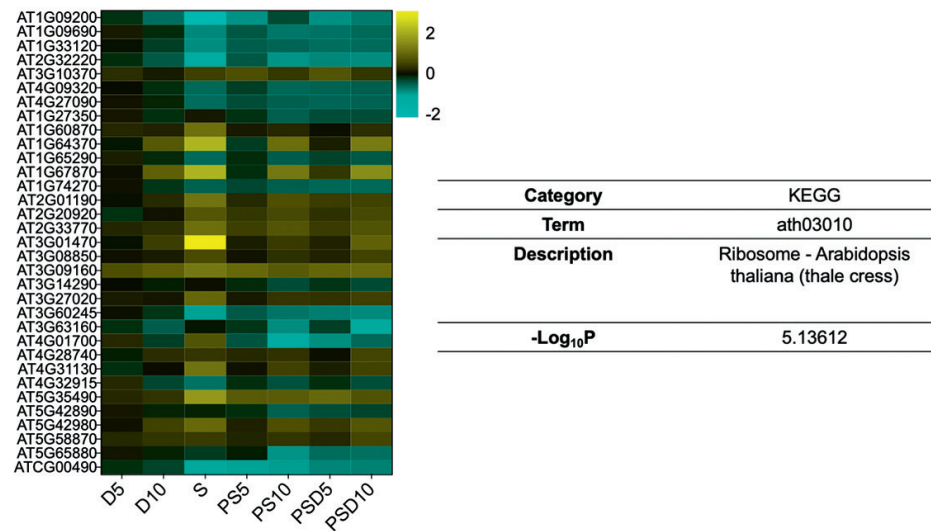


Figure S3.5: 33 DEGs regulated by both PS and PSD.

Heatmap shows relative expression of DEGs shared by both PS and PSD. For each DEG, the AGI gene locus ID is indicated. Color scales indicate Log_2FC value (relative to control (C) conditions), yellow and blue indicate up- and down- regulations, respectively. For abbreviations of stress treatments see figure 3.1 legend. The GO and KEGG enrichment analysis of the 31 DEGs are indicated in the table.

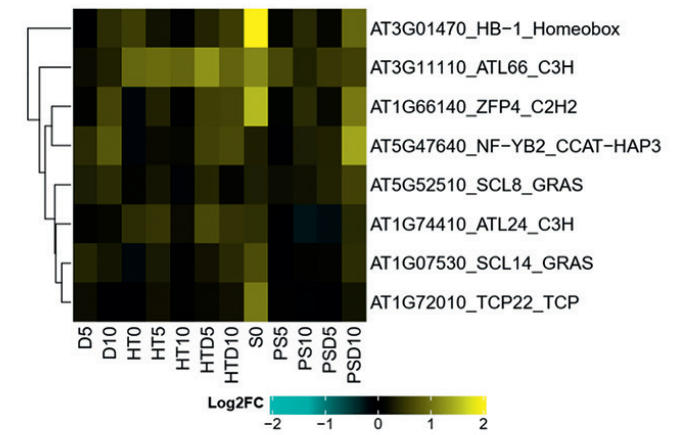


Figure S3.6: TFs upregulated in both combined and sequential stresses.

Heatmap presenting the expression patterns across individual and combinatorial stresses of 8 common TFs that are enriched in both the combined (HTD)- and sequential- (PSD) stress clusters with upregulated genes, compared to controls (C). Indicated are the AGI gene locus ID and the commonly used abbreviation. The color scale indicates the expression levels, yellow represents up- and blue represents down-regulation. For abbreviations of stress treatments see figure 3.1 legend.

Table S3.3: Significantly enriched GO terms (p < 0.01) of biological processes in each of the *k*-means clusters under combined high temperature and drought stress (HTD).

Indicated are the GO category (accession) and term description, p value of GO term enrichment and the *k*-means clusters in which the term was enriched. For abbreviations of stress treatments see figure 3.1 legend.

GO accession	Term description	p-Value	Cluster
GO:0042254	ribosome biogenesis	6.03979E-40	1
GO:0042273	ribosomal large subunit biogenesis	1.31912E-28	1
GO:0002181	cytoplasmic translation	4.54098E-20	1
GO:0042255	ribosome assembly	1.23714E-15	1
GO:0042274	ribosomal small subunit biogenesis	1.76745E-11	1
GO:0006119	oxidative phosphorylation	4.70525E-07	1
GO:0072344	rescue of stalled ribosome	2.7165E-05	1
GO:0001510	RNA methylation	3.61458E-05	1
GO:0032544	plastid translation	0.000431133	1
GO:0034728	nucleosome organization	0.000485249	1
GO:0000413	protein peptidyl-prolyl isomerization	0.000912284	1
GO:0016074	sno(s)RNA metabolic process	0.001450317	1
GO:0097549	chromatin organization involved in negative regulation of transcription	0.001494455	1
GO:0043038	amino acid activation	0.001783933	1
GO:0006091	generation of precursor metabolites and energy	0.00011082	2
GO:0016192	vesicle-mediated transport	0.00157761	2
GO:0007030	Golgi organization	0.00319522	2
GO:0006403	RNA localization	1.20322E-07	3
GO:0009657	plastid organization	1.30079E-06	3
GO:0000375	RNA splicing, via transesterification reactions	1.36781E-05	3
GO:0030433	ubiquitin-dependent ERAD pathway	2.27199E-05	3
GO:0034660	ncRNA metabolic process	2.84923E-05	3
GO:0000373	Group II intron splicing	3.26535E-05	3
GO:1903311	regulation of mRNA metabolic process	0.000139591	3
GO:0000959	mitochondrial RNA metabolic process	0.000185024	3
GO:0006457	protein folding	0.000276219	3
GO:0009790	embryo development	0.000381017	3
GO:0006281	DNA repair	0.002059724	3
GO:0048574	long-day photoperiodism, flowering	0.003376124	3

GO accession	Term description	p-Value	Cluster
GO:0140053	mitochondrial gene expression	0.004569125	3
GO:0065002	intracellular protein transmembrane transport	0.006145542	3
GO:0022613	ribonucleoprotein complex biogenesis	0.006222077	3
GO:0006897	endocytosis	0.006450208	3
GO:0090305	nucleic acid phosphodiester bond hydrolysis	0.007427573	3
GO:0042026	protein refolding	0.008236804	3
GO:0009408	response to heat	1.56187E-05	4
GO:0016560	protein import into peroxisome matrix, docking	3.73094E-05	4
GO:0006979	response to oxidative stress	0.000104547	4
GO:1901607	alpha-amino acid biosynthetic process	0.000192445	4
GO:0048878	chemical homeostasis	0.000337441	4
GO:0009644	response to high light intensity	0.000443147	4
GO:0006790	sulfur compound metabolic process	0.000716216	4
GO:0009611	response to wounding	0.000954123	4
GO:0120253	hydrocarbon catabolic process	0.001017665	4
GO:0016485	protein processing	0.00127862	4
GO:0010150	leaf senescence	0.001773684	4
GO:0046471	phosphatidylglycerol metabolic process	0.001807701	4
GO:0019684	photosynthesis, light reaction	0.00183533	4
GO:0042594	response to starvation	0.001857114	4
GO:0009620	response to fungus	0.001947046	4
GO:0009743	response to carbohydrate	0.002241505	4
GO:0006914	autophagy	0.003415799	4
GO:0006790	sulfur compound metabolic process	0.000716216	4

Table S3.4: Significantly enriched GO terms (p < 0.01) of biological processes of DEGs at HT at day 0.

Indicated are the direction of differential transcription (relative to control C; down or up), the GO category (accession) and term description, p value of GO term enrichment.

Regulation pattern	GO accession	Term description	p-Value
down	GO:0042254	ribosome biogenesis	9.95729E-22
down	GO:0002181	cytoplasmic translation	1.4703E-08
down	GO:0042255	ribosome assembly	2.13327E-08

Table S3.4: *Continued*

Regulation pattern	GO accession	Term description	p-Value
down	GO:0046148	pigment biosynthetic process	7.16182E-07
down	GO:0000470	maturation of LSU-rRNA	6.84428E-06
down	GO:0009812	flavonoid metabolic process	0.000668975
down	GO:0006515	protein quality control for misfolded or incompletely synthesized proteins	0.003913854
down	GO:0006626	protein targeting to mitochondrion	0.004064226
down	GO:0031167	rRNA methylation	0.004707484
down	GO:0010191	mucilage metabolic process	0.007093014
down	GO:0006417	regulation of translation	0.008076844
up	GO:0015979	photosynthesis	1.46374E-11
up	GO:0010275	NAD(P)H dehydrogenase complex assembly	1.57962E-07
up	GO:0044247	cellular polysaccharide catabolic process	0.000116583
up	GO:0010190	cytochrome b6f complex assembly	0.000117325
up	GO:0006790	sulfur compound metabolic process	0.000449286
up	GO:0006002	fructose 6-phosphate metabolic process	0.000890839
up	GO:0009069	serine family amino acid metabolic process	0.001109036
up	GO:0009658	chloroplast organization	0.00119019
up	GO:0009765	photosynthesis, light harvesting	0.001477437
up	GO:0000103	sulfate assimilation	0.00281855
up	GO:0009266	response to temperature stimulus	0.0050875
up	GO:0000373	Group II intron splicing	0.0056605

Table S3.5: Significantly enriched GO terms (p < 0.01) of biological processes in each of the k-means clusters under submergence followed by drought treatment.

Indicated are the GO category (accession) and term description, p value of GO term enrichment and the *k-means* clusters in which the term was enriched.

GO accession	Term description	p-Value	Cluster
GO:0034660	ncRNA metabolic process	2.91039E-05	1
GO:0042793	plastid transcription	6.05524E-05	1
GO:0000373	Group II intron splicing	0.001097608	1
GO:0000959	mitochondrial RNA metabolic process	0.00110131	1
GO:0006281	DNA repair	0.003283367	1
GO:0065002	intracellular protein transmembrane transport	0.003663384	1

Table S3.5: *Continued*

GO accession	Term description	p-Value	Cluster
GO:0006334	nucleosome assembly	0.004910088	1
GO:0072527	pyrimidine-containing compound metabolic process	0.008403109	1
GO:0042254	ribosome biogenesis	2.10002E-32	2
GO:0002181	cytoplasmic translation	1.61112E-18	2
GO:0042255	ribosome assembly	1.16976E-12	2
GO:0015995	chlorophyll biosynthetic process	4.91082E-09	2
GO:0042274	ribosomal small subunit biogenesis	5.72558E-08	2
GO:0006417	regulation of translation	9.99943E-05	2
GO:0032544	plastid translation	0.00039216	2
GO:0009657	plastid organization	0.000621101	2
GO:0045036	protein targeting to chloroplast	0.00114847	2
GO:1901259	chloroplast rRNA processing	0.003910888	2
GO:0015979	photosynthesis	1.6229E-06	3
GO:0010258	NADH dehydrogenase complex (plastoquinone) assembly	3.7316E-05	3
GO:0009110	vitamin biosynthetic process	0.00042279	3
GO:0009642	response to light intensity	0.00202643	3
GO:0006778	porphyrin-containing compound metabolic process	0.0020781	3
GO:0030001	metal ion transport	0.00403665	3
GO:0070417	cellular response to cold	0.00462344	3
GO:0016051	carbohydrate biosynthetic process	0.00488961	3
GO:0001101	response to acid chemical	0.00749204	3
GO:0051604	protein maturation	0.0084925	3
GO:0046148	pigment biosynthetic process	0.00149185	4
GO:0009639	response to red or far-red light	0.00677587	4

Table S3.6: Relative expression values of upregulated TFs identified in combined high temperature and drought.

Indicated are the the commonly used abbreviation (Gene name), AGI gene locus, Log₂FC effect on transcription and p values of the effect per treatment and timepoint. For abbreviations of stress treatments see figure 3.1 legend.

Gene Name	Locus ID	D5		D10		HT0		HT5		HT10		HTD5		HTD10	
		Log ₂ FC	P Value	Log ₂ FC	P Value	Log ₂ FC	P Value	Log ₂ FC	P Value	Log ₂ FC	P Value	Log ₂ FC	P Value	Log ₂ FC	P Value
H5FB2B	AT4G11660	0.425	0.210	0.243	0.782	0.220	0.353	0.358	0.540	0.675	0.260	0.977	1.600	0.015	
H5F4	AT4G36990	-0.320	0.754	0.377	0.629	0.430	0.231	1.103	0.311	0.365	0.541	0.797	1.363	0.024	
WHY2	AT1G71260	0.184	0.649	0.275	0.523	0.409	0.066	0.432	0.091	0.840	0.053	0.363	1.048	0.010	
VIP1	AT1G43700	0.264	0.303	0.175	0.480	0.113	0.732	0.845	0.045	0.571	0.039	0.712	0.924	0.002	
ATL66	AT3G11110	0.206	0.577	0.343	0.493	0.905	0.099	0.947	0.085	0.891	0.061	1.233	0.049	0.008	
DEAR3	AT2G23340	0.377	0.245	0.463	0.527	0.562	0.322	1.855	0.042	0.236	0.729	1.250	0.016	0.108	
NF-YB2	AT5G47640	0.420	0.150	0.779	0.481	-0.124	0.809	0.184	0.571	0.158	0.808	0.601	0.031	0.258	
ZFP4	AT1G66140	0.104	0.779	0.623	0.392	-0.156	0.683	0.355	0.497	0.059	0.826	0.587	0.095	0.019	
TLP7	AT1G53320	0.229	0.396	0.019	0.940	0.275	0.318	0.764	0.094	0.143	0.344	0.473	0.135	0.041	
BZIP28	AT3G10800	0.068	0.802	0.169	0.661	0.073	0.818	0.418	0.215	0.259	0.232	0.426	0.143	0.012	
ERF3	AT1G50640	0.270	0.369	0.338	0.507	0.544	0.122	1.074	0.029	0.312	0.302	0.780	0.060	0.056	
BZIP17	AT2G40950	0.175	0.533	0.168	0.456	-0.138	0.453	0.289	0.304	0.166	0.306	0.112	0.684	0.004	
HB1	AT3G01470	-0.034	0.872	0.437	0.444	0.567	0.270	0.254	0.286	0.092	0.522	0.375	0.045	0.063	
ATL24	AT1G74410	0.096	0.644	0.155	0.621	0.427	0.090	0.491	0.215	0.196	0.281	0.660	0.068	0.032	
ELF6	AT5G04240	0.355	0.111	0.226	0.462	0.143	0.584	0.334	0.235	0.152	0.373	0.323	0.131	0.018	
SE	AT2G27100	0.260	0.076	0.243	0.310	-0.201	0.554	0.001	0.995	0.240	0.079	0.127	0.147	0.024	
SCL14	AT1G07530	0.375	0.173	0.261	0.452	-0.160	0.505	0.292	0.408	0.048	0.752	0.248	0.361	0.008	
CDC5	AT1G09770	0.131	0.228	0.144	0.479	-0.165	0.482	0.100	0.301	0.054	0.712	-0.065	0.528	0.013	

Table S3.6: Continued

Gene Name	Locus ID	D5		D10		HT0		HT5		HT10		HTD5		HTD10	
		Log ₂ FC	P Value	Log ₂ FC	P Value	Log ₂ FC	P Value	Log ₂ FC	P Value	Log ₂ FC	P Value	Log ₂ FC	P Value	Log ₂ FC	P Value
PCF54	AT4G04885	0.212	0.376	0.139	0.515	-0.003	0.995	0.313	0.158	0.118	0.598	0.190	0.356	0.017	
MYBRI	AT5G67300	-0.142	0.805	0.406	0.755	0.239	0.826	1.630	0.030	0.418	0.700	0.267	0.741	0.662	
ARID5	AT3G43240	-0.153	0.522	0.110	0.532	-0.110	0.721	0.056	0.867	0.095	0.531	-0.212	0.418	0.023	
AT1G01930	AT1G01930	0.532	0.144	0.087	0.668	0.143	0.382	0.499	0.147	0.283	0.093	0.547	0.087	0.018	
TCP23	AT1G35560	0.211	0.364	0.225	0.661	0.343	0.093	0.654	0.082	0.304	0.270	0.847	0.018	0.098	
TCP9	AT2G45680	0.037	0.944	0.328	0.702	-0.316	0.409	0.783	0.025	0.856	0.164	-0.078	0.766	0.530	
AT5G12310	AT5G12310	0.379	0.237	0.251	0.481	0.302	0.252	0.275	0.435	0.257	0.294	0.474	0.135	0.040	
ILR3	AT5G54680	-0.108	0.472	-0.035	0.786	0.107	0.576	0.322	0.082	0.157	0.195	0.271	0.084	0.028	
ATL13	AT3G60080	0.389	0.088	0.243	0.524	0.256	0.144	0.204	0.167	0.228	0.351	0.414	0.032	0.216	
BEH4	AT1G78700	0.223	0.105	0.051	0.850	0.005	0.994	0.267	0.233	0.043	0.857	0.440	0.022	0.106	
TCP22	AT1G72010	0.209	0.382	-0.031	0.900	0.011	0.931	0.229	0.611	0.051	0.769	0.168	0.498	0.028	
SCL1	AT1G21450	0.321	0.105	0.031	0.903	0.320	0.198	0.419	0.074	0.082	0.351	0.299	0.026	0.029	
AT1G80400	AT1G80400	0.218	0.237	0.113	0.507	0.233	0.219	0.227	0.181	-0.009	0.948	0.418	0.042	0.033	
HB2	AT4G16780	0.447	0.215	0.265	0.574	0.761	0.022	0.947	0.038	-0.010	0.992	0.599	0.139	0.698	
SCL8	AT5G52510	0.319	0.153	0.422	0.361	0.113	0.458	0.264	0.286	-0.093	0.764	0.379	0.041	0.508	
BEL1	AT5G41410	0.460	0.190	0.273	0.479	0.490	0.128	0.112	0.792	-0.223	0.470	0.645	0.028	0.846	
MYB34	AT5G60890	0.414	0.391	0.243	0.782	0.901	0.188	1.368	0.031	-0.109	0.905	0.024	0.945	0.691	

Table S3.7: Relative expression values of upregulated TFs identified in submergence followed by drought.

Indicated are the the commonly used abbreviation (Gene name), AGI gene locus, Log₂FC effect on transcription and p values of the effect per treatment and timepoint. For abbreviations of stress treatments see figure 3.1 legend.

Gene Name	Locus ID	D5		D10		S/PS0		PS5		PS10		PSD5		PSD10	
		Log2FC	P Value	Log2FC	P Value	Log2FC	P Value	Log2FC	P Value	Log2FC	P Value	Log2FC	P Value	Log2FC	P Value
CGA1	AT4G26150	0.470	0.192	1.254	0.404	0.478	0.126	0.907	0.144	1.997	0.060	0.444	0.185	2.239	0.028
NF-YB2	AT5G47640	0.420	0.150	0.779	0.481	0.335	0.284	0.056	0.896	0.321	0.529	0.355	0.127	1.378	0.033
ZFP4	AT1G66140	0.104	0.779	0.623	0.392	1.511	0.000	0.100	0.816	0.423	0.164	0.183	0.701	1.052	0.013
HB1	AT3G01470	-0.034	0.872	0.437	0.444	3.098	0.000	0.138	0.843	0.398	0.048	0.171	0.309	0.904	0.011
NAC083	AT5G13180	0.451	0.175	0.230	0.604	0.785	0.001	0.087	0.819	0.155	0.644	0.271	0.469	0.784	0.041
WRKY17	AT2G24570	-0.083	0.804	0.654	0.444	0.039	0.884	0.003	0.995	1.174	0.048	0.094	0.856	0.733	0.097
FBH2	AT4G09180	0.375	0.076	0.507	0.443	0.090	0.597	0.504	0.116	0.341	0.145	0.145	0.528	0.656	0.012
ERF34	AT2G44940	0.282	0.506	0.395	0.478	0.279	0.402	0.351	0.528	0.119	0.635	0.410	0.613	0.641	0.037
RGAI	AT2G01570	0.101	0.503	0.406	0.444	0.534	0.007	0.290	0.155	0.576	0.087	0.198	0.262	0.610	0.037
SCL8	AT5G52510	0.319	0.153	0.422	0.361	0.331	0.027	0.215	0.247	0.242	0.344	0.358	0.111	0.605	0.035
ATL66	AT3G11110	0.206	0.577	0.343	0.493	1.166	0.014	0.652	0.223	0.351	0.155	0.518	0.195	0.594	0.041
DOF2	AT3G21270	0.243	0.551	0.198	0.603	1.243	0.001	0.296	0.485	0.398	0.197	0.238	0.497	0.559	0.045
DOF1	AT1G51700	0.369	0.129	0.484	0.584	0.295	0.272	0.551	0.334	0.592	0.327	0.537	0.045	0.520	0.223
SCL14	AT1G07530	0.375	0.173	0.261	0.452	0.692	0.001	0.015	0.971	0.098	0.316	0.129	0.679	0.438	0.013
HB34	AT3G28920	0.268	0.228	0.074	0.832	0.001	0.993	0.160	0.611	0.383	0.087	0.305	0.255	0.430	0.039
AT3G10760	AT3G10760	0.402	0.190	0.288	0.342	1.250	0.000	0.327	0.379	0.266	0.082	0.279	0.423	0.408	0.035
ATL24	AT1G74410	0.096	0.644	0.155	0.621	0.460	0.016	0.031	0.940	-0.247	0.149	-0.192	0.512	0.403	0.037
AL4	AT5G26210	0.217	0.237	0.277	0.426	-0.033	0.827	0.108	0.735	0.274	0.158	0.118	0.419	0.402	0.042

Table S3.7: Continued

Gene Name	Locus ID	D5		D10		S/PS0		PS5		PS10		PSD5		PSD10	
		Log2FC	P Value	Log2FC	P Value	Log2FC	P Value	Log2FC	P Value	Log2FC	P Value	Log2FC	P Value	Log2FC	P Value
CDF3	AT3G47500	0.333	0.226	0.232	0.507	0.363	0.024	0.002	0.996	-0.027	0.906	0.112	0.805	0.362	0.042
TCP22	AT1G72010	0.209	0.382	-0.031	0.900	1.045	0.000	0.058	0.891	-0.057	0.561	-0.005	0.990	0.253	0.045
ATL80	AT1G20823	0.126	0.792	0.284	0.684	0.117	0.662	1.232	0.150	0.569	0.410	1.021	0.024	0.209	0.618

Table S3.8: Identified candidate genes mediating acclimation to combined high temperature and drought (HTD) and/or submergence followed by drought (PSD) according to the transcriptomic analysis.

Indicated are the the commonly used abbreviation (Gene name), AGI gene locus, stress type, and selection criteria. For abbreviations of stress treatments see figure 3.1 legend.

Gene Name	Locus ID	Stress type	Selection criteria
<i>HSFB2B</i>	AT4G11660	HTD	Upregulated TF
<i>HSF4</i>	AT4G36990	HTD	Upregulated TF
<i>WHY2</i>	AT1G71260	HTD	Upregulated TF
<i>VIP1</i>	AT1G43700	HTD	Upregulated TF
<i>ATL66</i>	AT3G11110	HTD/PSD	Upregulated TF
<i>DEAR3</i>	AT2G23340	HTD	Upregulated TF
<i>NF-YB2</i>	AT5G47640	HTD/PSD	Upregulated TF/Hub genes in GRN
<i>ZFP4</i>	AT1G66140	HTD/PSD	Upregulated TF
<i>TLP7</i>	AT1G53320	HTD	Upregulated TF
<i>BZIP28</i>	AT3G10800	HTD	Upregulated TF
<i>ERF3</i>	AT1G50640	HTD	Upregulated TF
<i>BZIP17</i>	AT2G40950	HTD	Upregulated TF
<i>HB1</i>	AT3G01470	HTD/PSD	Upregulated TF
<i>ATL24</i>	AT1G74410	HTD/PSD	Upregulated TF
<i>ELF6</i>	AT5G04240	HTD	Upregulated TF
<i>SE</i>	AT2G27100	HTD	Upregulated TF
<i>SCL14</i>	AT1G07530	HTD/PSD	Upregulated TF
<i>CDC5</i>	AT1G09770	HTD	Upregulated TF
<i>PCFS4</i>	AT4G04885	HTD	Upregulated TF
<i>MYBR1</i>	AT5G67300	HTD	Upregulated TF
<i>ARID5</i>	AT3G43240	HTD	Upregulated TF
<i>AT1G01930</i>	AT1G01930	HTD	Upregulated TF
<i>TCP23</i>	AT1G35560	HTD	Upregulated TF
<i>TCP9</i>	AT2G45680	HTD	Upregulated TF
<i>AT5G12310</i>	AT5G12310	HTD	Upregulated TF
<i>ILR3</i>	AT5G54680	HTD	Upregulated TF
<i>ATL13</i>	AT3G60080	HTD	Upregulated TF
<i>BEH4</i>	AT1G78700	HTD	Upregulated TF
<i>TCP22</i>	AT1G72010	HTD/PSD	Upregulated TF
<i>SCL1</i>	AT1G21450	HTD	Upregulated TF
<i>AT1G80400</i>	AT1G80400	HTD	Upregulated TF
<i>HB2</i>	AT4G16780	HTD	Upregulated TF
<i>SCL8</i>	AT5G52510	HTD/PSD	Upregulated TF

Table S3.8: Continued

Gene Name	Locus ID	Stress type	Selection criteria
<i>BEL1</i>	AT5G41410	HTD	Upregulated TF
<i>MYB34</i>	AT5G60890	HTD	Upregulated TF
<i>CGA1/GNL</i>	AT4G26150	PSD	Upregulated TF
<i>NAC083</i>	AT5G13180	PSD	Upregulated TF
<i>WRKY17</i>	AT2G24570	PSD	Upregulated TF
<i>FBH2</i>	AT4G09180	PSD	Upregulated TF
<i>ERF34</i>	AT2G44940	PSD	Upregulated TF
<i>RGA1</i>	AT2G01570	PSD	Upregulated TF
<i>DOF2</i>	AT3G21270	PSD	Upregulated TF
<i>DOF1</i>	AT1G51700	PSD	Upregulated TF
<i>HB34</i>	AT3G28920	PSD	Upregulated TF
<i>AT3G10760</i>	AT3G10760	PSD	Upregulated TF
<i>AL4</i>	AT5G26210	PSD	Upregulated TF
<i>CDF3</i>	AT3G47500	PSD	Upregulated TF
<i>TCP22</i>	AT1G72010	PSD	Upregulated TF
<i>ATL80</i>	AT1G20823	PSD	Upregulated TF
<i>ABI5</i>	AT2G36270	HTD/PSD	Hub genes in GRN
<i>MYBR1</i>	AT5G67300	HTD	Hub genes in GRN
<i>AT1G16080</i>	AT1G16080	HTD	Hub genes in GRN
<i>ABF3</i>	AT4G34000	HTD	Hub genes in GRN
<i>PIF4</i>	AT2G43010	HTD	Hub genes in GRN
<i>GBF3</i>	AT2G46270	HTD/PSD	Hub genes in GRN
<i>ABF4</i>	AT3G19290	HTD	Hub genes in GRN
<i>TLP18.3</i>	AT1G54780	HTD	Hub genes in GRN
<i>ABF1</i>	AT1G49720	HTD/PSD	Hub genes in GRN
<i>CRL</i>	AT5G51020	HTD	Hub genes in GRN
<i>GBF2</i>	AT4G01120	PSD	Hub genes in GRN
<i>CCA1</i>	AT2G46830	PSD	Hub genes in GRN
<i>PRK</i>	AT1G32060	PSD	Hub genes in GRN
<i>AT5G65840</i>	AT5G65840	PSD	Hub genes in GRN
<i>AT5G62140</i>	AT5G62140	PSD	Hub genes in GRN
<i>GUN4</i>	AT3G59400	PSD	Hub genes in GRN
<i>AT1G66130</i>	AT1G66130	PSD	Hub genes in GRN
<i>GAMMA-VPE</i>	AT4G32940	-	Putative multi-stress associated gene
<i>AT4G16190</i>	AT4G16190	-	Putative multi-stress associated gene



4

Molecular components mediating multi-stress resilience in Arabidopsis

Zhang Jiang, Ava Verhoeven, Martijn van Zanten*, Rashmi Sasidharan*

* Shared senior authors

Plant Stress Resilience, Utrecht University, The Netherlands

Abstract

Plant response to multiple abiotic stresses involves intricate signal transduction pathways that can lead to acclimation. In Chapter 3, we demonstrated that sublethal combinatorial stresses, either simultaneously or sequentially imposed on *Arabidopsis thaliana*, trigger unique and more pronounced transcriptome signatures compared to the corresponding individual stresses. We identified a suite of molecular processes and candidate regulatory genes potentially participating in the acclimation to sublethal combinatorial stresses. In this chapter, we describe a reverse genetics approach to characterize the genetic effects of the identified candidates in regulating plant growth, development, and wilting, during *Arabidopsis* subjection to different types of sublethal combinatorial stresses; i) combined high temperature and drought and ii) submergence followed by drought. Furthermore, we validated the morphological and physiological effects of promising candidates during the subjection to the relative individual stresses.

Our results revealed that acclimation to different sublethal combinatorial stresses is likely coordinated by distinct candidate regulatory genes, acting as either positive or negative regulators to modulate plant growth, development, and wilting. EARLY FLOWERING 6 (ELF6) and ARABIDOPSIS TOXICOS EN LEVADURA 80 (ATL80) were identified as candidate master regulators of acclimation to combined and sequential stresses, respectively. Our results also confirmed the pivotal roles of previously identified molecular processes in response to combined or sequential stresses such as ABA signaling and chlorophyll accumulation. Overall, our work validates the phenotypic effects of previously identified candidate genes on the responsiveness to sublethal combinatorial stresses and provides important leads for future studies on the dedicated molecular mechanisms how identified multi-stress regulators control plant stress responsiveness.

Introduction

As sessile organisms, plants growing in natural or agricultural settings constantly encounter and must respond to diverse abiotic stresses (Jenks & Hasegawa, 2005; Mittler, 2006a; Zhang et al., 2022b). In recent years, there has been a tremendous increase in studies deciphering molecular and physiological mechanisms of plant abiotic-stress adaptation or acclimation (Hirayama & Shinozaki, 2010b; Pereira, 2016; Praveen et al., 2023). Many of these studies have primarily focused on the responsiveness to individual stresses, often involving severe, lethal conditions. However, in nature, abiotic stresses rarely occur in isolation. Additionally, the onset of abiotic stresses is in general gradual, and the stresses often occur at sublethal severities. Co-occurring stresses typically elicit distinct effects on plant growth, development, and physiology in comparison with the corresponding individual stresses, leading to unique acclimation strategies at both phenotypic and molecular levels (Choudhury et al., 2017; Balfagón et al., 2019a; Anwar et al., 2021b; Zandalinas & Mittler, 2022). The precise effect of a given combinatorial stress is determined by multiple parameters such as the duration, severity, order, and the number of applied stresses (Pandey et al., 2015; Fong et al., 2018; Zandalinas et al., 2021a; Zandalinas & Mittler, 2022).

Several plant species can induce a series of phenotypic changes at the whole-plant level when confronted with suboptimal environmental stimuli. For example, a slightly elevated ambient temperature, or a reduced red-to-far red ratio in the perceived light can drastically affect the rosette and root architectures of *Arabidopsis thaliana*, inducing traits like leaf elongation and hyponastic growth. Furthermore, under submerged or hypoxic conditions, cereal crops such as maize can form lysigenous aerenchyma in the root cortex to maintain adequate oxygen supply and enhance hypoxia tolerance (Drew et al., 1981; Evans, 2004; Ni et al., 2019). These changes are precisely regulated by complex signal transduction pathways involving a vast number of factors (Rajhi et al., 2011; Yamauchi et al., 2013; Zhu, 2016; Kleine et al., 2021). For example, responses to high temperature or light quality are among others regulated by PHYTOCHROME INTERACTING FACTOR (PIF) transcription factors (TFs), which target genes associated with e.g. auxin signaling and cell wall remodeling and thereby control plant growth and morphology (Hornitschek et al., 2012; Van Zanten et al., 2013; Courbier et al., 2021; Burko et al., 2022). However, when more than one stress occur simultaneously or sequentially, the combinatorial stresses can elicit distinct effects on the plant transcriptome when compared to the corresponding individual stresses (Mittler, 2006b; Coolen et al., 2016a; Anwar et al., 2021b; Zandalinas & Mittler, 2022).

Heat Shock Factors (HSFs) were shown to play a pivotal role in regulating Arabidopsis response to several stress combinations, including combined heat and drought, salinity and heat, and high light intensity in combination with heat (Rizhsky et al., 2004; Suzuki et al., 2016a; Balfagón et al., 2019a). Additionally, Arabidopsis mutants with impaired abscisic acid (ABA) signaling exhibited reduced growth and survival when subjected to combined high temperature and drought stress, accompanied by a high level of H₂O₂ compared to the wild-type plants (Zandalinas et al., 2016a). This underlines the importance of reactive oxygen species (ROS)-ABA interactions for the acclimation to combinatorial stresses (Devireddy et al., 2021). A recent study investigating molecular responses of Arabidopsis to single, double and triple combinations of heat, osmotic and salt stresses revealed many functionally uncharacterized genes as important regulators of stress acclimation, and are prospective candidates for engineering plant abiotic stress tolerance (Sewelam et al., 2020). Despite of this recent study, in many studies potential regulators of combinatorial stresses are suggested based on analysis of ~omics datasets, but subsequent experimental functional validation of these factors is lacking.

In Chapter 3 of this thesis, we performed an mRNA sequencing (RNA-seq) analysis to characterize the effects of two combinatorial sublethal stresses; i) combined high temperature and drought (HTD), ii) sequentially applied submergence and drought (PSD), and their corresponding individual stresses, on the transcriptome of young Arabidopsis leaves. We show that both combined and sequential stresses impose unique transcriptomic signatures in comparison to the relevant individual stresses. We also proposed several molecular processes to be putatively involved in the regulation of these combined and sequential stresses, such as plastid-nucleus communication (retrograde signaling), ABA signaling and photo-acclimation. Additionally, we highlighted a group of candidate genes (mostly TFs) as potential key regulators involved in mediating the acclimation to combinatorial sublethal stresses, which are considered of prime interest for further functional validation.

The selection of these candidate genes was based on their expression patterns under either HTD or PSD according to the RNA-seq dataset and met at least one of the following criteria; i) TFs that were transcriptionally upregulated (See; Chapter 3, Figure 3.5), ii) overrepresented genes from constructed gene regulatory networks (See; Chapter 3, Figure 3.6) and/or where iii) identified as multi-stress responsive genes (See; Chapter 3, Figure 3.8). In this chapter, we utilized a reverse genetics approach, using (mainly) Arabidopsis T-DNA insertion mutants, to confirm the involvement of these selected candidate genes on plant growth, development and wilting during subjection to the combined and sequential abiotic stresses. Mutants of confirmed

candidates were subsequently also validated for their role in mediating responses to the respective individually applied stresses.

Our results confirmed that several of the selected candidate genes, being generally transcriptionally upregulated (See; Chapter 3), coordinate the regulation of typical phenotypic acclimation traits (*e.g.*, leaf lengthening, dry weight accumulation, wilting, *etc.*) under HTD or PSD. The reverse genetics approach confirmed the significance of some previously identified key generic processes from the transcriptomics dataset, such as ABA signaling and chlorophyll accumulation for acclimation to HTD or PSD. Moreover, we identified novel candidate TFs, such as EARLY FLOWERING 6 (ELF6) and ARABIDOPSIS TOXICOS EN LEVADURA 80 (ATL80), with significant effects on not only plant growth and leaf development, but also on plant survival (wilting) during HTD and PSD, respectively. These are promising candidates for follow-up studies to gain more insights into the signaling networks controlling combinatorial stress acclimation and adaptation and might be of relevance for applied studies aiming on improving plant growth and yield under unstable and changing climatic conditions.

Results

In chapter 3 we identified a set of candidate genes potentially mediating responses to combined (HTD) and sequential (PSD) abiotic stresses, using a transcriptome profiling approach (See; Chapter 3 Table S3.8). Here we employed a reverse genetics approach to experimentally validate some of these candidates and probe their underlying physiological functions in combinatorial-stress acclimation. Arabidopsis T-DNA insertion mutants of the corresponding genes were subjected to combinatorial stresses and the effects on plant growth, development, and wilting were characterized (Figure S4.1). We selected TFs that were upregulated during either HTD or PSD ($\text{Log}_2 |\text{FC}| > 0$, $p < 0.05$) (See; Chapter 3 Figure 3.5), together with the overrepresented genes from the gene regulatory networks constructed based on the upregulated differentially expressed genes ($\text{Log}_2 |\text{FC}| > 0$, $p < 0.05$) under HTD or PSD (See; Chapter 3 Figure 3.6), and the identified multi-stress responsive genes ($\text{Log}_2 |\text{FC}| > 0$, $p < 0.05$, in at least one of the individual stress conditions (D, HT, PS)) (See; Chapter 3 Figure 3.8). In total, we successfully isolated 44 confirmed homozygous T-DNA insertion mutants, covering 31 HTD- and 22 PSD- candidate genes, respectively (Tables S4.1 and S4.2). We were unable to obtain homozygous lines for the remaining 11 mutants, mainly because of issues with seed germination. All confirmed homozygous mutants, along with the corresponding wild-type plants (WT), were subsequently assessed for their genetic effects on phenotypic traits under either HTD or PSD.

Characterization of mutants of candidate regulators controlling acclimation to combined high temperature and drought

We subjected the 31 *Arabidopsis* mutants with putative effect on HTD traits (Table S4.1) and their corresponding WT genotypes (Col-0, Col-3) to HTD conditions when the plants reached the 10-leaf stage (LS10) (Figure 4.1A). Traits indicative for plant growth and leaf development, including total rosette area, leaf (both petiole and blade) length and leaf number were measured at 0 and 10 days after the HTD treatment was initiated and the relative changes in trait values over the 10-day HTD treatment period were calculated. Subsequently, the HTD treatment was extended until the WT and mutants started to show wilting symptoms. At that moment, plant dry weight and leaf number, days to wilting and percentage of soil water content (%SWC) were recorded. All trait values were compared between mutants and their corresponding WTs.

Of the 31 mutants tested, five lines including *aba insensitive 5 (abi5-7)*, *early flowering 6 (elf6-3)*, *at5g12310*, *VIRE2-interacting protein 1 (vip1)* and *zinc finger protein 4 (zfp4)*, displayed early wilting phenotypes based on exhibiting either accelerated wilting time (days to wilting) and/or having a relatively high %SWC at the moment of wilting (Figure 4.1B, Table S4.3). As expected, the ABA signaling mutant *abi5-7* (Dekkers et al., 2016; Bi et al., 2017) showed substantial deviating phenotypes under HTD compared to the WT, such as lower total leaf area and reduced leaf initiation rate, and larger petioles, next to its clear wilting phenotypes (Figure 4.1B, Table S4.3). This points to a pivotal role for ABA signaling in modulating plant growth and leaf lengthening under HTD.

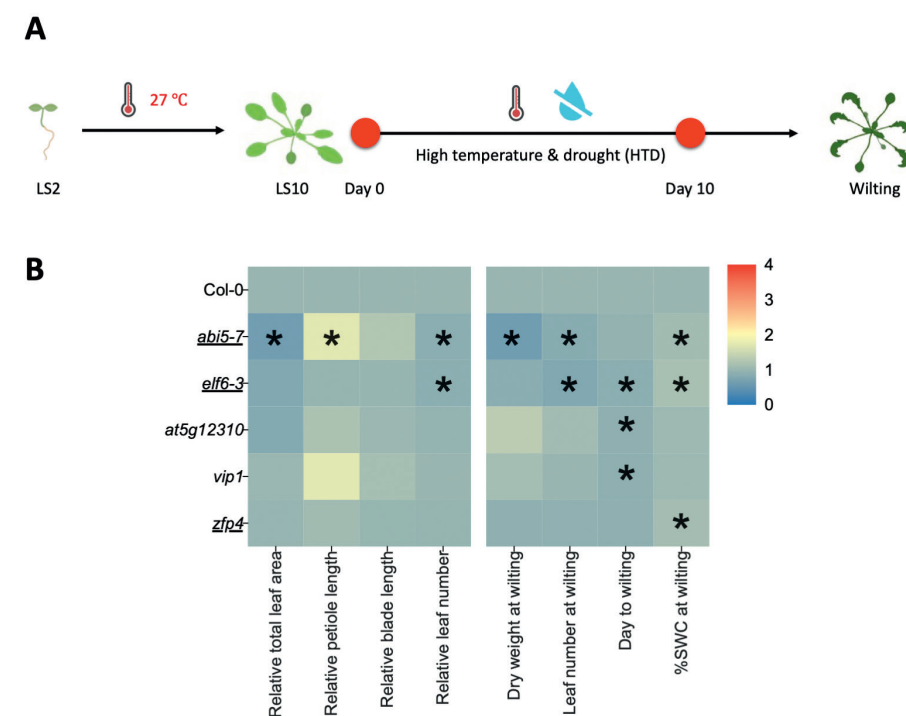
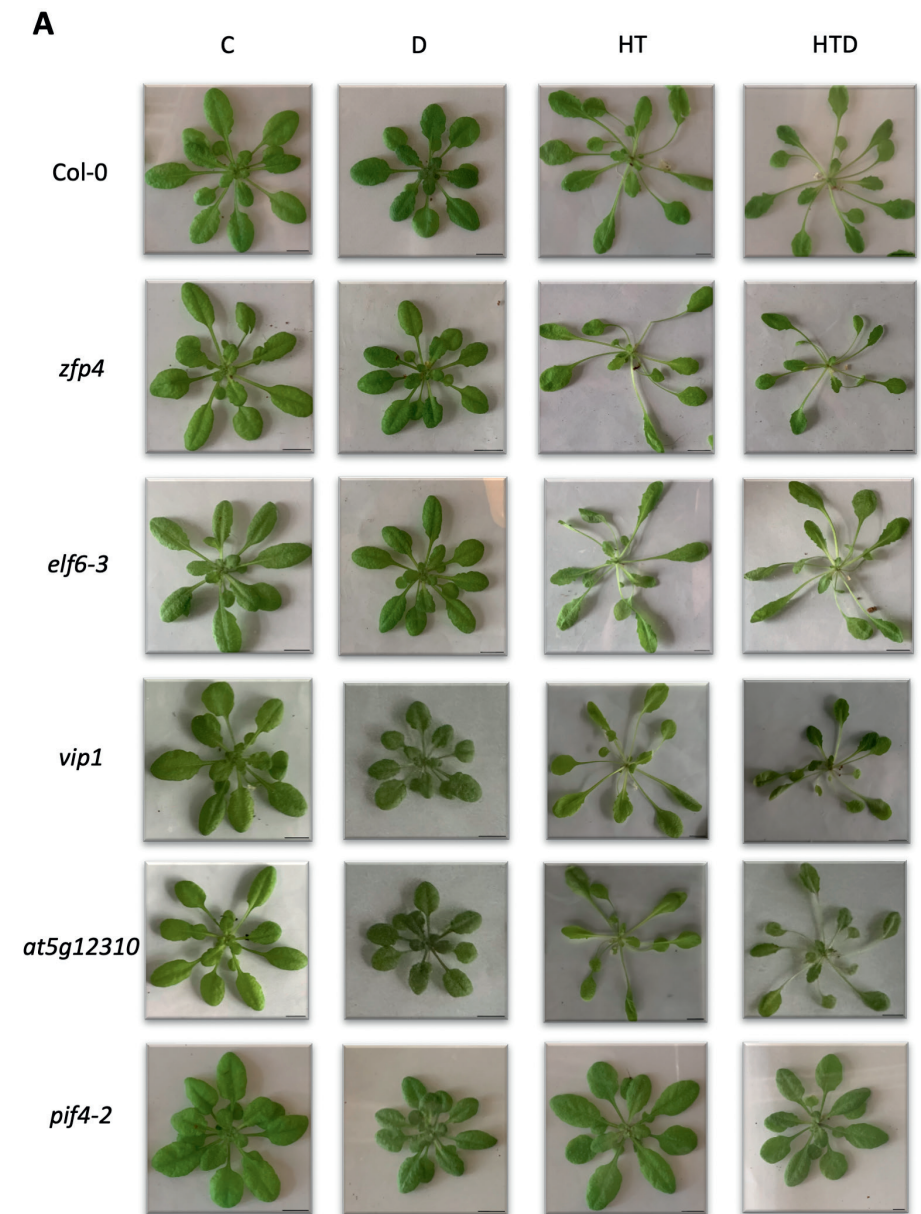


Figure 4.1 Effects of selected mutant genotypes on plant growth, development and wilting under HTD.

(A) Experimental scheme for the reverse genetic analysis. 2-leaf stage (LS2) *Arabidopsis* mutants and corresponding wild-type (WT) plants were pre-grown at 27 °C (day and night) until they reached the 10-leaf stage (LS10). Subsequently, the plants were subjected to combined high temperature and drought conditions (HTD) for 10 days and thereafter were left unwatered until wilting occurred. Measurements of phenotypic traits were carried out at day 0, 10 and at the moment of wilting (*i.e.*, timepoint differed per plant). **(B)** Heatmaps showing the phenotypic traits of *Arabidopsis* mutants with either significantly advanced wilting time and/or high %SWC relative to the corresponding wild-type plants (Col-0) during the exposure to HTD. The relative values of total leaf area, petiole/blade length and leaf number were calculated by normalizing the data obtained at day 10 by that of day 0 (left 4 panels). Dry weight and leaf number at wilting, days to wilting and %SWC at wilting are indicated as well (right 4 panels). The abbreviated names of tested mutants and the wild-type plants are indicated on the left. Color scales indicate relative values of measured traits (relative to the corresponding wild-type Col-0 plants). Underlined mutants indicate confirmed knockout of the corresponding genes based on previous studies (Table S4.1). Asterisks represent significant differences between mutants and the corresponding wild-type plants for the particular trait (Table S4.3) ($p < 0.05$, unpaired t-test). $n=8-12$.

The *elf6-3* mutant showed accelerated wilting compared to the WT, while also a high level of %SWC at wilting was observed (Figure 4.1B, Table S4.3). This mutant also

exhibited a considerable delay in leaf initiation rate. Compared to WT, both *at5g12310* and *vip1* mutants exhibited early wilting in terms of the number of days it took before the plants wilted. The *zfp4* mutant wilted at a high %SWC, but the number of days until wilting was unaffected. Although the *at5g12310*, *vip1* and *zfp4* mutants did not exhibit clear phenotypes at the morphological level compared to the WT under HTD (Figure 4.1B, Table S4.3), we set out to further validate the genetic effects of these genes, and of *elf3-6* on plant growth, development and physiological responses under control conditions (C; 21 °C), high temperatures (HT; 27 °C), single drought (D; 21 °C) and combined high temperature and drought conditions (HTD) (Figures 4.2 and 4.3). Since ABA signaling is a known universal player in plant acclimation to diverse stresses (Skubacz et al., 2016; Wang et al., 2021), we omitted the ABA signaling mutant *abi5-7* from further validation. Instead, we included the *phytochrome interacting factor 4* (*pif4-2*) mutant as a phenotypic control for high-temperature responses, as this mutant is unable to acclimate to high-temperature conditions and its response to drought is only poorly studied (Leivar et al., 2008; Van Der Woude et al., 2019). Of these mutant lines, dry weight, and leaf traits (total leaf area, leaf lengthening and initiation) were measured at 0, 5 and 10 days after the respective treatments were initiated (Figures 4.2A-C, S4.2A-C). The *elf6-3* mutant showed significantly higher dry weight and rosette area compared to the WT during HTD (Figure 4.2B). Additionally, *elf6-3* also displayed enhanced levels of dry weight accumulation and total rosette area (relative to the WT) at 0-day (pre-growth) at HT, but neither at later time points of HT nor under C and D treatments. Collectively, our result thus indicates that ELF6 could potentially be a negative regulator in controlling plant growth and rosette expansion under HTD.



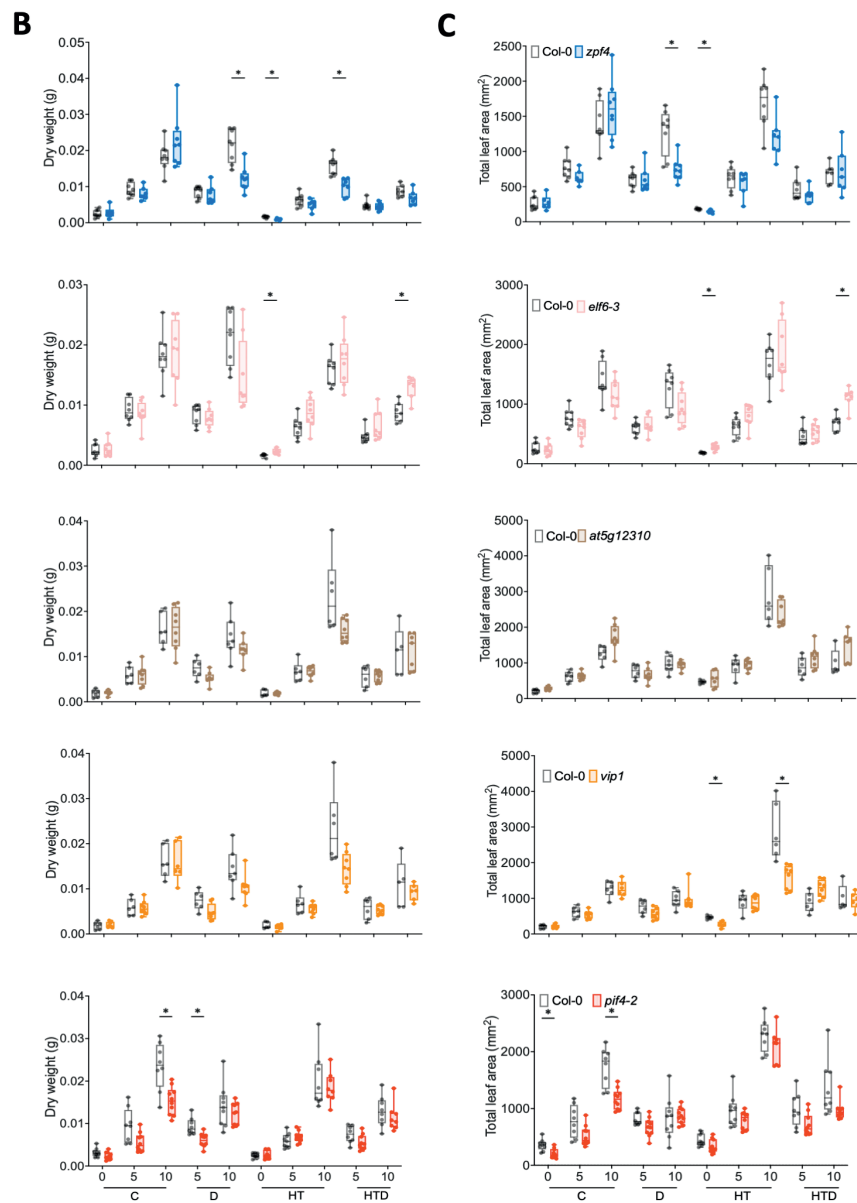


Figure 4.2 Effect of combined stress; HTD, the individual stresses of D, HT and control (C) on phenotypic traits of selected Arabidopsis mutants and the corresponding wild-type plants.

(A) Representative images of whole rosettes of the selected mutants and the corresponding wild-type plants (Col-0) grown on Jiffy coco pellet growth substrate and subjected to single and combined stresses at 10 days after the treatments initiated. Scale bars indicate 1 cm.

Note the inability of *pif4-2* to respond to high temperature in terms of petiole elongation. (B, C) Rosette dry weight (B) and total leaf area (C) of Arabidopsis mutants (*zfp4* (blue), *elf6-3* (pink), *at5g12310* (brown), *vip1* (orange) and *pif4-2* (red)) and the wild-type plants (Col-0; gray). For plants that wilted before the harvesting time points, the traits were measured at the day of wilting onset. Boxes indicate boundaries of the second and third quartiles (Q) of the data distribution. Horizontal bars indicate median and whiskers Q1 and Q4 values within 1.5 times the interquartile range. Asterisks represent significant differences between the mutant and the corresponding wild-type plants within the same time point ($p < 0.05$, multiple unpaired t-test with Holm-Šidák correction). Numbers indicate days after treatments started. Abbreviations; C; control, D; drought, HT; high temperature, HTD; high temperature & drought. $n = 5-10$.

The *zfp4* mutant showed a reduction in dry weight accumulation and total leaf area compared to the WT under both D and HT treatment, whereas *vip1* only showed smaller total leaf area than the WT under 0- or 10- day HT (Figure 4.2B-C), suggesting that both ZFP4 and VIP1 might be involved in mediating plant growth during HT and/or D but not HTD. The values of dry weight accumulation and rosette expansion of *at5g12310* and the WT were comparable at all treatment conditions (Figure 4.2B-C). The *pif4-2* mutants displayed significant reduction in dry weight accumulation under C and D, but not under HT or HTD (Figure 4.2B). Moreover, *pif4-2* showed reduced blade length relative to the WT during the subjection to D, but the petiole length of *pif4-2* was constitutively inhibited in almost all treatments relative to the WT (Figure S4.2 A-B). PIF4 is thus likely a general regulator of petiole elongation including under drought conditions, next to its role under HT (Koini et al., 2009; Van Zanten et al., 2013; Lee et al., 2021a).

Upon the HTD treatment, all tested mutants with accelerated wilting phenotypes (note, here *pif4-2* was not included as it only served as a morphological control for the phenotypic validation) displayed a significant decrease in chlorophyll content compared to the WT (Figure 4.3A). Of note, both *vip1* and *at5g12310* displayed significantly increased chlorophyll content under 10-day single drought treatment (D) relative to the WT. No significant differences were observed between mutants and the WT in terms of chlorophyll abundance during HT treatment. Under HT and HTD, stomatal conductance of mutants and the WTs was comparable (Figure 4.3B). However, 5-day D resulted in a reduction in stomatal conductance in both *vip1* and *at5g12310* mutants.

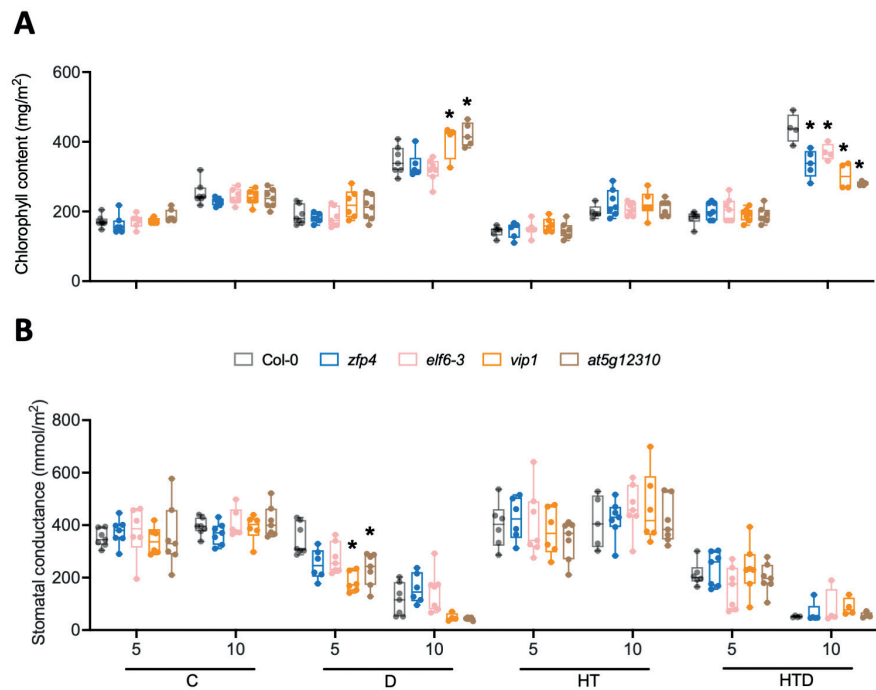


Figure 4.3 Effects of combined stress HTD, the individual stresses of D, HT and control (C) on chlorophyll content and stomatal conductance of selected mutants.

(A, B) Chlorophyll content (A) and stomatal conductance (B) of Arabidopsis mutants (*zfp4* (blue), *elf6-3* (pink), *vip1* (orange), *at5g12310* (brown)) and the wild-type plants (Col-0; gray). Box plots show the median and boxes indicate boundaries of the second and third quartiles (Q1 and Q3) of the data distribution. Whiskers indicate Q1 and Q4 values within 1.5 times the interquartile range. Asterisks represent significant differences between the mutant and the corresponding wild-type plants within the same time point ($p < 0.05$, one-way ANOVA with Dunnett test). Numbers on the X-axis indicate days after treatments started. Abbreviations; C; control, D; drought, HT; high temperature, HTD; high temperature & drought. $n = 4-7$.

Principal component analysis reveals trait correlations and validates mutant effects under combined high temperature and drought

To define correlations among traits and identify mutants with significantly different composite phenotypes in addition to wilting, a principal component analysis (PCA) was conducted including all measured phenotypic data (Table S4.3) of 31 HTD candidate genes and the WTs (Figure 4.4A-B). This indicated that, for example, *thylakoid lumen protein 18.3* (*tlp18.3*) and *bca2a zinc finger at113* (*btl13*, Col-3 background) mutants, showed high correlation with traits related to leaf lengthening (RPL; relative petiole length, RBL; relative blade length). These mutants displayed significantly increased (young) leaf lengthening compared to the corresponding WT plants (Col-0 or

Col-3) (Figure 4.4, Table S4.3). In particular *tlp18.3*, whose relative petiole length was approximately 3-fold higher than Col-0 (Figure 4.4A and Table S4.3). This suggests that the TPL18 and BTL13 transcription factors might play a role in controlling leaf elongation during HTD, likely as negative regulators.

The mutant *homeobox 2* (*hb2*), *nuclear factor y subunit b2* (*nf-yb2*), *arabidopsis toxicos en levadura 66* (*atl66*) and *teosinte branched1 /cycloidea/proliferating cell factor 22* (*tcp22*), exhibited enhanced relative petiole and/or blade elongation (RPL and RBL) compared to the WT under HTD (Figure 4.4A, Table S4.3). Likewise, *btl13*, *whirly2* (*why2-1*) and *serrate* (*se-1*) showed reduced total leaf area and leaf number at wilting in comparison to the WT. This implies that BTL13, WHY2 and SE transcription factors may act as positive regulators of plant rosette development during the HTD treatment.

The basic region/leucine zipper motif (bZIP) TFs, bZIP17 and bZIP28 act as key regulators in the so called ‘unfolded protein’ response (UPR) (Kim et al., 2018) and have also been implicated in heat stress responses (Kataoka et al., 2017; Gao et al., 2022). Compared to the WT, *bzip17* displayed significantly reduced total rosette area, blade lengthening and leaf formation under HTD, while *bzip28* only showed reduction in the number of formed leaves (Figure 4.4A, Table S4.3). The *bzip28 bzip60* double mutant, in which the UPR is constitutively hampered (Samperna et al., 2021), showed significant delay in both leaf formation and dry weight accumulation (Figure 4.4A, Table S4.3), implying that UPR might be important in acclimation to HTD.

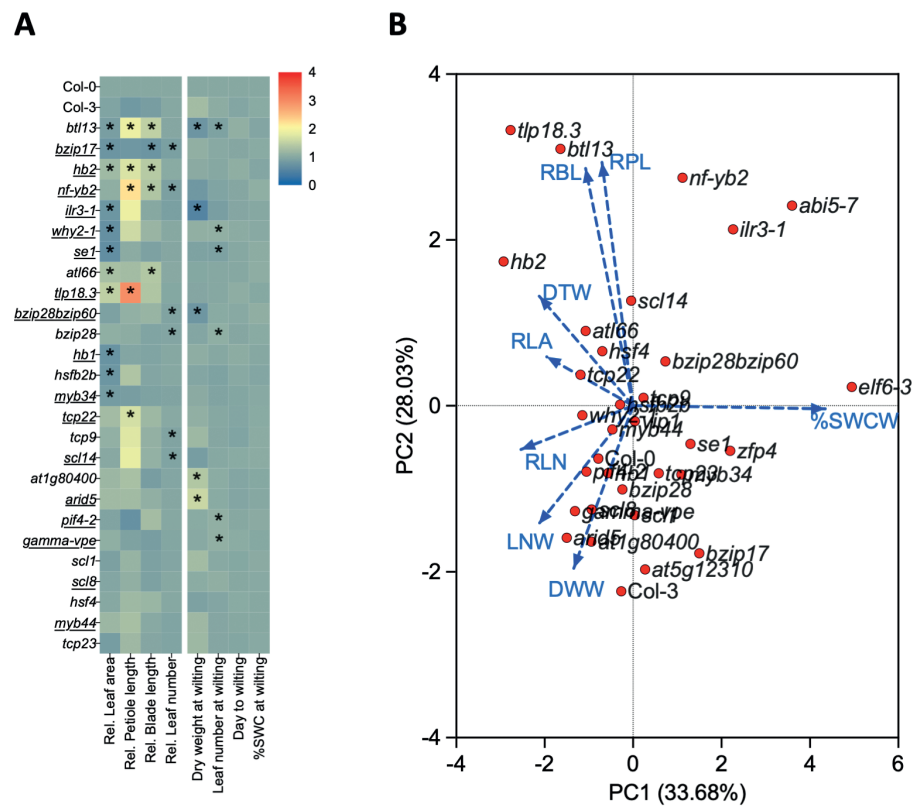


Figure 4.4 Effects of selected mutant genotypes on plant growth, development and wilting under combined high temperature and drought stress.

(A) Heatmaps showing the phenotypic traits of Arabidopsis mutants, without early wilting phenotypes (opposed to those indicated in Figure 4.1) along with the corresponding wild-type plants (Col-0 and Col-3) in response to subjection to HTD. Relative values of total leaf area, petiole/blade length and leaf number were calculated by normalizing the data obtained at day 10 by that of day 0 (left 4 panels). Dry weight and leaf number at wilting, days to wilting and %SWC at wilting were indicated as well (right 4 panels). Abbreviated names of mutants and the wild-type plants are indicated on the left. Color scales indicate relative values of measured traits (relative to the corresponding wild-type plants, with Col-3 relative to Col-0). Underlined mutants indicate confirmed knockout mutants of the corresponding genes based on previous studies (Table S4.1). Asterisks represent significant differences between mutants and the corresponding wild-type plants for the particular trait (Table S4.3) ($p < 0.05$, unpaired t-test), $n=8-12$. **(B)** Principal component analysis (PCA) of all measured traits of all mutants and corresponding wild-type plants. Visualized are the distributions of mutants and wild-type plants indicated by symbols and correlations between measured traits by arrows. Abbreviations of traits: RLA; relative total leaf area, RPL; relative petiole length, RBL; relative blade length, RLN; relative leaf number, DWW; dry weight at wilting, LNW; leaf number at wilting, DTW; day to wilting, %SWCW; percentage of soil water content (%SWC) at wilting.

Several mutants displayed significant changes in only one of the measured traits. For example, *hb1* only showed significantly reduced relative total leaf area compared to the WT during HTD (Figure 4.4A, Table S4.3). HSFs and MYELOBLASTOSIS (MYBs) proteins are well-known TFs controlling responses to various types of abiotic stresses (Katiyar et al., 2012; Scharf et al., 2012; Guo et al., 2016; Li et al., 2022b). Like the *hb1* mutant, two of the tested HSF and MYB mutants, *hsfb2b* and *myb34*, exhibited significantly reduced relative rosette area compared to the WT during HTD (Figure 4.4A, Table S4.3). However, two other mutants of these gene families, *hsf4* and *myb44*, did not show significant differences relative to the WT in measured traits. Additionally, *tcp9* and *scarecrow-like 14* (*scl14*) displayed significantly reduced relative leaf number relative to the WT, while *at1g80400* and *at-rich interacting domain 5* (*arid5*) were able to accumulate significantly higher dry weight levels than the WT at the moment of wilting (Figure 4.4A, Table S4.3), suggesting that *AT1G80400* and *ARID5* might negatively govern biomass gain during HTD. Both *pif4-2* and the previously identified multi-stress mutant, *gamma-vpe*, were only compromised in leaf initiation compared to the WT under HTD (Figure 4.4A, Table S4.3).

According to the PCA, *ilr3-1* phenotypically resembles *abi5-7* (Figure 4.4B). We observed that *ilr3-1* mutant plants exhibited enhanced hyponastic growth when grown at elevated ambient temperature (27 °C) relative to the WT. However, the presence of drought seemingly did not alter the enhanced hyponastic growth phenotype of *ilr3-1* (Figure S4.3A-B). Nonetheless, the enhanced hyponastic phenotype under HTD did not contribute to plant wilting as no significant differences between *ilr3-1* and the WT were observed in either days to wilting or %SWC at wilting (Figure 4.4A).

Traits associated with leaf development, including the relative petiole (RPL) and blade (RBL) length and total leaf area (RLA), are highly correlated (Figure 4.4B). Likewise, traits relevant to leaf initiation (relative leaf number (RLN), leaf number at wilting (LNW)) and relative dry weight at wilting (DWW) were positively correlated. As expected, days to wilting (DTW) and %SWC at wilting (%SWCW) negatively correlated, indicating that fast-wilting mutants indeed also generally contained a high %SWC at the moment of wilting.

Characterization of mutants of candidate regulators for acclimation to post-submergence drought

To investigate the effects of selected candidate genes on responses to submergence followed by drought (PSD), we tested (mainly) T-DNA mutants of 22 candidate genes (Table S4.2) and WT (Col-0) (Figure 4.5A, Table S4.4). Measurements (same traits as measured for HTD described above) were taken at day 0 and 10-day PSD. The data of

10-day PSD plants were normalized to 0-day PSD (the onset of post-submergence). Wilting-related traits were obtained at the moment the plants showed symptoms of wilting.

Of all tested mutant lines, 6 lines exhibited early wilting phenotypes (either a lower number of days to reach the wilting point and/or retention of a high level of %SWC at wilting) (Figure 4.5B, Table S4.4). This included the *NAC domain containing protein 83* (*nac083*), *hb1*, *genomes uncoupled 4* (*gun4*), *abi5-7* and *atl80* mutants (Figure 4.5B). In terms of phenotypic changes under PSD, *nac083*, *hb1* and *abi5-7* exhibited a significant increase in total leaf area and/or leaf lengthening compared to the WT (Figure 4.5B, Table S4.4). Both *gun4* and *at3g10760* had significantly reduced levels of leaf initiation relative to the WT. Notably, *gun4* was only ~50% of the (dry) weight at the moment of wilting compared to the WT (Table S4.4). Despite exhibiting wilting already at a high %SWC level, the phenotypic traits of the *atl80* mutant were comparable with those of the WT (Figure 4.5B, Table S4.4).

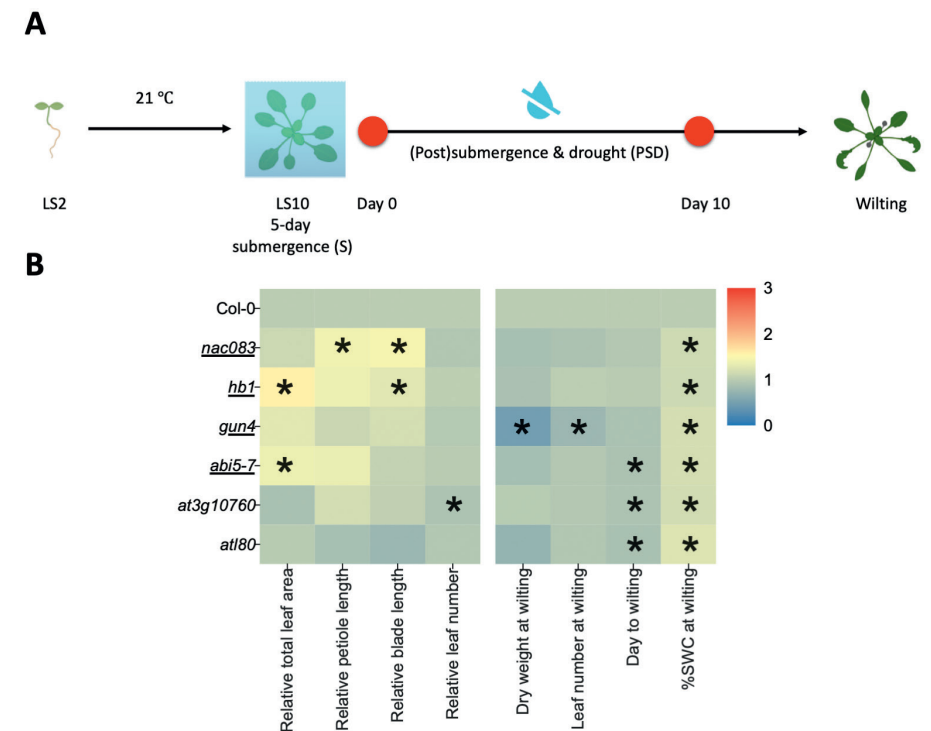
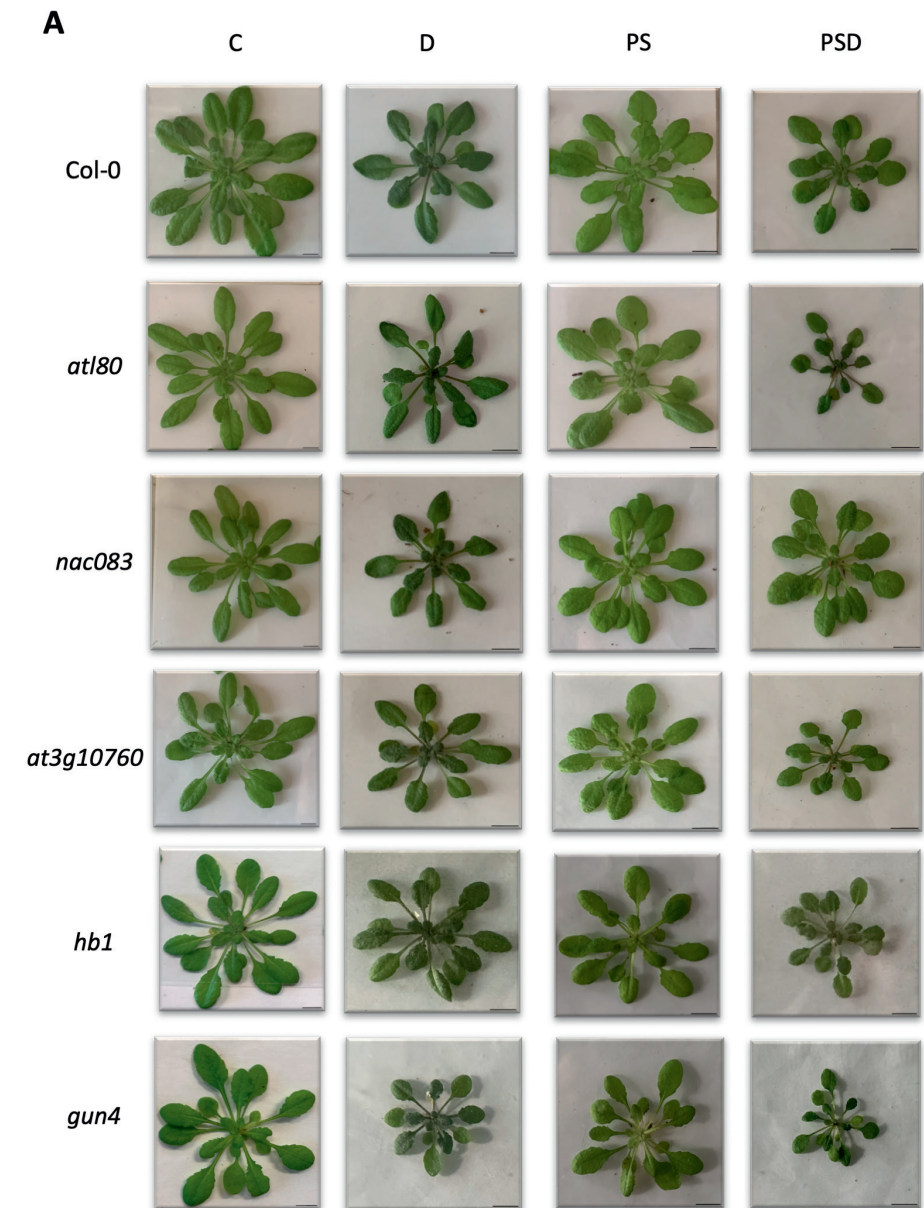


Figure 4.5 Effects of selected mutant genotypes on plant growth, development and wilting under PSD.

(A) Experimental scheme for the reverse genetic analysis. 2-leaf stage (LS2) *Arabidopsis* mutants and corresponding wild-type (WT) plants were pre-grown at 21°C (day and night) until they reached the 10-leaf stage (LS10). Subsequently, the plants were subjected to a 5-day submergence treatment in the light, followed by progressive drought (PSD) treatment upon de-submergence until wilting. Measurements of phenotypic traits were carried out at day 0 (moment of de-submergence), day 10 and the moment of wilting (*i.e.*, time point differed per plant). **(B)** Heatmaps showing the phenotypic traits of *Arabidopsis* mutants exhibiting either significantly advanced wilting time and/or a high %SWC relative to the corresponding wild-type plants (Col-0) during the subjection to PSD. The relative values of total leaf area, petiole/blade length and leaf number were calculated by normalizing the data obtained at day 10 to that of day 0 (left 4 panels). Dry weight and leaf number at wilting, days to wilting and %SWC at wilting are indicated as well (right 4 panels). The abbreviated names of tested mutants and the wild-type plants are indicated on the left. Color scales indicate relative values of measured traits (relative to the corresponding wild-type plants, Col-0). Underlined mutants indicate confirmed knockout of the corresponding genes based on previous studies (Table S4.2). Asterisks represent significant differences between mutants and the corresponding wild-type plants (Table S4.4) ($p < 0.05$, unpaired t-test, $n=8-12$).

We next tested the effects of the *atl80*, *nac083*, *at3g10760*, *hb1* and *gun4* mutants as well as the WT Col-0 on plant growth, development, and physiological responses

when drought (D) and post submergence (PS under well-watered conditions) were individually applied next to PSD (Figures 4.6 and 4.7). Given the universal effects of ABA signaling (Skubacz et al., 2016), the *abi5* mutants were not included for the validation test. Measurements of rosette traits and dry weight were taken at 0, 5, and 15 days after the treatments were initiated (note that for both PS and PSD, the 15-day treatment thus refers to 10-day PS/PSD) (Figures 4.6A-C, S4.4A-C). Of the five tested mutants, only *at180* showed a significant decrease in both dry weight accumulation and total leaf area compared to the WT when subjected to PSD and developed smaller rosettes and shorter leaves than the WT during both C and D (Figures 4.6A-C, S4.4A-C).



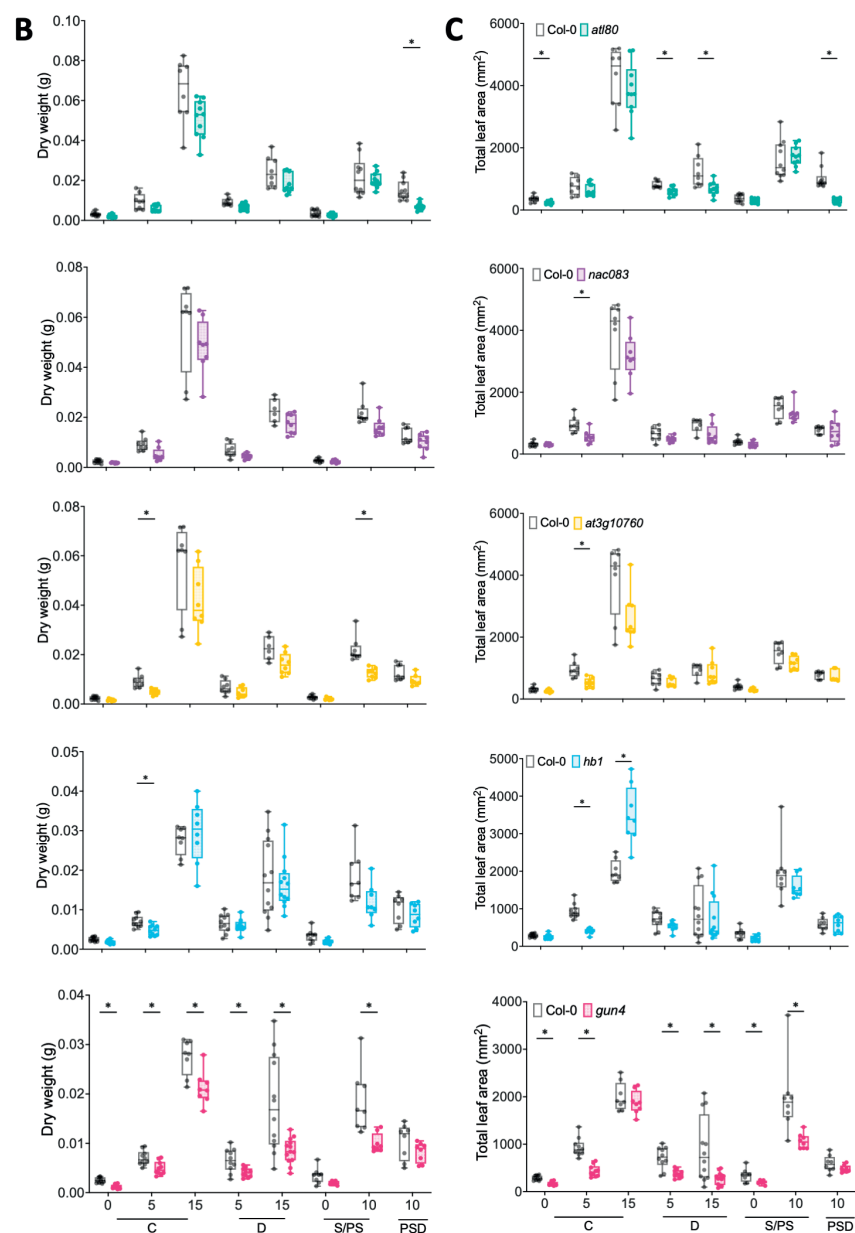


Figure 4.6 Effect of sequential stress; PSD, the related individual stresses of D, S/PS and control (C) on phenotypic traits of selected *Arabidopsis* mutants and the corresponding wild-type plants.

(A) Representative images of whole rosettes of the selected mutants and the corresponding wild-type plants (Col-0) on Jiffy coco pellet growth substrate subjected to single and sequential stresses 15 days after the treatments started. Scale bars indicate 1 cm. (B, C) Rosette dry weight (B) and total leaf area (C) of *Arabidopsis* mutants (*at180* (aqua), *nac083* (purple),

at3g10760 (yellow), *hb1* (azure) and *gun4* (magenta)) and the wild-type plants (Col-0; gray). For plants that wilted before the harvesting time points, the traits were measured on the day of wilting onset. Boxes indicate boundaries of the second and third quartiles (Q) of the data distribution. Horizontal bars indicate median and whiskers Q1 and Q4 values within 1.5 times the interquartile range. Asterisks represent significant differences between the mutant and the corresponding wild-type plants within the same time point ($p < 0.05$, multiple unpaired t-test with Holm-Šidák correction). Numbers indicate days after treatment started. Abbreviations; C; control, D; drought, S/PS; 5-day submergence / (post-)submergence & recovery, PSD; (post-)submergence & drought. $n = 6-13$.

Both *nac083* and *hb1* mutants had similar dry weights and total leaf area as the WT during the subjection to individual (D, S/PS) and sequential stresses (PSD) (Figure 4.6B-C). However, prolonged PS treatment resulted in decreased blade length and leaf number in *nac083* compared to the WT (Figures S4.4A and 4.4C). As reflected by a reduced dry weight accumulation, blade length and number of leaves during 10-day PS, the *at3g10760* mutant was unable to recover to the same extent as WT after submergence (PS), despite sufficient water being supplied during the post-submergence phase (Figures 4.6B, S4.4B-C). The *gun4* mutant appeared to be highly sensitive to both D and PS, as dry weight, total leaf area, leaf length and leaf initiation rate traits were significantly lower than the WT, even though *gun4* also exhibited a significant reduction in the above-mentioned traits relative to the WT under control conditions (C) (Figures 4.6B-C, S4.4A-C).

Measurements of chlorophyll content and stomatal conductance revealed that most of the mutants displayed comparable levels of chlorophyll and similar stomatal conductance as the WT (Figure 4.7A-B). The exception to this was *gun4*, which exhibited a high level of chlorophyll and a high stomatal conductance under 10-day C.

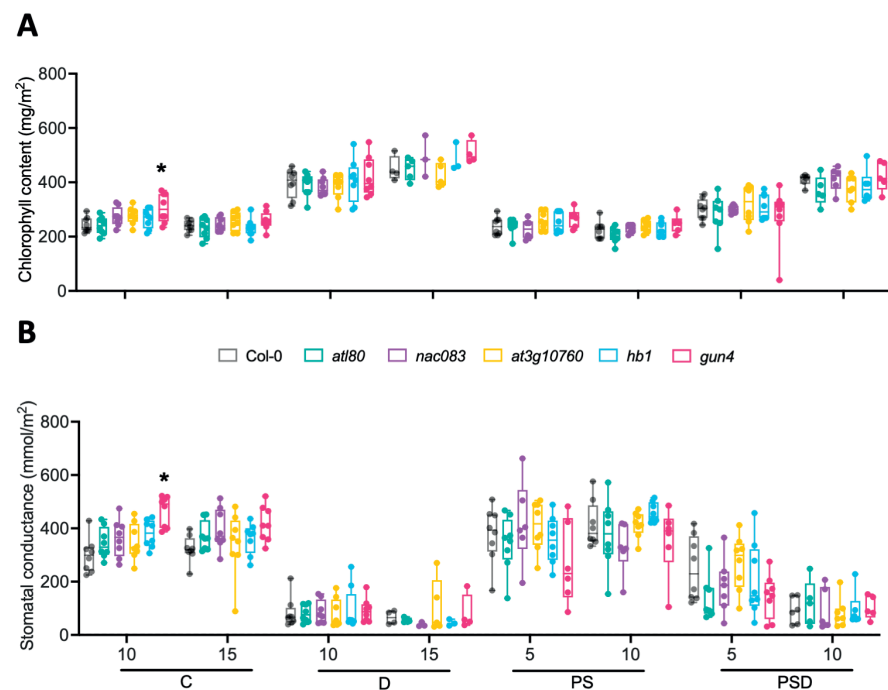


Figure 4.7 Effect of sequential stress PSD, and the related individual stresses of D, S/PS and control (C) on chlorophyll content and stomatal conductance of selected Arabidopsis mutants and corresponding wild-type plants.

(A, B) chlorophyll content (A) and stomatal conductance (B) of Arabidopsis mutants (*atl80* (aqua), *nac083* (purple), *at3g10760* (yellow), *hb1* (azure) and *gun4* (magenta)) and the wild-type plants (Col-0; gray). Boxes indicate boundaries of the second and third quartiles (Q) of the data distribution. Horizontal bars indicate median and whiskers Q1 and Q4 values within 1.5 times the interquartile range. Asterisks represent significant differences between the mutant and the corresponding wild-type plants within the same time point ($p < 0.05$, one-way ANOVA with Dunnett test). Numbers indicates days after treatment started. Abbreviations; C; control, D; drought, S/PS; 5-day submergence / (post-)submergence & recovery, PSD; (post-)submergence & drought. $n = 3-8$.

Principal component analysis reveals trait correlations and validates mutant effects under submergence followed by drought

Like with HTD, PCA analysis revealed clear correlations among measured traits under PSD (Figure 4.8B). Traits related to leaf development (relative total leaf area (RLA), relative petiole length (RPL) / relative blade length (RBL)) were positively correlated. Moreover, dry weight (DWW) and traits associated with leaf initiation (relative increase in leaf number (RLN) and leaf number at wilting (LNW)) were also correlated (Figure 4.8B). Days to wilting (DTW) and %SWC at wilting (%SWCW) were as expected

negatively correlated. Dry weight and total leaf area were selected to describe the genetic effects of mutations in selected candidate genes on plant growth and development.

Considering the mutants with no clear early wilting phenotype (Figure 4.8A), *DNA binding with one finger 2 (dof2)* showed a notable reduction in leaf formation rate and dry weight accumulation compared to the WT in response to PSD treatment (Figure 4.8A, Table S4.4). The *scl14* mutant showed increased relative total leaf area, whereas the number of leaves counted at wilting was lower than the WT (Figure 4.8A, Table S4.4). Interestingly, *hb34*, which displayed decreased petiole length and leaf formation rate relative to the WT, exhibited a typical leaf-rolling phenotype in response to PSD, but not under control (C) conditions (Figure S4.5A-B). Additionally, both *tcp22* and *nf-yb2* mutants had significantly longer leaf blades but had a reduced leaf initiation rate in comparison to the WT (Figure 4.8A, Table S4.4). This implies that both TCP22 and NF-YB2 might regulate blade lengthening and new leaf initiation during PSD. The *zfp4* mutant, only showed a lag in leaf formation in PSD (Figure 4.8A, Table S4.4). The *cytokinin-responsive GATA factor 1 (cga1)*, also known as *gnl* (Richter et al., 2013) mutant did not differ from WT in any of the measured traits during PSD (Figure 4.8A, Table S4.4). However, in combination with a knockout of a homolog of *CGA1*, *GATA NITRATE-INDUCIBLE CARBON-METABOLISM INVOLVED (GNC)* (the *gnlgnc* double mutant), plants accumulated less dry weight and had impaired leaf initiation in comparison with the WT (Figure 4.8A, Table S4.4). Additionally, both *atl66* and *cycling dof factor 3 (cdf3)* mutants had a larger leaf area and larger relative blade length (Figure 4.8A, Table S4.4), indicating that ATL66 and CDF3 might act as negative regulators of leaf development during PSD. Additionally, *flowering bhlh 2 (fbh2)* and *repressor of ga1-3 1 (rga1)* showed a significant reduction in relative leaf number compared to the WT when exposed to PSD (Figure 4.8A, Table S4.4).

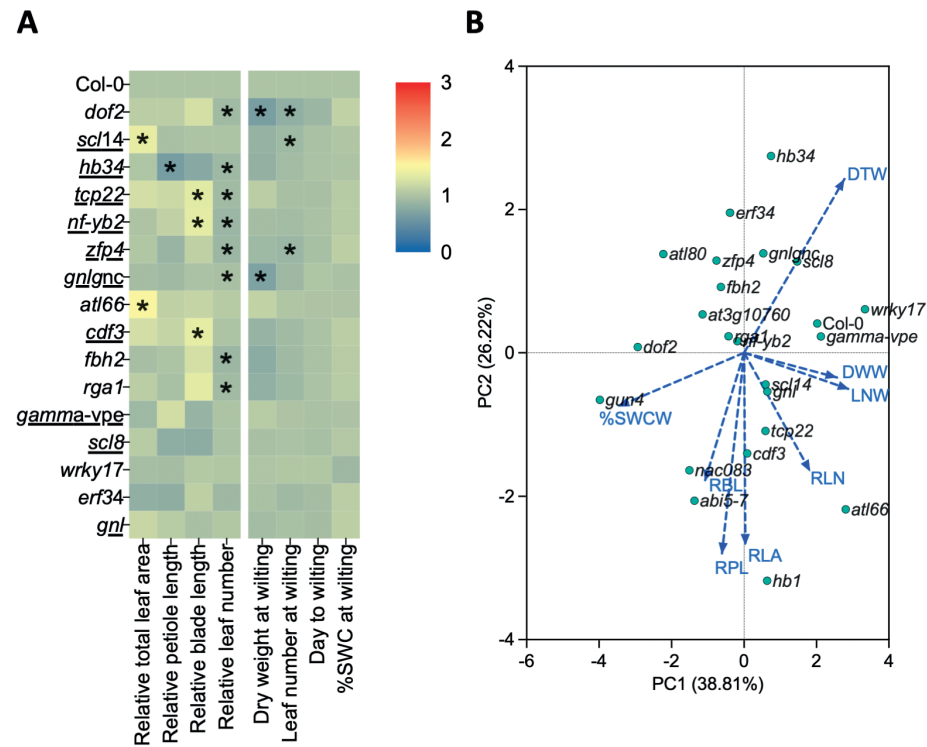


Figure 4.8 Effects of selected mutant genotypes on plant growth, development and wilting under PSD.

(A) Heatmaps showing the phenotypic traits of Arabidopsis mutants without early wilting phenotypes (opposed to those indicated in Figure 4.5) along with the corresponding wild-type plants (Col-0) in response to subjection to PSD. Relative values of total leaf area, petiole/blade length and leaf number were calculated by normalizing the data obtained at day 10 to that of day 0 (left 4 panels). Dry weight and leaf number at wilting, days to wilting and %SWC at wilting are indicated as well (right 4 panels). The abbreviated names of tested mutants and the wild-type plants are indicated on the left. Color scales indicate relative values of measured traits (relative to the corresponding wild-type Col-0). Underlined mutants indicate confirmed knockout of the corresponding genes as described in previous studies (Table S4.2). Asterisks represent significant differences between mutants and the corresponding wild-type plants for the particular trait (Table S4.4) ($p < 0.05$, unpaired t-test, $n=8-12$). **(B)** Principal component analysis (PCA) of measured traits of mutants and the corresponding wild-type plants (Col-0). Visualized are the distributions of mutants and wild-type plant indicated by symbols and correlations between measured traits, indicated by arrows. Abbreviations of traits: RLA; relative total leaf area, RPL; relative petiole length, RBL; relative blade length, RLN; relative leaf number, DWW; dry weight at wilting, LNW; leaf number at wilting, DTW; day to wilting, %SWCW; percentage of soil water content (%SWC) at wilting.

Discussion

Plant acclimation to abiotic stresses is governed by numerous molecular regulators and complex signal transduction networks, especially when multiple stresses co-occur (Zhang & Sonnewald, 2017; Zandalinas et al., 2020b). Signaling molecules controlling responsiveness to combinatorial stress can be different from those regulating the corresponding individual stresses (Rizhsky et al., 2004; Mittler, 2006a; Balfagón et al., 2019a; Zandalinas & Mittler, 2022; Da Ros et al., 2023).

In chapter 3, following a transcriptome profiling approach, we identified a set of candidate genes that putatively mediate the responses to combined (HTD) or sequential (PSD) sublethal stresses. In this chapter, we performed a reverse genetics analysis to validate the physiological functions of several of the identified candidate genes in combinatorial-stress response using T-DNA insertion mutants, of which several are confirmed knockouts as described in literature (Table S4.1 and S4.2). Our aim was to identify novel gene(s) mediating plant responses to combinatorial and/or the relevant individual stresses at the morphological, developmental, and physiological levels. The selection of candidate genes was based on upregulation of transcription factors under HTD or PSD in the RNA-seq data (See; Chapter 3 Figure 3.5). We also included putative (upregulated) regulators based on constructed gene regulatory networks (See; Chapter 3 Figure 3.6), and multi-stress responsive genes (See; Chapter 3 Figure 3.8). Although downregulation was not among the selection criteria, it is likely that some or several of the significantly downregulated DEGs in our RNA-seq dataset also play important roles in mediating responses to either combined or sequential stresses and are worthwhile to test in future experiments, despite these may not be easily identified using the mutant characterization approach, as used in this chapter.

A reverse genetics approach as conducted here is useful to screen for effects genes of interest may have. However, it should be interpreted with care, as this approach is not fully conclusive on the roles of factors whose single knock-out mutants are lacking phenotypes, as gene redundancy might mask their roles (Tax & Vernon, 2001). For further elucidation of the relevant functions of a certain candidate in response to a given combinatorial stress, additional research including assessment of independent mutant alleles, generation of overexpression lines, or functional validation of the homologs is needed (Bhaskara et al., 2022). Of note, in this chapter, our aim was to unveil genetic effects based on probing a broad range of candidates (TFs, Figure S4.1), rather than focusing on deciphering the precise molecular mechanisms underlying

selected genes, which would be the next stage in disclosing the roles of confirmed candidate genes in multi-stress tolerance.

Although most of the T-DNA insertion lines used in our study were confirmed as knockout mutants according to previous studies (Tables S4.1 and S4.2) and were additionally examined to ensure homozygosity here, it is still essential to verify whether the target genes are functionally knocked-out at the transcriptional and translational levels before drawing definite conclusions on their physiological functions under a certain stress condition, based on the observed phenotypes. Put in other words, absence of phenotypes in this study should be interpreted with care as long as the mutations are not all (yet) effectively characterized.

ABA signaling is relevant for plant acclimation to combined and sequential abiotic stresses

ABA signaling plays a pivotal role in plant responses to various individual and combinatorial abiotic stresses (Tuteja, 2007b; Sah et al., 2016; Suzuki et al., 2016c; Zandalinas et al., 2016a; Segarra-Medina et al., 2023). Considering its well-established role in drought responses (Sreenivasulu et al., 2012; Zhao et al., 2016c), the involvement of ABA signaling in stress combinations containing drought is perhaps not surprising. Our results confirmed the importance of ABA signaling in regulating plant growth, leaf development and wilting under both HTD and PSD and we observed pronounced phenotypic differences between *abi5-7*, an ABA insensitive mutant with pleiotropic defects in ABA responses (Finkelstein & Lynch, 2000; Skubacz et al., 2016), and the WT (Figure 4.1B, Table S4.3). In response to HTD, *abi5-7* showed in general enhanced leaf lengthening, but suppressed rosette expansion, leaf formation rate and dry weight accumulation relative to the WT (Figure 4.1B, Table S4.3), suggesting that ABA (signaling) may have a dual function in regulating plant growth and leaf development during HTD. This dual role aligns well with previous studies in which ABA was identified to have both inhibiting and stimulating effects on plant shoot growth, especially under water stress conditions (Saab et al., 1990; Sharp & LeNoble, 2002). In contrast to HTD, in which *abi5-7* displayed reduced total leaf area compared to the WT, ABA signaling seemingly controls rosette growth in a negative manner during PSD, as *abi5-7* mutant plants had a larger leaf area compared to the WT (Figure 4.5B, Table S4.4). This negative effect of ABA under PSD can possibly be explained by the observation that ABA-induced stomatal closure under water-limited conditions can compromise plant photosynthesis (Sreenivasulu et al., 2012; Negin et al., 2019).

ABA accumulation is closely associated with stress-induced plant wilting (Wright & Hiron, 1972; Zhang & Zhang, 1994; Tuteja, 2007b). In our study, both HTD and PSD

resulted in significantly accelerated wilting and/or a high level of %SWC retainment at wilting in *abi5-7* relative to the WT (Figures 4.1B and 4.5B, Table S4.3 and S4.4). Likely, the early wilting phenotype of *abi5-7* is attributed to the inability to close stomata (Kang et al., 2018; Liu et al., 2022b). This suggests an involvement of ABI5 / ABA signaling in the acclimation to both HTD and PSD.

Additionally, some mutants displayed phenotypic similarities to *abi5-7* when exposed to HTD or PSD, such as *nf-yb2* and *ilr3-1* under HTD or *nac083* under PSD (Figure 4.4B and 4.8B). This leads to the speculation that the corresponding TFs of these mutants might control plant growth and leaf development under combined or sequential stresses by affecting ABA in an unknown manner. ILR3 has, to the best of our knowledge, not been directly linked to ABA biosynthesis or signaling so far. But NF-YB2 is indeed known to function during ABA-mediated seed germination and dehydration stress response through an ABA dependent pathway (Kumimoto et al., 2013; Sato et al., 2019), while NAC083 has been demonstrated by previous studies to be an ABA responsive TF involved in modulating abiotic stress responses and plant senescence (Seo & Park, 2011; Yang et al., 2011). Taken together, NF-YB2 and NAC083 may control the morphological response to HTD or PSD downstream of ABA-signaling, but more work is needed to confirm this.

Novel regulators of combinatorial-stress responses

Although *elf6-3* did not differ pronouncedly from the WT in terms of rosette growth and development (*i.e.* relative leaf lengthening, total leaf area and dry weight at wilting) according to the initial reverse genetics screen data (Figure 4.1B), the subsequent functional validation of early wilting mutants (*zfp4*, *elf6-3*, *at5g12310* and *vip1*) highlighted that ELF6 might be negatively controlling biomass (dry weight) accumulation and rosette development, but positively regulates plant wilting under HTD (Figure 4.2B-C). ELF6 was initially identified as a repressor in the photoperiodic flowering pathway as its loss-of-function mutant leads to an early flowering phenotype (Noh et al., 2004; Yu et al., 2008). Additionally, both ELF6 and its close homolog RELATIVE OF EARLY FLOWERING 6 (REF6), are characterized as main histone H3 at Lys27 trimethylation (H3K27me3) demethylases in Arabidopsis (Lu et al., 2011; Crevillén et al., 2014; He et al., 2022). H3K27me3 is crucial for the regulation of plant thermomorphogenesis and heat stress memory (Casal & Balasubramanian, 2019; Yamaguchi et al., 2021; Perrella et al., 2022). For example, enhanced hypocotyl elongation (a typical shoot thermomorphogenesis phenotype (Park et al., 2017; Delker et al., 2022)) of plants grown under high ambient temperature is likely accomplished by PICKLE (PKL)-dependent removal of H3K27me3 (Jing et al., 2013; Zha et al., 2017; Perrella et al., 2022). Therefore, it can be hypothesized that the involvement of ELF6 in

regulating plant growth and development under HTD in our work may be somehow related to H3K27me3-mediated high temperature responses. The physiological and molecular function of ELF6 in governing the acclimation to HTD or HT deserves further investigation.

Of the 5 early wilting mutants characterized under PSD conditions (*atl80*, *nac083*, *at3g10760*, *hb1* and *gun4*), ATL80 stood out as the only TF that apparently positively modulates plant growth, leaf development as well as wilting during PSD (Figures 4.5B). Moreover, ATL80 may participate in controlling leaf lengthening during individually applied D conditions (Figures 4.6B and S4.4A-B). Next to acting as a TF controlling the expression of downstream target genes, ATL80 protein is known as a plasma membrane-localized RING E3 ubiquitin ligase that negatively regulates cold stress response and phosphate mobilization (Suh & Kim, 2015). However, it is unclear whether ATL80 regulates the response to PSD and/or D through a similar regulatory mechanism. Nonetheless, future studies on deciphering the molecular mechanisms underlying the acclimation strategy of PSD can particularly focus on the ATL80 and its target proteins.

Next to ELF6 and ATL80 as master regulators for combinatorial stresses, our results also highlighted several genes governing morphological response to multiple isolated stresses. For example, ZFP4 was identified as a positive regulator of plant growth and leaf development under HT and D, but not HTD (Figures 4.2B and 4.2C), although the *zfp4* mutant retained high %SWC at wilting (Figure 4.1B). Previous research implicates ZFP4 in vascular development and aliphatic glucosinolate biosynthesis (Li et al., 2018b; Smit et al., 2020). Together with its homolog ZFP3, ZFP4 has at least a partially redundant biological function in controlling ABA response during seed germination (Joseph et al., 2014). A recent finding discovered that ZFP1, another close homolog of ZFP4, controls root hair initiation and elongation (Han et al., 2020), which is relevant to plant drought resilience (Comas et al., 2013; Marin et al., 2021; Duddek et al., 2022). Further investigations are needed to determine whether ZFP4 governs the acclimation to D and HTD through analogous mechanisms as its homologs (*e.g.*, via the control of ABA signaling and/or root hair development).

Under PSD, GUN4 appeared to positively regulate plant dry weight accumulation and leaf initiation. GUN4 is identified as a crucial factor in regulating multiple generic processes such as chlorophyll synthesis, ROS homeostasis, photoprotection and plastid retrograde signaling (Li et al., 2021b), thus the precise role of GUN4 in PSD acclimation remains ambiguous, especially since we did not observe a deviating chlorophyll content in the *gun4* mutant. However, because our transcriptomic data implicates the relevance of photosynthesis-related processes in PSD acclimation (See; Chapter

3, Figure 3.4), we hypothesize that GUN4 may positively modulate plant development through retrograde signaling under PSD.

In Chapter 2, we demonstrated that increased chlorophyll content in young leaves under D (also HTD and PSD) is likely part of the acclimation strategy plants adopt to cope with stressful conditions (See, Chapter 2 Figures 2.6 and 2.8). Here, our results showed that all tested HTD-relative mutants with altered wilting phenotypes (*zfp4*, *elf6-3*, *vip1*, *at5g12310*) had a lower chlorophyll abundance in young leaves than the WT, specifically under 10-day HTD (Figure 4.3A). On the contrary, *vip1* and *at5g12310* had a higher chlorophyll abundance than WT under D, but not HT. This suggests that the corresponding TFs of the mutants may control HTD-triggered plant wilting, at least partly, through the regulation of chlorophyll accumulation in a complex and not yet understood manner. However, both *vip1* and *at5g12310* mutants exhibited a remarkable decrease in stomatal conductance under D. Together with the increased chlorophyll content, our result implicates possible (novel) functions of both VIP1 and AT5G12310 in antagonizing chlorophyll accumulation and stomatal closure during the subjection to D. Our results also showed that the five selected early wilting mutants (*atl80*, *nac083*, *at3g10760*, *hb1* and *gun4*) exhibited similar levels of chlorophyll content and stomatal conductance under D, PS and PSD (Figure 4.7A-B). This suggests that these TFs might not directly affect plant growth, leaf development or wilting via effects on stomata or chlorophyll but the control of other physiological processes.

Finally, some of the candidate genes tested might also impact root phenotypes and thereby the responsiveness to HTD or PSD, since root traits are important in acclimation to drought-associated stresses (Comas et al., 2013; Kang et al., 2022; Reinelt et al., 2023). However, it is hard to draw reliable conclusions here considering the focus on shoot traits in our present study.

Genetic factors coordinate the phenotypic responses to combinatorial stresses

According to observed diversity in phenotypic traits of the mutants (Figures 4.1B, 4.4A-B, 4.5B and 4.8A-B, Table S4.3 and S4.4), different aspects of the overall acclimation strategies of plant growth, development and wilting under HTD or PSD, are coordinated by different genetic factors (candidate genes or TFs). These factors may together or individually contribute to a certain phenotypic response. For example, in response to HTD, TFs such as TLP18.3, BTL13, TCP22 and HB2 are likely involved in orchestrating leaf elongation, possibly as negative regulators, as their corresponding mutant lines displayed induced relative leaf lengthening (Figure 4.4 A-B, Table S4.3).

Upon PSD treatment, HB1 and CDF3 seemingly inhibit the lengthening of petiole and blade (Figures 4.5B and 4.6B, Table S4.3).

We found that certain genetic factors have specific roles depending on the identity of the applied (combinatorial) stress. For example, HB1 is likely a positive regulator of rosette development under HTD (Figure 4.4A), whereas it might negatively control both rosette expansion and blade lengthening during PSD (Figure 4.5B). The role of HB1 in controlling leaf development is in line with a previous study (Miguel et al., 2020), in which *HB1* overexpression in *Arabidopsis* led to an atypical leaf phenotype of deep serration. However, in subsequent functional validation, the *hb1* mutant only showed distinct growth and leaf development/lengthening (relative to the WT) under control conditions (C), but not under any of the stress conditions (Figures 4.6 and S4.4). Although we do not fully grasp the cause of this inconsistency, it may arise from the experimental settings as small variations in soil water loss when manipulating drought in the growth chamber. Additionally, the adopted approaches for data normalization and statistic analysis can also be reasons for some inconsistencies in our work. For example, the *pif4-2* mutant displays a significant reduction in petiole lengthening in combined stress (HTD) and the corresponding control conditions (C, D and HT) compared to the WT (Figure S4.2). However, according to the results of reverse genetics screening, the reduction in relative petiole length of *pif4-2* is not statistically significant (Figure 4.4, Table S4.3).

Intriguingly, we observed that the *ilr3-1* mutant displayed an exaggerated hyponastic growth phenotype under both HT and HTD conditions (Figure S4.3A-B). In *Arabidopsis*, leaf hyponasty is considered a typical morphological adaptation to elevated ambient temperature, driven by increased auxin levels and signaling following PIF4 activation (Koini et al., 2009; Quint et al., 2016; Park et al., 2019). However, the *ilr3-1* mutant has been documented to show diminished sensitivity to indole-3-acetic acid (IAA) conjugates IAA-Leu and IAA-Phe, while maintaining WT response to free bioactive IAA (Rampey et al., 2006). Additionally, the downstream target genes of ILR3 are responsible for encoding metal transporters, which might indirectly modulate IAA-conjugate hydrolysis by controlling the availability of metals that influence IAA-amino acid hydrolase protein activity (Rampey et al., 2006). Accordingly, the exaggerated hyponastic growth phenotype of *ilr3-1* under high ambient temperature (HT and HTD) may be associated with the altered sensitivity of auxin conjugate(s). Further investigation into crosstalk between ILR3-regulated iron homeostasis and high temperature response is therefore a potentially promising way forward.

We also found that *hb34* displayed a distinctive leaf rolling phenotype upon PSD (Figure S4.5A-B). Leaf rolling serves as a protective mechanism against excessive water loss by transpiration (Kadioglu et al., 2012; Yang et al., 2022a). Among the factors accounting for plant leaf rolling are proteins related to cell wall, particularly secondary cell wall biosynthesis or formation (Zhu et al., 2022b; De Souza et al., 2023). It has recently been discovered that *SQUAMOSA PROMOTER BINDING PROTEIN-LIKE 10 (SPL10)*, which is characterized to be functionally associated with cell wall development (Bascom, 2023), is a direct downstream target of HB34 (Lee et al., 2022). Collectively, HB34 in our study thus may participate in negatively controlling cell wall development and thereby affect leaf rolling and (possibly) lengthening during PSD, which may consequently lead to enhanced transpiration and thereafter water loss.

In conclusion, the reverse genetics approach adopted here to validate selected candidate genes identified from our transcriptomics dataset yielded several promising candidates for further investigations into the complex regulatory networks mediating multi-stress acclimation.

Acknowledgements

This work is supported by the Netherlands Organization for Scientific Research (NWO) (project no. 867.15.031 to AV) and the China Scholarship Council (CSC) (project no. 20186170025 to ZJ). We thank Christian Dubos (University of Montpellier, France) for providing us with the seeds of *ilr3-1* and *ilr3-3* and Yorit van de Kaa for seed harvesting.

Materials and methods

Plant materials and growth conditions

Arabidopsis thaliana wild-type Columbia-0 (Col-0; NASC stock center ID: N1092), Columbia-3 (Col-3; NASC stock center ID: N908) and T-DNA insertion mutants (Tables S4.1 and S4.2) were grown as described in Chapter 2. In brief, stratified seeds were germinated in a climate-controlled growth chamber (8 h photoperiod / 16 h darkness, 21 °C, 120-150 $\mu\text{mol m}^{-2} \text{s}^{-1}$ PAR with LED lightening, 70% relative humidity) until they reached 2-true-leaf stage (LS2). Individual plants were then transferred to Jiffy 7c coconut pellets (Jiffy Products International BV, Zwijndrecht, The Netherlands) presoaked in 50 mL Hoagland solution (Millenaar et al., 2005) followed by saturation with deionized water to a final weight of 250 ± 20 g per pellet. Plants subjected to high temperature treatments (HT and HTD) were transferred to a growth chamber set at 27 °C, with otherwise identical conditions as used for the rest of treatments at 21

°C (C, D, S/PS, PSD). Nutrition supplementation and randomization were performed as described in Chapter 2 (See; Chapter 2 Materials and Methods).

Stress treatments

Plants were subjected to individual (S, PS, D, HT) or combinatorial stresses (HTD, PSD) or kept at control conditions (C). Stress treatments for phenotypic and physiological validations were applied on plants that reached the 10-true-leaf stage (LS10), as described in Chapter 2. For each stress treatment, wild-type and mutant plants were randomized in the experimental setups and growth chambers to avoid position effects.

Confirmation of T-DNA insertion lines

Fresh leaves were detached and gDNA was extracted using Direct PCR-Phire and Phusion kit (Thermo Scientific, Inc, USA) following the manufacturers protocol. In brief, dissected leaves were initially submerged in the Dilution Buffer (Thermo Scientific, Inc, USA). Subsequently, leaves were briefly crushed against the tube wall with a pipette tip. When the solution became greenish, the supernatant was used for PCR after centrifugation. The presence of the T-DNA insertions and the homozygosity were determined by PCR using the primer pairs indicated in Tables S4.1 and S4.2.

Measurements of rosette traits and dry weight

Rosette traits and dry weight were measured as described in Chapter 2. Briefly, side and top pictures of the rosette plants subjected to different stress treatments and controls were taken with a regular camera. Thereafter the entire rosette was oven-dried at 80 °C for 3 days to dry weight was determined using an ultra-balance. The number of leaves, plant hyponasty, total rosette area, and petiole and blade length of the young leaves (7th - 10th leaves, counting from the earliest emerged leaves after LS2) were quantified using ImageJ software (National Institutes of Health, USA).

Measurements of physiological traits

Chlorophyll content and stomatal conductance were measured as described in Chapter 2. In brief, young leaves (7th - 10th leaves) of plants were dissected and chlorophyll content and stomatal conductance were immediately measured using a pre-calibrated CM-300 Chlorophyll Meter (Opti-Sciences Inc., Hudson, USA) and an SC-1 Leaf Porometer (Decagon Devices, Inc., Pullman, USA), respectively.

Statistical analysis

Figures in this chapter were generated using GraphPad Prism 9 (GraphPad Software, La Jolla, USA) and Biorender.com. Unpaired t-test, multiple t-test and one-way ANOVA

followed by post hoc analysis of Holm-Šidák correction (multiple t-test) or Dunnett test (one-way ANOVA), were performed by GraphPad Prism 9. Significance was considered as $p < 0.05$.

Supplemental data

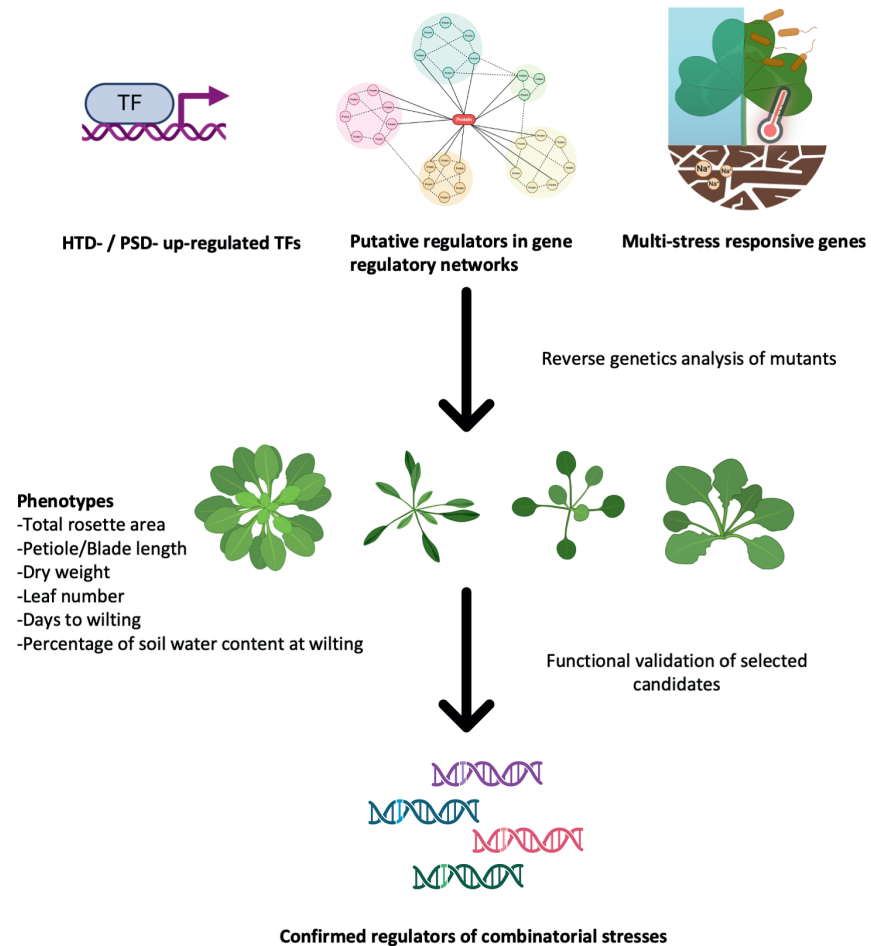


Figure S4.1 Experimental approach for the characterization of effects of selected candidate genes on plant growth, development, and physiology during the subjection to combinatorial abiotic stresses.

Mutants of selected (upregulated) candidate genes identified by a transcriptomics approach (Chapter 3) were tested for their phenotypic responses upon subjection to combinatorial stresses; i) combined high temperature and drought (HTD) and ii) submergence followed by drought (PSD). Thereafter mutants that exhibited a clear effect on plant survival (wilting) were selected for further functional validation by assessing developmental, morphological, and physiological responses under both combinatorial stresses and the corresponding individual stresses in more detail.

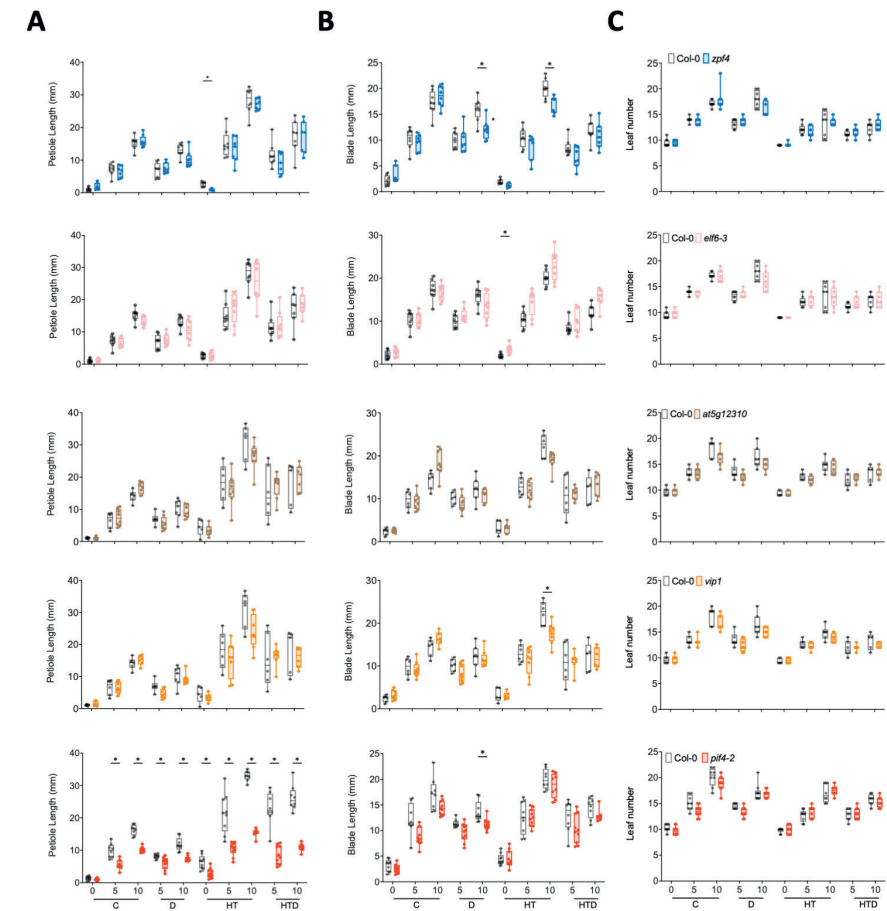


Figure S4.2 Effect of combined HTD stress, the individual stresses D, HT and controls (C) on leaf development traits of selected Arabidopsis mutants.

(A, B, C) Average lengths of petiole (A) and blade (B) of young leaves, and leaf number (C) of Arabidopsis mutants (*zfp4* (blue), *elf6-3* (pink), *at5g12310* (brown), *vip1* (orange) and *pif4-2* (red)) and the wild-type plants (Col-0; grey). Box plots show the median and boxes indicate boundaries of the second and third quartiles (Q1 and Q3) of the data distribution. Whiskers indicate Q1 and Q4 values within 1.5 times the interquartile range. Asterisks represent significant differences between the mutant and the corresponding wild-type plants within the same timepoint ($p < 0.05$, multiple unpaired t-test with Holm-Šidák correction). Numbers indicates days after treatment started. Abbreviations; C; control, D; drought, HT; high temperature, HTD; high temperature & drought. $n = 5-10$.

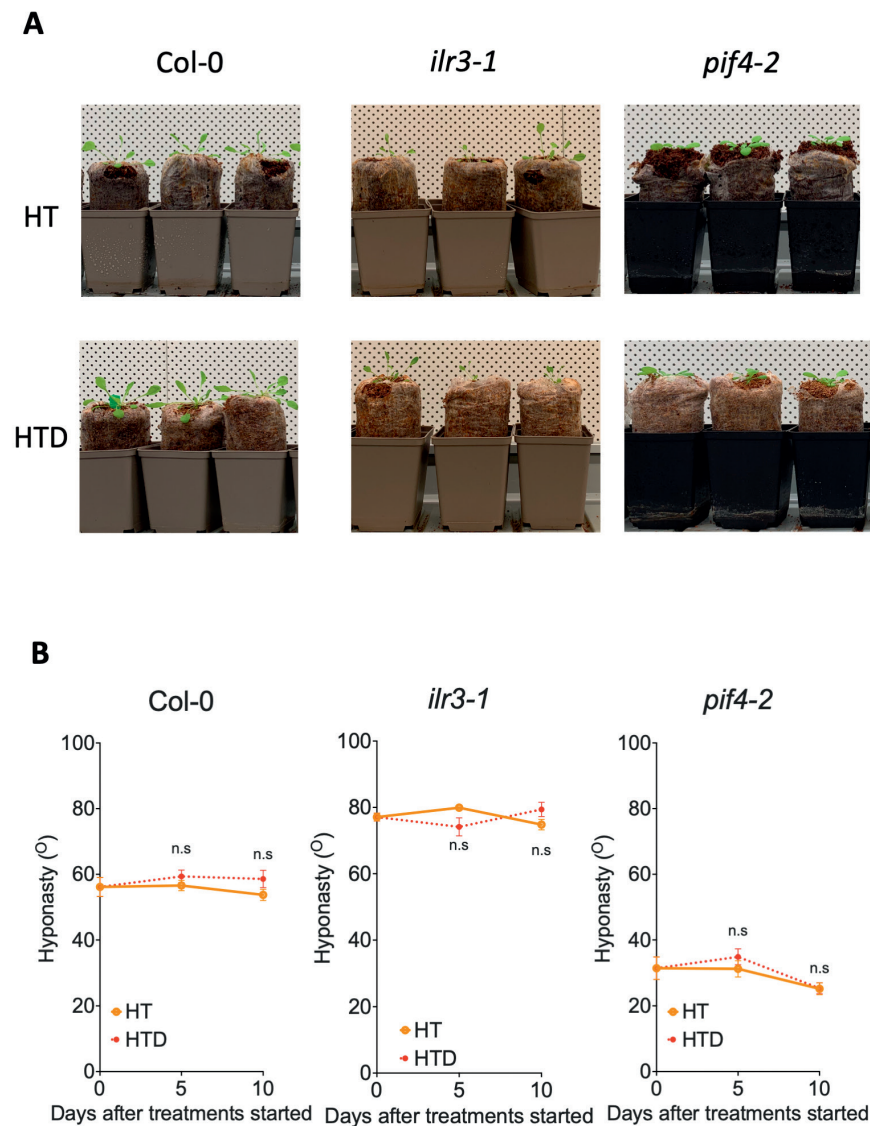


Figure S4.3 Leaf hyponasty of *ilr3* and *pif4* mutants and wild-type plants during subjection to high temperature-related treatments.

(A) Representative rosette (side) images of Col-0 (left), *ilr3-1* (middle) and *pif4-2* (right) upon 5-day high temperature (HT, upper row) or combined high temperature and drought (HTD, lower row) treatment. Note the exaggerated hyponastic response of *ilr3-1* and absence of response in *pif4-2*. (B) Average angles of the 2 most hyponastic leaves of individual plants, relative to the horizontal. Red dashed lines represent HTD treatment and solid orange lines indicate HT treatment. The letter 'n.s.' represents no significant differences between treatments within the same timepoint ($p > 0.05$, unpaired t-test). Abbreviations; C; control, D; drought, HT; high temperature, HTD; high temperature & drought. $n = 5-10$.

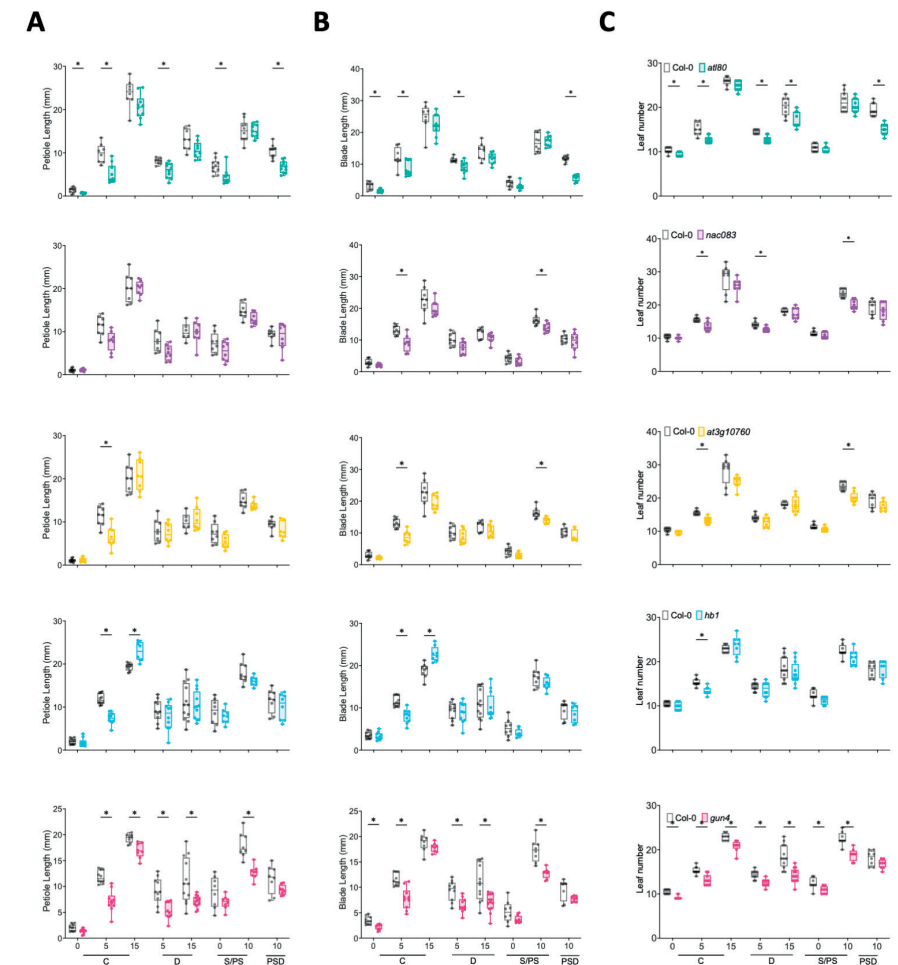


Figure S4.4 Effect of sequential stress PSD, the individual stresses D, S/PS and control (C) on leaf development of the selected Arabidopsis mutants.

(A, B, C) Average lengths of petiole (A) and blade (B) of young leaves, and (C) leaf number of Arabidopsis mutants (*at180* (aqua), *nac083* (purple), *at3g10760* (yellow), *hb1* (azure) and *gun4* (magenta)) and the wild-type plants (Col-0; grey). Box plots show the median and boxes indicate boundaries of the second and third quartiles (Q1 and Q3) of the data distribution. Whiskers indicate Q1 and Q4 values within 1.5 times the interquartile range. Asterisks represent significant differences between the mutant and the corresponding wild-type plants within the same timepoint ($p < 0.05$, multiple unpaired t-test with Holm-Sídák correction). Numbers indicate days after treatment started. Abbreviations; C; control, D; drought, S/PS; 5-day submergence / (post-)submergence & recovery, PSD; (post-)submergence & drought. $n = 6-13$.

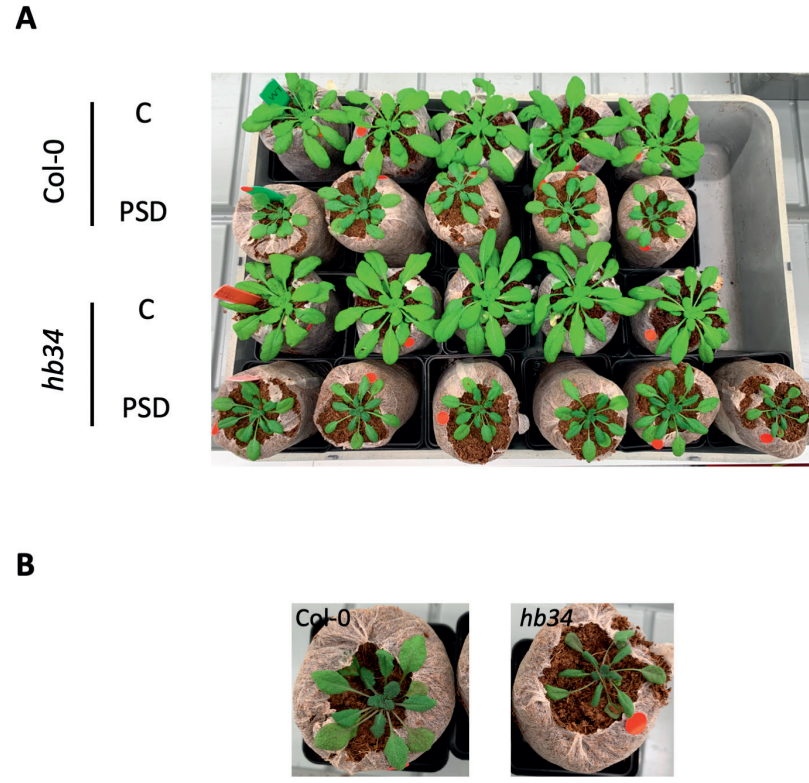


Figure S4.5 Representative images of Col-0 (upper two rows) and *hb34* mutant (lower two rows) plants on Jiffy coco pellet growth substrate, subjected to control (C; 1st and 3rd row) and submergence followed by drought (PSD; 2nd and 4th row) at (A) 15 days after treatments started (B) the day of wilting.

Table S4.1 List of T-DNA insertion mutants used for HTD in this study.

Indicated are AGI gene locus ID, the commonly used abbreviation of the mutants, SALK number or resource publications, primers used for genotyping (including forward, reverse and insertion primers), publications that confirmed the knockout of the corresponding SALK line, status of homozygosity and the insertion position of T-DNA.

Locus ID	Mutant Name	SALK ID/ Resource	Forward primer	Reverse primer	Insertion primer	Studies confirmed knockout function	Homozygous availability	T-DNA insertion position
AT1G50640	<i>erf3</i>	SALK_200697C	CGATCTGGGCATTAATTTTG	CCTCTCTCTCTAATCTCCG	CGTCAAGCTCTAAATCGGGG		No	
AT2G23340	<i>dear3</i>	SALK_116495	TGATCGGCCTTCACATTTTC	ATGCATCCAACTCGATTTCC	CGTCAAGCTCTAAATCGGGG		No	
AT3G43240	<i>arid5</i>	SALK_111627C	AGCCCACTCCACATGATC	TGCCAACAGAAAAAGATCC	CGTCAAGCTCTAAATCGGGG	(Zhao et al., 2021b)	Yes	Exon
AT5G54680	<i>ilr3-1</i>	(Rampey et al., 2006)	AGAAATCGCTATGGAATTG TTTATGGTTCT	CATTGTTCAACACAGATAACAGT TACGATGAT	-	(Tissot et al., 2019)	Yes	Exon
AT2G40950	<i>bzip17</i>	SALK_004048C	GAGAGGATGCTGACGCTAGTG	ATTACCTGCAACACCTTTCACG	ATTTTGCCGATTTTCGGAAC	(Cifuentes-Esquivel et al., 2018)	Yes	Exon
AT3G10800	<i>bzip28</i>	SALK_132285	CACCATTAATTTCTTAACCCAAGC	GTTGCCCTTAAAGGACATTTCTC	GCGTGGACCGCTTGCTGCAACT	(Gao et al., 2008)	Yes	Exon
AT3G10800/ At1g42990	<i>bzip28/bzip60</i>	SALK_132285 (BZIP28), SALK_050203 (BZIP60)	GGAAGAAAAGTCCTCTCGGAG (BZIP60)	CACAGCATCATCGTCTCTCTTC (BZIP60)	CGTCAAGCTCTAAATCGGGG	(Sun et al., 2013b)	Yes	Exon (Both)
AT1G43700	<i>vip1</i>	SALK_080470C	CAAGGGATGCAACAATCATG	CCTCAGGGGAATGGAATTC	CGTCAAGCTCTAAATCGGGG		Yes	3'UTR
AT1G78700	<i>beh4</i>	SALK_025953	TTTTTGGGAAAGCAAGTTGG	AAAAGATTACGGTCGGGGAC	CGTCAAGCTCTAAATCGGGG		No	
AT1G66140	<i>zfp4</i>	SALK_038923C	TGCCATTATGTGTCAGCAAC	CTGCTGCTCCGGTTACTAC	CGTCAAGCTCTAAATCGGGG	(Joseph et al., 2014)	Yes	5'UTR
AT1G01930	<i>at1g01930</i>	-	-	-	-		No	
AT5G04240	<i>elf6-3</i>	SALK_074694C	AGCCAAAAGCAATAAGACC	TACCCAAGCCATCGAAAAG	CGTCAAGCTCTAAATCGGGG	(Keyzor et al., 2021)	Yes	Exon
AT2G27100	<i>se-1</i>	SALK_059424	AGGACGTGGAGTTATGGTG	CAGAAAGGAAACTGAGAGCG	CGTCAAGCTCTAAATCGGGG	(Lobbes et al., 2006)	Yes	CDS

Table S4.1: Continued

Locus ID	Mutant Name	SALK ID/ Resource	Forward primer	Reverse primer	Insertion primer	Studies confirmed knockout function	Homozygous availability	T-DNA insertion position
AT4G04885	<i>pcf5-1</i>	SALK_102934C	GAAGAGGATGCATGGCTTC	ATGCATCATGTGTCGTTTGG	CGTCAAGCTCTAAATCGGGG		No	
AT5G12310	<i>at5g12310</i>	SALK_123983C	TACACCACCAAAATTTGGC	ATTTTCTCAATGTCACGGC	CGTCAAGCTCTAAATCGGGG		Yes	CDS
AT1G74410	<i>at124</i>	SALK_046988	TCTTCCGACTTGGACACAG	AGTTTGCATGTCATGCATGC	CGTCAAGCTCTAAATCGGGG		No	
AT1G80400	<i>at1g80400</i>	SALK_023687C	AAGCTGGGTTTCAAGTTTG	TTGGCCTCAATTAATTTGGG	CGTCAAGCTCTAAATCGGGG		Yes	Exon
AT3G60080	<i>bh13</i>	SAIL_1153_F01	CATCAAACGGTTGTCGTTTG	AATCATCGGTGGAACAGAC	CTGAATTTTATAAACC AATCTCG		Yes, Col-3 background with multiple loci	5'UTR
AT3G11110	<i>at166</i>	WisDslLoxHs 207_06D	AAACAACCCAGCTGCTTACG	AGTCTGGTGTGGCAAATTC	TTTCTCCATTTGACCATCAT ACTCATTG		Yes, with multiple loci	3'UTR
AT5G47640	<i>nf-yb2</i>	SALK_025666	ATCACC AACACCAATGTTCCG	AGATCAATTC AATCCGAGC	CGTCAAGCTCTAAATCGGGG	(Sato et al., 2019)	Yes	Exon
AT1G21450	<i>scl1</i>	SALK_102071	TTTTGGAGATTACCAAGCG	TCTGGGAAAGAACGGTGGAAG	CGTCAAGCTCTAAATCGGGG		Yes	Exon
AT5G52510	<i>scl8</i>	SALK_129947	GTCCACCTTCTCCGATATCG	GTGGTGGTGGATTTTTAC	CGTCAAGCTCTAAATCGGGG	(Ziemer, 2008)	Yes	CDS
AT1G07530	<i>scl14</i>	SALK_126931	GGTCTCACACAAAATAATG	AGCAGTTGAAGACCCAAAG	CGTCAAGCTCTAAATCGGGG	(Fode et al., 2008)	Yes	5'UTR
AT3G01470	<i>hb1</i>	SALK_207381C	CCTGGATCTGAGCTTATCG	GGTATAAAAAGACGGCGCTTG	CGTCAAGCTCTAAATCGGGG	(Capella et al., 2015)	Yes	5'UTR
AT4G16780	<i>hb2</i>	SALK_106790C	CTCAGCACTCAACGATCTAACC	ATTCTCTTTGAGCCTTGTGG	CGTCAAGCTCTAAATCGGGG	(Stamm et al., 2012)	Yes	Exon
AT4G11660	<i>hsfb2b</i>	SALK_137357C	AAAAAAGAAATACATTTTCCAA CTTATCTC	TTCTGTTCCACGAGATCAATTC	CGTCAAGCTCTAAATCGGGG		Yes	Exon
AT4G36990	<i>hsf4</i>	SALK_070065C	TCTCTTTTCTGTCGTGTTTG	AAGGTTTTCTCACCAACCC	CGTCAAGCTCTAAATCGGGG		Yes	5'UTR
AT5G60890	<i>myb34</i>	WisDslLox424F3	TCCGGGAATTTTCAATAAC	ATGGTGAGGACACCATGTTG	TTTCTCCATTTGACCATCAT ACTCATTG	(Frerigmann & Gigolashvili, 2014)	Yes	CDS

Table S4.1: Continued

Locus ID	Mutant Name	SALK ID/ Resource	Forward primer	Reverse primer	Insertion primer	Studies confirmed knockout function	Homozygous availability	T-DNA insertion position
AT5G67300	<i>myb44</i>	SALK_008606	TTGTC AATTTGTCATGCACTG	TCGCCCATTTAATCCGAAC	CGTCAAGCTCTAAATCGGGG	(Zhao et al., 2016b)	Yes	Exon
AT1G09770	<i>cdc5</i>	SAIL_207_F03	TGTACGACCACAAATAGGAGC	ATACTTGAATGCCGAAACCC	CTGAATTTTATAAACC AATCTCG		No	
AT2G45680	<i>tcp9</i>	SALK_143587	TAAAAATCCGACGACGAC	GGACCATGACTTAGAGAGGGC	CGTCAAGCTCTAAATCGGGG		Yes	
AT1G35560	<i>tcp23</i>	SALK_203816C	ATATCCGGCTAACCCCTAG	TCAAGATCACCTAACCCGGG	CGTCAAGCTCTAAATCGGGG		Yes	3'UTR
AT1G72010	<i>tcp22</i>	SALK_027490	TGTTGGGTTCTCTATCTCG	GAGTTAGCTCAGGGTCGTGG	CGTCAAGCTCTAAATCGGGG	(Aguilar-Martinez & Sinha, 2013)	Yes	Exon
AT1G53320	<i>tlp7</i>	SALK_120547	GATTTTACCCGGGTATAC	CGAATTTTGTGTAAGC AACTTC	CGTCAAGCTCTAAATCGGGG		No	
AT1G71260	<i>why2</i>	SALK_016156C	CCATGCAGGGTAAATTTAAC	CGCTTACTTCAAATCCGAGG	CGTCAAGCTCTAAATCGGGG	(Cappadocia et al., 2010)	Yes	CDS
AT2G43010	<i>plf4-2</i>	SAIL_1288_E07	GGGAAACAGAAATGGAACAG	ACCTAGTGTCCAAAGAGA	CTGAATTTTATAAACC AATCTCG	(Sang et al., 2023)	Yes	CDS&Exon
AT2G36270	<i>abi5-7</i>	(Nambara et al., 2002)	CGTCAGAGCGAAGTAGAG	GCGGGCGGGGCGCGGGGGG ATGTTATTATTCTCTCTGCGAT	-	(Zhao et al., 2020a)	Yes	G-to-A mutation at 225 bp
AT4G32940	<i>gamma-vpe</i>	SALK_010372	GGTGCTTTTCGGTACTTCAIG	TTTGCTGTGATCCTTGGAGAC	CGTCAAGCTCTAAATCGGGG	(Albertini et al., 2014)	Yes	Exon
AT1G54780	<i>tlp18.3</i>	SALK_109618	TGTCGGTTGCTAGTACTGC	TCAAAAACCCACCACTTCTC	CGTCAAGCTCTAAATCGGGG	(Ansari & Lin, 2010)	Yes	Intron
AT5G41410	<i>bel1</i>	-	-	-	-		No	

Table S4.2 List of T-DNA insertion mutants used for PSD in this study.

Indicated are AGI gene locus ID, the commonly used abbreviation of the mutants, SALK number or resource publications, primers used for genotyping (including forward, reverse and insertion primers), publications that confirmed the knockout of the corresponding SALK line, status of homozygosity and the insertion position of T-DNA.

Locus ID	Mutant Name	SALK ID/ Resource	Forward primer	Reverse primer	Insertion primer	Studies confirmed knockout function	Homozygous availability	T-DNA insertion position
AT5G26210	<i>al4</i>	SALK_087658	TACTGGTCCGAAAACCCCTG	GGCTCAAGGAAAAGCATCTC	CGTCAAGCTCTAAATCGGGG		No	
AT2G44940	<i>erf34</i>	SALK_020979C	TTAAGAGGTGACGCACATGC	CCGAGAAGAAACAAC TGAGCC	CGTCAAGCTCTAAATCGGGG		No	
AT4G09180	<i>fbh2</i>	SALK_063665C	TTGCATTTTGCAGACATAGG	AATCTCGAAGACTTGGTCAAGC	CGTCAAGCTCTAAATCGGGG		Yes	Exon
AT1G51700	<i>dorf1</i>	SALK_065359	TGGCTAAACATTTGACAGGTG	AGGCAAAAGCATGGAATTTG	CGTCAAGCTCTAAATCGGGG		No	
AT3G21270	<i>dorf2</i>	SALK_097322C	GAAAAATGGAACCAAAACAAG	TTCTCAAAAACCGGATTTGG	CGTCAAGCTCTAAATCGGGG		Yes	
AT3G47500	<i>cdf3</i>	GK-808G05	AATCATCTCCATTCTTACCCGAG	CATAGTTCACGTTGTGTTACCA	ATATTGACCATCATACTCATTGC	(Corrales et al., 2017)	Yes	CDS
AT4G26150	<i>gml (cpa1)</i>	SALK_003995	CACCGCAACAAAATTTTCATG	AGCCAAAAGCATGGAATTTG	ATTTTCCCGATTTCGGAAC	(Chiang et al., 2012)	Yes	Intron
AT4G26150/ AT5G56860	<i>gmlgnc</i>	SALK_003995 (GNL), SALK_001778 (GNC)	TTTGATCTTGACATTTTGGC	AGCCAAAAGCATGGAATTTG	ATTTTCCCGATTTCGGAAC	(Chiang et al., 2012)	Yes	Exon & Intron
AT1G66140	<i>zfp4</i>	SALK_038923C	TGCCATTTATGTGTGACGCAAC	CTGTGCTCCGGGTTACTAC	CGTCAAGCTCTAAATCGGGG	(Joseph et al., 2014)	Yes	5'UTR
AT3G11110	<i>atl66</i>	WisDslxHs207_06D	AAACAACCCAGCTGCTTACG	AGTCTGGTGTGGCCAATTC	TTTCTCCATTTGACCCATCAT ACTCATTG		Yes, with multiple loci	3'UTR
AT1G74410	<i>atl24</i>	SALK_046988	TCTTCTCGACTTGGACACAG	AGTTTCGATGTGATGCATGC	CGTCAAGCTCTAAATCGGGG		No	
AT1G20823	<i>atl80</i>	SALK_088190	AGCCATATTTGTACGTGAAAG	CTTCTCAGGCCTTGTTCG	CGTCAAGCTCTAAATCGGGG		Yes	Promoter

Table S4.2: Continued

Locus ID	Mutant Name	SALK ID/ Resource	Forward primer	Reverse primer	Insertion primer	Studies confirmed knockout function	Homozygous availability	T-DNA insertion position
AT5G47640	<i>nf-yb2</i>	SALK_025666	ATCACCAACACCAATGTTTCG	AGATCAATTTCCAATCCGAGC	CGTCAAGCTCTAAATCGGGG	(Sato et al., 2019)	Yes	Exon
AT3G10760	<i>at3g10760</i>	SALK_011176C	CCTGAAGGTGCTTGAGCTTC	TCAGACTGGTTCGCAAGATG	CGTCAAGCTCTAAATCGGGG		Yes	Exon
AT1G07530	<i>sc14</i>	SALK_126931	GGTCTACACACAAAAATAATG	AGCAGCTTGAAGAGCCAAAG	CGTCAAGCTCTAAATCGGGG	(Fode et al., 2008)	Yes	5'UTR
AT5G52510	<i>sc18</i>	SALK_129947	GTCACCTTCTCCGATATCG	GTTGGTGGTCCGGATTTTAC	CGTCAAGCTCTAAATCGGGG	(Ziemer, 2008)	Yes	CDS
AT2G01570	<i>rga1</i>	SALK_137951	AAACCTTTTTCATGAAATATCGC	ACCGTGGATTGTTGCTAAC	CGTCAAGCTCTAAATCGGGG		Yes	
AT3G01470	<i>hb1</i>	SALK_207381C	CCTGGGATCTGAGCTTATCG	GGTATAAAAAGACGGCGCTTG	CGTCAAGCTCTAAATCGGGG	(Capella et al., 2015)	Yes	5'UTR
AT5G13180	<i>nac083</i>	SALK_143793	AATGACCATATTGCCCTTGG	ATCGGTTCTTGAGCCATGAG	CGTCAAGCTCTAAATCGGGG	(Yang et al., 2011)	Yes	Exon
AT1G72010	<i>tcp22</i>	SALK_027490	TGTTGGGTTCTCTATCTTCG	GAGTTAGCTCAGGGTCGTGG	CGTCAAGCTCTAAATCGGGG	(Aguilar-Martinez & Sinha, 2013)	Yes	Exon
AT2G24570	<i>wrky17</i>	SALK_142377	CAAGAAGCTGCATCACAAGG	CTTACCGCCGGTACTCTCAC	CGTCAAGCTCTAAATCGGGG		Yes	Intron
AT3G28920	<i>hb34</i>	SALK_085482C	GAAGACGACGAGGCGGTTTAC	GCAACATTCATCAACCAGAGC	CGTCAAGCTCTAAATCGGGG	(Lee et al., 2022)	Yes	Exon
AT2G36270	<i>abi5-7</i>	-	CGTCAGACGAGAAAGTAGAG	GCGGGGCGGGGCGACGGGGGGGATT GTTATTCTCTCTGCGGAT			Yes	
AT3G59400	<i>gun4</i>	SALK_011461	GACTCTGCCCATGTGCTTAG	AGGTGAAAACAATCTCCCC	CGTCAAGCTCTAAATCGGGG	(Fölsche et al., 2022)	Yes	Exon
AT4G32940	<i>gamma-vpe</i>	SALK_010372	GGTGCTTTTCGGTACTTTCATG	TTTGCTGTGATCCTTGGAGAC	CGTCAAGCTCTAAATCGGGG	(Albertini et al., 2014)	Yes	Exon

Table 4.3 Relative values of measured phenotypic traits of Arabidopsis mutants and wild-type plants under HTD.

Indicated are genotypes (mutants or wild-type plants) and the values of measured traits relative to the corresponding wild-type plants. Asterisks represent significant differences between mutants and the corresponding wild-type plants for the particular trait ($p < 0.05$, unpaired t-test).

Genotype	Relative total leaf area	Relative petiole length	Relative blade length	Relative leaf number	Dry weight at wilting	Leaf number at wilting	Day to wilting	%SWC at wilting
Col-0	1.000	1.000	1.000	1.000	1.000	1.000	1.000	1.000
<i>abi5-7</i>	0.631*	1.720*	1.245	0.865*	0.615*	0.842*	0.953	1.084*
<i>elf6-3</i>	0.783	0.969	0.986	0.881*	0.863	0.782*	0.884*	1.148*
<i>at5g12310</i>	0.811	1.182	1.023	0.958	1.342	1.088	0.913*	1.041
<i>vip1</i>	1.011	1.735	1.133	0.997	1.114	0.998	0.902*	1.040
<i>zfp4</i>	0.978	1.069	0.981	0.969	0.912	0.924	0.896	1.107*
Col-3	0.931	0.793	0.861	0.992	1.240	1.045	0.959	1.025
<i>btf13</i>	0.868*	1.883*	1.490*	0.979	0.745*	0.923*	1.081	0.945
<i>bzip17</i>	0.737*	0.766	0.742*	0.892*	1.076	1.013	0.980	1.020
<i>hb2</i>	1.215*	1.714*	1.411*	1.022	1.015	0.988	1.062	0.964
<i>nf-yb2</i>	1.059	2.218*	1.363*	0.902*	0.780	0.934	0.976	1.071
<i>ilr3-1</i>	0.749*	1.898	0.995	0.878	0.512*	0.868	0.967	0.990
<i>why2-1</i>	0.679*	1.598	1.159	0.996	1.077	1.086*	1.026	1.010
<i>sei</i>	0.636*	1.028	0.907	0.979	0.920	0.906*	0.987	1.035
<i>atf66</i>	1.285*	1.241	1.384*	1.005	0.982	0.988	0.992	1.055
<i>tfp18.3</i>	1.480*	2.956*	1.362	0.982	0.967	0.987	1.055	0.994
<i>bzip28bzip60</i>	0.910	1.098	1.152	0.935*	0.755*	1.023	1.011	1.066

Table 4.3: Continued

Genotype	Relative total leaf area	Relative petiole length	Relative blade length	Relative leaf number	Dry weight at wilting	Leaf number at wilting	Day to wilting	%SWC at wilting
<i>bzip28</i>	1.072	1.041	0.934	0.946*	0.965	1.085*	0.978	1.020
<i>hb1</i>	0.713*	0.960	0.934	0.991	1.050	0.986	1.044	0.989
<i>hsfb2b</i>	0.749*	1.348	0.948	0.993	0.964	0.917	1.008	0.962
<i>myb34</i>	0.828*	0.859	0.920	0.939	1.016	0.936	0.969	1.014
<i>tcp22</i>	1.238	1.658*	1.194	1.011	1.090	0.990	0.959	1.022
<i>tcp9</i>	1.099	1.754	1.109	0.936*	1.192	0.979	0.934	1.030
<i>scl14</i>	1.005	1.841	1.114	0.930*	0.853	1.004	1.021	1.029
<i>at1g80400</i>	1.185	1.290	0.860	0.957	1.369*	1.035	0.965	0.994
<i>arid5</i>	1.220	1.229	1.089	0.975	1.571*	1.025	0.946	0.991
<i>pif4-2</i>	0.935	0.688	1.250	0.992	1.021	1.093*	0.997	1.018
<i>gamma-vpe</i>	1.075	0.925	0.864	0.973	1.009	1.095*	1.034	0.994
<i>scl1</i>	0.895	1.142	0.913	0.949	1.240	1.014	0.982	1.018
<i>scl8</i>	0.964	1.079	0.907	1.004	1.035	1.070	1.000	1.015
<i>hsf4</i>	1.003	1.200	1.164	0.986	0.911	0.949	1.022	0.997
<i>myb44</i>	1.178	1.286	1.011	0.935	1.196	0.967	0.996	1.000
<i>tcp23</i>	0.840	1.199	0.966	0.934	1.190	0.966	0.970	1.012

Table 4.4 Relative values of measured phenotypic traits of Arabidopsis mutants and wild-type plants under PSD.

Indicated are genotypes (mutants or wild-type plants) and the values of measured traits relative to the corresponding wild-type plants. Asterisks represent significant differences between mutants and the corresponding wild-type plants for the particular trait ($p < 0.05$, unpaired t-test).

Genotype	Relative total leaf area	Relative petiole length	Relative blade length	Relative leaf number	Dry weight at wilting	Leaf number at wilting	Day to wilting	%SWC at wilting
Col-0	1.000	1.000	1.000	1.000	1.000	1.000	1.000	1.000
<i>nac083</i>	1.117	1.411*	1.469*	0.929	0.856	0.885	0.947	1.138*
<i>hb1</i>	1.570*	1.366	1.276*	1.020	0.876	1.008	0.988	1.127*
<i>gun4</i>	1.294	1.104	1.188	0.962	0.482*	0.764*	0.881	1.194*
<i>abi5-7</i>	1.369*	1.354	1.057	0.992	0.842	0.943	0.888*	1.198*
<i>at3g10760</i>	0.867	1.176	1.045	0.895*	0.978	0.948	0.898*	1.169*
<i>at180</i>	0.985	0.858	0.755	0.942	0.720	0.928	0.868*	1.255*
<i>dof2</i>	1.088	1.093	1.250	0.920*	0.649*	0.815*	0.889	1.129
<i>scf14</i>	1.386*	0.973	1.002	1.000	0.848	0.912	0.981	1.025
<i>hb34</i>	1.016	0.631*	0.760	0.904*	0.830	0.933	0.993	0.999
<i>tcp22</i>	1.231	1.189	1.346*	0.923*	1.093	0.966	0.965	1.057
<i>nf-yb2</i>	1.004	1.132	1.352*	0.875*	0.947	0.930	0.985	1.061
<i>zfp4</i>	1.030	0.868	1.120	0.884*	0.911	0.880*	0.963	1.094
<i>gnlgnc</i>	0.943	0.908	0.992	0.976*	0.690*	0.899	1.017	0.984
<i>at166</i>	1.498*	1.121	1.159	1.062	1.135	1.024	1.003	1.003
<i>cdf3</i>	1.233	1.160	1.368*	0.998	0.856	0.927	0.990	1.089
<i>fbh2</i>	0.958	0.997	1.242	0.887*	0.776	0.917	0.986	1.073

Table 4.4: Continued

Genotype	Relative total leaf area	Relative petiole length	Relative blade length	Relative leaf number	Dry weight at wilting	Leaf number at wilting	Day to wilting	%SWC at wilting
<i>rga1</i>	1.090	0.970	1.344	0.924*	0.824	0.892	0.993	1.066
<i>gamma-vpe</i>	0.904	1.229	0.859	0.997	1.068	1.005	0.986	0.996
<i>scl8</i>	1.067	0.786	0.777	0.988	0.975	0.993	0.964	1.045
<i>wrky17</i>	0.950	0.948	1.048	1.027	1.013	1.033	1.031	0.899
<i>erf34</i>	0.816	0.793	1.108	0.900	0.983	0.905	0.945	1.091
<i>gnl</i>	1.171	1.066	0.977	1.026	0.930	0.970	0.947	1.096



5

The transcription factor GOLDEN2-LIKE 2 regulates thermomorphogenesis in Arabidopsis in a complex manner that may involve PIF4 and auxin

Zhang Jiang, Romy Geertsma, Elias Bernard, Ava Verhoeven, Rashmi Sasidharan*, Martijn van Zanten*

* Shared senior authors

Plant Stress Resilience, Utrecht University

Abstract

Plants are susceptible to environmental cues including temperature. Even a mild increase in ambient temperature can cause substantial changes in growth, physiology and development. Changes in plant morphology/architecture in response to mild increases in temperature are referred to as thermomorphogenesis. High temperature can also pronouncedly affect chloroplast functions and thereby photosynthesis. While plant temperature perception, signalling and regulation of thermomorphogenesis are increasingly well understood, the role of chloroplasts in thermal responses remains poorly explored.

The transcriptomics experiments described in Chapter 3 pointed to a potential involvement of chloroplast-associated genes in mediating responsiveness to high temperature conditions (including individually applied high temperature and the combination with drought). Here, we show that one of the identified candidates; GOLDEN2-LIKE 2 (GLK2), a transcription factor responsible for the expression of photosynthesis-associated nuclear genes and chloroplast development, regulates thermomorphogenesis in *Arabidopsis thaliana*. We demonstrate that GLK2 protein is stabilized by high temperature. Both mutation and overexpression of *GLK* impeded thermomorphogenic responses, suggesting that GLK2 regulates thermomorphogenesis in a complex manner. Furthermore, we show that GLK2 governs plant thermal responses likely independent of GENOMES UNCOUPLED 1 (GUN1)-dependent retrograde signalling pathway. Results of experiments conducted to test if GLK2 affects thermomorphogenesis through the regulation of auxin signalling or/and biosynthesis were inconclusive. However our data suggest that GLK2 might attenuate PIF4 in a not yet understood manner. Together, our finding uncovers a novel role for GLK2 in modulating thermomorphogenesis and points to a potential link between chloroplast functioning, auxin biology and temperature responses.

Introduction

Ambient temperature is an important environmental factor that affects plant growth, development and yield (Hatfield & Prueger, 2015; Susila et al., 2018; Lee et al., 2021b). Even a slight increase in ambient temperature, below the heat stress level, can lead to a multitude of phenotypic changes in some plant species, including *Arabidopsis thaliana* (Proveniers & Van Zanten, 2013; Praat et al., 2021; Burko et al., 2022). High-temperature triggered growth and morphological acclimation at the whole plant level are referred to as ‘thermomorphogenesis’. Thermomorphogenesis is characterized by traits like petiole and hypocotyl elongation, leaf hyponasty and early flowering (Casal & Balasubramanian, 2019; Vu et al., 2019). These phenotypic changes are able to mitigate the negative effects of high temperature and help plants maintain optimal growth under sub-optimal growth environments (Bita & Gerats, 2013; Van Der Woude et al., 2019).

At the molecular level, thermomorphogenesis is governed by a complex signalling network involving diverse receptors and regulators (Quint et al., 2016; Lee et al., 2021a; Ai et al., 2023). For example, the perception of high temperature in *Arabidopsis* is partially accomplished by the Phytochrome B photoreceptor (phyB), which directs the expression of a subset of high-temperature responsive genes (Mathur et al., 2014; Jung et al., 2016). Another crucial signal integrator in thermomorphogenesis is PHYTOCHROME INTERACTING FACTOR 4 (PIF4), a transcription factor that among others stimulates auxin biosynthesis and signalling, which are required for the induction of thermomorphogenesis (Sun et al., 2012; Proveniers & Van Zanten, 2013; Delker et al., 2022). Recently, some studies highlighted the importance of epigenetic processes involving histone modifications and histone variants in thermomorphogenic responses (Perrella et al., 2022). For example, HISTONE DEACETYLASE 9 (HDA9) is required for *YUCCA8* (*YUC8*)-dependent auxin biosynthesis during thermomorphogenesis in *Arabidopsis* in a phyB independent manner (Van Der Woude et al., 2019; Hou et al., 2022), while the SANT-domain protein POWERDRESS (PWR) can interact with HDA9 and regulate its function (Chen et al., 2016; Tasset et al., 2018).

Unlike mildly elevated temperatures that do not elicit permanent damage in plants (Praat et al., 2021), more extreme high temperatures (heat stress) can considerably disrupt photosynthesis and chloroplast activities including chlorophyll biosynthesis, photochemical reactions, electron transport and carbon assimilation and eventually lead to retardation in plant growth, development and sometimes even death (Mathur et al., 2014; Hu et al., 2020). To survive heat stress, plants must restore their energy homeostasis via recovery of perturbed photosynthesis, which involves the

reprogramming of gene expression in the nucleus and cellular metabolism. This requires mutual signalling events, called retrograde signalling, to take place between organelles (chloroplast, mitochondria *etc.*) and the nucleus and thereby control nuclear-gene expression in response to functional changes in organelles (Baena-González, 2010; Crawford et al., 2018; Dogra & Kim, 2019; Wang et al., 2020).

Retrograde signals can derive from various sources, such as the tetrapyrrole pathway, organellar gene expression or reactive oxygen species (ROS) (Leister, 2012). Of all known retrograde signalling pathways, GUN1-dependent chloroplast-to-nuclear retrograde signalling is among the best studied (Koussevitzky et al., 2007; Richter et al., 2023). GUN1 is a chloroplast-localized pentatricopeptide-repeat protein and is involved in plastid development (Koussevitzky et al., 2007; Gommers et al., 2020). When chloroplasts are stressed by photodamage, GUN1 is activated and transcriptionally represses *GOLDEN2-LIKE1 (GLK1)*, a transcription factor controlling the expression of photosynthesis associated nuclear genes (*PhANGs*) in the nucleus (Waters et al., 2009; Martín et al., 2016; Veciana et al., 2022b). A recent study demonstrated that GUN1-mediated retrograde signaling also directs the expression of antioxidant related genes to scavenge excess ROS caused by perturbed chloroplast functioning in Arabidopsis seedlings (Fortunato et al., 2022). To the best of our knowledge, GUN1-mediated retrograde signaling has not been linked to high ambient temperature signaling events so far, despite the apparent close connections between chloroplast and temperature responses (Hu et al., 2020; Schwenkert et al., 2022).

The transcriptomic analysis described in Chapter 3 demonstrated that many chloroplast-related genes were differentially regulated in response to high ambient temperature stresses, both in the presence (HTD) and absence (HT) of drought (See; Chapter 3 Figure 3.3C, Tables S3.3 and S3.4). Furthermore, we noted that *GLK2*, a transcription factor regulating chloroplast development and the expression of chloroplast-associated genes (including *PhANGs*), was upregulated upon high temperature conditions. These results hinted at a potential (novel) role for chloroplasts in high temperature responses. In this chapter, we demonstrate that overexpression, but also mutation of *GLK2*, suppresses plant thermomorphogenesis in seedling and rosette stage plants. *GLK2* protein is stabilized under high temperature conditions and its overexpression triggers the upregulation of *PIF4* and *YUC8* at the transcriptional level. Surprisingly, *GLK2*-mediated high temperature responses occur independently of GUN1-dependent retrograde signalling. Our findings uncover a novel role for *GLK2* in thermomorphogenesis, adding to our current understanding of the complex regulatory networks mediating plant responses to high temperatures.

Results

According to the Gene Ontology (GO) analysis of upregulated differentially expressed genes (DEGs) under high temperature conditions (HT and HTD) in chapter 3, genes associated with plastid organisation (GO:0009657) were significantly enriched (See; Chapter 3 Figures 3.3C, Tables S3.3 and S3.4). This implies a role for chloroplasts in regulating responses to high temperature signals. Chloroplasts being semi-autonomous organelles retaining their own genomes, are responsible for photosynthesis and plant development (Zhang et al., 2020c). Chloroplast biogenesis and functionality are fine-tuned by genes, termed photosynthesis-associated plastid (*PhAPGs*; encoded in the plastid genome), and photosynthesis-associated nuclear genes (*PhANGs*; encoded in the nuclear genome) (Dubreuil et al., 2018; Lv et al., 2019; Ji, 2020; Yoo et al., 2020).

To assess the role of chloroplasts in regulating high temperature responses, we examined the expression patterns of genes that associate with chloroplast and/or photosynthesis, including *PhAPGs*, *PhANGs* and two well-characterized transcription factors governing chloroplast development and the expression of *PhANGs*; *GLK1* and *GLK2* (Chen et al., 2016; Hernández-Verdeja and Lundgren, 2023; Li et al., 2022; Nagatoshi et al., 2016), upon high temperature treatments in the RNA-seq dataset (Figures 5.1A-B, S5.1A-B). Our results indicate that high temperature treatment indeed pronouncedly downregulated several *PhANGs*, but upregulated many *PhAPGs* (Figure S5.1B). In our analysis of the RNA-seq data, *GLK1* was not identified as a DEG, while *GLK2* was found in the HT/HTD upregulated clusters by the *k*-means clustering approach (See; Chapter 3, Figures 3.3C). Both *GLK1* and *GLK2* showed low transcripts per million (TPM) rates, whereas 5-day HT boosted the TPM rate of *GLK2* (Figure 5.1B). Moreover, HT also upregulated the expression of *GLK2* (Log_2FC). These findings suggest that the chloroplast, and the GLKs may have a role in acclimation to high temperature conditions (*i.e.*, thermomorphogenesis). *GLK1* and *GLK2* are partially redundant in their functions (Waters et al., 2009). Due to the absence of *GLK1* in our DEGs (See; Chapter 3), and the fact that the overexpression line of *GLK1* (*35S::GLK1*) (Waters et al., 2008) failed to germinate in the trial experiments, we only investigated the function of *GLK2* in thermomorphogenesis.

***GLK2* affects chlorophyll accumulation under both control and high temperature conditions**

To study the genetic effects of *GLK2* on thermal acclimation, a suite of rosette phenotypic traits were assessed using wild-type Col-0, a *GLK2* overexpressing line (*35S::GLK2*) (Waters et al., 2008) and the double mutant *glk1glk2* (Fitter et al., 2002a).

Traits included were chlorophyll content and leaf initiation rate (score of leaf number across time). The results showed that plants grown under HT accumulated less chlorophyll in young leaves than plants grown under control temperatures (C) (Figure 5.1C). Both Col-0 and *35S::GLK2* maintained comparable levels of chlorophyll content regardless of the growth temperature, while the *glk1glk2* double mutant displayed remarkably low chlorophyll levels in accordance with its pale green phenotype (Figure S5.2A), despite all plants being at a similar developmental stages (Figure 5.1C).

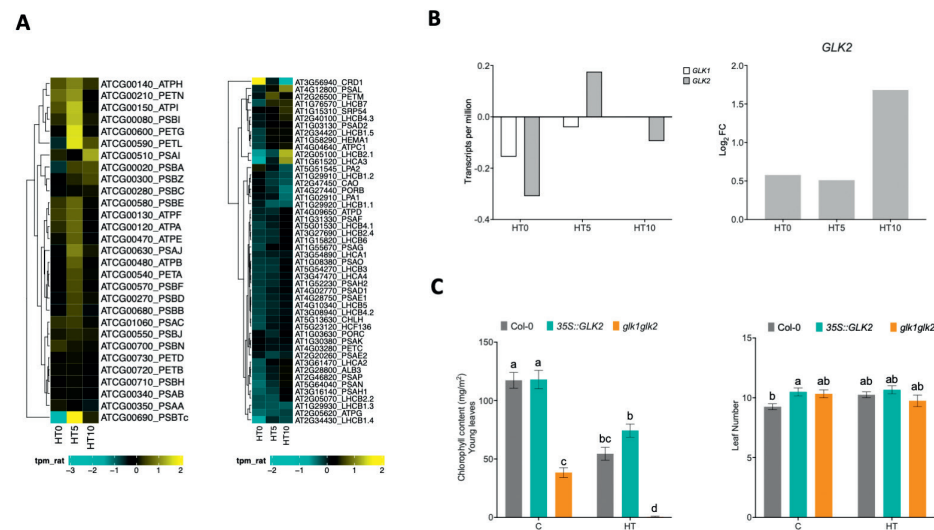


Figure 5.1. Effects of high temperature on photosynthesis-associated genes and effect of GLK on high temperature-mediated phenotypic traits.

(A) Heatmap presenting the expression (Transcript per million, TPM) of photosynthesis-associated chloroplast genes (*PhAPGs*, left panel) and photosynthesis-associated nuclear genes (*PhANGs*, right panel) in response to high temperature (HT) treatments. Data are derived from the transcriptomics experiments described in chapter 3. Indicated are the AGI gene locus ID and the commonly used abbreviation. The colour scale indicates the expression levels; yellow represents up- and blue represents down-regulation. For abbreviations see chapter 3, legend figure 3.1. (B) Expression levels of *GLK1* and *GLK2* indicated as transcripts per million (*GLK1* and *GLK2*, left) or Log₂FC (*GLK2*, relative to the corresponding controls (C), right). Data are derived from the RNA-seq dataset (Chapter 3) at high temperature (HT) conditions on day 0, 5 and 10 (HT0, HT5, HT10). (C) Chlorophyll content (left) and number of leaves (right) of wild-type Col-0 (black), *35S::GLK2* (aqua) and *glk1glk2* (orange) grown under control (C) and high temperature (HT) conditions from 2-leaf stage till the 10-leaf stage. Error bars indicate means \pm SEM. Letters denote significant differences between different treatments and genotypes ($p < 0.05$, 2-way ANOVA with Tukey's Post-hoc test). $n=3-8$.

We next examined if *35S::GLK2* and *glk1glk2* affected wilting time when high temperature was combined with drought (HTD). Upon HTD, Col-0 wild-type and

glk1glk2 wilted at 18 days after the drought treatment started, while *35S::GLK2* plants were on average one day delayed (Figure S5.2B). When plants were subjected to 10-day C or HTD, the chlorophyll content of young leaves of *35S::GLK2* plants was significantly higher than that observed in wild-type Col-0, while on the contrary *glk1glk2* again exhibited considerably low chlorophyll levels (Figure S5.2C). The leaf initiation rate of Col-0 and *glk1glk2* under C and HTD conditions were comparable (Figure S5.2D). However, *35S::GLK2* plants overall generated more leaves per unit of time. Taken together, our results suggest that *GLK2* may act as a positive regulator of plant growth and development. It should however be noted that this is not strictly linked to HT or HTD conditions, as similar genetic effects were also observed under C conditions (Figures 5.1, S5.2).

Overexpression of *GLK2* attenuates thermomorphogenesis

To test for a possible effect of *GLK2* on plant thermomorphogenesis, we quantified petiole length and leaf angles (hyponasty) of the wild-type plants, *glk1glk2* mutant and *GLK2* overexpression line at control (C, 21 °C) and high temperature (HT, 27 °C) conditions (Figure 5.2A-C). Col-0 wild-type and *glk1glk2* mutant plants grown exhibited significant induction of leaf hyponasty under HT compared to control conditions as expected, while *35S::GLK2* plants were unable to induce hyponastic growth in response to high temperature (Figure 5.2B). All three lines displayed significantly enhanced petiole elongation in response to high temperature, but surprisingly, both *35S::GLK2* and *glk1glk2* did so to a much lesser extent than Col-0 wild-type (Figure 5.2C).

Next, we tested whether the observed differences in thermomorphogenic responses of Col-0, *35S::GLK2* and *glk1glk2* were consistent in seedlings by quantifying the ability to induce hypocotyl elongation in response to high temperature (Figure 5.2D-E), a key characteristic of thermomorphogenesis (Proveniers & Van Zanten, 2013; Delker et al., 2022). We included two phenotypic controls for high temperature responses, *phytochrome interacting factor 4* (*pif4-2*) and *phytochrome b* (*phyb-9*) mutants. The *pif4-2* mutant is unable to acclimate to high temperature conditions and is disturbed in hypocotyl elongation in response to high temperature (Leivar et al., 2008; Van Der Woude et al., 2019), while *phyb-9* has constitutively elongated hypocotyl, regardless of the growth conditions (Reed et al., 2000). As expected, Col-0 seedlings showed enhanced hypocotyl length under 27 °C relative to 21 °C (Figure 5.2E) and the known *pif4-2* and *phyb-9* phenotypes could be recapitulated. Hypocotyl elongation of both of *35S::GLK2* and *glk1glk2* was considerably reduced compared to Col-0, although not to the level of *pif4-2* (Figure 5.2E). Given that both *GLK2* overexpression and mutation result in largely similar phenotypes under high temperature in seedlings (hypocotyl elongation) and vegetative plants (petiole elongation), but also clearly differed in

temperature responsiveness when hyponasty is considered as output, suggest that GLKs, particularly GLK2, acts as a regulator of plant thermomorphogenesis in a complex manner.

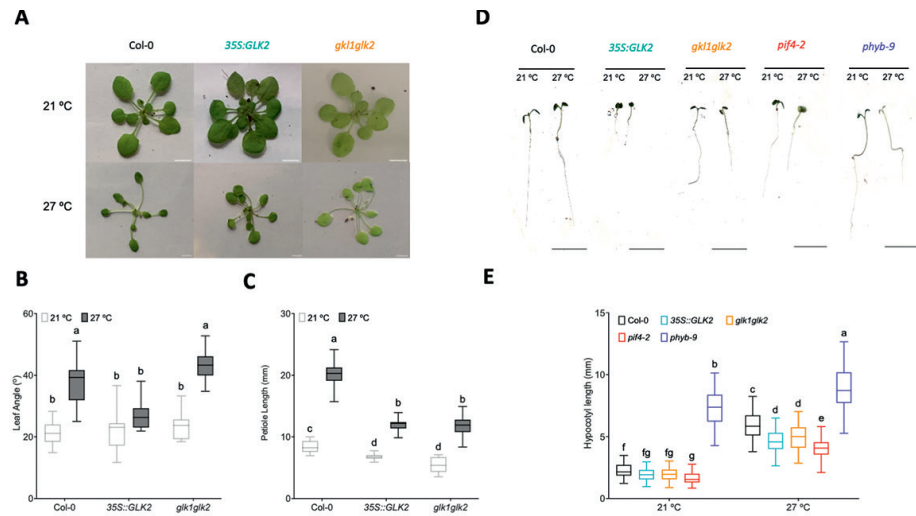


Figure 5.2. Genetic effects of GLK2 on thermomorphogenesis.

(A) Representative images of 10-leaf stage (LS10) Col-0, 35S::GLK2 and *glk1glk2* pre-grown at either control temperature 21 °C (upper row) or high temperature 27 °C (lower row). Scale bars indicate 1 cm. (B) Average angles of the two most hyponastic leaves of individual plants, relative to the horizontal. $n = 12-15$. (C) Average length of the petioles of the 3rd-6th youngest leaf. $n = 12-15$. (D) Representative images of 8-day old seedlings of Col-0, 35S::GLK2, *glk1glk2*, *pif4-2* and *phyb-9* grown at control (21 °C) or high temperature (27 °C). Scale bars indicate 1 cm. (E) Quantification of hypocotyl length of Col-0 (black), 35S::GLK2 (aqua), *glk1glk2* (orange), *pif4-2* (red) and *phyb-9* (purple) seedlings grown at 21 °C or 27 °C for 8 days. $n = 4$ independent replicates, each containing 25-30 seedlings. (B,C) Temperatures are indicated by different colors; 21 °C white, 27 °C; gray. (B,C,E) Boxes indicate boundaries of the second and third quartiles (Q) of the data distribution. Black horizontal bars indicate median and whiskers Q1 and Q4 values within 1.5 times the interquartile range. Letters denote significant differences between different treatments and genotypes ($p < 0.05$, 2-way ANOVA with Tukey's Post-hoc test).

GLK2 modulation of thermomorphogenesis occurs independent from GUN1-mediated retrograde signalling

The expression of *PhAPGs* is associated with chloroplast biogenesis and can be triggered by the photoactivation of phytochromes (Yoo et al., 2019), while *PhANGs* are considered marker genes of GUN1-mediated retrograde signalling and are direct downstream targets of GLKs (Wu et al., 2018; Zhao et al., 2019a; Li et al., 2022a). It has been previously demonstrated that the transcription factor GLK1 acts downstream

of the chloroplast-derived retrograde signalling regulator GUN1 and is repressed upon photodamaging conditions to mediate the expression of *PhANGs* and seedling morphogenesis (Martin et al., 2016; Veciana et al., 2022a). We therefore explored the hypothesis that GUN1 controls plant thermomorphogenesis at high temperature conditions through GLK2 (Figure 5.3A), as GLK1 and GLK2 are redundant in their functions (Waters et al., 2009). To test this, hypocotyl lengths of Col-0 and mutant *gun1* plants grown at 21 °C and 27 °C were compared (Figure 5.3B) in the expectation that the *gun1* mutant line would exhibit a similar phenotype as 35S::GLK2 under high temperature conditions. However, we found that the hypocotyl lengths of Col-0 and the mutant line *gun1* did not significantly differ (Figure 5.3B). This result indicates that GUN1 is likely not a regulator of GLKs under high temperature conditions when acclimation to high temperature is considered.

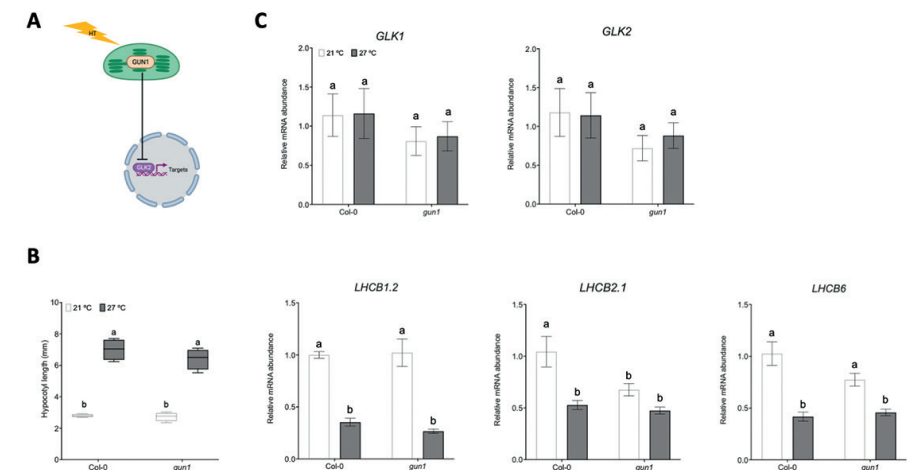


Figure 5.3. Phenotypic and transcriptional analysis of Col-0 and *gun1* mutant in response to high temperature.

(A) Hypothesized scheme indicating the potential inhibition of GLK2 under high temperature through GUN1-dependent retrograde signalling. (B) Hypocotyl lengths of Col-0 wild-type and *gun1* mutant seedlings grown at 21 °C (white bars) or 27 °C (gray bars) for 8 days. Boxes indicate boundaries of the second and third quartiles (Q) of the data distribution. Black horizontal bars indicate median and whiskers Q1 and Q4 values within 1.5 times the interquartile range. $n = 4$, with each containing 25-30 seedlings. (C) Relative mRNA abundance (expression) of GLK1, GLK2 and their known downstream target genes (*LHC1.2*, *LHC2.1* and *LHC6*) at 21 °C (white bars) or 27 °C (gray bars), as determined by RT-qPCR. $n = 4$, each containing 30-50 pooled seedlings. Error bars indicate means \pm SEM. (B,C) Letters denote significant differences between different treatments and genotypes ($p < 0.05$, 2-way ANOVA with Tukey's Post-hoc test).

Our finding that GUN1 is not involved in thermomorphogenesis regulation via *GLK2* was largely confirmed by analysis of the expression of *GLKs* and their target genes (Hills et al., 2015): *LIGHT-HARVESTING CHLOROPHYLL B-BINDING (LHCB) 1.2*, *LHCB2.1* and *LHCB6*, at 21°C and 27°C in the mutant line *gun1* and wild-type Col-0 (Figure 5.3C). qRT-PCR experiments revealed that the expression of both *GLK1* and *GLK2* was not affected by high temperature. Moreover, GUN1 had no effect on *GLK1* or *GLK2* expression. Expression of the *GLK* downstream targets (*LHCB1.2*, *LHCB2.1* and *LHCB6*) was overall decreased at 27°C relative to 21°C, but this effect occurred regardless of the presence of GUN1 (Figure 5.3C). Together, these results show that the *GLK2*-mediated regulation of thermomorphogenesis occurs independent of GUN1-mediated retrograde signalling. The decrease of the core-photosynthesis associated genes *LHCB1.2*, *LHCB2.1* and *LHCB6* at 27°C indicates that high temperature might have a direct negative effect on plant photosynthesis.

***GLKs* regulate thermomorphogenesis at the transcription and translational levels**

To understand the molecular mechanism underlying *GLK* regulation of plant thermomorphogenesis, we first quantified the relative expression levels of *GLK2* in Col-0 wild-type, *35S::GLK2* overexpression and *glk1glk2* double mutant backgrounds at 21°C and 27°C (Figure 5.4A). This confirmed our previous results (Figure 5.3C) that *GLK2* expression is not affected by high temperature. Moreover, our data also confirmed the overexpression of *GLK2* in *35S::GLK2* and the absence of *GLK2* transcript in *glk1glk2* at both 21°C and 27°C.

We next examined the protein levels of *GLK2* at 21°C and 27°C by Western blot analysis using a line expressing *35S::GLK2-GFP* (Waters et al., 2008) (Figures 5.4B, S5.3). The results showed that *GLK2* protein accumulated more under high ambient temperature compared to control temperature conditions, suggesting that *GLK2* is stabilized by high temperature even though it may be considered a negative regulator of thermomorphogenesis based on our genetic analyses.

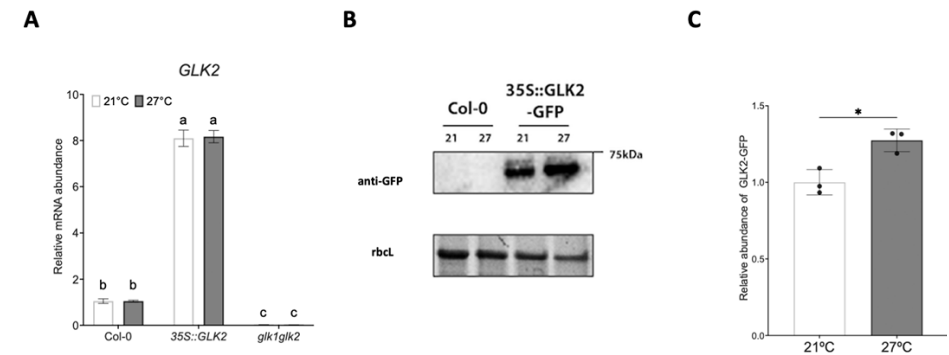


Figure 5.4. Transcriptional regulation and protein stability of *GLK2* under high temperature conditions.

(A) Relative mRNA abundance of Col-0 wild-type, *35S::GLK2* and *glk1glk2* at 21°C (white bars) or 27°C (gray bars), as determined by RT-qPCR. $n=4-5$ replicates of 30-50 pooled seedlings each. Letters denote significant differences between different treatments and genotypes ($p < 0.05$, 2-way ANOVA with Tukey's Post-hoc test). **(B)** Western blots showing the level of *GLK2-GFP* in Col-0 and *35S::GLK2-GFP* expressing seedlings grown at 21°C or 27°C for 8 days. Stain-free imaging of Rubisco protein (*rbcL*) was used as loading control. $n=3$, each containing approximately 30-50 pooled seedlings. The original uncropped blot images are indicated in Figure S5.3. **(C)** Quantification of relative *GLK2-GFP* abundance at 21°C (white bars) or 27°C (gray bars) from the Western blots shown in panel C and Figure S5.3. Asterisks represent significant differences ($*p < 0.05$, unpaired t-test). **(A,C)** Error bars indicate means \pm SEM.

To connect our findings on *GLK2* to the existing knowledge framework of thermomorphogenesis regulation, we tested the effect of *GLK2* on the expression (mRNA) levels of several marker genes that are known to be affected by high temperature and/or are key factors in the thermomorphogenesis regulatory network, including *HEAT SHOCK PROTEIN 70 (HSP70)*, *PIF4* and *YUCCA8* (Figure 5.5), and several *PIF4* target genes (Figure S5.4). *HSP70* has no apparent role in thermomorphogenesis regulation, but its expression level is considered a molecular thermometer as *HSP70* mRNA abundance scales with temperature (Kumar & Wigge, 2010; Van Der Woude et al., 2019). Our data showed that expression of *HSP70* was consistently induced at 27°C in all three genotypes, suggesting that *GLKs* do not affect sensitivity to high temperature.

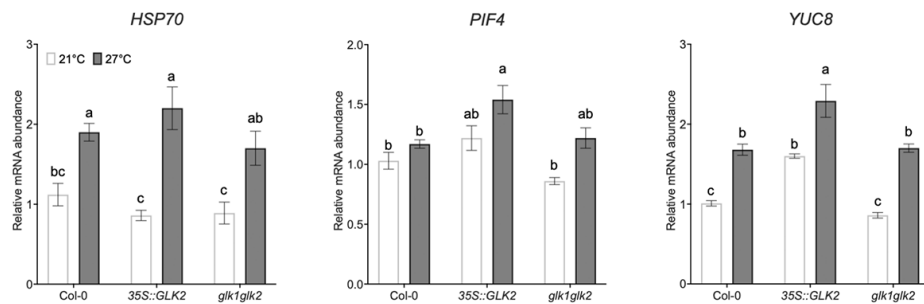


Figure 5.5 Effect of GLK2 on the expression of temperature-regulated genes.

Relative mRNA abundance of *HSP70*, *PIF4* and *YUC8* at 21 °C (white bars) or 27 °C (gray bars), as determined by RT-qPCR. n=4-5, each containing 30-50 pooled seedlings harvested at ZT = 9 h. Error bars indicate means \pm SEM. Letters denote significant differences between different treatments and genotypes ($p < 0.05$, 2-way ANOVA with Tukey's Post-hoc test).

The expression of *PIF4* (Gangappa et al., 2017; Hwang et al., 2017; Lee et al., 2021a) showed no significant differences at 21°C in *glk1glk2* and *35S::GLK2*, but a notably increased expression in *PIF4* was found in *35S::GLK2* at 27 °C, compared to Col-0. However, no differences in *PIF4* expression were found between *glk1glk2* and Col-0. High temperature-induced hypocotyl elongation requires auxin biosynthesis (Sun et al., 2012; Van Der Woude et al., 2021). In line with the upregulation of *PIF4*, *YUCCA8* (*YUC8*), a rate-limiting auxin biosynthesis gene directly targeted by *PIF4* under high temperatures (Sun et al., 2012), was significantly induced by high temperature in all tested genotypes, but most notably in *35S::GLK2*, despite that two auxin responsive genes responsible for hypocotyl elongation, *INDOLE-3-ACETIC ACID INDUCIBLE 19* and *29* (*IAA19* and *IAA29*) (Tatematsu et al., 2004; Sun et al., 2013a), showed in general a decrease at 27 °C relative to 21 °C in all the three genotypes (Figure S5.4).

The role of auxin in GLK2-mediated thermomorphogenesis is ambiguous

Our qRT-PCR data on *PIF4* and *YUCA8* (Figures 5.5 and S5.4) suggested that GLKs might directly or indirectly interfere with auxin levels and response under high temperature conditions. This interference could also potentially explain our apparent contradictory finding that both overexpression and mutation of *GLK2* results in the abolishment of thermomorphogenesis capacity. This is because the same response strength phenotype could be explained by both high (hyper-optimal) and low (supra-optimal), but still enhanced (relative to 21°C) levels of auxin, despite having auxin concentrations that are highly offset from the maximal response concentration (Van Der Woude et al., 2021; Zhu et al., 2022a).

To investigate whether *GLKs* affect auxin transport or biosynthesis in response to high temperature, we compared auxin dose-responsiveness of hypocotyl elongation of *35S::GLK2*, *glk1glk2* and Col-0, as well as *pif4-2* and *phyb-9* (as phenotypic controls) by applying different concentrations of the synthetic auxin chemical Picloram or the auxin transport inhibitor N-1-naphthylphthalamic acid (NPA) (Prigge et al., 2016; Abas et al., 2020) (Figure 5.6A-B). Overall, low levels of Picloram stimulated hypocotyl elongation as expected (Figure 5.6A). Higher concentrations repressed hypocotyl from $\sim 2.5 \mu\text{M}$ onwards at 21 °C and from $\sim 1 \mu\text{M}$ onwards at 27°C in Col-0 and *glk1glk2*, whereas for *35S::GLK2* a higher concentration was required to repress elongation (Figure 5.6A). Remarkably, *glk1glk2* showed a rather similar trend of hypocotyl growth as the wild-type Col-0 in response to Picloram treatment, while *35S::GLK2* and *pif4-2* overall showed comparable elongation responses without restoring comparable trends as Col-0 upon high concentrations of Picloram (Figure 5.6A).

NPA inhibits auxin transport and thereby inhibits hypocotyl elongation. It was observed that NPA causes a decrease in hypocotyl length in all genotypes at 27°C. Intriguingly, *35S::GLK2* and *pif4-2* displayed clear similarities in hypocotyl elongation at 27°C. Similarly, *pif4-2* did not fully restore the elongation trend to a comparable level as Col-0 upon high concentrations of NPA treatment. These results may suggest that *GLK2* attenuates thermomorphogenic response through repression of *PIF4*.

Agravitropism is induced by disturbance of auxin distribution and/or signalling in the plant and is strongly induced by NPA and Picloram (Rakusová et al., 2011). In our study, with an increase in the concentration of Picloram and NPA, *35S::GLK2* displayed stronger agravitropy than at lower concentrations. *35S::GLK2* even reaches 75%, meaning total absence of gravitropism response (Figure 5.6B). At total absence of Picloram and NPA, both *pif4-2* and *35S::GLK2* were already showing some degree of agravitropism. Taken together, these results again implicate that *GLK2* may negatively regulate *PIF4* and thereby the downstream auxin response, although this regulatory mechanism needs to be supported by additional work, for example, by measuring the absolute auxin concentrations in *GLK2* mutation and overexpression lines.

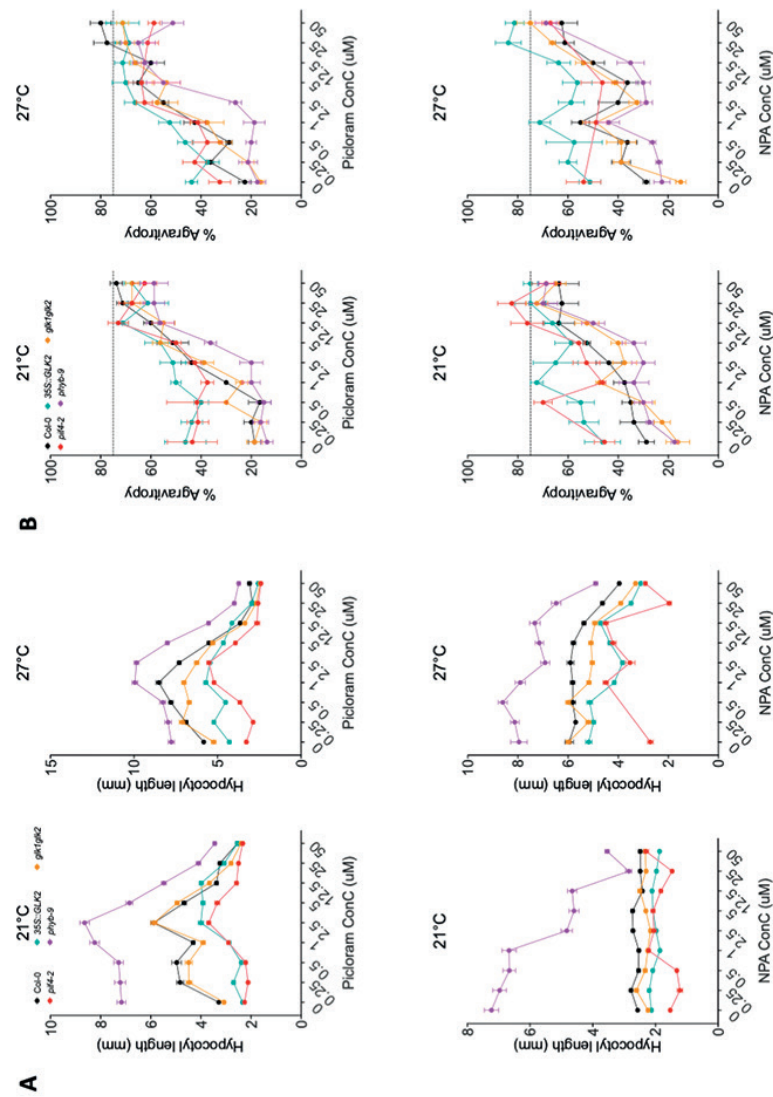


Figure 5.6. Effects of Picloram and NPA on hypocotyl length and shoot (a)gravity. Hypocotyl length (A) and percentage of agravitropic seedlings (B) of 8 day-old Col-0 wild-type (black), *35S::GLK2* (orange), *glk1glk2* (aqua), *pif4-2* (red) and *pif4-9* (purple) seedlings over a range of concentrations of Picloram (upper rows) and NPA (bottom rows), at 22 °C (left) or 27 °C (right). Error bars indicate means \pm SEM. Dashed horizontal lines in panel B indicate 75%, which equals complete agravity.

Discussion

Chloroplasts serve as stress sensors in perceiving environmental signals (Song et al., 2021; Li & Kim, 2022). Sub-optimal growth conditions like stressful high temperatures can drastically disrupt photosynthetic activities (Mathur et al., 2014). In this chapter, we present a novel role for GLK2, a transcription factor that controls chloroplast development (Waters et al., 2009; Martín et al., 2016), in modulating thermomorphogenesis in Arabidopsis. Our results however indicate that GLK2 affects thermomorphogenesis likely independent of GUN1-dependent retrograde signaling events but might involve manipulation of auxin biosynthesis and/or signaling possibly by attenuating PIF4 function in a yet unknown manner.

Our data show that overexpression of *GLK2* (*35S::GLK2*) in rosette plants resulted in significant increased chlorophyll levels and a higher leaf initiation rate under C, HT and HTD conditions (Figures 5.1C and S5.2C-D), accompanied by slightly delayed leaf wilting under HTD (Figure S5.2B). These results are consistent with prior studies (Macková et al., 2013; Nankishore & Farrell, 2016) and our findings in Chapter 2 (See; Chapter 2 Figures 2.2 and 2.3) that increase in chlorophyll content likely accounts for better performance of plant growth and the survival of stresses. In this chapter, we did not investigate if and how GLK2 contributes to acclimation to the other combinatorial stress that is the focus of this thesis; submergence followed by drought (post-submergence & drought, PSD). PSD was not included in this chapter as the chloroplast-associated GO terms found in response to HT and HTD were not enriched in PSD-upregulated gene clusters (See; Chapter 3 Figure 3.4C and Table S3.5). However, we did observe the overrepresentation of another GUN protein, GUN4, in the gene regulatory network constructed by PSD-upregulated genes (See; Chapter 3, Figure 3.6). Given that GUN4 plays a pivotal role in activating Mg chelatase during chlorophyll biosynthesis and retrograde signaling (Tarahi Tabrizi et al., 2016; Li et al., 2023; Richter et al., 2023), its presence during PSD hints at a potential involvement of retrograde signaling regulation that distinct from the GUN1-mediated retrograde signaling. On the other hand, considering the fact that GLK2 overexpression is known to enhance chlorophyll content, further investigation into plant stress responses (e.g., wilting, leaf development) under PSD in *GLK2* mutant and overexpression lines might be enlightening. This would help in further corroborating our findings that accumulation of chlorophyll content in young leaves could contribute to the acclimation of both HTD and PSD (See; Chapter 2; Results and Discussion).

Our data indicate that GLK2 is stabilized under 27 °C at the protein level and is an apparent negative regulator of thermomorphogenesis, as its overexpression resulted

in attenuated petiole elongation, hyponastic growth in rosette plants and hypocotyl elongation in seedlings (Figure 5.2). The (increase in) protein abundance of GLK2 under high temperature may fine tune plant thermomorphogenesis by translationally repressing high-temperature responsive regulator(s) (*i.e.*, *PIF4*) in a feedback loop and therefore controls plant growth. However, *glk1glk2* also displayed impeded petiole and hypocotyl lengthening, but displayed a hyponastic response similar to Col-0 wild-type under high temperature, which is likely due to the inhibition of plant development and carbon acquisition caused by impaired chloroplast biogenesis and photosynthesis when *GLK1* and *GLK2* are both knocked-out (Waters et al., 2009; Zubo et al., 2018; Hernández-Verdeja et al., 2022; Li et al., 2022a). GLKs thus control thermomorphogenesis in a complex manner and additional work is needed to better understand its role. Testing the expression or protein abundance of other marker genes of thermomorphogenesis in the *35S::GLK2* and *glk1glk2* backgrounds should resolve if indeed the phenotypic similarities observed in *35S::GLK2* vs. *glk1glk2* have a different origin, *i.e.*, thermomorphogenesis is impaired in *GLK2* overexpression lines due to disruption of native signaling events and in the double mutant because it has issues with energy homeostasis. Most notably, future studies should focus on assessing protein stability of *PIF4* as our data on *GLK2* could be explained in part by *GLK2* attenuating *PIF4* and its effects.

GUN1-mediated retrograde signaling can transcriptionally repress *GLKs* and thereby the expression of *PhANGs* and chloroplast biogenesis (Waters et al., 2009; Lee et al., 2023). Because the GUN1/GLK1 retrograde signaling inhibits photomorphogenesis upon chloroplast damage (Martín et al., 2016; Veciana et al., 2022a), we tested the hypothesis that *GLK2* might negatively control plant thermomorphogenesis through the GUN1-mediated plastid-to-nuclear retrograde signaling pathway. However, based on the observation that hypocotyl elongation as well as the expression of *GLK*-targeted *PhANG* genes were similar in the *gun1* mutant line and Col-0 at both control and high temperature (Figure 5.3B-C), we conclude that the impeded thermomorphogenesis caused by *GLK2* is likely not GUN1-dependent. Despite *LHCB* genes being direct targets of *GLK2*, the observed downregulation of these genes by high temperature likely occurs independent of *GLK2* (and GUN1), as *GLK2* has been shown to act as a positive regulator of nuclear-coded photosynthesis genes, including *LHCB1.2*, *LHCB2.1* and *LHCB6* and *GLK2* is stabilized by high temperature (Figure 5.4). Because *GLK1* was not fully assessed in this study, it is possible that *GLK1* has a more dominant effect on the expression of *LHCBs* than *GLK2*, despite *GLK1* and *GLK2* being partially redundant in their functions (Waters et al., 2009). Moreover, despite *GLK1* not being a significant DEG in our RNA-seq dataset (See; Chapter 3), its expression, indicated as transcripts per million, decreased during HT (Figure 5.1B). Whether

GLK1 has a (dominant over *GLK2*) role in the expression regulation of *LHCBs* under high temperature conditions needs to be further verified by checking the protein abundance of *GLK1* upon high temperature conditions and by assaying single *glk1* mutants and an *GLK1* overexpression line. Given that multiple pathways and mediators are involved in communication between plastids and nucleus upon stress conditions (Jan et al., 2022a), it is also possible that other retrograde signaling pathways are involved in controlling *GLK2* to mediate high temperature responses rather than GUN1. For example, *ETHYLENE-DEPENDENT GRAVITROPISM-DEFICIENT AND YELLOW-GREEN-LIKE 3 (EGY3)* is able to mediate chloroplast ROS homeostasis and promotes retrograde signaling in response to salt stress in *Arabidopsis* (Zhuang et al., 2021). Additionally, a recent study pointed out that GUN1 is necessary for H₂O₂-dependent oxidation of the cellular environment (Fortunato et al., 2022). Thus, future studies should focus on if and how retrograde signaling controls thermomorphogenesis, perhaps by focusing on cellular ROS signaling.

The induced expression of *YUC8* in *35S::GLK2* compared to *glk1glk2* and Col-0 under both normal and high temperature conditions implicates a potential role of *GLK2* in controlling auxin responses (Figure 5.5), which is further validated by comparing the dose-responsive hypocotyl growth between *GLK* mutants (*35S::GLK2* and *glk1glk2*), wild-type Col-0 and the phenotypic controls (*pif4-2* and *phyb-9*) (Figure 5.6A-B). Our results demonstrated that upon Picloram treatment, *35S::GLK2* resembles *pif4-2* in hypocotyl growth under both normal and high temperature conditions, while *glk1glk2* responded similar as the wild-type plants (Figure 5.6A). Together with the high percentage of agravitropism observed in *35S::GLK2*, it is possible that the attenuated thermomorphogenesis reflected by the inhibition of hypocotyl elongation in *35S::GLK2* is attributed to the lack of auxin response, or overaccumulation of auxin, that triggers inhibition (Bellstaedt et al., 2019; Van Der Woude et al., 2021). However, upon higher concentrations of Picloram or NPA treatments, *pif4-2* was unable to reach a comparable level of hypocotyl elongation as the wild-type plants, which is inconsistent with previous studies carried out on *pif4-2* mutants using the same treatments and experimental setups (Van Der Woude et al., 2021). Thus, due to the presence of the inconsistencies at diverse levels, we were not able to conclude whether or not *GLK2* manipulates auxin response through the regulation of *PIF4*, or otherwise directs auxin biosynthesis and/or signaling. To elucidate this, additional work such as replicating the dose-responsive experiment, or quantifying auxin levels in the *GLK2* overexpression line in the presence or absence of high temperature, is necessary. Additionally, further studies should also address whether the reduced hypocotyl elongation in *glk1glk2*, compared to Col-0, is due to the metabolic imbalance brought on by the compromised chloroplast function.

Previous studies have highlighted multiple negative regulators of thermomorphogenesis such as EARLY FLOWERING 3 (ELF3) and CRYPTOCHROME 1 (CRY1) (Raschke et al., 2015; Ma et al., 2016). These factors can directly interact with PIF4, a transcription factor that is induced by high temperature at both the transcriptional and the protein stability level, and constitutes a main signaling hub in thermomorphogenic responses (Proveniers & Van Zanten, 2013; Quint et al., 2016). It has been demonstrated that *GLKs* (*GLK1* and *GLK2*) are transcriptionally repressed by PIF4 and are direct PIF4 targets (Oh et al., 2012; Song et al., 2014; Martín et al., 2016). Our results showed that high levels of *GLK2* (in the *35S::GLK2* overexpression line, Figure 5.4A-C) result in enhanced *PIF4* mRNA abundance (Figure 5.5), suggesting that *GLK2* positively regulates *PIF4*. It is possible that *GLK2* and *PIF4* form a positive feedback regulatory loop; *PIF4* abundance represses *GLK2*, while *GLK2* in turn stimulates *PIF4* and thereafter promotes auxin biosynthesis. This likely explains why the overexpression of *GLK2* resembled the phenotypes of *pif4-2* upon high temperature and/or exogenous auxin treatment (Figures 5.2 and 5.5). We also propose that the impeded thermomorphogenesis caused by *GLK2* overexpression in this study might be due to feedback regulation of *PIF4* as *PIF4* can modulate its own expression by binding its own promoter (Lee et al., 2021b; Shapulatov et al., 2023). *GLK2* thus may affect the expression of *PIF4*, downstream of *PIF4*, and acts as an autofeedback regulator to modulate thermomorphogenesis. In the native (wild-type plants, Col-0) situation, *GLK2* may be stabilized on the protein level by high temperature to boost *PIF4* expression, needed to initially trigger auxin biosynthesis in early stages after high temperature perception, followed by the induction of thermomorphogenesis, but later participates in repression of thermomorphogenesis via *PIF4* feedback attenuation. This system may be out of balance in the *35S::GLK2* line with repression of thermomorphogenesis as a phenotypic outcome. However, high expression levels of *YUC8* were observed in *35S::GLK2*, which does not necessarily fit this *PIF4* attenuation hypothesis. Nevertheless feedback attenuation of (and by) *PIF4* is not unprecedented, as a recent study presented a autoregulatory composite negative feedback loop of *PIF4*-HECATE (*HEC*)s in thermomorphogenic responses, where *HEC2* can be transcriptionally activated by *PIFs*, while conversely, *HEC2* physically heterodimerizes *PIF4* to inhibit its function (Lee et al., 2021b). Moreover, it is known that *PIF4* induces the *Arabidopsis* RNA-binding protein *FCA*, which thereafter attenuates *PIF4* effectiveness by mediating *PIF4* dissociation from the *YUC8* promoter by removing H3K4me2 from the promoter (Lee et al., 2014; Choi & Oh, 2016). It is clear that major question marks remain and to further test the role of *GLK2* in general, and the *PIF4*-*GLK2* feedback-loop hypothesis in particular, additional work such as characterization of physical interactions between *PIF4* and *GLK2*, or the quantification of *PIF4* protein abundance in the genetic background of *GLK2* overexpression, are needed.

Acknowledgements

This work is supported by the Netherlands Organization for Scientific Research (NWO) (project no. 867.15.031 to AV) and the China Scholarship Council (CSC) (project no. 20186170025 to ZJ). We thank Dr. Charlotte Gommers (Wageningen University & Research, The Netherlands) for providing the seeds of *35S::GLK1*, *35S::GLK2*, *glk1glk2* and *gun1* and for discussions on retrograde signalling. We also thank Tatjana Kleine (Ludwig-Maximilians-Universität München, Germany) for providing the seeds of *35S::GLK2-GFP* and Nil Veciana and Elena Monte (Ramon Llull University, Spain) for sharing the information of the PCR reaction for genotyping, and Yorrit van de kaa for harvesting seeds.

Material and methods

Plant material and growth conditions

Arabidopsis thaliana seeds were obtained from the NASC stock center or were obtained via colleagues. The following lines were included in this study: wild-type Columbia-0 (Col-0; NASC stock center ID: N1092), *35S::GLK2* (NASC stock center ID: N9906), *35S::GLK2-GFP* (NASC stock center ID: N2107721) (Waters et al., 2008), *glk1glk2* (Fitter et al., 2002b), *gun1* (NASC stock center ID: N72518), (Ruckle et al., 2008), *pif4-2* (NASC stock center ID: N879261) and *phyb-9* (NASC stock center ID: N71625 (Yoshida et al., 2018)).

Plants for rosette trait measurements were grown as described in Chapter 2. In brief, seeds were sown on moist potting soil (Primasta BV, Asten, The Netherlands) and thereafter stratified at 4 °C in darkness for 4 days. The stratified seeds were then transferred to a growth chamber (MD1400; Snijders, The Netherlands) for germination with the following conditions: 8 h photoperiod / 16 h darkness, 21 °C, 120-150 $\mu\text{mol m}^{-2} \text{s}^{-1}$ PAR with LED lightening, 70% relative humidity. On the day the plants reached the 2-true leaf stage (LS2), the seedlings were individually transplanted to Jiffy 7c coconut pellets (Jiffy Products International BV, Zwijndrecht, The Netherlands) that were presoaked in 50 mL Hoagland solution (Millenaar et al., 2005), followed by saturation with deionized water to a final weight of 250 ± 20 g per pellet. Plants that were to be subjected to (combined) high temperature treatments (HT and HTD) were placed in the growth chamber set at 27 °C, with otherwise identical conditions as used for the control treatments (C) at 21 °C. Nutrition supplementation and randomization were performed as described in Chapter 2 (See; Chapter 2 Materials and Methods).

For hypocotyl measurements, seedlings were grown on MS-agar plates. Seeds were sterilized for 2 hours in a mixture of commercial bleach (Glorix) and concentrated hydrochloric acid (Sigma-Aldrich) before sowing. After sterilization, seeds were sown on sterile 1% plant agar supplied with 1 x Murashige-Skoog medium (MS, Duchefa M0255) without sucrose in square petri dishes (120 x 120 x 17 mm, Greiner Bio One). Plates containing the seeds were kept at 4 °C for 4 days in the darkness for sterilization before being placed vertically in growth chambers set at 21 °C or 27 °C and other conditions as described above, for 8 days.

Stress treatments

Plants for rosette trait measurements were subjected to individual (HT) or combined stresses (HTD) or kept at control conditions (C). Stress treatments were applied as described in Chapter 2.

Measurements of rosette and seedling traits

Petiole length was recorded by averaging the lengths of the 3rd–6th youngest leaf per plant. The hyponasty (leaf angle) was obtained by calculating the average of the angles of two opposing petioles relative to the horizontal.

To measure hypocotyl lengths, plates were scanned by an Epson V800 scanner (EPSON, Japan) and thereafter the hypocotyl length was measured per seedling using ImageJ (National Institutes of Health, USA). Seedling agravitropy was scored by counting the percentage of seedlings with agravitropic growth (hypocotyls deviated more than 45° from the opposite of the direction of gravity). Notably, when encountering total absence of gravitropic response, about 75% of the seedlings would show agravitropic growth, as a population of plants that is fully agravitropic has on average 25% of its seedlings within 45° from the opposite of the direction of gravity by chance.

Chlorophyll content measurements

Chlorophyll content was determined using a CM-300 Chlorophyll Meter (Opti-Sciences Inc., Hudson, USA) with a fluorescent detector. After calibration, the detector was placed at 5 mm distance from the leaf for 3 seconds and chlorophyll content per square meter (mg / m²) was automatically calculated based on the fluorescent intensity.

RNA isolation and quantitative real-time PCR (RT-qPCR)

Approximately 30–50 seedlings were harvested at ZT = 9 h and pooled together as one biological replicate and thereafter snap-frozen in liquid nitrogen. Frozen samples were subsequently grinded using a cryogenic grinding mill (Retsch, Haan, Germany) to a fine powder. Total RNA was extracted using the RNeasy kit (Qiagen, Germany)

following the manufacturers protocol. cDNA was synthesised using RNase H Reverse Transcriptase (Thermo Fisher Scientific) and random hexamer primers (Thermo Fisher Scientific). RT-qPCRs were performed using the Applied Biosystems ViiA 7 Real-time PCR system (Thermo Fisher Scientific) with a 5 µL reaction mixture containing 2.5 µL 2X SYBR Green MasterMix (Bio-Rad), 0.25 µL forward and reverse primer (10 µM) and 2 µL of 5 ng/µL cDNA. Relative mRNA abundance (indication of gene expression) was calculated by normalizing the CT values derived from the average of two technical replicates, by that of the housekeeping gene, *ACTIN2* and *PROTEIN PHOSPHATASE 2A* (*PP2A*), and thereafter normalized to Col-0 wild-type values under control temperature (21 °C). Primers used for RT-qPCR are indicated in Table S5.1.

Confirmation of T-DNA insertion lines

The confirmation of T-DNA insertion lines was performed using the same approach as described in Chapter 4. In brief, fresh leaves were detached and gDNA was extracted using Direct PCR-Phire and Phusion kit (Thermo Scientific, Inc, USA) following the manufacturers protocol. The presence of the T-DNA insertions and the homozygosity were determined by PCR using the primer pairs indicated in Table S5.1.

Western blotting

Approximately 30–50 seedlings were pooled together and pulverized in liquid nitrogen. Protein was extracted by incubating the samples in modified RIPA lysis buffer (Zhang et al., 2018; Hartman et al., 2019) for 30 min on ice and thereafter protein concentration was quantified using a BCA kit (Pierce). 30 µg protein was loaded into a pre-cast Mini-PROTEAN Stain Free TGX Gel (Bio Rad). Rubisco large subunit was visualized using stain-free imaging. Protein was then transferred to a 0.2 µm PVDF membrane (Bio Rad) using trans-blot turbo transfer system (BioRad). Membranes were then blocked for 1 hour in blocking solution (TBS-T (TBS supplied with 0.1% Tween 20) + 5% milk) at room temperature before being probed with primary antibody (anti-GFP, 1:2500, Roche #11814460001) in blocking solution at 4°C overnight. Membranes were rinsed for 4 times with 1x TBS-T and thereafter incubated with secondary antibody (rabbit anti-mouse, 1:2500, Cell Signaling #7076) at room temperature. After incubation, membranes were washed with TBS-T for 3 times and subsequently with TBS for 2 times. Membranes were incubated with Femto chemiluminescence substrate (Thermo Fisher Scientific) and imaged under a ChemiDoc imaging system (BioRad) to visualize the Horseradish Peroxidase (HRP) activity.

Pharmacological assays

N-1-Naphthylphthalamic acid (NPA; Duchefa) and Picloram (Sigma-Aldrich) were first dissolved in DMSO (Sigma-Aldrich) to a 100 mM stock solution. The stock solutions

were further diluted into required concentrations (here 50 μM , 25 μM , 12.5 μM , 5 μM , 2.5 μM , 1 μM , 0.5 μM and 0.1 μM) with DMSO and thereafter dissolved in the MS-agar medium to a final DMSO concentration of 0.1%. For mock treatments, DMSO lacking other chemical compounds were supplied to the agar medium.

Statistical analysis

Figures in this chapter were generated using GraphPad Prism 9 (GraphPad Software, La Jolla, USA) and Biorender.com. One-way or two-way ANOVA followed by Tukey's multiple test were performed by GraphPad Prism 9. The significance was considered as $p < 0.05$.

Supplemental data

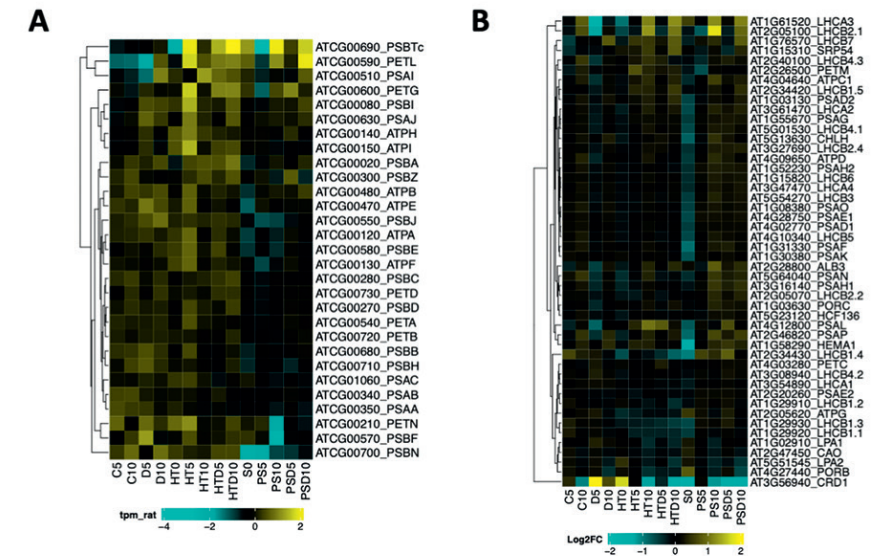


Figure S5.1. Expression levels of photosynthesis associated genes.

Heatmap presenting the expression (Transcript per million, TPM) of photosynthesis-associated chloroplast genes (*PhAPGs*) (**A**) and photosynthesis-associated nuclear genes (*PhANGs*) (**B**) in response to combined, sequential and single stresses. Data are derived from the transcriptome experiments described in chapter 3. Indicated are the AGI gene locus IDs and the commonly used abbreviations. The color scale indicates the expression levels, yellow represents up- and blue represents down-regulation. For abbreviations see chapter 3, legend figure 3.1.

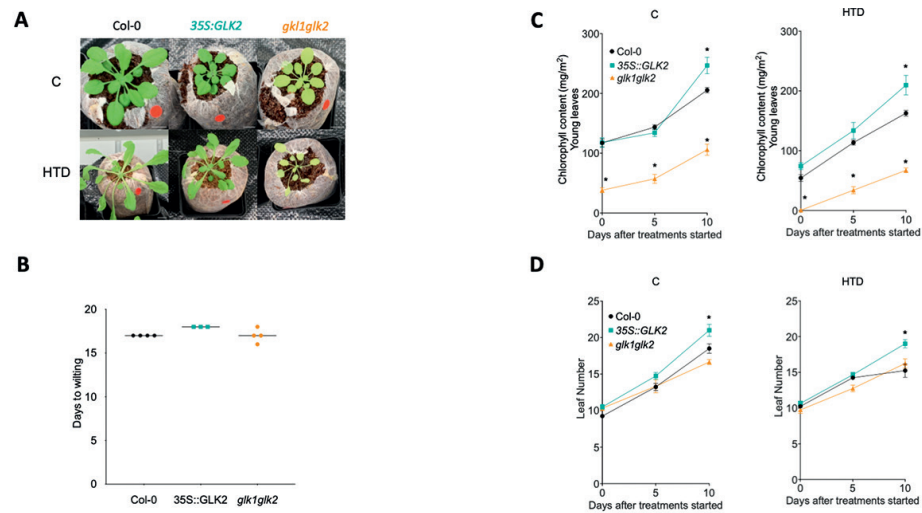


Figure S5.2. Effects of combined high temperature (HT), HT in combination with drought (HTD) and control (C) conditions on rosette phenotypic traits of Col-0 wild-type, 35S::GLK2 and *glk1glk2*.

(A) Representative images of Col-0, 35S::GLK2 and *glk1glk2* plants subjected to control (C) and combined high temperature and drought (HTD) treatment for 10 days. (B) Number of days till wilting occurred of Col-0 (black), 35S::GLK2 (aqua) and *glk1glk2* (orange) during the subjection of high temperature combined with drought (HTD). Dots represent individual biological replicates (plants). Black lines indicate the mean values. $n=3-4$. (C,D) Chlorophyll content (C) and number of leaves (D) of Col-0 (black), 35S::GLK2 (aqua) and *glk1glk2* (orange) under control (C, left) and combined high temperature and drought (HTD, right) treatments at different timepoints after the treatments started. Error bars indicate means \pm SEM. Asterisks represent significant differences between mutants (35S::GLK2 and *glk1glk2*) and the wild-type plants (Col-0) at the same time points ($p < 0.05$, 2-way ANOVA with Tukey's Post-hoc test). $n=3-8$.

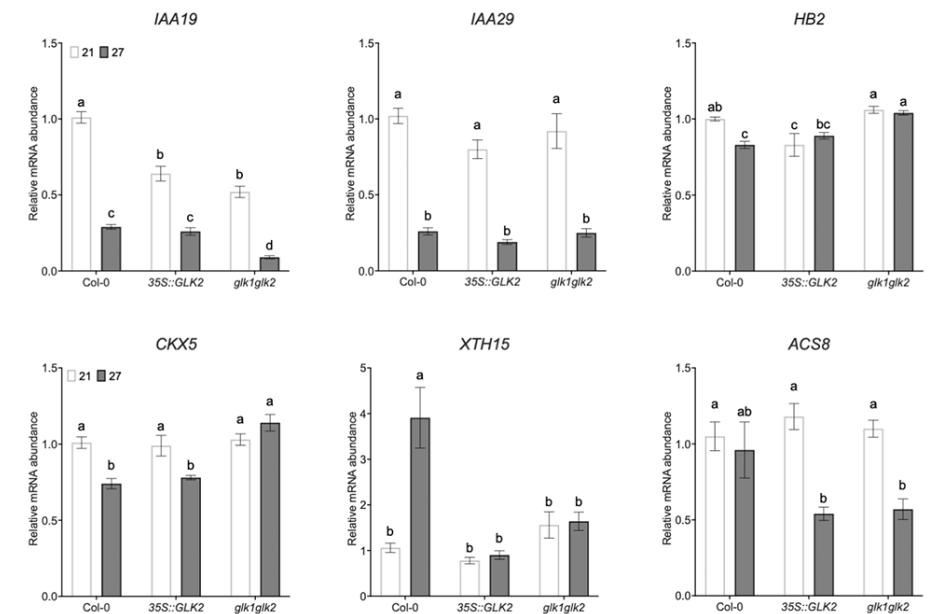


Figure S5.4. Relative mRNA abundance of PIF4 target genes *IAA19*, *IAA29*, *HB2*, *CKX5*, *XTH15* and *ACS8* at 21 °C or 27 °C, as determined by RT-qPCR.

$n=4-5$, each containing 30-50 seedlings as a pool harvested at ZT = 9 h. Error bars indicate means \pm SEM. Letters denote significant differences between different treatments and genotypes ($p < 0.05$, 2-way ANOVA with Tukey's Post-hoc test).

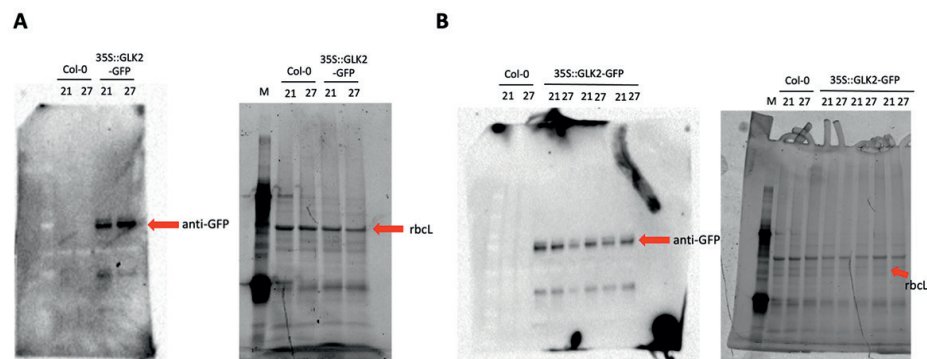


Figure S5.3. Full images of original uncropped Western blots used to detect GLK2. Uncropped Western blots (left) and Stain-free imaging of Rubisco protein (rbcl) (right) of Figure 5.4B (A) and the biological replicate (B).

Table S5.1 Primers used in this study.

Indicated are oligo name (FW; forward primer, RV; reverse primer), primer sequence, purpose for the primer pairs and the corresponding AGI identifier code.

Oligo Name	Sequence (5' - 3')	Purpose	AGI
<i>GUN1</i> FW	ATGCTGCATATCAGATTTCCGG	Genotyping	AT2G31400
<i>GUN1</i> RV	GTGGGTCTGCTGTTTCTTTG	Genotyping	AT2G31400
<i>GLK1</i> FW	TATGACGGTGACAGTGACCGG	qPCR/Genotyping	AT2G20570
<i>GLK1</i> RV	AACTGTTCCACTGCCTCCACG	qPCR/Genotyping	AT2G20570
<i>GLK2</i> FW	TGTGTGTAAGCAAGAGGGTGG	qPCR/Genotyping	AT5G44190
<i>GLK2</i> RV	CTACCCCTAATTGCTCCACCG	qPCR/Genotyping	AT5G44190
<i>LHCB2.1</i> FW	GGAAACCCTAACTGATCCACG	qPCR	AT2G05100
<i>LHCB2.1</i> RV	GACCGTCTTAAGCTCCTTCAC	qPCR	AT2G05100
<i>PIF4</i> FW	CTCGATTTCCGGTTATGG	qPCR	AT2G43010
<i>PIF4</i> RV	CAGACGGTTGATCATCTG	qPCR	AT2G43010
<i>LHCB6</i> FW	AACCCAATTGCTTCTCATGG	qPCR	AT1G15820
<i>LHCB6</i> RV	CCAACGGATCGAAGAATCTC	qPCR	AT1G15820
<i>LHCB1.2</i> FW	CTTCGTTCAAGCCATTGTCA	qPCR	AT1G29910
<i>LHCB1.2</i> RV	AACAAAGTTGGTTGCGAAGG	qPCR	AT1G29910
<i>HSP70</i> FW	CTGACAGCGAGCGTCTCAT	qPCR	AT4G16660
<i>HSP70</i> RV	GGATCACTGTATCTTCTCCGATT	qPCR	AT4G16660
<i>YUC8</i> FW	CGTCCCATATTGGCTACAAG	qPCR	AT4G28720
<i>YUC8</i> RV	CCTTCTCGTAAACCCAAC	qPCR	AT4G28720
<i>IAA19</i> FW	TAAGCTCTTCGGTTTCCGTG	qPCR	AT3G15540
<i>IAA19</i> RV	ACATCCCCAAGGTACATCA	qPCR	AT3G15540
<i>HB2</i> FW	CGAGCAAGACAAGTGAAGT	qPCR	AT4G16780
<i>HB2</i> RV	ATTCTCGCAGCATCTCCGTA	qPCR	AT4G16780
<i>CKX5</i> FW	TCGACGTTGTAAGTGGAAAGGAG	qPCR	AT1G75450
<i>CKX5</i> RV	AGAGAGATTCGTGCTCGAGTGATG	qPCR	AT1G75450
<i>XTH5</i> FW	TAGTTGGAATGGGTTTGACGGCGT AAGTCATCTAA	qPCR	AT5G13870
<i>XTH5</i> RV	TTATGGAGTTGGGTTTTGGGTTTG GTTGATAGAA	qPCR	AT5G13870
<i>ACS8</i> FW	TGGGTCTAGCAGAAAATCAGTTG	qPCR	AT4G37770
<i>ACS8</i> RV	TCCGACATGAAATCCGCCAT	qPCR	AT4G37770
<i>IAA29</i> FW	AAGATGGATGGTGTGGCAAT	qPCR	AT4G32280
<i>IAA29</i> RV	GTCACCCTCTTCCCTTGGA	qPCR	AT4G32280
<i>ACTIN2</i> FW	TTCGTGGTGGTGAAGTTTGT	qPCR	AT3G19780

Table S5.1: Continued

Oligo Name	Sequence (5' - 3')	Purpose	AGI
<i>ACTIN2</i> RV	GCATCATCACAAGCATCCTAA	qPCR	AT3G19780
<i>PP2A</i> FW	TAACGTGGCCAAAATGATGC	qPCR	AT1G10430
<i>PP2A</i> RV	GTTCTCCACAACCGCTTGGT	qPCR	AT1G10430
<i>Spm5</i>	CGGGATCCGACACTCTTAATT AACTGACACTC	Genotyping	
<i>2bgs</i>	AACTGCAGGTTACTGATCCGA TTGTTCTT	Genotyping	
<i>Spm8</i>	GTTTTGGCCGACACTCCTTACC	Genotyping	
<i>ara4</i>	TCCGATGTGACCTATATTC	Genotyping	
<i>SALK LB</i>	GCATCTGAATTCATAACCAATC	Genotyping	



6

Summarizing Discussion

Zhang Jiang, Martijn van Zanten*, Rashmi Sasidharan*
* Shared senior authors

Plant stress resilience, Utrecht University

The notable increase in average global temperatures due to climate change has already become problematic for earth's inhabitants, as its occurrence leads to not only temperature extremes like heat waves, but also an increase in episodes of drought and flooding events (Mimura, 2013; Stott, 2016; Schiermeier, 2018; Sutanto et al., 2020; Intergovernmental Panel On Climate Change (Ipc), 2023; Tripathy et al., 2023). Such weather extremes can have a substantial negative impact on the growth and yield of agricultural crops and jeopardize food security (Kumar, 2020; Raymond et al., 2020; Kopecká et al., 2023).

Being sessile organisms, plants rely on timely sensing of environmental signals to trigger various acclimation mechanisms that increase resilience in stressful environments (Zhang et al., 2020a; Kleine et al., 2021). In the past few decades, extensive research has contributed to our understanding of these mechanisms, but these have been predominantly focused on individual abiotic stresses. Plants in the field, however, are often exposed to variations in several environmental parameters and abiotic stresses rarely occur in isolation in nature (Mittler, 2006b; Zhang & Sonnewald, 2017). The understanding of how plants cope with multiple environmental threats and the mechanisms conferring multi-stress resilience therefore remains poorly understood. In this thesis, we characterized the responses of the model plant species *Arabidopsis thaliana* to two commonly occurring abiotic stress combinations; i) simultaneous imposition of high temperature and drought, and ii) sequential application of flooding followed by drought. Research on these stress combinations is relevant due to the heightened occurrence of the corresponding isolated stresses driven by unpredictable weather imposed by climate change (Anwar et al., 2021a; Morales et al., 2022). For instance, an elevation in temperature can accelerate soil drying and consequently leads to the co-occurrence of high temperature and drought (Lamaoui et al., 2018). Similarly, persistent heavy rainfall during the wet season can swiftly alternate with dry spells, resulting in a sequential presence of flooding events and drought episodes (Miao et al., 2009). The choice of *Arabidopsis* allowed us to leverage the vast amount of knowledge from previous studies on individual abiotic stresses. Together with its short life cycle, this facilitated an easier and faster optimization of combined stress treatments. Additionally, the compact and well-characterized genome along with numerous accessible mutations make *Arabidopsis* an optimal model for functional genetics studies of plant stress resilience (Pederson, 1968; Dean, 1993; Hays, 2002).

In natural and agricultural settings, abiotic stresses often occur at a gradual and sublethal severity. This contrasts with the often lethal stress levels applied in experimental laboratory studies to test for plant tolerance (Bailey-Serres & Colmer, 2014; Clauw et al., 2015; De Smet et al., 2021). As indicated above, sublethal stresses can

often evoke acclimation responses to cope with the environmental stress (Proveniers & Van Zanten, 2013; Pantazopoulou et al., 2017; Lee et al., 2020). To date, there is only a limited number of publications that focus on the acclimation capacity of plants to prolonged stress combinations at a sublethal severity.

While our understanding of plant multi-stress resilience is relatively poor compared to the knowledge on acclimation to individual stresses, it is known that co-occurring stresses can elicit distinct effects at both transcriptome and phenotypic levels compared to the corresponding individual stresses (Mittler, 2006b; Choudhury et al., 2017; Anwar et al., 2021a; Zandalinas et al., 2021b). The findings described in this thesis align with this. We observed unique response characteristics that were only apparent when stresses were applied in combination or sequentially, compared to the individual stresses. These responses included diverse *Arabidopsis* (rosette) growth, development, and physiological characteristics such as chlorophyll content, stomatal conductance and traits associated with leaf lengthening (Chapter 2). Through a comparative mRNA sequencing (RNA-seq) approach, we elucidated that the observed differences in phenotypic responses upon combined or sequential stresses correlate to differential gene regulation at the transcriptome level, as combined and sequential stresses led to a distinct set of differentially expressed genes (DEGs) that were not differentially regulated in response to either of the corresponding individual stresses (Chapter 3). The analysis of RNA-seq data also permitted the identification of crucial molecular processes and putative candidate genes that contribute to the acclimation to individual or combinatorial abiotic stresses, which were thereafter validated by a mutant analysis approach using identical experimental settings (Chapter 4&5). We also demonstrated the robustness of the phenotypes we studied by generating reproducible outcomes regardless of whether the stress treatments were conducted under LED or fluorescence-tube lighting systems (Chapter 2, Figure S2.3).

Considerations on mild drought treatments.

Drought stress is among the major environmental stresses hindering plant growth and productivity (Seleiman et al., 2021; Chieb & Gachomo, 2023). Our work showed that individually applied progressive drought (D) for 5 or 10 days did not elicit considerable changes at the morphological or the transcriptome level (Chapter 2 Figures 2.5 and 2.7, Chapter 3 Figures 3.3 and 3.4), even though the percentage of soil water content (%SWC) had dropped to approximately 30% after 10-days of progressive drought (Chapter 2 Figures S2.1 and S2.3). However, plants displayed some typical drought responses including elongated roots and reduced stomatal conductance (Chapter 2 Figures 2.6, 2.7, 2.8 and 2.9). This implies that the plants used in our experimental setup did perceive the water deficit.

Because the main goal of our study was to decipher the molecular underpinning of acclimation strategies of prolonged sublethal stresses, rather than focusing on the tolerance to stresses at a lethal severity, the transcriptomic profiling was conducted on young leaves that continued to expand while being subjected to the stress. Therefore, the limited number of detected DEGs under D were considered the ‘just right’ drought response, which enabled the initiation of chlorophyll abundance at the physiological level (Chapter 2 Figure 2.3), but did not alter the expression of a multifold of genes associated with *e.g.* metabolic changes as frequently observed under more severe drought conditions (Guo et al., 2018; Fàbregas & Fernie, 2019; Lozano-Elena et al., 2022). However, when D was imposed on the plants in combination with high temperature (HTD) or prior submergence (PSD), more DEGs were significantly differentially regulated compared to control conditions (Chapter 3 Figures 3.3 and 3.4). We propose that the three detected drought-associated DEGs (*GUARD-CELL-ENRICHED GDSL LIPASE 3 (GGL3)*, *PHOSPHOFRUCTOKINASE 1 (PFK1)* and *AT5G16990*) can be considered as potential marker genes for acclimation to mild drought stress and are worthy of further investigation into their physiological functions in drought acclimation. Obviously, since drought is primarily sensed in the roots and we did note root elongation in response to drought (Chapter 2 Figures 2.5G and 2.7G), it is plausible that in these below-ground tissues drought triggers a more extensive transcriptome reconfiguration, than the three genes detected in young leaves.

Some aspects of our experimental setup might also have contributed to the subtle effects of drought treatment, such as the high relative humidity (70%) in the growing chamber, or variation in soil water evaporation due to (uneven) ventilation. Given the relatively uncontrolled soil water loss during progressive drought, a controlled (moderated) drought application, where soil water content is sustained at a defined low level might be more optimal for studying drought stress resilience in future experiments. Such a controlled drought treatment can help sustain low soil water moisture at a sublethal severity for a long period of time, allowing probing long-term effects of mild drought as well (Harb et al., 2010; Ma et al., 2014; Abid et al., 2016). Moreover, a better controlled sustained drought system can also facilitate the precise comparison of performances and acclimation phenotypes between different plant genotypes with different growth characteristics (Harb et al., 2010). This can help studies aiming to determine the (natural) genetic basis of (differences in) drought susceptibility.

Acclimation to combinatorial abiotic stress in different plant tissues

While our study on the molecular responses to combined or sequential stresses only focused on expanding (young) leaves, as we aimed to identify genetic regulators

mediating ‘stress acclimation’ rather than ‘stress tolerance’, different plant organs such as the aboveground and belowground tissues can exhibit variations in response signatures to a certain environmental signal (Sarwat, 2017; Ambroise et al., 2020; Vives-Peris et al., 2020). Roots are the primary organ to perceive the stress signals for osmotic stresses such as salt or drought (Li et al., 2021a). When exposed to drought, plants attempt to invest in longer primary roots for water capture in deeper soil (Markhart, 1985). This typical drought response was confirmed by our study where primary root elongation was observed under D relative to controls (C) (Chapter 2 Figures 2.5G and 2.7G). Drought in combination with high ambient temperature can enhance the intensity of soil drying relative to isolated drought occurrence and roots thus need to penetrate into deeper soil for a better plant hydraulic status (Bengough et al., 2011). Indeed, drought in combination with either high temperature or prior submergence treatment further stimulated primary root lengthening (Chapter 2 Figures 2.5G and 2.7G), which can be considered an additional effect caused by combinatorial stresses. Possibly, induced root elongation under combinatorial stresses is attributed to changes in shoot-to-root resource allocation upon stress treatments (Agathokleous et al., 2019; Reinelt et al., 2023). However, to better elucidate the mechanisms underlying shoot-to-root communications under combinatorial stresses, further investigation on root responses to combinatorial stresses at the molecular level is needed. A recent study highlighted that a prior waterlogging stress can trigger a rapid systemic hydraulic wave from root to shoot, inducing a heightened state of tolerance to a subsequent submergence stress (Peláez-Vico et al., 2023). In addition, the systematic response upon combinatorial stresses occurs not only between above- and below-ground, but also between leaves (Zandalinas et al., 2020). These studies have provided valuable insights for future studies of the whole-plant acclimation to combinatorial abiotic stresses in the particular context of signaling communication between different tissues. For example, whether hydraulic waves in root can facilitate the shoot/leaf responsiveness to combinatorial stresses, or if signals derived from leaves can initiate the acclimation response in belowground tissues.

Cross-acclimation to sequentially combinatorial stresses

In response to sequentially combinatorial stress, the initial stress can prime plants to enhance the effective responses to the subsequent stress (Coolen et al., 2016a; Perincherry et al., 2021; Liu et al., 2022a). While our work identified molecular components, including transcription factors and phytohormones, that potentially govern acclimation to either combined or sequential stresses (Chapter 3&4), we did not investigate cross-acclimation between sequentially occurring stresses such as submergence (S) and PSD. We argue that potential key regulators of cross-acclimation in a sequential combinatorial stress should reside in the fraction of genes/proteins

that are actively regulated in response to both the first and second stresses. In our study, genes potentially involved in cross-acclimation should therefore be among the 599 DEGs ($\text{Log}_2 |\text{FC}| > 0$, $p < 0.05$) overlapping between submergence (S) and PSD in the transcriptomic dataset (Figure 6.1). Among these are putative cross-acclimation candidates genes that have a functional association with responsiveness to both submergence and drought (*i.e.*, DEGs relevant to energy consumption, ABA or ethylene response (Tamang et al., 2021)), and are of particular interest for further studies.

Epigenetic regulation is known to play a crucial role in cross acclimation processes (Luo & He, 2020; Miryeganeh, 2021). Therefore, future work on (sequentially) combinatorial stress resilience should include an investigation of changes occurring at the post-transcriptional level, such as sRNA-mediated regulation, DNA methylation and histone modifications.

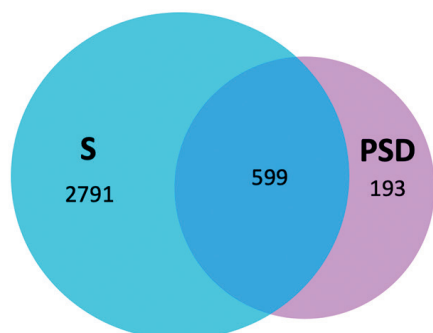


Figure 6.1. Putative cross-acclimation regulators.

Venn diagram showing the number of differentially expressed genes (DEGs, $|\text{Log}_2 \text{FC}| > 0$, $p < 0.05$) commonly (overlap) or differentially expressed upon submergence in the light (S) and post-submergence and drought (PSD) stresses, compared to control conditions.

Improving plant multi-stress resilience

Plant responses to abiotic stresses are usually age-dependent (Rankenberg et al., 2021). Juvenile tissues are in general more responsive to environmental stresses than mature tissues, while also being more tolerant (Berens et al., 2019; Bui et al., 2020). In our study, young *Arabidopsis* leaves tended to maintain a higher level of chlorophyll content under D, PSD, and HTD, compared to the corresponding controls, while the old(er) leaves did not (Chapter 2 Figure 2.3). Additionally, increased chlorophyll abundance linked to *GLK2* overexpression under HTD could contribute to improved survival under

drought (*i.e.*, delayed wilting) (Chapter 5 Figure S5.2). Seemingly, tweaking chlorophyll content can be a promising strategy to improve plant resilience to abiotic stresses like drought, as an enhanced abundance of chlorophyll content enables more efficient photosynthetic activities under certain conditions if photon capture is limiting (Zhao et al., 2019b; Mandal & Dutta, 2020; Monteoliva et al., 2021).

Frequently implicated molecules in combinatorial-stress responses, such as reactive oxygen species (ROS) or genes encoding Heat Shock Proteins (HSPs) or Heat Shock Factors (HSFs) (Zandalinas et al., 2020; Zandalinas et al., 2021; Zandalinas and Mittler, 2022; Zhang and Sonnewald, 2017), were not overrepresented in our RNA-seq dataset. This is potentially attributed to the sublethal stress severity, as well as the focus of our study on identifying genes responsible for ‘stress acclimation’ rather than ‘stress tolerance’ by assaying young expanding leaves which consequently resulted in the enrichment of putative candidates linked to sublethal stress acclimation instead of lethal-stress associated genes.

The presence of *Arabidopsis* Latent Virus 1 (ArLV1) in our RNA-seq dataset (and thus plants) was unexpected. We showed that the presence of this comovirus has only very subtle effects on the *Arabidopsis* transcriptome and measured phenotypic traits (whole rosette area, leaf initiations) (Chapter 3, Figures S3.1, S3.2). *Arabidopsis* plants inoculated with ArLV1 exhibited a higher level of chlorophyll, accompanied by delayed wilting time under progressive drought (Verhoeven et al., 2023). This implies that ArLV1 infection likely confers plants with mild drought tolerance, which is consistent with the concept from previous studies that many plant viruses can have protective effects on their host by mitigating the negative effects of abiotic stresses such as high temperature (Anfoka et al., 2016), drought (Mishra et al., 2022) or salinity (Sinha et al., 2021a). Given the beneficial effect of ArLV1 and other plant viruses on the responsiveness to environmental stimuli, the mechanism of virus-triggered stress resilience to combinatorial stresses is interesting to investigate in future studies. In agricultural settings, crops inoculated with beneficial plant viruses might improve crop tolerance to abiotic stresses while maintaining growth and yield.

Phytohormones are crucial signaling compounds governing plant growth, development and physiology (Wani et al., 2016; El Sabagh et al., 2022) and are well-known for steering plant tolerance to different environmental signals (Zheng et al., 2023). For example, an ethylene pre-treatment can activate molecular processes that promote resilience against multiple abiotic stresses, including hypoxia (Hartman et al., 2019; Liu et al., 2022c), salinity (Cao et al., 2007; Peng et al., 2014) and drought (Zhu et al., 2018). Manipulation of phytochromes to enhance plant growth and

metabolism under stress conditions can be accomplished by several strategies, including exogenous application of bio-active hormones or precursor compounds, or by genetic manipulation of hormone-target genes (Sawers et al., 2005; Mockler, 2016; Yuan et al., 2019; Zhang et al., 2021a). We show that ABA signaling is likely involved in acclimation to both HTD and PSD (Chapter 3 & 4). However, investigation into ABA downstream targets and their roles in mediating typical phenotypic traits is currently lacking. γ -Aminobutyric acid (GABA), which is another plant metabolite, might be an emerging candidate for endogenous application to reinforce (combinatorial) stress resilience. GABA accumulates rapidly in plants upon biotic or abiotic stresses (Roberts, 2007; Shelp et al., 2021). GABA is also proposed as a key player in the acclimation of Arabidopsis to combined high light and heat stress, potentially through the promotion of autophagy (Balfagón et al., 2022). Moreover, multiple studies have evidenced that exogenous application of GABA has beneficial effects on the resistance of abiotic stresses such as drought (Yong et al., 2017) or salt (Mishra et al., 2023). Additional work is necessary to elucidate the target processes of GABA in the context of combinatorial stress acclimation, as well as to determine the most optimal dosage for application in field breeding.

By combining RNA-seq and reverse genetics analysis, we uncovered *EARLY FLOWERING 6 (ELF6)* as a negative regulator of the phenotypic acclimation to HTD, while *ARABIDOPSIS TOXICOS EN LEVADURA 80 (ATL80)* is a positive regulator for PSD (Chapter 3 & Chapter 4). Additionally, we identified regulators such as *ZINC FINGER PROTEIN 4 (ZFP4)* and *GENOMES UNCOUPLED 4 (GUN4)*, as relevant factors in controlling plant wilting under HTD or PSD. Interestingly, *ZFP4* and *GUN4* appear to participate in governing rosette expansion and/or dry weight accumulation under individually applied stresses such as D, high temperature (HT) or post-submergence (PS), but not combinatorial stresses (Chapter 4 Figures 4.2 and 4.6). These genes are putative *bonafide* multi-stress tolerance genes and are of much value for further studies into their molecular functions during (sublethal) isolated or combinatorial stresses. It could be that orthologs of these candidates in commercial crop species also contribute to combinatorial stress resilience.

Concluding remarks and future perspectives

Relative to the corresponding isolated stresses, co-occurring abiotic stresses usually cause distinct effects on plants and elicit unique acclimation responses and underlying transcriptomic changes. Here we catalogued phenotypic and transcriptomic characteristics contributing to the acclimation and resilience of Arabidopsis to either simultaneously or sequentially occurring sublethal combinatorial stresses. We provided examples of how selected identified molecular components affect plant

growth, development, and physiology upon the sublethal stress treatments. Our study provides a platform that can be built on further in future investigations on long-term acclimation to stress combinations at a gradual and sublethal severity, which is highly relevant in natural or agricultural settings due to unpredictable climate change.

It is important to note that in our work, the terms 'resilience' and 'acclimation' primarily refer to morphological and physiological changes adopted by plants in order to counteract (combinatorial) abiotic stresses, rather than to traits that are of prime commercial significance such as seed yield or food productivity. In the future, it would be interesting to investigate how the sublethal combinatorial stresses affect productivity in different plant species including agronomical crops, and whether the identified multi-stress regulators and traits that we describe in this thesis can contribute to the actual breeding and/or engineering of climate change-ready field crops. Identification of orthologues that share functionality and a common ancestor is often regarded as a first step for the knowledge transfer (Spannagl et al., 2011). Followed by genome editing techniques (CRISPR/Cas9), it will be hopefully possible to develop modern agricultural crops that possess enhanced resilience to multiple combinatorial stresses.

References

- Abas, L., Kolb, M., Stadlmann, J., Janacek, D.P., Lukic, K. & Schwechheimer, C.**, 2020. Naphthylphthalamic acid associates with and inhibits PIN auxin transporters. 1–8. doi: 10.1073/pnas.2020857118
- Abid, M., Tian, Z., Ata-Ul-Karim, S.T., Liu, Y., Cui, Y., Zahoor, R., Jiang, D. & Dai, T.**, 2016. Improved tolerance to post-anthesis drought stress by pre-drought priming at vegetative stages in drought-tolerant and -sensitive wheat cultivars. *Plant Physiology and Biochemistry* **106**: 218–227. doi: 10.1016/j.plaphy.2016.05.003
- Agathokleous, E., Belz, R.G., Kitao, M., Koike, T. & Calabrese, E.J.**, 2019. Does the root to shoot ratio show a hormetic response to stress? An ecological and environmental perspective. *Journal of Forestry Research* **30**(5): 1569–1580. doi: 10.1007/s11676-018-0863-7
- Aguilar-Martínez, J.A. & Sinha, N.**, 2013. Analysis of the role of Arabidopsis class I TCP genes AtTCP7, AtTCP8, AtTCP22, and AtTCP23 in leaf development. *Frontiers in Plant Science* **4**. doi: 10.3389/fpls.2013.00406
- Aharoni, A. & Galili, G.**, 2011. Metabolic engineering of the plant primary–secondary metabolism interface. *Current Opinion in Biotechnology* **22**(2): 239–244. doi: 10.1016/j.copbio.2010.11.004
- Ahmed, I.M., Cao, F., Zhang, M., Chen, X., Zhang, G. & Wu, F.**, 2013. Difference in Yield and Physiological Features in Response to Drought and Salinity Combined Stress during Anthesis in Tibetan Wild and Cultivated Barleys. *PLoS ONE* **8**(10): e77869. doi: 10.1371/journal.pone.0077869
- Ahmed, I.M., Nadira, U.A., Bibi, N., Cao, F., He, X., Zhang, G. & Wu, F.**, 2015a. Secondary metabolism and antioxidants are involved in the tolerance to drought and salinity, separately and combined, in Tibetan wild barley. *Environmental and Experimental Botany* **111**: 1–12. doi: 10.1016/j.envexpbot.2014.10.003
- Ahmed, I.M., Nadira, U.A., Bibi, N., Zhang, G. & Wu, F.**, 2015b. Tolerance to Combined Stress of Drought and Salinity in Barley. In: R. Mahalingam (ed.): *Combined Stresses in Plants*. Springer International Publishing (Cham): pp. 93–121. doi: 10.1007/978-3-319-07899-1_5
- Ai, H., Bellstaedt, J., Bartusch, K.S., Eschen-Lippold, L., Babben, S., Balcke, G.U., Tissier, A., Hause, B., Andersen, T.G., Delker, C. & Quint, M.**, 2023. Auxin-dependent regulation of cell division rates governs root thermomorphogenesis. *The EMBO Journal* **42**(11): e111926. doi: 10.15252/embj.2022111926
- Albertini, A., Simeoni, F., Galbiati, M., Bauer, H., Tonelli, C. & Cominelli, E.**, 2014. Involvement of the vacuolar processing enzyme γ VPE in response of Arabidopsis thaliana to water stress. *Biologia Plantarum* **58**(3): 531–538. doi: 10.1007/s10535-014-0417-6
- Albertos, P., Dünder, G., Schenk, P., Carrera, S., Cavelius, P., Sieberer, T. & Poppenberger, B.**, 2022. Transcription factor BES1 interacts with HSFA1 to promote heat stress resistance of plants. *The EMBO Journal* **41**(3): e108664. doi: 10.15252/embj.2021108664
- Ambrose, V., Legay, S., Guerriero, G., Hausman, J.-F., Cuypers, A. & Sergeant, K.**, 2020. The Roots of Plant Frost Hardiness and Tolerance. *Plant and Cell Physiology* **61**(1): 3–20. doi: 10.1093/pcp/pcz196
- Andrási, N., Rigó, G., Zsigmond, L., Pérez-Salamó, I., Papdi, C., Klement, E., Pettkó-Szandtner, A., Baba, A.I., Ayaydin, F., Dasari, R., Cséplő, Á. & Szabados, L.**, 2019. The mitogen-activated protein kinase 4-phosphorylated heat shock factor A4A regulates responses to combined salt and heat stresses. *Journal of Experimental Botany* **70**(18): 4903–4918. doi: 10.1093/jxb/erz217

- Anfoka, G., Moshe, A., Fridman, L., Amrani, L., Rotem, O., Kolot, M., Zeidan, M., Czosnek, H. & Gorovits, R.**, 2016. Tomato yellow leaf curl virus infection mitigates the heat stress response of plants grown at high temperatures. *Scientific Reports* **6**(1): 19715. doi: 10.1038/srep19715
- Ansari, M.I. & Lin, T.-P.**, 2010. Arabidopsis thaliana thylakoid lumen 18.3 protein (TLP 18.3) gene regulate developmental process.
- Anwar, K., Joshi, R., Dhankher, O.P., Singla-Pareek, S.L. & Pareek, A.**, 2021a. Elucidating the Response of Crop Plants towards Individual, Combined and Sequentially Occurring Abiotic Stresses. *International Journal of Molecular Sciences* **22**(11): 6119. doi: 10.3390/ijms22116119
- Anwar, K., Joshi, R., Dhankher, O.P., Singla-Pareek, S.L. & Pareek, A.**, 2021b. Elucidating the Response of Crop Plants towards Individual, Combined and Sequentially Occurring Abiotic Stresses. *International Journal of Molecular Sciences* **22**(11): 6119. doi: 10.3390/ijms22116119
- Ascencio-Ibáñez, J.T., Sozzani, R., Lee, T.-J., Chu, T.-M., Wolfinger, R.D., Cella, R. & Hanley-Bowdoin, L.**, 2008. Global Analysis of Arabidopsis Gene Expression Uncovers a Complex Array of Changes Impacting Pathogen Response and Cell Cycle during Geminivirus Infection. *Plant Physiology* **148**(1): 436–454. doi: 10.1104/pp.108.121038
- Ashburner, M., Ball, C.A., Blake, J.A., Botstein, D., Butler, H., Cherry, J.M., Davis, A.P., Dolinski, K., Dwight, S.S., Eppig, J.T., Harris, M.A., Hill, D.P., Issel-Tarver, L., Kasarskis, A., Lewis, S., Matese, J.C., Richardson, J.E., Ringwald, M., Rubin, G.M. & Sherlock, G.**, 2000. Gene Ontology: tool for the unification of biology. *Nature Genetics* **25**(1): 25–29. doi: 10.1038/75556
- Azodi, C.B., Lloyd, J.P. & Shiu, S.-H.**, 2020. The cis-regulatory codes of response to combined heat and drought stress in Arabidopsis thaliana. *NAR Genomics and Bioinformatics* **2**(3): lqaa049. doi: 10.1093/nargab/lqaa049
- Bader, G.D. & Hogue, C.W.**, 2003. An automated method for finding molecular complexes in large protein interaction networks. *BMC Bioinformatics* **4**(1): 2. doi: 10.1186/1471-2105-4-2
- Baek, D., Kim, M.C., Kumar, D., Park, B., Cheong, M.S., Choi, W., Park, H.C., Chun, H.J., Park, H.J., Lee, S.Y., Bressan, R.A., Kim, J.-Y. & Yun, D.-J.**, 2019. AtPR5K2, a PR5-Like Receptor Kinase, Modulates Plant Responses to Drought Stress by Phosphorylating Protein Phosphatase 2Cs. *Frontiers in Plant Science* **10**: 1146. doi: 10.3389/fpls.2019.01146
- Baena-González, E.**, 2010. Energy Signaling in the Regulation of Gene Expression during Stress. *Molecular Plant* **3**(2): 300–313. doi: 10.1093/mp/ssp113
- Bai, Y., Sunarti, S., Kissoudis, C., Visser, R.G.F. & Van Der Linden, C.G.**, 2018. The Role of Tomato WRKY Genes in Plant Responses to Combined Abiotic and Biotic Stresses. *Frontiers in Plant Science* **9**: 801. doi: 10.3389/fpls.2018.00801
- Bailey-Serres, J. & Colmer, T.D.**, 2014. Plant tolerance of flooding stress – recent advances. *Plant, Cell & Environment* **37**(10): 2211–2215. doi: 10.1111/pce.12420
- Bailey-Serres, J. & Voeselek, L.A.C.J.**, 2008. Flooding Stress: Acclimations and Genetic Diversity. *Annual Review of Plant Biology* **59**(1): 313–339. doi: 10.1146/annurev.arplant.59.032607.092752
- Balfagón, D., Gómez-Cadenas, A., Rambla, J.L., Granell, A., De Ollas, C., Bassham, D.C., Mittler, R. & Zandalinas, S.I.**, 2022. γ -Aminobutyric acid plays a key role in plant acclimation to a combination of high light and heat stress. *Plant Physiology* **188**(4): 2026–2038. doi: 10.1093/plphys/kiac010
- Balfagón, D., Sengupta, S., Gómez-Cadenas, A., Fritschi, F.B., Azad, R.K., Mittler, R. & Zandalinas, S.I.**, 2019a. Jasmonic Acid Is Required for Plant Acclimation to a Combination of High Light and Heat Stress. *Plant Physiology* **181**(4): 1668–1682. doi: 10.1104/pp.19.00956
- Balfagón, D., Sengupta, S., Gómez-Cadenas, A., Fritschi, F.B., Azad, R.K., Mittler, R. & Zandalinas, S.I.**, 2019b. Jasmonic Acid Is Required for Plant Acclimation to a Combination of High Light and Heat Stress. *Plant Physiology* **181**(4): 1668–1682. doi: 10.1104/pp.19.00956

- Balfagón, D., Zandalinas, S.I., De Reis De Oliveira, T., Santa-Catarina, C. & Gómez-Cadenas, A.**, 2023. Omics analyses in citrus reveal a possible role of RNA translation pathways and UPR regulators in the tolerance to combined drought, high irradiance and heat stress. *Horticulture Research* uhad107. doi: 10.1093/hr/uhad107
- Baniwal, S.K., Bharti, K., Chan, K.Y., Fauth, M., Ganguli, A., Kotak, S., Mishra, S.K., Nover, L., Port, M., Scharf, K.-D., Tripp, J., Weber, C., Zielinski, D. & Von Koskull-Döring, P.**, 2004. Heat stress response in plants: a complex game with chaperones and more than twenty heat stress transcription factors. *Journal of Biosciences* **29**(4): 471–487. doi: 10.1007/BF02712120
- Banti, V., Loreti, E., Novi, G., Santaniello, A., Alpi, A. & Perata, P.**, 2008. Heat acclimation and cross-tolerance against anoxia in *Arabidopsis*. *Plant, Cell & Environment* **31**(7): 1029–1037. doi: 10.1111/j.1365-3040.2008.01816.x
- Bao, G., Tang, W., An, Q., Liu, Y., Tian, J., Zhao, N. & Zhu, S.**, 2020. Physiological effects of the combined stresses of freezing-thawing, acid precipitation and deicing salt on alfalfa seedlings. *BMC Plant Biology* **20**(1): 204. doi: 10.1186/s12870-020-02413-4
- Bascom, C.**, 2023. Shape-shifting leaves depend on SPL10. *The Plant Cell* **35**(5): 1292–1293. doi: 10.1093/plcell/koad046
- Batista-Silva, W., Heinemann, B., Rugen, N., Nunes-Nesi, A., Araújo, W.L., Braun, H. & Hildebrandt, T.M.**, 2019. The role of amino acid metabolism during abiotic stress release. *Plant, Cell & Environment* **42**(5): 1630–1644. doi: 10.1111/pce.13518
- Bechtold, U., Penfold, C.A., Jenkins, D.J., Legaie, R., Moore, J.D., Lawson, T., Matthews, J.S.A., Violet-Chabrand, S.R.M., Baxter, L., Subramaniam, S., Hickman, R., Florance, H., Sambles, C., Salmon, D.L., Feil, R., Bowden, L., Hill, C., Baker, N.R., Lunn, J.E., Finkenstädt, B., Mead, A., Buchanan-Wollaston, V., Beynon, J., Rand, D.A., Wild, D.L., Denby, K.J., Ott, S., Smirnov, N. & Mullineaux, P.M.**, 2016. Time-Series Transcriptomics Reveals That AGAMOUS-LIKE22 Affects Primary Metabolism and Developmental Processes in Drought-Stressed *Arabidopsis*. *The Plant Cell* **28**(2): 345–366. doi: 10.1105/tpc.15.00910
- Beckers, G.J.M., Jaskiewicz, M., Liu, Y., Underwood, W.R., He, S.Y., Zhang, S. & Conrath, U.**, 2009. Mitogen-Activated Protein Kinases 3 and 6 Are Required for Full Priming of Stress Responses in *Arabidopsis thaliana*. *The Plant Cell* **21**(3): 944–953. doi: 10.1105/tpc.108.062158
- Begcy, K. & Dresselhaus, T.**, 2018. Epigenetic responses to abiotic stresses during reproductive development in cereals. *Plant Reproduction* **31**(4): 343–355. doi: 10.1007/s00497-018-0343-4
- Bellstaedt, J., Trenner, J., Lippmann, R., Poeschl, Y., Zhang, X., Friml, J., Quint, M. & Delker, C.**, 2019. A Mobile Auxin Signal Connects Temperature Sensing in Cotyledons with Growth Responses in Hypocotyls. *Plant Physiology* **180**(2): 757–766. doi: 10.1104/pp.18.01377
- Bengough, A.G., McKenzie, B.M., Hallett, P.D. & Valentine, T.A.**, 2011. Root elongation, water stress, and mechanical impedance: a review of limiting stresses and beneficial root tip traits. *Journal of Experimental Botany* **62**(1): 59–68. doi: 10.1093/jxb/erq350
- Benschop, J.J., Jackson, M.B., Gühl, K., Vreeburg, R.A.M., Croker, S.J., Peeters, A.J.M. & Voeselek, L.A.C.J.**, 2005. Contrasting interactions between ethylene and abscisic acid in *Rumex* species differing in submergence tolerance: ABA-regulated growth in *Rumex*. *The Plant Journal* **44**(5): 756–768. doi: 10.1111/j.1365-313X.2005.02563.x
- Berens, M.L., Wolinska, K.W., Spaepen, S., Ziegler, J., Nobori, T., Nair, A., Krüler, V., Winkelmüller, T.M., Wang, Y., Mine, A., Becker, D., Garrido-Oter, R., Schulze-Lefert, P. & Tsuda, K.**, 2019. Balancing trade-offs between biotic and abiotic stress responses through leaf age-dependent variation in stress hormone cross-talk. *Proceedings of the National Academy of Sciences* **116**(6): 2364–2373. doi: 10.1073/pnas.1817233116
- Berkowitz, O., De Clercq, I., Van Breusegem, F. & Whelan, J.**, 2016. Interaction between hormonal and mitochondrial signalling during growth, development and in plant defence responses. *Plant, Cell & Environment* **39**(5): 1127–1139. doi: 10.1111/pce.12712
- Bernoux, M., Timmers, T., Jauneau, A., Brière, C., De Wit, P.J.G.M., Marco, Y. & Deslandes, L.**, 2008. RD19, an *Arabidopsis* Cysteine Protease Required for RRS1-R–Mediated Resistance, Is Relocalized to the Nucleus by the *Ralstonia solanacearum* PopP2 Effector. *The Plant Cell* **20**(8): 2252–2264. doi: 10.1105/tpc.108.058685
- Bharath, P., Gahir, S. & Raghavendra, A.S.**, 2021. Abscisic Acid-Induced Stomatal Closure: An Important Component of Plant Defense Against Abiotic and Biotic Stress. *Frontiers in Plant Science* **12**: 615114. doi: 10.3389/fpls.2021.615114
- Bhaskara, G.B., Lasky, J.R., Razzaque, S., Zhang, L., Haque, T., Bonnette, J.E., Civelek, G.Z., Verslues, P.E. & Juenger, T.E.**, 2022. Natural variation identifies new effectors of water-use efficiency in *Arabidopsis*. *Proceedings of the National Academy of Sciences* **119**(33): e2205305119. doi: 10.1073/pnas.2205305119
- Bi, C., Ma, Y., Wu, Z., Yu, Y.-T., Liang, S., Lu, K. & Wang, X.-F.**, 2017. *Arabidopsis* ABI5 plays a role in regulating ROS homeostasis by activating CATALASE 1 transcription in seed germination. *Plant Molecular Biology* **94**(1–2): 197–213. doi: 10.1007/s11103-017-0603-y
- Bin Rahman, A.N.M.R. & Zhang, J.**, 2016. Flood and drought tolerance in rice: opposite but may coexist. *Food and Energy Security* **5**(2): 76–88. doi: 10.1002/fes3.79
- Bitá, C.E. & Gerats, T.**, 2013. Plant tolerance to high temperature in a changing environment: scientific fundamentals and production of heat stress-tolerant crops. *Frontiers in Plant Science* **4**. doi: 10.3389/fpls.2013.00273
- Bittner, A., Cieřla, A., Gruden, K., Lukan, T., Mahmud, S., Teige, M., Vothknecht, U.C. & Wurzinger, B.**, 2022. Organelles and phytohormones: a network of interactions in plant stress responses. *Journal of Experimental Botany* **73**(21): 7165–7181. doi: 10.1093/jxb/erac384
- Bosco, C.D., Lezhneva, L., Biehl, A., Leister, D., Strotmann, H., Wanner, G. & Meurer, J.**, 2004. Inactivation of the Chloroplast ATP Synthase γ Subunit Results in High Non-photochemical Fluorescence Quenching and Altered Nuclear Gene Expression in *Arabidopsis thaliana*. *Journal of Biological Chemistry* **279**(2): 1060–1069. doi: 10.1074/jbc.M308435200
- Bouzi, M., He, F., Schmitz, G., Häusler, R.E., Weber, A.P.M., Mettler-Altman, T. & De Meaux, J.**, 2019. *Arabidopsis* species deploy distinct strategies to cope with drought stress. *Annals of Botany* **124**(1): 27–40. doi: 10.1093/aob/mcy237
- Bowler, C. & Fluhr, R.**, 2000. The role of calcium and activated oxygens as signals for controlling cross-tolerance. *Trends in Plant Science* **5**(6): 241–246. doi: 10.1016/S1360-1385(00)01628-9
- Bray, N.L., Pimentel, H., Melsted, P. & Pachter, L.**, 2016. Near-optimal probabilistic RNA-seq quantification. *Nature Biotechnology* **34**(5): 525–527. doi: 10.1038/nbt.3519
- Bueno, A., Alfarhan, A., Arand, K., Burghardt, M., Deininger, A.-C., Hedrich, R., Leide, J., Seufert, P., Staiger, S. & Riederer, M.**, 2019. Effects of temperature on the cuticular transpiration barrier of two desert plants with water-spender and water-saver strategies. *Journal of Experimental Botany* **70**(5): 1613–1625. doi: 10.1093/jxb/erz018
- Bui, L.T., Shukla, V., Giorgi, F.M., Trivellini, A., Perata, P., Licausi, F. & Giuntoli, B.**, 2020. Differential submergence tolerance between juvenile and adult *Arabidopsis* plants involves the ANAC017 transcription factor. *The Plant Journal* **104**(4): 979–994. doi: 10.1111/tpj.14975
- Burko, Y., Willige, B.C., Seluzicki, A., Novák, O., Ljung, K. & Chory, J.**, 2022. PIF7 is a master regulator of thermomorphogenesis in shade. *Nature Communications* **13**(1): 4942. doi: 10.1038/s41467-022-32585-6
- Çakırlar, H., Çiçek, N., Fedina, I., Georgieva, K., Doğru, A. & Velitchkova, M.**, 2008. NaCl induced cross-acclimation to UV-B radiation in four Barley (*Hordeum vulgare* L.) cultivars. *Acta Physiologiae Plantarum* **30**(4): 561–567. doi: 10.1007/s11738-008-0155-5

- Calixto, C.P.G., Guo, W., James, A.B., Tzioutziou, N.A., Entizne, J.C., Panter, P.E., Knight, H., Nimmo, H.G., Zhang, R. & Brown, J.W.S.**, 2018. Rapid and Dynamic Alternative Splicing Impacts the Arabidopsis Cold Response Transcriptome. *The Plant Cell* **30**(7): 1424–1444. doi: 10.1105/tpc.18.00177
- Cao, W.-H., Liu, J., He, X.-J., Mu, R.-L., Zhou, H.-L., Chen, S.-Y. & Zhang, J.-S.**, 2007. Modulation of Ethylene Responses Affects Plant Salt-Stress Responses. *Plant Physiology* **143**(2): 707–719. doi: 10.1104/pp.106.094292
- Capella, M., Ribone, P.A., Arce, A.L. & Chan, R.L.**, 2015. Arabidopsis thaliana HomeoBox 1 (At HB 1), a Homedomain-Leucine Zipper I (HD -Zip I) transcription factor, is regulated by PHYTOCHROME-INTERACTING FACTOR 1 to promote hypocotyl elongation. *New Phytologist* **207**(3): 669–682. doi: 10.1111/nph.13401
- Cappadocia, L., Maréchal, A., Parent, J.-S., Lepage, É., Sygusch, J. & Brisson, N.**, 2010. Crystal Structures of DNA-Whirly Complexes and Their Role in Arabidopsis Organelle Genome Repair. *The Plant Cell* **22**(6): 1849–1867. doi: 10.1105/tpc.109.071399
- Carmo-Silva, A.E., Gore, M.A., Andrade-Sanchez, P., French, A.N., Hunsaker, D.J. & Salvucci, M.E.**, 2012. Decreased CO₂ availability and inactivation of Rubisco limit photosynthesis in cotton plants under heat and drought stress in the field. *Environmental and Experimental Botany* **83**: 1–11. doi: 10.1016/j.envexpbot.2012.04.001
- Casal, J.J. & Balasubramanian, S.**, 2019. Thermomorphogenesis. *Annual Review of Plant Biology* **70**(1): 321–346. doi: 10.1146/annurev-arplant-050718-095919
- Castro, J.N.D., Müller, C., Almeida, G.M. & Costa, A.C.**, 2019. Physiological tolerance to drought under high temperature in soybean cultivars. *Australian Journal of Crop Science* (13(06) 2019): 976–987. doi: 10.21475/ajcs.19.13.06.p1767
- Castroverde, C.D.M. & Dina, D.**, 2021. Temperature regulation of plant hormone signaling during stress and development. *Journal of Experimental Botany* erab257. doi: 10.1093/jxb/erab257
- Caverzan, A., Casassola, A. & Brammer, S.P.**, 2016. Antioxidant responses of wheat plants under stress. *Genetics and Molecular Biology* **39**(1): 1–6. doi: 10.1590/1678-4685-GMB-2015-0109
- Chang, H.-C., Tsai, M.-C., Wu, S.-S. & Chang, I.-F.**, 2019. Regulation of AB15 expression by ABF3 during salt stress responses in Arabidopsis thaliana. *Botanical Studies* **60**(1): 16. doi: 10.1186/s40529-019-0264-z
- Chatr-aryamontri, A., Oughtred, R., Boucher, L., Rust, J., Chang, C., Kolas, N.K., O'Donnell, L., Oster, S., Theesfeld, C., Sellam, A., Stark, C., Breitkreutz, B.-J., Dolinski, K. & Tyers, M.**, 2017. The BioGRID interaction database: 2017 update. *Nucleic Acids Research* **45**(D1): D369–D379. doi: 10.1093/nar/gkw1102
- Chaves, M.M., Flexas, J. & Pinheiro, C.**, 2009. Photosynthesis under drought and salt stress: regulation mechanisms from whole plant to cell. *Annals of Botany* **103**(4): 551–560. doi: 10.1093/aob/mcn125
- Chen, K., Huang, Y., Liu, C., Liang, Y. & Li, M.**, 2021a. Transcriptome Profile Analysis of Arabidopsis Reveals the Drought Stress-Induced Long Non-coding RNAs Associated With Photosynthesis, Chlorophyll Synthesis, Fatty Acid Synthesis and Degradation. *Frontiers in Plant Science* **12**: 643182. doi: 10.3389/fpls.2021.643182
- Chen, M., Ji, M., Wen, B., Liu, L., Li, S., Chen, X., Gao, D. & Li, L.**, 2016a. GOLDEN 2-LIKE Transcription Factors of Plants. *Frontiers in Plant Science* **7**. doi: 10.3389/fpls.2016.01509
- Chen, Q., Hu, T., Li, X., Song, C.-P., Zhu, J.-K., Chen, L. & Zhao, Y.**, 2021b. Phosphorylation of SWEET sucrose transporters regulates plant root:shoot ratio under drought. *Nature Plants* **8**(1): 68–77. doi: 10.1038/s41477-021-01040-7
- Chen, X., Lu, L., Mayer, K.S., Scalf, M., Qian, S., Lomax, A., Smith, L.M. & Zhong, X.**, 2016b. POWERDRESS interacts with HISTONE DEACETYLASE 9 to promote aging in Arabidopsis. *eLife* **5**: e17214. doi: 10.7554/eLife.17214
- Chen, X., Visser, E.J.W., De Kroon, H., Pierik, R., Voeseenek, L.A.C.J. & Huber, H.**, 2011. Fitness consequences of natural variation in flooding-induced shoot elongation in *Rumex palustris*. *New Phytologist* **190**(2): 409–420. doi: 10.1111/j.1469-8137.2010.03639.x
- Chiang, Y.-H., Zubo, Y.O., Tapken, W., Kim, H.J., Lavanway, A.M., Howard, L., Pilon, M., Kieber, J.J. & Schaller, G.E.**, 2012. Functional Characterization of the GATA Transcription Factors GNC and CGA1 Reveals Their Key Role in Chloroplast Development, Growth, and Division in Arabidopsis. *Plant Physiology* **160**(1): 332–348. doi: 10.1104/pp.112.198705
- Chieb, M. & Gachomo, E.W.**, 2023. The role of plant growth promoting rhizobacteria in plant drought stress responses. *BMC Plant Biology* **23**(1): 407. doi: 10.1186/s12870-023-04403-8
- Choi, H., Hong, J., Ha, J., Kang, J. & Kim, S.Y.**, 2000. ABFs, a Family of ABA-responsive Element Binding Factors. *Journal of Biological Chemistry* **275**(3): 1723–1730. doi: 10.1074/jbc.275.3.1723
- Choi, H. & Oh, E.**, 2016. PIF4 Integrates Multiple Environmental and Hormonal Signals for Plant Growth Regulation in Arabidopsis. *Molecules and Cells* **39**(8): 587–593. doi: 10.14348/molcells.2016.0126
- Choudhury, F.K., Rivero, R.M., Blumwald, E. & Mittler, R.**, 2017. Reactive oxygen species, abiotic stress and stress combination. *The Plant Journal* **90**(5): 856–867. doi: 10.1111/tpj.13299
- Chun, S.C., Paramasivan, M. & Chandrasekaran, M.**, 2018. Proline Accumulation Influenced by Osmotic Stress in Arbuscular Mycorrhizal Symbiotic Plants. *Frontiers in Microbiology* **9**: 2525. doi: 10.3389/fmicb.2018.02525
- Cifuentes-Esquivel, N., Celiz-Balboa, J., Henriquez-Valencia, C., Mitina, I., Arraño-Salinas, P., Moreno, A.A., Meneses, C., Blanco-Herrera, F. & Orellana, A.**, 2018. bZIP17 regulates the expression of genes related to seed storage and germination, reducing seed susceptibility to osmotic stress. *Journal of Cellular Biochemistry* **119**(8): 6857–6868. doi: 10.1002/jcb.26882
- Clauw, P., Coppens, F., De Beuf, K., Dhondt, S., Van Daele, T., Maleux, K., Storme, V., Clement, L., Gonzalez, N. & Inzé, D.**, 2015. Leaf Responses to Mild Drought Stress in Natural Variants of Arabidopsis. *Plant Physiology* **167**(3): 800–816. doi: 10.1104/pp.114.254284
- Cleland, R.E.**, 2001. Unlocking the mysteries of leaf primordia formation. *Proceedings of the National Academy of Sciences* **98**(20): 10981–10982. doi: 10.1073/pnas.211443498
- Cohen, I., Zandalinas, S.I., Huck, C., Fritschi, F.B. & Mittler, R.**, 2021. Meta-analysis of drought and heat stress combination impact on crop yield and yield components. *Physiologia Plantarum* **171**(1): 66–76. doi: 10.1111/ppl.13203
- Comas, L.H., Becker, S.R., Cruz, V.M.V., Byrne, P.F. & Dierig, D.A.**, 2013. Root traits contributing to plant productivity under drought. *Frontiers in Plant Science* **4**. doi: 10.3389/fpls.2013.00442
- Coolen, S., Proietti, S., Hickman, R., Davila Olivas, N.H., Huang, P.-P., Van Verk, M.C., Van Pelt, J.A., Wittenberg, A.H.J., De Vos, M., Prins, M., Van Loon, J.J.A., Aarts, M.G.M., Dicke, M., Pieterse, C.M.J. & Van Wees, S.C.M.**, 2016a. Transcriptome dynamics of Arabidopsis during sequential biotic and abiotic stresses. *The Plant Journal* **86**(3): 249–267. doi: 10.1111/tpj.13167
- Coolen, S., Proietti, S., Hickman, R., Davila Olivas, N.H., Huang, P.-P., Van Verk, M.C., Van Pelt, J.A., Wittenberg, A.H.J., De Vos, M., Prins, M., Van Loon, J.J.A., Aarts, M.G.M., Dicke, M., Pieterse, C.M.J. & Van Wees, S.C.M.**, 2016b. Transcriptome dynamics of Arabidopsis during sequential biotic and abiotic stresses. *The Plant Journal* **86**(3): 249–267. doi: 10.1111/tpj.13167

- Cornic, G.**, 2000. Drought stress inhibits photosynthesis by decreasing stomatal aperture – not by affecting ATP synthesis. *Trends in Plant Science* **5**(5): 187–188. doi: 10.1016/S1360-1385(00)01625-3
- Corrales, A., Carrillo, L., Lasierra, P., Nebauer, S.G., Dominguez-Figueroa, J., Renau-Morata, B., Pollmann, S., Granell, A., Molina, R., Vicente-Carbajosa, J. & Medina, J.**, 2017. Multifaceted role of cycling DOF factor 3 (CDF3) in the regulation of flowering time and abiotic stress responses in Arabidopsis. *Plant, Cell & Environment* **40**(5): 748–764. doi: 10.1111/pce.12894
- Correia, B., Hancock, R.D., Amaral, J., Gomez-Cadenas, A., Valledor, L. & Pinto, G.**, 2018. Combined Drought and Heat Activates Protective Responses in Eucalyptus globulus That Are Not Activated When Subjected to Drought or Heat Stress Alone. *Frontiers in Plant Science* **9**: 819. doi: 10.3389/fpls.2018.00819
- Courbier, S., Snoek, B.L., Kajala, K., Li, L., Van Wees, S.C.M. & Pierik, R.**, 2021. Mechanisms of far-red light-mediated dampening of defense against Botrytis cinerea in tomato leaves. *Plant Physiology* **187**(3): 1250–1266. doi: 10.1093/plphys/kiab354
- Crawford, A.J., McLachlan, D.H., Hetherington, A.M. & Franklin, K.A.**, 2012. High temperature exposure increases plant cooling capacity. *Current Biology* **22**(10): R396–R397. doi: 10.1016/j.cub.2012.03.044
- Crawford, T., Lehotai, N. & Strand, Å.**, 2018. The role of retrograde signals during plant stress responses. *Journal of Experimental Botany* **69**(11): 2783–2795. doi: 10.1093/jxb/erx481
- Crebillón, P., Yang, H., Cui, X., Greeff, C., Trick, M., Qiu, Q., Cao, X. & Dean, C.**, 2014. Epigenetic reprogramming that prevents transgenerational inheritance of the vernalized state. *Nature* **515**(7528): 587–590. doi: 10.1038/nature13722
- Crisp, P.A., Ganguly, D., Eichten, S.R., Borevitz, J.O. & Pogson, B.J.**, 2016. Reconsidering plant memory: Intersections between stress recovery, RNA turnover, and epigenetics. *Science Advances* **2**(2): e1501340. doi: 10.1126/sciadv.1501340
- Cushman, J.C., Denby, K. & Mittler, R.**, 2022. Plant responses and adaptations to a changing climate. *The Plant Journal* **109**(2): 319–322. doi: 10.1111/tpj.15641
- Da Ros, L., Bollina, V., Soolanayakanahally, R., Pahari, S., Elferjani, R., Kulkarni, M., Vaid, N., Risseuw, E., Cram, D., Pasha, A., Esteban, E., Konkin, D., Provart, N., Nambara, E. & Kagale, S.**, 2023. Multi-omics atlas of combinatorial abiotic stress responses in wheat. *The Plant Journal* **tpj.16332**. doi: 10.1111/tpj.16332
- Das, A., Eldakak, M., Paudel, B., Kim, D.-W., Hemmati, H., Basu, C. & Rohila, J.S.**, 2016. Leaf Proteome Analysis Reveals Prospective Drought and Heat Stress Response Mechanisms in Soybean. *BioMed Research International* **2016**: 1–23. doi: 10.1155/2016/6021047
- Davila Olivas, N.H., Coolen, S., Huang, P., Severing, E., Verk, M.C., Hickman, R., Wittenberg, A.H.J., Vos, M., Prins, M., Loon, J.J.A., Aarts, M.G.M., Wees, S.C.M., Pieterse, C.M.J. & Dicke, M.**, 2016. Effect of prior drought and pathogen stress on Arabidopsis transcriptome changes to caterpillar herbivory. *New Phytologist* **210**(4): 1344–1356. doi: 10.1111/nph.13847
- De Smet, I., Quint, M. & van Zanten, M.**, 2021. High and low temperature signalling and response. *Journal of Experimental Botany* **72**(21): 7339–7344. doi: 10.1093/jxb/erab447
- De Souza, W.R., Mitchell, R.A.C. & Cesarino, I.**, 2023. Editorial: The plant cell wall: advances and current perspectives. *Frontiers in Plant Science* **14**: 1235749. doi: 10.3389/fpls.2023.1235749
- Dean, C.**, 1993. Advantages of Arabidopsis for cloning plant genes. *Philosophical Transactions of the Royal Society of London. Series B: Biological Sciences* **342**(1301): 189–195. doi: 10.1098/rstb.1993.0146
- Dekkers, B.J.W., He, H., Hanson, J., Willems, L.A.J., Jamar, D.C.L., Cueff, G., Rajjou, L., Hilhorst, H.W.M. & Bentsink, L.**, 2016. The Arabidopsis DELAY OF GERMINATION 1 gene affects ABSCISIC ACID INSENSITIVE 5 (ABI5) expression and genetically interacts with ABI3 during Arabidopsis seed development. *The Plant Journal* **85**(4): 451–465. doi: 10.1111/tpj.13118
- Delker, C., Quint, M. & Wigge, P.A.**, 2022. Recent advances in understanding thermomorphogenesis signaling. *Current Opinion in Plant Biology* **68**: 102231. doi: 10.1016/j.pbi.2022.102231
- Devireddy, A.R., Zandalinas, S.I., Fichman, Y. & Mittler, R.**, 2021. Integration of reactive oxygen species and hormone signaling during abiotic stress. *The Plant Journal* **105**(2): 459–476. doi: 10.1111/tpj.15010
- Divi, U.K., Rahman, T. & Krishna, P.**, 2010. Brassinosteroid-mediated stress tolerance in Arabidopsis shows interactions with abscisic acid, ethylene and salicylic acid pathways. *BMC Plant Biology* **10**(1): 151. doi: 10.1186/1471-2229-10-151
- Dixit, S.K., Gupta, A., Fatima, U. & Senthil-Kumar, M.**, 2019. AtGBF3 confers tolerance to Arabidopsis thaliana against combined drought and Pseudomonas syringae stress. *Environmental and Experimental Botany* **168**: 103881. doi: 10.1016/j.envexpbot.2019.103881
- Dogra, V. & Kim, C.**, 2019. Chloroplast protein homeostasis is coupled with retrograde signaling. *Plant Signaling & Behavior* **14**(11): 1656037. doi: 10.1080/15592324.2019.1656037
- Dong, S. & Beckles, D.M.**, 2019. Dynamic changes in the starch-sugar interconversion within plant source and sink tissues promote a better abiotic stress response. *Journal of Plant Physiology* **234–235**: 80–93. doi: 10.1016/j.jplph.2019.01.007
- Dopp, I.J., Yang, X. & Mackenzie, S.A.**, 2021. A new take on organelle-mediated stress sensing in plants. *New Phytologist* **230**(6): 2148–2153. doi: 10.1111/nph.17333
- Dos Santos, T.B., Ribas, A.F., De Souza, S.G.H., Budzinski, I.G.F. & Domingues, D.S.**, 2022. Physiological Responses to Drought, Salinity, and Heat Stress in Plants: A Review. *Stresses* **2**(1): 113–135. doi: 10.3390/stresses2010009
- Dreher, K.A., Brown, J., Saw, R.E. & Callis, J.**, 2006. The Arabidopsis Aux/IAA Protein Family Has Diversified in Degradation and Auxin Responsiveness. *The Plant Cell* **18**(3): 699–714. doi: 10.1105/tpc.105.039172
- Drew, M.C., Jackson, M.B., Giffard, S.C. & Campbell, R.**, 1981. Inhibition by silver ions of gas space (aerenchyma) formation in adventitious roots of Zea mays L. subjected to exogenous ethylene or to oxygen deficiency. *Planta* **153**(3): 217–224. doi: 10.1007/BF00383890
- Duan, L., Dietrich, D., Ng, C.H., Chan, P.M.Y., Bhalerao, R., Bennett, M.J. & Dinneny, J.R.**, 2013. Endodermal ABA Signaling Promotes Lateral Root Quiescence during Salt Stress in Arabidopsis Seedlings. *The Plant Cell* **25**(1): 324–341. doi: 10.1105/tpc.112.107227
- Dubreuil, C., Jin, X., Barajas-López, J.D.D., Hewitt, T.C., Tanz, S.K., Dobrenel, T., Schröder, W.P., Hanson, J., Pesquet, E., Grönlund, A., Small, I. & Strand, Å.**, 2018. Establishment of Photosynthesis through Chloroplast Development Is Controlled by Two Distinct Regulatory Phases. *Plant Physiology* **176**(2): 1199–1214. doi: 10.1104/pp.17.00435
- Duddek, P., Carminati, A., Koebernick, N., Ohmann, L., Lovric, G., Delzon, S., Rodriguez-Dominguez, C.M., King, A. & Ahmed, M.A.**, 2022. The impact of drought-induced root and root hair shrinkage on root–soil contact. *Plant Physiology* **189**(3): 1232–1236. doi: 10.1093/plphys/kiac144
- El Sabagh, A., Islam, M.S., Hossain, A., Iqbal, M.A., Mubeen, M., Waleed, M., Reginato, M., Battaglia, M., Ahmed, S., Rehman, A., Arif, M., Athar, H.-U.-R., Ratnasekera, D., Danish, S., Raza, M.A., Rajendran, K., Mushtaq, M., Skalicky, M., Brestic, M., Soufan, W., Fahad, S., Pandey, S., Kamran, M., Datta, R. & Abdelhamid, M.T.**, 2022. Phytohormones as Growth Regulators During Abiotic Stress Tolerance in Plants. *Frontiers in Agronomy* **4**: 765068. doi: 10.3389/fagro.2022.765068

- Evans, D.E.**, 2004. Aerenchyma formation. *New Phytologist* **161**(1): 35–49. doi: 10.1046/j.1469-8137.2003.00907.x
- Fàbregas, N. & Fèrnie, A.R.**, 2019. The metabolic response to drought. *Journal of Experimental Botany* **70**(4): 1077–1085. doi: 10.1093/jxb/ery437
- Fahad, S., Bajwa, A.A., Nazir, U., Anjum, S.A., Farooq, A., Zohaib, A., Sadia, S., Nasim, W., Adkins, S., Saud, S., Ihsan, M.Z., Alharby, H., Wu, C., Wang, D. & Huang, J.**, 2017. Crop Production under Drought and Heat Stress: Plant Responses and Management Options. *Frontiers in Plant Science* **8**. doi: 10.3389/fpls.2017.01147
- Fernando, V.C.D., Al Khateeb, W., Belmonte, M.F. & Schroeder, D.F.**, 2018. Role of Arabidopsis ABF1/3/4 during det1 germination in salt and osmotic stress conditions. *Plant Molecular Biology* **97**(1–2): 149–163. doi: 10.1007/s11103-018-0729-6
- Fernando, V.C.D. & Schroeder, D.F.**, 2016. Role of ABA in Arabidopsis Salt, Drought, and Desiccation Tolerance. In: A.K. Shanker & C. Shanker (eds.): *Abiotic and Biotic Stress in Plants - Recent Advances and Future Perspectives*. InTech. doi: 10.5772/61957
- Finkelstein, R.R. & Lynch, T.J.**, 2000. The Arabidopsis Abscisic Acid Response Gene ABI5 Encodes a Basic Leucine Zipper Transcription Factor. *The Plant Cell* **12**(4): 599–609. doi: 10.1105/tpc.12.4.599
- Fitter, D.W., Martin, D.J., Copley, M.J., Scotland, R.W. & Langdale, J.A.**, 2002a. GLK gene pairs regulate chloroplast development in diverse plant species. *The Plant Journal* **31**(6): 713–727. doi: 10.1046/j.1365-313X.2002.01390.x
- Fitter, D.W., Martin, D.J., Copley, M.J., Scotland, R.W. & Langdale, J.A.**, 2002b. GLK gene pairs regulate chloroplast development in diverse plant species. **31**.
- Fode, B., Siemsen, T., Thurow, C., Weigel, R. & Gatz, C.**, 2008. The Arabidopsis GRAS Protein SCL14 Interacts with Class II TGA Transcription Factors and Is Essential for the Activation of Stress-Inducible Promoters. *The Plant Cell* **20**(11): 3122–3135. doi: 10.1105/tpc.108.058974
- Fölsche, V., Großmann, C. & Richter, A.S.**, 2022. Impact of Porphyrin Binding to GENOMES UNCOUPLED 4 on Tetrapyrrole Biosynthesis in planta. *Frontiers in Plant Science* **13**: 850504. doi: 10.3389/fpls.2022.850504
- Fong, C.R., Bittick, S.J. & Fong, P.**, 2018. Simultaneous synergist, antagonistic and additive interactions between multiple local stressors all degrade algal turf communities on coral reefs. *Journal of Ecology* **106**(4): 1390–1400. doi: 10.1111/1365-2745.12914
- Fonseca De Lima, C.F., Kleine-Vehn, J., De Smet, I. & Feraru, E.**, 2021. Getting to the root of belowground high temperature responses in plants. *Journal of Experimental Botany* **erab202**. doi: 10.1093/jxb/erab202
- Fortunato, S., Lasorella, C., Tadini, L., Jeran, N., Vita, F., Pesaresi, P. & De Pinto, M.C.**, 2022. GUN1 involvement in the redox changes occurring during biogenic retrograde signaling. *Plant Science* **320**: 111265. doi: 10.1016/j.plantsci.2022.111265
- Foyer, C.H. & Hanke, G.**, 2022. ROS production and signalling in chloroplasts: cornerstones and evolving concepts. *The Plant Journal* **111**(3): 642–661. doi: 10.1111/tbj.15856
- Foyer, C.H., Rasool, B., Davey, J.W. & Hancock, R.D.**, 2016. Cross-tolerance to biotic and abiotic stresses in plants: a focus on resistance to aphid infestation. *Journal of Experimental Botany* **67**(7): 2025–2037. doi: 10.1093/jxb/erw079
- Foyer, C.H. & Shigeoka, S.**, 2011. Understanding Oxidative Stress and Antioxidant Functions to Enhance Photosynthesis. *Plant Physiology* **155**(1): 93–100. doi: 10.1104/pp.110.166181
- Frerigmann, H. & Gigolashvili, T.**, 2014. MYB34, MYB51, and MYB122 Distinctly Regulate Indolic Glucosinolate Biosynthesis in Arabidopsis thaliana. *Molecular Plant* **7**(5): 814–828. doi: 10.1093/mp/ssu004
- Fujita, Y., Fujita, M., Shinozaki, K. & Yamaguchi-Shinozaki, K.**, 2011. ABA-mediated transcriptional regulation in response to osmotic stress in plants. *Journal of Plant Research* **124**(4): 509–525. doi: 10.1007/s10265-011-0412-3

- Fukao, T., Yeung, E. & Bailey-Serres, J.**, 2011. The Submergence Tolerance Regulator SUB1A Mediates Crosstalk between Submergence and Drought Tolerance in Rice. *The Plant Cell* **23**(1): 412–427. doi: 10.1105/tpc.110.080325
- Gaillochet, C., Burko, Y., Platre, M.P., Zhang, L., Simura, J., Willige, B.C., Kumar, S.V., Ljung, K., Chory, J. & Busch, W.**, 2020. HY5 and phytochrome activity modulate shoot-to-root coordination during thermomorphogenesis in Arabidopsis. *Development* **147**(24): dev192625. doi: 10.1242/dev.192625
- Gan, P., Liu, F., Li, R., Wang, S. & Luo, J.**, 2019. Chloroplasts— Beyond Energy Capture and Carbon Fixation: Tuning of Photosynthesis in Response to Chilling Stress. *International Journal of Molecular Sciences* **20**(20): 5046. doi: 10.3390/ijms20205046
- Gangappa, S.N., Berriri, S. & Kumar, S.V.**, 2017. PIF4 Coordinates Thermosensory Growth and Immunity in Arabidopsis. *Current Biology* **27**(2): 243–249. doi: 10.1016/j.cub.2016.11.012
- Gao, H., Brandizzi, F., Benning, C. & Larkin, R.M.**, 2008. A membrane-tethered transcription factor defines a branch of the heat stress response in Arabidopsis thaliana. *Proceedings of the National Academy of Sciences* **105**(42): 16398–16403. doi: 10.1073/pnas.0808463105
- Gao, J., Wang, M.-J., Wang, J.-J., Lu, H.-P. & Liu, J.-X.**, 2022. bZIP17 regulates heat stress tolerance at reproductive stage in Arabidopsis. *ABIOTECH* **3**(1): 1–11. doi: 10.1007/s42994-021-00062-1
- Gao, L., Liu, Y., Wang, X., Li, Y. & Han, R.**, 2019. Lower levels of UV-B light trigger the adaptive responses by inducing plant antioxidant metabolism and flavonoid biosynthesis in *Medicago sativa* seedlings. *Functional Plant Biology* **46**(10): 896. doi: 10.1071/FP19007
- Garner, K.L., Chang, M.Y., Fulda, M.T., Berlin, J.A., Freed, R.E., Soo-Hoo, M.M., Revell, D.L., Ikegami, M., Flint, L.E., Flint, A.L. & Kendall, B.E.**, 2015. Impacts of sea level rise and climate change on coastal plant species in the central California coast. *PeerJ* **3**: e958. doi: 10.7717/peerj.958
- Genzel, F., Dicke, M.D., Junker-Frohn, L.V., Neuwohner, A., Thiele, B., Putz, A., Usadel, B., Wormit, A. & Wiese-Klinkenberg, A.**, 2021. Impact of Moderate Cold and Salt Stress on the Accumulation of Antioxidant Flavonoids in the Leaves of Two Capsicum Cultivars. *Journal of Agricultural and Food Chemistry* **69**(23): 6431–6443. doi: 10.1021/acs.jafc.1c00908
- Gibbs, D.J., Lee, S.C., Md Isa, N., Gramuglia, S., Fukao, T., Bassel, G.W., Correia, C.S., Corbineau, F., Theodoulou, F.L., Bailey-Serres, J. & Holdsworth, M.J.**, 2011. Homeostatic response to hypoxia is regulated by the N-end rule pathway in plants. *Nature* **479**(7373): 415–418. doi: 10.1038/nature10534
- Giuntoli, B. & Perata, P.**, 2018. Group VII Ethylene Response Factors in Arabidopsis: Regulation and Physiological Roles. *Plant Physiology* **176**(2): 1143–1155. doi: 10.1104/pp.17.01225
- Goda, H., Sasaki, E., Akiyama, K., Maruyama-Nakashita, A., Nakabayashi, K., Li, W., Ogawa, M., Yamauchi, Y., Preston, J., Aoki, K., Kiba, T., Takatsuto, S., Fujioka, S., Asami, T., Nakano, T., Kato, H., Mizuno, T., Sakakibara, H., Yamaguchi, S., Nambara, E., Kamiya, Y., Takahashi, H., Hirai, M.Y., Sakurai, T., Shinozaki, K., Saito, K., Yoshida, S. & Shimada, Y.**, 2008. The AtGenExpress hormone and chemical treatment data set: experimental design, data evaluation, model data analysis and data access. *The Plant Journal* **55**(3): 526–542. doi: 10.1111/j.1365-313X.2008.03510.x
- Gommers, C.M.M., Ruiz-sola, M.Á., Ayats, A., Pereira, L. & Pujol, M.**, 2020. GUN1-independent retrograde signaling targets the ethylene pathway to repress photomorphogenesis.
- Gourlay, G., Hawkins, B.J., Albert, A., Schnitzler, J. & Peter Constabel, C.**, 2022. Condensed tannins as antioxidants that protect poplar against oxidative stress from drought and UV-B. *Plant, Cell & Environment* **45**(2): 362–377. doi: 10.1111/pce.14242
- Guo, M., Liu, J.-H., Ma, X., Luo, D.-X., Gong, Z.-H. & Lu, M.-H.**, 2016. The Plant Heat Stress Transcription Factors (HSFs): Structure, Regulation, and Function in Response to Abiotic Stresses. *Frontiers in Plant Science* **7**. doi: 10.3389/fpls.2016.00114

- Guo, Q., Li, X., Niu, L., Jameson, P.E. & Zhou, W.**, 2021. Transcription-associated metabolomic adjustments in maize occur during combined drought and cold stress. *Plant Physiology* **186**(1): 677–695. doi: 10.1093/plphys/kiab050
- Guo, R., Shi, L., Jiao, Y., Li, M., Zhong, X., Gu, F., Liu, Q., Xia, X. & Li, H.**, 2018. Metabolic responses to drought stress in the tissues of drought-tolerant and drought-sensitive wheat genotype seedlings. *AoB PLANTS* **10**(2). doi: 10.1093/aobpla/ply016
- Gupta, A., Hisano, H., Hojo, Y., Matsuura, T., Ikeda, Y., Mori, I.C. & Senthil-Kumar, M.**, 2017. Global profiling of phytohormone dynamics during combined drought and pathogen stress in *Arabidopsis thaliana* reveals ABA and JA as major regulators. *Scientific Reports* **7**(1): 4017. doi: 10.1038/s41598-017-03907-2
- Gupta, A., Patil, M., Qamar, A. & Senthil-Kumar, M.**, 2020. ath-miR164c influences plant responses to the combined stress of drought and bacterial infection by regulating proline metabolism. *Environmental and Experimental Botany* **172**: 103998. doi: 10.1016/j.envexpbot.2020.103998
- Gurrieri, L., Del Giudice, A., Demitri, N., Falini, G., Pavel, N.V., Zaffagnini, M., Polentarutti, M., Crozet, P., Marchand, C.H., Henri, J., Trost, P., Lemaire, S.D., Sparla, F. & Fermani, S.**, 2019. *Arabidopsis* and *Chlamydomonas* phosphoribulokinase crystal structures complete the redox structural proteome of the Calvin–Benson cycle. *Proceedings of the National Academy of Sciences* **116**(16): 8048–8053. doi: 10.1073/pnas.1820639116
- Gurrieri, L., Sparla, F., Zaffagnini, M. & Trost, P.**, 2023. Dark complexes of the Calvin–Benson cycle in a physiological perspective. *Seminars in Cell & Developmental Biology* **S1084952123000496**. doi: 10.1016/j.semcdb.2023.03.002
- Guzmán, P.**, 2012. The prolific ATL family of RING-H2 ubiquitin ligases. *Plant Signaling & Behavior* **7**(8): 1014–1021. doi: 10.4161/psb.20851
- H Wani, S.**, 2015. Plant Stress Tolerance: Engineering ABA: A Potent Phytohormone. *Transcriptomics: Open Access* **03**(02). doi: 10.4172/2329-8936.1000113
- Habibpourmehraban, F., Wu, Y., Wu, J.X., Hamzelou, S., Masoomi-Aladizgeh, F., Kamath, K.S., Amirkhani, A., Atwell, B.J. & Haynes, P.A.**, 2022. Multiple Abiotic Stresses Applied Simultaneously Elicit Distinct Responses in Two Contrasting Rice Cultivars. *International Journal of Molecular Sciences* **23**(3): 1739. doi: 10.3390/ijms23031739
- Han, G., Wei, X., Dong, X., Wang, C., Sui, N., Guo, J., Yuan, F., Gong, Z., Li, X., Zhang, Y., Meng, Z., Chen, Z., Zhao, D. & Wang, B.**, 2020. *Arabidopsis* ZINC FINGER PROTEIN1 Acts Downstream of GL2 to Repress Root Hair Initiation and Elongation by Directly Suppressing bHLH Genes. *The Plant Cell* **32**(1): 206–225. doi: 10.1105/tpc.19.00226
- Harb, A., Krishnan, A., Ambavaram, M.M.R. & Pereira, A.**, 2010. Molecular and Physiological Analysis of Drought Stress in *Arabidopsis* Reveals Early Responses Leading to Acclimation in Plant Growth. *Plant Physiology* **154**(3): 1254–1271. doi: 10.1104/pp.110.161752
- Hartman, S., Liu, Z., Van Veen, H., Vicente, J., Reinen, E., Martopawiro, S., Zhang, H., Van Dongen, N., Bosman, F., Bassel, G.W., Visser, E.J.W., Bailey-Serres, J., Theodoulou, F.L., Hebelstrup, K.H., Gibbs, D.J., Holdsworth, M.J., Sasidharan, R. & Voeselek, L.A.C.J.**, 2019. Ethylene-mediated nitric oxide depletion pre-adapts plants to hypoxia stress. *Nature Communications* **10**(1): 4020. doi: 10.1038/s41467-019-12045-4
- Hasanuzzaman, M., Bhuyan, M.H.M., Zulfiqar, F., Raza, A., Mohsin, S., Mahmud, J., Fujita, M. & Fotopoulos, V.**, 2020. Reactive Oxygen Species and Antioxidant Defense in Plants under Abiotic Stress: Revisiting the Crucial Role of a Universal Defense Regulator. *Antioxidants* **9**(8): 681. doi: 10.3390/antiox9080681
- Hatfield, J.L. & Prueger, J.H.**, 2015. Temperature extremes: Effect on plant growth and development. *Weather and Climate Extremes* **10**: 4–10. doi: 10.1016/j.wace.2015.08.001

- Hatsugai, N., Yamada, K., Goto-Yamada, S. & Hara-Nishimura, I.**, 2015. Vacuolar processing enzyme in plant programmed cell death. *Frontiers in Plant Science* **6**. doi: 10.3389/fpls.2015.00234
- Hayat, S., Hayat, Q., Alyemeni, M.N., Wani, A.S., Pichtel, J. & Ahmad, A.**, 2012. Role of proline under changing environments: A review. *Plant Signaling & Behavior* **7**(11): 1456–1466. doi: 10.4161/psb.21949
- Hays, J.B.**, 2002. *Arabidopsis thaliana*, a versatile model system for study of eukaryotic genome-maintenance functions. *DNA Repair* **1**(8): 579–600. doi: 10.1016/S1568-7864(02)00093-9
- He, K., Mei, H., Zhu, J., Qiu, Q., Cao, X. & Deng, X.**, 2022. The histone H3K27 demethylase REF6/JMJ12 promotes thermomorphogenesis in *Arabidopsis*. *National Science Review* **9**(5): nwab213. doi: 10.1093/nsr/nwab213
- Hemantaranjan, A.**, 2014. Heat Stress Responses and Thermotolerance. *Advances in Plants & Agriculture Research* **1**(3). doi: 10.15406/apar.2014.01.00012
- Hernandez, I., Alegre, L. & Munne-Bosch, S.**, 2004. Drought-induced changes in flavonoids and other low molecular weight antioxidants in *Cistus clusii* grown under Mediterranean field conditions. *Tree Physiology* **24**(11): 1303–1311. doi: 10.1093/treephys/24.11.1303
- Hernández-Verdeja, T. & Lundgren, M.R.**, 2023. GOLDEN2-LIKE transcription factors: A golden ticket to improve crops? *PLANTS, PEOPLE, PLANET* ppp3.10412. doi: 10.1002/ppp3.10412
- Hernández-Verdeja, T., Vuorijoki, L., Jin, X., Vergara, A., Dubreuil, C. & Strand, Å.**, 2022. GENOMES UNCOUPLED1 plays a key role during the de-etiolation process in *Arabidopsis*. *New Phytologist* **235**(1): 188–203. doi: 10.1111/nph.18115
- Hildebrandt, T.M.**, 2018. Synthesis versus degradation: directions of amino acid metabolism during *Arabidopsis* abiotic stress response. *Plant Molecular Biology* **98**(1–2): 121–135. doi: 10.1007/s11103-018-0767-0
- Hilker, M., Schwachtje, J., Baier, M., Balazadeh, S., Bäurle, I., Geiselhardt, S., Hinch, D.K., Kunze, R., Mueller-Roeber, B., Rillig, M.C., Rolff, J., Romeis, T., Schmölling, T., Steppuhn, A., Van Dongen, J., Whitcomb, S.J., Wurst, S., Zuther, E. & Kopka, J.**, 2016. Priming and memory of stress responses in organisms lacking a nervous system: Priming and memory of stress responses. *Biological Reviews* **91**(4): 1118–1133. doi: 10.1111/brv.12215
- Hills, A.C., Khan, S. & López-Juez, E.**, 2015. Chloroplast biogenesis-associated nuclear genes: Control by plastid signals evolved prior to their regulation as part of photomorphogenesis. *Frontiers in Plant Science* **6**(DEC): 1–13. doi: 10.3389/fpls.2015.01078
- Hirayama, T. & Shinozaki, K.**, 2010a. Research on plant abiotic stress responses in the post-genome era: past, present and future. *The Plant Journal* **61**(6): 1041–1052. doi: 10.1111/j.1365-313X.2010.04124.x
- Hirayama, T. & Shinozaki, K.**, 2010b. Research on plant abiotic stress responses in the post-genome era: past, present and future. *The Plant Journal* **61**(6): 1041–1052. doi: 10.1111/j.1365-313X.2010.04124.x
- Hornitschek, P., Kohnen, M.V., Lorrain, S., Rougemont, J., Ljung, K., López-Vidriero, I., Franco-Zorrilla, J.M., Solano, R., Trevisan, M., Pradervand, S., Xenarios, I. & Fankhauser, C.**, 2012. Phytochrome interacting factors 4 and 5 control seedling growth in changing light conditions by directly controlling auxin signaling: PIF4 and PIF5 control auxin signaling. *The Plant Journal* **71**(5): 699–711. doi: 10.1111/j.1365-313X.2012.05033.x
- Hossain, M.A., Burritt, D.J. & Fujita, M.**, 2016. Cross-Stress Tolerance in Plants: Molecular Mechanisms and Possible Involvement of Reactive Oxygen Species and Methylglyoxal Detoxification Systems. In: N. Tuteja & S.S. Gill (eds.): *Abiotic Stress Response in Plants*. Wiley-VCH Verlag GmbH & Co. KGaA (Weinheim, Germany): pp. 327–380. doi: 10.1002/9783527694570.ch16

- Hossain, M.A., Li, Z.-G., Hoque, T.S., Burritt, D.J., Fujita, M. & Munné-Bosch, S.**, 2018. Heat or cold priming-induced cross-tolerance to abiotic stresses in plants: key regulators and possible mechanisms. *Protoplasma* **255**(1): 399–412. doi: 10.1007/s00709-017-1150-8
- Hou, Y., Yan, Y. & Cao, X.**, 2022. Epigenetic regulation of thermomorphogenesis in *Arabidopsis thaliana*. *aBIOTECH* **3**(1): 12–24. doi: 10.1007/s42994-022-00070-9
- Hu, S., Ding, Y. & Zhu, C.**, 2020. Sensitivity and Responses of Chloroplasts to Heat Stress in Plants. *Frontiers in Plant Science* **11**: 375. doi: 10.3389/fpls.2020.00375
- Huang, C., Yu, J., Cai, Q., Chen, Y., Li, Y., Ren, Y. & Miao, Y.**, 2020. Triple-localized WHIRLY2 Influences Leaf Senescence and Silique Development via Carbon Allocation. *Plant Physiology* **184**(3): 1348–1362. doi: 10.1104/pp.20.00832
- Huang, Y., Guo, Y., Liu, Y., Zhang, F., Wang, Z., Wang, H., Wang, F., Li, D., Mao, D., Luan, S., Liang, M. & Chen, L.**, 2018. 9-cis-Epoxycarotenoid Dioxygenase 3 Regulates Plant Growth and Enhances Multi-Abiotic Stress Tolerance in Rice. *Frontiers in Plant Science* **9**: 162. doi: 10.3389/fpls.2018.00162
- Hudson, D., Guevara, D., Yaish, M.W., Hannam, C., Long, N., Clarke, J.D., Bi, Y.-M. & Rothstein, S.J.**, 2011. GNC and CGA1 Modulate Chlorophyll Biosynthesis and Glutamate Synthase (GLU1/Fd-GOGAT) Expression in *Arabidopsis*. *PLoS ONE* **6**(11): e26765. doi: 10.1371/journal.pone.0026765
- Hura, T., Hura, K. & Ostrowska, A.**, 2022. Drought-Stress Induced Physiological and Molecular Changes in Plants. *International Journal of Molecular Sciences* **23**(9): 4698. doi: 10.3390/ijms23094698
- Hussain, H.A., Men, S., Hussain, S., Chen, Y., Ali, S., Zhang, S., Zhang, K., Li, Y., Xu, Q., Liao, C. & Wang, L.**, 2019. Interactive effects of drought and heat stresses on morpho-physiological attributes, yield, nutrient uptake and oxidative status in maize hybrids. *Scientific Reports* **9**(1): 3890. doi: 10.1038/s41598-019-40362-7
- Hwang, G., Zhu, J.-Y., Lee, Y.K., Kim, S., Nguyen, T.T., Kim, J. & Oh, E.**, 2017. PIF4 Promotes Expression of LNG1 and LNG2 to Induce Thermomorphogenic Growth in *Arabidopsis*. *Frontiers in Plant Science* **8**: 1320. doi: 10.3389/fpls.2017.01320
- Ibrahim, W., Zhu, Y.-M., Chen, Y., Qiu, C.-W., Zhu, S. & Wu, F.**, 2019. Genotypic differences in leaf secondary metabolism, plant hormones and yield under alone and combined stress of drought and salinity in cotton genotypes. *Physiologia Plantarum* **165**(2): 343–355. doi: 10.1111/ppl.12862
- Intergovernmental Panel On Climate Change (ipcc)**, 2023. *Climate Change 2022 – Impacts, Adaptation and Vulnerability: Working Group II Contribution to the Sixth Assessment Report of the Intergovernmental Panel on Climate Change*. Cambridge University Press: 1st ed. doi: 10.1017/9781009325844
- Jackson, M.B. & Armstrong, W.**, 1999. Formation of Aerenchyma and the Processes of Plant Ventilation in Relation to Soil Flooding and Submergence. *Plant Biology* **1**(3): 274–287. doi: 10.1111/j.1438-8677.1999.tb00253.x
- Jan, M., Liu, Z., Rochaix, J.-D. & Sun, X.**, 2022a. Retrograde and anterograde signaling in the crosstalk between chloroplast and nucleus. *Frontiers in Plant Science* **13**: 980237. doi: 10.3389/fpls.2022.980237
- Jan, R., Khan, M.-A., Asaf, S., Lubna, Waqas, M., Park, J.-R., Asif, S., Kim, N., Lee, I.-J. & Kim, K.-M.**, 2022b. Drought and UV Radiation Stress Tolerance in Rice Is Improved by Overaccumulation of Non-Enzymatic Antioxidant Flavonoids. *Antioxidants* **11**(5): 917. doi: 10.3390/antiox11050917
- Jenks, M. A. & Hasegawa, P. M. (eds.)**, 2005. *Plant Abiotic Stress*. Blackwell Publishing Ltd (Oxford, UK). doi: 10.1002/9780470988503
- Jensen, M.K., Kjaersgaard, T., Nielsen, M.M., Galberg, P., Petersen, K., O’Shea, C. & Skriver, K.**, 2010. The *Arabidopsis thaliana* NAC transcription factor family: structure–function relationships and determinants of ANAC019 stress signalling. *Biochemical Journal* **426**(2): 183–196. doi: 10.1042/BJ20091234
- Jeong, M.-J. & Shih, M.-C.**, 2003. Interaction of a GATA factor with cis-acting elements involved in light regulation of nuclear genes encoding chloroplast glyceraldehyde-3-phosphate dehydrogenase in *Arabidopsis*. *Biochemical and Biophysical Research Communications* **300**(2): 555–562. doi: 10.1016/S0006-291X(02)02892-9
- Jia, W., Ma, M., Chen, J. & Wu, S.**, 2021. Plant Morphological, Physiological and Anatomical Adaptation to Flooding Stress and the Underlying Molecular Mechanisms. *International Journal of Molecular Sciences* **22**(3): 1088. doi: 10.3390/ijms22031088
- Jin, J., He, K., Tang, X., Li, Z., Lv, L., Zhao, Y., Luo, J. & Gao, G.**, 2015. An *Arabidopsis* Transcriptional Regulatory Map Reveals Distinct Functional and Evolutionary Features of Novel Transcription Factors. *Molecular Biology and Evolution* **32**(7): 1767–1773. doi: 10.1093/molbev/msv058
- Jing, Y., Zhang, D., Wang, X., Tang, W., Wang, W., Huai, J., Xu, G., Chen, D., Li, Y. & Lin, R.**, 2013. *Arabidopsis* Chromatin Remodeling Factor PICKLE Interacts with Transcription Factor HY5 to Regulate Hypocotyl Cell Elongation. *The Plant Cell* **25**(1): 242–256. doi: 10.1105/tpc.112.105742
- Joseph, M.P., Papdi, C., Kozma-Bognár, L., Nagy, I., López-Carbonell, M., Rigó, G., Koncz, C. & Szabados, L.**, 2014. The *Arabidopsis* ZINC FINGER PROTEIN3 Interferes with Abscisic Acid and Light Signaling in Seed Germination and Plant Development. *Plant Physiology* **165**(3): 1203–1220. doi: 10.1104/pp.113.234294
- Jumrani, K. & Bhatia, V.S.**, 2018. Impact of combined stress of high temperature and water deficit on growth and seed yield of soybean. *Physiology and Molecular Biology of Plants* **24**(1): 37–50. doi: 10.1007/s12298-017-0480-5
- Jung, J.-H., Domijan, M., Klose, C., Biswas, S., Ezer, D., Gao, M., Khattak, A.K., Box, M.S., Charoensawan, V., Cortijo, S., Kumar, M., Grant, A., Locke, J.C.W., Schäfer, E., Jaeger, K.E. & Wigge, P.A.**, 2016. Phytochromes function as thermosensors in *Arabidopsis*. *Science* **354**(6314): 886–889. doi: 10.1126/science.aaf6005
- Kadioglu, A., Terzi, R., Saruhan, N. & Saglam, A.**, 2012. Current advances in the investigation of leaf rolling caused by biotic and abiotic stress factors. *Plant Science* **182**: 42–48. doi: 10.1016/j.plantsci.2011.01.013
- Kanehisa, M.**, 2000. KEGG: Kyoto Encyclopedia of Genes and Genomes. *Nucleic Acids Research* **28**(1): 27–30. doi: 10.1093/nar/28.1.27
- Kang, J., Peng, Y. & Xu, W.**, 2022. Crop Root Responses to Drought Stress: Molecular Mechanisms, Nutrient Regulations, and Interactions with Microorganisms in the Rhizosphere. *International Journal of Molecular Sciences* **23**(16): 9310. doi: 10.3390/ijms23169310
- Kang, X., Xu, G., Lee, B., Chen, C., Zhang, H., Kuang, R. & Ni, M.**, 2018. HRB2 and BBX21 interaction modulates *Arabidopsis* ABI5 locus and stomatal aperture. *Plant, Cell & Environment* **41**(8): 1912–1925. doi: 10.1111/pce.13336
- Kanojia, A., Shrestha, D.K. & Dijkwel, P.P.**, 2021. Primary metabolic processes as drivers of leaf ageing. *Cellular and Molecular Life Sciences* **78**(19–20): 6351–6364. doi: 10.1007/s00018-021-03896-6
- Kataoka, R., Takahashi, M. & Suzuki, N.**, 2017. Coordination between bZIP28 and HSFA2 in the regulation of heat response signals in *Arabidopsis*. *Plant Signaling & Behavior* **12**(11): e1376159. doi: 10.1080/15592324.2017.1376159

- Katiyar, A., Smita, S., Lenka, S.K., Rajwanshi, R., Chinnusamy, V. & Bansal, K.C.**, 2012. Genome-wide classification and expression analysis of MYB transcription factor families in rice and Arabidopsis. *BMC Genomics* **13**(1): 544. doi: 10.1186/1471-2164-13-544
- Kawase, M. & Whitmoyer, R.E.**, 1980. AERENCHYMA DEVELOPMENT IN WATERLOGGED PLANTS. *American Journal of Botany* **67**(1): 18–22. doi: 10.1002/j.1537-2197.1980.tb07620.x
- Keleş, Y. & Öncel, I.**, 2002. Response of antioxidative defence system to temperature and water stress combinations in wheat seedlings. *Plant Science* **163**(4): 783–790. doi: 10.1016/S0168-9452(02)00213-3
- Kende, H., Van Der Knaap, E. & Cho, H.-T.**, 1998. Deepwater Rice: A Model Plant to Study Stem Elongation. *Plant Physiology* **118**(4): 1105–1110. doi: 10.1104/pp.118.4.1105
- Keyzor, C., Mermaz, B., Trigazis, E., Jo, S. & Song, J.**, 2021. Histone Demethylases ELF6 and JM13 Antagonistically Regulate Self-Fertility in Arabidopsis. *Frontiers in Plant Science* **12**: 640135. doi: 10.3389/fpls.2021.640135
- Kim, C., Kim, S.J., Jeong, J., Park, E., Oh, E., Park, Y.-I., Lim, P.O. & Choi, G.**, 2020. High Ambient Temperature Accelerates Leaf Senescence via PHYTOCHROME-INTERACTING FACTOR 4 and 5 in Arabidopsis.
- Kim, J.-S., Yamaguchi-Shinozaki, K. & Shinozaki, K.**, 2018. ER-Anchored Transcription Factors bZIP17 and bZIP28 Regulate Root Elongation. *Plant Physiology* **176**(3): 2221–2230. doi: 10.1104/pp.17.01414
- Kim, Y.Y., Cui, M.H., Noh, M.S., Jung, K.W. & Shin, J.S.**, 2017. The FBA motif-containing protein AFBA1 acts as a novel positive regulator of ABA response in Arabidopsis. *Plant and Cell Physiology* **58**(3): 574–586. doi: 10.1093/pcp/pcx003
- Kinoshita, T., Yamada, K., Hiraiwa, N., Kondo, M., Nishimura, M. & Hara-Nishimura, I.**, 1999. Vacuolar processing enzyme is up-regulated in the lytic vacuoles of vegetative tissues during senescence and under various stressed conditions. *The Plant Journal* **19**(1): 43–53. doi: 10.1046/j.1365-313X.1999.00497.x
- Kleine, T., Nägele, T., Neuhaus, H.E., Schmitz-Linneweber, C., Fernie, A.R., Geigenberger, P., Grimm, B., Kaufmann, K., Klipp, E., Meurer, J., Möhlmann, T., Mühlhaus, T., Naranjo, B., Nickelsen, J., Richter, A., Ruwe, H., Schroda, M., Schwenkert, S., Trentmann, O., Willmund, F., Zoschke, R. & Leister, D.**, 2021. Acclimation in plants – the Green Hub consortium. *The Plant Journal* **106**(1): 23–40. doi: 10.1111/tpj.15144
- Klermund, C., Ranftl, Q.L., Diener, J., Bastakis, E., Richter, R. & Schwechheimer, C.**, 2016. LLM-Domain B-GATA Transcription Factors Promote Stomatal Development Downstream of Light Signaling Pathways in Arabidopsis thaliana Hypocotyls. *The Plant Cell* **28**(3): 646–660. doi: 10.1105/tpc.15.00783
- Koini, M.A., Alvey, L., Allen, T., Tilley, C.A., Harberd, N.P., Whitelam, G.C. & Franklin, K.A.**, 2009. High Temperature-Mediated Adaptations in Plant Architecture Require the bHLH Transcription Factor PIF4. *Current Biology* **19**(5): 408–413. doi: 10.1016/j.cub.2009.01.046
- Kolb, S., Senizza, B., Araniti, F., Lewin, S., Wende, S. & Lucini, L.**, 2022. A multi-omics approach to unravel the interaction between heat and drought stress in the Arabidopsis thaliana holobiont [Preprint]. Preprints. doi: 10.22541/au.167030830.06849298/v1
- Kong, R.S. & Henry, H.A.L.**, 2016. Prior exposure to freezing stress enhances the survival and recovery of *Poa pratensis* exposed to severe drought. *American Journal of Botany* **103**(11): 1890–1896. doi: 10.3732/ajb.1600176
- Kong, R.S. & Henry, H.A.L.**, 2019. Cross acclimation effects of spring freezing and summer drought on plant functional groups and ecosystem properties. *Environmental and Experimental Botany* **164**: 52–57. doi: 10.1016/j.envexpbot.2019.05.001
- Kopecká, R., Kameniarová, M., Černý, M., Brzobohatý, B. & Novák, J.**, 2023. Abiotic Stress in Crop Production. *International Journal of Molecular Sciences* **24**(7): 6603. doi: 10.3390/ijms24076603
- Kosová, K., Vítámvás, P., Urban, M.O., Prášil, I.T. & Renaut, J.**, 2018. Plant Abiotic Stress Proteomics: The Major Factors Determining Alterations in Cellular Proteome. *Frontiers in Plant Science* **9**: 122. doi: 10.3389/fpls.2018.00122
- Kotak, S., Larkindale, J., Lee, U., Von Koskull-Döring, P., Vierling, E. & Scharf, K.-D.**, 2007. Complexity of the heat stress response in plants. *Current Opinion in Plant Biology* **10**(3): 310–316. doi: 10.1016/j.pbi.2007.04.011
- Koussevitzky, S., Nott, A., Mockler, T.C., Hong, F., Sachetto-Martins, G., Surpin, M., Lim, J., Mittler, R. & Chory, J.**, 2007. Signals from Chloroplasts Converge to Regulate Nuclear Gene Expression. *Science* **316**(5825): 715–719. doi: 10.1126/science.1140516
- Krasensky, J. & Jonak, C.**, 2012. Drought, salt, and temperature stress-induced metabolic rearrangements and regulatory networks. *Journal of Experimental Botany* **63**(4): 1593–1608. doi: 10.1093/jxb/err460
- Kreibich, H., Van Loon, A.F., Schröter, K., Ward, P.J., Mazzoleni, M., Sairam, N., Abeshu, G.W., Agafonova, S., AghaKouchak, A., Aksoy, H., Alvarez-Garretón, C., Aznar, B., Balkhi, L., Barendrecht, M.H., Biancamaria, S., Bos-Burgering, L., Bradley, C., Budiyo, Y., Buytaert, W., Capewell, L., Carlson, H., Cavus, Y., Couasnon, A., Coxon, G., Daliakopoulos, I., de Ruiter, M.C., Delus, C., Erfurt, M., Esposito, G., François, D., Frappart, F., Freer, J., Frolova, N., Gain, A.K., Grillakis, M., Grima, J.O., Guzmán, D.A., Huning, L.S., Ionita, M., Kharlamov, M., Khoi, D.N., Kieboom, N., Kireeva, M., Koutroulis, A., Lavado-Casimiro, W., Li, H.-Y., Llasat, M.C., Macdonald, D., Mård, J., Mathew-Richards, H., McKenzie, A., Mejia, A., Mendiondo, E.M., Mens, M., Mobini, S., Mohor, G.S., Nagavciuc, V., Ngo-Duc, T., Thao Nguyen Huynh, T., Nhi, P.T.T., Petrucci, O., Nguyen, H.Q., Quintana-Seguí, P., Razavi, S., Ridolfi, E., Riegel, J., Sadik, M.S., Savelli, E., Sazonov, A., Sharma, S., Sörensen, J., Arguello Souza, F.A., Stahl, K., Steinhausen, M., Stoelzle, M., Szalińska, W., Tang, Q., Tian, F., Tokarczyk, T., Tovar, C., Tran, T.V.T., Van Huijgevoort, M.H.J., van Vliet, M.T.H., Vorogushyn, S., Wagener, T., Wang, Y., Wendt, D.E., Wickham, E., Yang, L., Zambrano-Bigiarini, M., Blöschl, G. & Di Baldassarre, G.**, 2022. The challenge of unprecedented floods and droughts in risk management. *Nature* **608**(7921): 80–86. doi: 10.1038/s41586-022-04917-5
- Kulkarni, S.R., Vanechoutte, D., Van de Velde, J. & Vandepoele, K.**, 2018. TF2Network: predicting transcription factor regulators and gene regulatory networks in Arabidopsis using publicly available binding site information. *Nucleic Acids Research* **46**(6): e31–e31. doi: 10.1093/nar/gkx1279
- Kumar, D., Datta, R., Hazra, S., Sultana, A., Mukhopadhyay, R. & Chattopadhyay, S.**, 2015. Transcriptomic Profiling of Arabidopsis thaliana Mutant pad2.1 in Response to Combined Cold and Osmotic Stress. *PLOS ONE* **10**(3): e0122690. doi: 10.1371/journal.pone.0122690
- Kumar, L., Chhogyel, N., Gopalakrishnan, T., Hasan, M.K., Jayasinghe, S.L., Kariyawasam, C.S., Kogo, B.K. & Ratnayake, S.**, 2022. Climate change and future of agri-food production. In: *Future Foods*. Elsevier: pp. 49–79. doi: 10.1016/B978-0-323-91001-9.00009-8
- Kumar, S.**, 2020. Abiotic Stresses and Their Effects on Plant Growth, Yield and Nutritional Quality of Agricultural Produce. *International Journal of Food Science and Agriculture* **4**(4): 367–378. doi: 10.26855/ijfsa.2020.12.002
- Kumar, S.V. & Wigge, P.A.**, 2010. H2A.Z-Containing Nucleosomes Mediate the Thermosensory Response in Arabidopsis. *Cell* **140**(1): 136–147. doi: 10.1016/j.cell.2009.11.006
- Kumimoto, R.W., Sirwardana, C.L., Gayler, K.K., Risinger, J.R., Siefers, N. & Holt, B.F.**, 2013. NUCLEAR FACTOR Y Transcription Factors Have Both Opposing and Additive Roles in ABA-Mediated Seed Germination. *PLoS ONE* **8**(3): e59481. doi: 10.1371/journal.pone.0059481

- Küpers, J.J., Snoek, B.L., Oskam, L., Pantazopoulou, C.K., Matton, S.E.A., Reinen, E., Liao, C.-Y., Eggermont, E.D.C., Weekamp, H., Biddanda-Devaiah, M., Kohlen, W., Weijers, D. & Pierik, R., 2023. Local light signaling at the leaf tip drives remote differential petiole growth through auxin-gibberellin dynamics. *Current Biology* **33**(1): 75–85.e5. doi: 10.1016/j.cub.2022.11.045
- Lamaoui, M., Jemo, M., Datla, R. & Bekkaoui, F., 2018. Heat and Drought Stresses in Crops and Approaches for Their Mitigation. *Frontiers in Chemistry* **6**: 26. doi: 10.3389/fchem.2018.00026
- Lamers, J., van der Meer, T. & Testerink, C., 2020. How Plants Sense and Respond to Stressful Environments1 [OPEN]. *Plant Physiology* **182**(4): 1624–1635. doi: 10.1104/pp.19.01464
- Langan, P., Bernád, V., Walsh, J., Henchy, J., Khodaeiaminjan, M., Mangina, E. & Negrão, S., 2022. Phenotyping for waterlogging tolerance in crops: current trends and future prospects. *Journal of Experimental Botany* **73**(15): 5149–5169. doi: 10.1093/jxb/erac243
- Larkin, R.M., Alonso, J.M., Ecker, J.R. & Chory, J., 2003. GUN4, a Regulator of Chlorophyll Synthesis and Intracellular Signaling. *Science* **299**(5608): 902–906. doi: 10.1126/science.1079978
- Larkindale, J., Hall, J.D., Knight, M.R. & Vierling, E., 2005. Heat Stress Phenotypes of Arabidopsis Mutants Implicate Multiple Signaling Pathways in the Acquisition of Thermotolerance. *Plant Physiology* **138**(2): 882–897. doi: 10.1104/pp.105.062257
- Lê, S., Josse, J. & Husson, F., 2008. **FactoMineR**: An R Package for Multivariate Analysis. *Journal of Statistical Software* **25**(1). doi: 10.18637/jss.v025.i01
- Lee, H.-J., Jung, J.-H., Cortés Llorca, L., Kim, S.-G., Lee, S., Baldwin, I.T. & Park, C.-M., 2014. FCA mediates thermal adaptation of stem growth by attenuating auxin action in Arabidopsis. *Nature Communications* **5**(1): 5473. doi: 10.1038/ncomms6473
- Lee, J.-H., Kim, J.Y., Kim, J.-I., Park, Y.-J. & Park, C.-M., 2020. Plant Thermomorphogenic Adaptation to Global Warming. *Journal of Plant Biology* **63**(1): 1–9. doi: 10.1007/s12374-020-09232-y
- Lee, K.P., Li, M., Li, M., Liu, K., Medina-Puche, L., Qi, S., Cui, C., Lozano-Duran, R. & Kim, C., 2023. Hierarchical regulatory module GENOMES UNCOUPLED1–GOLDEN2–LIKE1/2–WRKY18/40 modulates salicylic acid signaling. *Plant Physiology* **192**(4): 3120–3133. doi: 10.1093/plphys/kiad251
- Lee, S., Wang, W. & Huq, E., 2021a. Spatial regulation of thermomorphogenesis by HY5 and PIF4 in Arabidopsis. *Nature Communications* **12**(1): 3656. doi: 10.1038/s41467-021-24018-7
- Lee, S., Zhu, L. & Huq, E., 2021b. An autoregulatory negative feedback loop controls thermomorphogenesis in Arabidopsis. *PLOS Genetics* **17**(6): e1009595. doi: 10.1371/journal.pgen.1009595
- Lee, S.C., Mastroph, A., Sasidharan, R., Vashisht, D., Pedersen, O., Oosumi, T., Voeselek, L.A.C.J. & Bailey-Serres, J., 2011. Molecular characterization of the submergence response of the Arabidopsis thaliana ecotype Columbia. *New Phytologist* **190**(2): 457–471. doi: 10.1111/j.1469-8137.2010.03590.x
- Lee, Y.K., Kumari, S., Olson, A., Hauser, F. & Ware, D., 2022. Role of a ZF-HD Transcription Factor in miR157-Mediated Feed-Forward Regulatory Module That Determines Plant Architecture in Arabidopsis. *International Journal of Molecular Sciences* **23**(15): 8665. doi: 10.3390/ijms23158665
- Leipner, J., Fracheboud, Y. & Stamp, P., 1997. Acclimation by suboptimal growth temperature diminishes photooxidative damage in maize leaves. *Plant, Cell and Environment* **20**(3): 366–372. doi: 10.1046/j.1365-3040.1997.d01-76.x
- Leister, D., 2012. Retrograde signaling in plants: from simple to complex scenarios. *Frontiers in Plant Science* **3**. doi: 10.3389/fpls.2012.00135

- Leivar, P., Monte, E., Al-Sady, B., Carle, C., Storer, A., Alonso, J.M., Ecker, J.R. & Quail, P.H., 2008. The Arabidopsis Phytochrome-Interacting Factor PIF7, Together with PIF3 and PIF4, Regulates Responses to Prolonged Red Light by Modulating phyB Levels. *The Plant Cell* **20**(2): 337–352. doi: 10.1105/tpc.107.052142
- Li, B., Gao, K., Ren, H. & Tang, W., 2018a. Molecular mechanisms governing plant responses to high temperatures: Plant high temperature response mechanisms. *Journal of Integrative Plant Biology* **60**(9): 757–779. doi: 10.1111/jipb.12701
- Li, B., Tang, M., Nelson, A., Caligagan, H., Zhou, X., Clark-Wiest, C., Ngo, R., Brady, S.M. & Kliebenstein, D.J., 2018b. Network-Guided Discovery of Extensive Epistasis between Transcription Factors Involved in Aliphatic Glucosinolate Biosynthesis. *The Plant Cell* **30**(1): 178–195. doi: 10.1105/tpc.17.00805
- Li, M. & Kim, C., 2022. Chloroplast ROS and stress signaling. *Plant Communications* **3**(1): 100264. doi: 10.1016/j.xplc.2021.100264
- Li, M., Lee, K.P., Liu, T., Dogra, V., Duan, J., Li, M., Xing, W. & Kim, C., 2022a. Antagonistic modules regulate photosynthesis-associated nuclear genes via GOLDEN2-LIKE transcription factors. *Plant Physiology* **188**(4): 2308–2324. doi: 10.1093/plphys/kiab600
- Li, P., Yang, X., Wang, H., Pan, T., Yang, J., Wang, Y., Xu, Y., Yang, Z. & Xu, C., 2021a. Metabolic responses to combined water deficit and salt stress in maize primary roots. *Journal of Integrative Agriculture* **20**(1): 109–119. doi: 10.1016/S2095-3119(20)63242-7
- Li, R.-Q., Jiang, M., Huang, J.-Z., Møller, I.M. & Shu, Q.-Y., 2021b. Mutations of the Genomes Uncoupled 4 Gene Cause ROS Accumulation and Repress Expression of Peroxidase Genes in Rice. *Frontiers in Plant Science* **12**: 682453. doi: 10.3389/fpls.2021.682453
- Li, W., Li, X., Chao, J., Zhang, Z., Wang, W. & Guo, Y., 2018c. NAC Family Transcription Factors in Tobacco and Their Potential Role in Regulating Leaf Senescence. *Frontiers in Plant Science* **9**: 1900. doi: 10.3389/fpls.2018.01900
- Li, X., Guo, C., Li, Z., Wang, G., Yang, J., Chen, L., Hu, Z., Sun, J., Gao, J., Yang, A., Pu, W. & Wen, L., 2022b. Deciphering the roles of tobacco MYB transcription factors in environmental stress tolerance. *Frontiers in Plant Science* **13**: 998606. doi: 10.3389/fpls.2022.998606
- Li, X., Yang, Y., Sun, X., Lin, H., Chen, J., Ren, J., Hu, X. & Yang, Y., 2014. Comparative Physiological and Proteomic Analyses of Poplar (*Populus yunnanensis*) Plantlets Exposed to High Temperature and Drought. *PLoS ONE* **9**(9): e107605. doi: 10.1371/journal.pone.0107605
- Li, Y., Liu, H., Ma, T., Li, J., Yuan, J., Xu, Y.-C., Sun, R., Zhang, X., Jing, Y., Guo, Y.-L. & Lin, R., 2023. Arabidopsis EXECUTER1 interacts with WRKY transcription factors to mediate plastid-to-nucleus singlet oxygen signaling. *The Plant Cell* **35**(2): 827–851. doi: 10.1093/plcell/koac330
- Licausi, F., Kosmacz, M., Weits, D.A., Giuntoli, B., Giorgi, F.M., Voeselek, L.A.C.J., Perata, P. & Van Dongen, J.T., 2011. Oxygen sensing in plants is mediated by an N-end rule pathway for protein destabilization. *Nature* **479**(7373): 419–422. doi: 10.1038/nature10536
- Lin, K.-F., Tsai, M.-Y., Lu, C.-A., Wu, S.-J. & Yeh, C.-H., 2018. The roles of Arabidopsis HSFA2, HSFA4a, and HSFA7a in the heat shock response and cytosolic protein response. *Botanical Studies* **59**(1): 15. doi: 10.1186/s40529-018-0231-0
- Linden, K.J., Chen, Y., Kyaw, K., Schultz, B. & Callis, J., 2021. Factors that affect protein abundance of a positive regulator of abscisic acid signalling, the basic leucine zipper transcription factor ABRE-binding factor 2 (ABF2). *Plant Direct* **5**(6). doi: 10.1002/pld3.330
- Liu, H., Able, A.J. & Able, J.A., 2020. Integrated Analysis of Small RNA, Transcriptome, and Degradome Sequencing Reveals the Water-Deficit and Heat Stress Response Network in Durum Wheat. *International Journal of Molecular Sciences* **21**(17): 6017. doi: 10.3390/ijms21176017
- Liu, H., Able, A.J. & Able, J.A., 2022a. Priming crops for the future: rewiring stress memory. *Trends in Plant Science* **27**(7): 699–716. doi: 10.1016/j.tplants.2021.11.015

- Liu, H., Song, S., Zhang, H., Li, Y., Niu, L., Zhang, J. & Wang, W.**, 2022b. Signaling Transduction of ABA, ROS, and Ca²⁺ in Plant Stomatal Closure in Response to Drought. *International Journal of Molecular Sciences* **23**(23): 14824. doi: 10.3390/ijms232314824
- Liu, L., White, M.J. & MacRae, T.H.**, 1999. Transcription factors and their genes in higher plants. Functional domains, evolution and regulation. *European Journal of Biochemistry* **262**(2): 247–257. doi: 10.1046/j.1432-1327.1999.00349.x
- Liu, M. & Lu, S.**, 2016. Plastoquinone and Ubiquinone in Plants: Biosynthesis, Physiological Function and Metabolic Engineering. *Frontiers in Plant Science* **7**. doi: 10.3389/fpls.2016.01898
- Liu, X. & Hou, X.**, 2018. Antagonistic Regulation of ABA and GA in Metabolism and Signaling Pathways. *Frontiers in Plant Science* **9**: 251. doi: 10.3389/fpls.2018.00251
- Liu, X.-D., Xie, L., Wei, Y., Zhou, X., Jia, B., Liu, J. & Zhang, S.**, 2014. Abiotic Stress Resistance, a Novel Moonlighting Function of Ribosomal Protein RPL44 in the Halophilic Fungus *Aspergillus glaucus*. *Applied and Environmental Microbiology* **80**(14): 4294–4300. doi: 10.1128/AEM.00292-14
- Liu, Y. & Li, T.**, 2022. NaCl Pretreatment Enhances the Low Temperature Tolerance of Tomato Through Photosynthetic Acclimation. *Frontiers in Plant Science* **13**.
- Liu, Z., Hartman, S., Van Veen, H., Zhang, H., Leeggangers, H.A.C.F., Martopawiro, S., Bosman, F., De Deugd, F., Su, P., Hummel, M., Rankenberg, T., Hassall, K.L., Bailey-Serres, J., Theodoulou, F.L., Voesenek, L.A.C.J. & Sasidharan, R.**, 2022c. Ethylene augments root hypoxia tolerance via growth cessation and reactive oxygen species amelioration. *Plant Physiology* **190**(2): 1365–1383. doi: 10.1093/plphys/kiac245
- Llorens, E., González-Hernández, A.I., Scalschi, L., Fernández-Crespo, E., Camañes, G., Vicedo, B. & García-Agustín, P.**, 2020. Priming mediated stress and cross-stress tolerance in plants: Concepts and opportunities. In: *Priming-Mediated Stress and Cross-Stress Tolerance in Crop Plants*. Elsevier: pp. 1–20. doi: 10.1016/B978-0-12-817892-8.00001-5
- Lobbes, D., Rallapalli, G., Schmidt, D.D., Martin, C. & Clarke, J.**, 2006. SERRATE: a new player on the plant microRNA scene. *EMBO Reports* **7**(10): 1052–1058. doi: 10.1038/sj.embor.7400806
- Löw, M., Herbinger, K., Nunn, A.J., Häberle, K.-H., Leuchner, M., Heerdt, C., Werner, H., Wipfler, P., Pretzsch, H., Tausz, M. & Matyssek, R.**, 2006. Extraordinary drought of 2003 overrules ozone impact on adult beech trees (*Fagus sylvatica*). *Trees* **20**(5): 539–548. doi: 10.1007/s00468-006-0069-z
- Lozano-Elena, F., Fàbregas, N., Coletto-Alcudia, V. & Caño-Delgado, A.I.**, 2022. Analysis of metabolic dynamics during drought stress in *Arabidopsis* plants. *Scientific Data* **9**(1): 90. doi: 10.1038/s41597-022-01161-4
- Lu, F., Cui, X., Zhang, S., Jenuwein, T. & Cao, X.**, 2011. *Arabidopsis* REF6 is a histone H3 lysine 27 demethylase. *Nature Genetics* **43**(7): 715–719. doi: 10.1038/ng.854
- Lu, K.X., Cao, B.H., Feng, X.P., He, Y. & Jiang, D.A.**, 2009. Photosynthetic response of salt-tolerant and sensitive soybean varieties. *Photosynthetica* **47**(3): 381–387. doi: 10.1007/s11099-009-0059-7
- Luo, F.-L., Nagel, K.A., Zeng, B., Schurr, U. & Matsubara, S.**, 2009. Photosynthetic acclimation is important for post-submergence recovery of photosynthesis and growth in two riparian species. *Annals of Botany* **104**(7): 1435–1444. doi: 10.1093/aob/mcp257
- Luo, X. & He, Y.**, 2020. Experiencing winter for spring flowering: A molecular epigenetic perspective on vernalization. *Journal of Integrative Plant Biology* **62**(1): 104–117. doi: 10.1111/jipb.12896
- Lv, R., Li, Z., Li, M., Dogra, V., Lv, S., Liu, R., Lee, K.P. & Kim, C.**, 2019. Uncoupled Expression of Nuclear and Plastid Photosynthesis-Associated Genes Contributes to Cell Death in a Lesion Mimic Mutant. *The Plant Cell* **31**(1): 210–230. doi: 10.1105/tpc.18.00813

- Ma, D., Li, X., Guo, Y., Chu, J., Fang, S., Yan, C., Noel, J.P. & Liu, H.**, 2016. Cryptochrome 1 interacts with PIF4 to regulate high temperature-mediated hypocotyl elongation in response to blue light. *Proceedings of the National Academy of Sciences* **113**(1): 224–229. doi: 10.1073/pnas.1511437113
- Ma, X., Sukiran, N., Ma, H. & Su, Z.**, 2014. Moderate drought causes dramatic floral transcriptomic reprogramming to ensure successful reproductive development in *Arabidopsis*. *BMC Plant Biology* **14**(1): 164. doi: 10.1186/1471-2229-14-164
- Macková, H., Hronková, M., Dobrá, J., Turečková, V., Novák, O., Lubovská, Z., Motyka, V., Haisel, D., Hájek, T., Prášil, I.T., Gaudinová, A., Štorchová, H., Ge, E., Werner, T., Schmölling, T. & Vanková, R.**, 2013. Enhanced drought and heat stress tolerance of tobacco plants with ectopically enhanced cytokinin oxidase/dehydrogenase gene expression. *Journal of Experimental Botany* **64**(10): 2805–2815. doi: 10.1093/jxb/ert131
- Mahalingam, R.**, 2015. Consideration of Combined Stress: A Crucial Paradigm for Improving Multiple Stress Tolerance in Plants. In: R. Mahalingam (ed.): *Combined Stresses in Plants*. Springer International Publishing (Cham): pp. 1–25. doi: 10.1007/978-3-319-07899-1_1
- Malefo, M.B., Mathibela, E.O., Crampton, B.G. & Makgopa, M.E.**, 2020. Investigating the role of Bowman-Birk serine protease inhibitor in *Arabidopsis* plants under drought stress. *Plant Physiology and Biochemistry* **149**: 286–293. doi: 10.1016/j.plaphy.2020.02.007
- Mamaeva, A., Taliansky, M., Filippova, A., Love, A.J., Golub, N. & Fesenko, I.**, 2020. The role of chloroplast protein remodeling in stress responses and shaping of the plant peptidome. *New Phytologist* **227**(5): 1326–1334. doi: 10.1111/nph.16620
- Mandal, R. & Dutta, G.**, 2020. From photosynthesis to biosensing: Chlorophyll proves to be a versatile molecule. *Sensors International* **1**: 100058. doi: 10.1016/j.sintl.2020.100058
- Mano, J., Belles-Boix, E., Babiychuk, E., Inzé, D., Torii, Y., Hiraoka, E., Takimoto, K., Slooten, L., Asada, K. & Kushnir, S.**, 2005. Protection against Photooxidative Injury of Tobacco Leaves by 2-Alkenal Reductase. Detoxication of Lipid Peroxide-Derived Reactive Carbonyls. *Plant Physiology* **139**(4): 1773–1783. doi: 10.1104/pp.105.070391
- Marchin, R.M., Backes, D., Ossola, A., Leishman, M.R., Tjoelker, M.G. & Ellsworth, D.S.**, 2022. Extreme heat increases stomatal conductance and drought-induced mortality risk in vulnerable plant species. *Global Change Biology* **28**(3): 1133–1146. doi: 10.1111/gcb.15976
- Marin, M., Feeney, D.S., Brown, L.K., Naveed, M., Ruiz, S., Koebernick, N., Bengough, A.G., Hallett, P.D., Roose, T., Puértolas, J., Dodd, I.C. & George, T.S.**, 2021. Significance of root hairs for plant performance under contrasting field conditions and water deficit. *Annals of Botany* **128**(1): 1–16. doi: 10.1093/aob/mcaa181
- Markhart, A.H.**, 1985. Comparative Water Relations of *Phaseolus vulgaris* L. and *Phaseolus acutifolius* Gray. *Plant Physiology* **77**(1): 113–117. doi: 10.1104/pp.77.1.113
- Martín, G., Leivar, P., Ludevid, D., Tepperman, J.M., Quail, P.H. & Monte, E.**, 2016. Phytochrome and retrograde signalling pathways converge to antagonistically regulate a light-induced transcriptional network. *Nature Communications* **7**(1): 11431. doi: 10.1038/ncomms11431
- Martín, G., Leivar, P., Ludevid, D., Tepperman, J.M., Quail, P.H. & Monte, E.**, 2016. Phytochrome and retrograde signalling pathways converge to antagonistically regulate a light-induced transcriptional network. *Nature Communications* **7**(May). doi: 10.1038/ncomms11431
- Martin, M.**, 2011. Cutadapt removes adapter sequences from high-throughput sequencing reads. *EMBnet.Journal* **17**(1): 10. doi: 10.14806/ej.17.1.200
- Maruta, T., Noshi, M., Tanouchi, A., Tamoi, M., Yabuta, Y., Yoshimura, K., Ishikawa, T. & Shigeoka, S.**, 2012. H₂O₂-triggered Retrograde Signaling from Chloroplasts to Nucleus Plays Specific Role in Response to Stress. *Journal of Biological Chemistry* **287**(15): 11717–11729. doi: 10.1074/jbc.M111.292847

- Masson-Delmotte, V., Zhai, P. & Pirani, A.**, 2021. Climate change 2021: the physical science basis : summary for policymakers : working group I contribution to the sixth Assessment report of the Intergovernmental Panel on Climate Change. IPCC (Geneva, Switzerland).
- Mathur, S., Agrawal, D. & Jajoo, A.**, 2014. Photosynthesis: Response to high temperature stress. *Journal of Photochemistry and Photobiology B: Biology* **137**: 116–126. doi: 10.1016/j.jphotobiol.2014.01.010
- Mecey, C., Hauck, P., Trapp, M., Pumplun, N., Plovanich, A., Yao, J. & He, S.Y.**, 2011. A Critical Role of STAYGREEN /Mendel's I Locus in Controlling Disease Symptom Development during *Pseudomonas syringae* pv tomato Infection of Arabidopsis. *Plant Physiology* **157**(4): 1965–1974. doi: 10.1104/pp.111.181826
- Miao, S., Zou, C.B. & Breshears, D.D.**, 2009. Vegetation Responses to Extreme Hydrological Events: Sequence Matters. *The American Naturalist* **173**(1): 113–118. doi: 10.1086/593307
- Mignolli, F., Barone, J.O. & Vidoz, M.L.**, 2021. Root submergence enhances respiration and sugar accumulation in the stem of flooded tomato plants. *Plant, Cell & Environment* **44**(11): 3643–3654. doi: 10.1111/pce.14152
- Miguel, V.N., Manavella, P.A., Chan, R.L. & Capella, M.**, 2020. The AtHB1 Transcription Factor Controls the miR164-CUC2 Regulatory Node to Modulate Leaf Development. *Plant and Cell Physiology* **61**(3): 659–670. doi: 10.1093/pcp/pcz233
- Millenaar, F.F., Cox, M.C.H., Van Berkel, Y.E.M.D.J., Welschen, R.A.M., Pierik, R., Voeselek, L.A.J.C. & Peeters, A.J.M.**, 2005. Ethylene-Induced Differential Growth of Petioles in Arabidopsis. Analyzing Natural Variation, Response Kinetics, and Regulation. *Plant Physiology* **137**(3): 998–1008. doi: 10.1104/pp.104.053967
- Mimura, N.**, 2013. Sea-level rise caused by climate change and its implications for society. *Proceedings of the Japan Academy, Series B* **89**(7): 281–301. doi: 10.2183/pjab.89.281
- Miryeganeh, M.**, 2021. Plants' Epigenetic Mechanisms and Abiotic Stress. *Genes* **12**(8): 1106. doi: 10.3390/genes12081106
- Mishra, R., Shteinberg, M., Shkolnik, D., Anfoka, G., Czosnek, H. & Gorovits, R.**, 2022. Interplay between abiotic (drought) and biotic (virus) stresses in tomato plants. *Molecular Plant Pathology* **23**(4): 475–488. doi: 10.1111/mpp.13172
- Mishra, V., Gahlawt, P., Singh, S., Dubey, N.K., Singh, S.P., Tripathi, D.K. & Singh, V.P.**, 2023. GABA: a key player of abiotic stress regulation. *Plant Signaling & Behavior* **18**(1): 2163343. doi: 10.1080/15592324.2022.2163343
- Mittler, R.**, 2002. Oxidative stress, antioxidants and stress tolerance. *Trends in Plant Science* **7**(9): 405–410. doi: 10.1016/S1360-1385(02)02312-9
- Mittler, R.**, 2006a. Abiotic stress, the field environment and stress combination. *Trends in Plant Science* **11**(1): 15–19. doi: 10.1016/j.tplants.2005.11.002
- Mittler, R.**, 2006b. Abiotic stress, the field environment and stress combination. *Trends in Plant Science* **11**(1): 15–19. doi: 10.1016/j.tplants.2005.11.002
- Mittler, R.**, 2017. ROS Are Good. *Trends in Plant Science* **22**(1): 11–19. doi: 10.1016/j.tplants.2016.08.002
- Mittler, R. & Blumwald, E.**, 2010. Genetic Engineering for Modern Agriculture: Challenges and Perspectives. *Annual Review of Plant Biology* **61**(1): 443–462. doi: 10.1146/annurev-arplant-042809-112116
- Mittler, R., Vanderauwera, S., Gollery, M. & Van Breusegem, F.**, 2004. Reactive oxygen gene network of plants. *Trends in Plant Science* **9**(10): 490–498. doi: 10.1016/j.tplants.2004.08.009
- Mittler, R., Zandalinas, S.I., Fichman, Y. & Van Breusegem, F.**, 2022. Reactive oxygen species signalling in plant stress responses. *Nature Reviews Molecular Cell Biology* **23**(10): 663–679. doi: 10.1038/s41580-022-00499-2

- Mockler, T.C.**, 2016. Modulation of phytochrome signaling networks for improved biomass accumulation using a bioenergy crop model (No. DOE-DDPSC--0006627, 1331003; p. DOE-DDPSC--0006627, 1331003). p. DOE-DDPSC--0006627, 1331003. doi: 10.2172/1331003
- Mohanty, B.**, 2003. Contrasting Effects of Submergence in Light and Dark on Pyruvate Decarboxylase Activity in Roots of Rice Lines Differing in Submergence Tolerance. *Annals of Botany* **91**(2): 291–300. doi: 10.1093/aob/mcf050
- Mommer, L. & Visser, E.J.W.**, 2005. Underwater Photosynthesis in Flooded Terrestrial Plants: A Matter of Leaf Plasticity. *Annals of Botany* **96**(4): 581–589. doi: 10.1093/aob/mci212
- Monteoliva, M.I., Guzzo, M.C. & Posada, G.A.**, 2021. Breeding for Drought Tolerance by Monitoring Chlorophyll Content. (165).
- Morales, A., de Boer, H.J., Douma, J.C., Elsen, S., Engels, S., Glimmerveen, T., Sajeev, N., Huber, M., Luimes, M., Luitjens, E., Raatjes, K., Hsieh, C., Teapal, J., Wildenbeest, T., Jiang, Z., Pareek, A., Singla-Pareek, S., Yin, X., Evers, J., Anten, N.P.R., van Zanten, M. & Sasidharan, R.**, 2022. Effects of sublethal single, simultaneous and sequential abiotic stresses on phenotypic traits of Arabidopsis thaliana. *AoB PLANTS* **14**(4): plac029. doi: 10.1093/aobpla/plac029
- Morales, M. & Munné-Bosch, S.**, 2019. Malondialdehyde: Facts and Artifacts. *Plant Physiology* **180**(3): 1246–1250. doi: 10.1104/pp.19.00405
- Muhammad Aslam, M., Waseem, M., Jakada, B.H., Okal, E.J., Lei, Z., Saqib, H.S.A., Yuan, W., Xu, W. & Zhang, Q.**, 2022. Mechanisms of Abscisic Acid-Mediated Drought Stress Responses in Plants. *International Journal of Molecular Sciences* **23**(3): 1084. doi: 10.3390/ijms23031084
- Munné-Bosch, S. & Alegre, L.**, 2013. Cross-stress tolerance and stress “memory” in plants: An integrated view. *Environmental and Experimental Botany* **94**: 1–2. doi: 10.1016/j.envexpbot.2013.02.002
- Murphy, A.**, 2015. Hormone crosstalk in plants. *Journal of Experimental Botany* **66**(16): 4853–4854. doi: 10.1093/jxb/erv339
- Mustroph, A., Zanetti, M.E., Jang, C.J.H., Holtan, H.E., Repetti, P.P., Galbraith, D.W., Girke, T. & Bailey-Serres, J.**, 2009. Profiling translomes of discrete cell populations resolves altered cellular priorities during hypoxia in Arabidopsis. *Proceedings of the National Academy of Sciences* **106**(44): 18843–18848. doi: 10.1073/pnas.0906131106
- Nadeem, H., Khan, A., Gupta, R., Hashem, M., Alamri, S., Ahmad Siddiqui, M. & Ahmad, F.**, 2022. Stress combination—when two negatives may become antagonistic, synergistic, or additive for plants: A review. *Pedosphere* **S1002016022000376**. doi: 10.1016/j.pedsph.2022.06.031
- Nagatoshi, Y., Mitsuda, N., Hayashi, M., Inoue, S., Okuma, E., Kubo, A., Murata, Y., Seo, M., Saji, H., Kinoshita, T. & Ohme-Takagi, M.**, 2016. GOLDEN 2-LIKE transcription factors for chloroplast development affect ozone tolerance through the regulation of stomatal movement. *Proceedings of the National Academy of Sciences* **113**(15): 4218–4223. doi: 10.1073/pnas.1513093113
- Nambara, E., Suzuki, M., Abrams, S., McCarty, D.R., Kamiya, Y. & McCourt, P.**, 2002. A Screen for Genes That Function in Abscisic Acid Signaling in Arabidopsis thaliana. *Genetics* **161**(3): 1247–1255. doi: 10.1093/genetics/161.3.1247
- Nankishore, A. & Farrell, A.D.**, 2016. The response of contrasting tomato genotypes to combined heat and drought stress. *Journal of Plant Physiology* **202**: 75–82. doi: 10.1016/j.jplph.2016.07.006
- Nardeli, S.M., Zacharaki, V., Rojas-Murcia, N., Collani, S., Wang, K., Bayer, M., Schmid, M. & Goretti, D.**, 2023. Temperature-dependent regulation of Arabidopsis thaliana growth and development by LSM7 [Preprint]. *Plant Biology*. doi: 10.1101/2023.03.28.534379

- Nascimento, L.B.D.S., Leal-Costa, M.V., Menezes, E.A., Lopes, V.R., Muzitano, M.F., Costa, S.S. & Tavares, E.S.**, 2015. Ultraviolet-B radiation effects on phenolic profile and flavonoid content of *Kalanchoe pinnata*. *Journal of Photochemistry and Photobiology B: Biology* **148**: 73–81. doi: 10.1016/j.jphotobiol.2015.03.011
- Naseer, S., Lee, Y., Lapiere, C., Franke, R., Nawrath, C. & Geldner, N.**, 2012. Casparian strip diffusion barrier in Arabidopsis is made of a lignin polymer without suberin. *Proceedings of the National Academy of Sciences* **109**(25): 10101–10106. doi: 10.1073/pnas.1205726109
- Neelam; YANG, A.**, 2013. Determination of heat tolerance of interspecific (*Cucurbita maxima* x *Cucurbita moschata*) inbred line of squash 'Maxchata' and its parents through photosynthetic response. *Tarım Bilimleri Dergisi* **19**(3): 188–197. doi: 10.1501/Tarimbil_0000001244
- Negin, B., Yaaran, A., Kelly, G., Zait, Y. & Moshelion, M.**, 2019. Mesophyll Abscisic Acid Restrains Early Growth and Flowering But Does Not Directly Suppress Photosynthesis. *Plant Physiology* **180**(2): 910–925. doi: 10.1104/pp.18.01334
- Netshimbupfe, M.H., Berner, J. & Gouws, C.**, 2022. The interactive effects of drought and heat stress on photosynthetic efficiency and biochemical defense mechanisms of *Amaranthus* species. *Plant-Environment Interactions* **3**(5): 212–225. doi: 10.1002/pei3.10092
- Ni, X.-L., Gui, M.-Y., Tan, L.-L., Zhu, Q., Liu, W.-Z. & Li, C.-X.**, 2019. Programmed Cell Death and Aerenchyma Formation in Water-Logged Sunflower Stems and Its Promotion by Ethylene and ROS. *Frontiers in Plant Science* **9**: 1928. doi: 10.3389/fpls.2018.01928
- Nielsen, F., Mikkelsen, B.B., Nielsen, J.B., Andersen, H.R. & Grandjean, P.**, 1997. Plasma malondialdehyde as biomarker for oxidative stress: reference interval and effects of life-style factors. *Clinical Chemistry* **43**(7): 1209–1214. doi: 10.1093/clinchem/43.7.1209
- Ning, L.-H., Du, W., Song, H.-N., Shao, H.-B., Qi, W.-C., Sheteiwy, M.S.A. & Yu, D.**, 2019. Identification of responsive miRNAs involved in combination stresses of phosphate starvation and salt stress in soybean root. *Environmental and Experimental Botany* **167**: 103823. doi: 10.1016/j.envexpbot.2019.103823
- Nishiyama, Y. & Murata, N.**, 2014. Revised scheme for the mechanism of photoinhibition and its application to enhance the abiotic stress tolerance of the photosynthetic machinery. *Applied Microbiology and Biotechnology* **98**(21): 8777–8796. doi: 10.1007/s00253-014-6020-0
- Noh, B., Lee, S.-H., Kim, H.-J., Yi, G., Shin, E.-A., Lee, M., Jung, K.-J., Doyle, M.R., Amasino, R.M. & Noh, Y.-S.**, 2004. Divergent Roles of a Pair of Homologous Jumonji/Zinc-Finger-Class Transcription Factor Proteins in the Regulation of Arabidopsis Flowering Time. *The Plant Cell* **16**(10): 2601–2613. doi: 10.1105/tpc.104.025353
- Obata, T., Witt, S., Lisec, J., Palacios-Rojas, N., Florez-Sarasa, I., Arous, J.L., Cairns, J.E., Yousfi, S. & Fernie, A.R.**, 2015. Metabolite profiles of maize leaves in drought, heat and combined stress field trials reveal the relationship between metabolism and grain yield. *Plant Physiology* pp.01164.2015. doi: 10.1104/pp.15.01164
- Oh, E., Zhu, J.-Y. & Wang, Z.-Y.**, 2012. Interaction between BZR1 and PIF4 integrates brassinosteroid and environmental responses. *Nature Cell Biology* **14**(8): 802–809. doi: 10.1038/ncb2545
- Ohbayashi, I. & Sugiyama, M.**, 2018. Plant Nucleolar Stress Response, a New Face in the NAC-Dependent Cellular Stress Responses. *Frontiers in Plant Science* **8**: 2247. doi: 10.3389/fpls.2017.02247
- Paakkonen, E., Vahala, J., Pohjola, M., Holopainen, T. & Karenlampi, L.**, 1998. Physiological, stomatal and ultrastructural ozone responses in birch (*Betula pendula* Roth.) are modified by water stress. *Plant, Cell and Environment* **21**(7): 671–684. doi: 10.1046/j.1365-3040.1998.00303.x
- Pagès, L.**, 2011. Links between root developmental traits and foraging performance: Root developmental traits and foraging performance. *Plant, Cell & Environment* **34**(10): 1749–1760. doi: 10.1111/j.1365-3040.2011.02371.x
- Pal, G., Bakade, R., Deshpande, S., Sureshkumar, V., Patil, S.S., Dawane, A., Agarwal, S., Niranjana, V., PrasannaKumar, M.K. & Vemanna, R.S.**, 2022. Transcriptomic responses under combined bacterial blight and drought stress in rice reveal potential genes to improve multi-stress tolerance. *BMC Plant Biology* **22**(1): 349. doi: 10.1186/s12870-022-03725-3
- Pandey, P., Irulappan, V., Bagavathiannan, M.V. & Senthil-Kumar, M.**, 2017. Impact of Combined Abiotic and Biotic Stresses on Plant Growth and Avenues for Crop Improvement by Exploiting Physio-morphological Traits. *Frontiers in Plant Science* **8**. doi: 10.3389/fpls.2017.00537
- Pandey, P., Ramegowda, V. & Senthil-Kumar, M.**, 2015. Shared and unique responses of plants to multiple individual stresses and stress combinations: physiological and molecular mechanisms. *Frontiers in Plant Science* **6**. doi: 10.3389/fpls.2015.00723
- Pantazopoulou, C.K., Bongers, F.J., Küpers, J.J., Reinen, E., Das, D., Evers, J.B., Anten, N.P.R. & Pierik, R.**, 2017. Neighbor detection at the leaf tip adaptively regulates upward leaf movement through spatial auxin dynamics. *Proceedings of the National Academy of Sciences* **114**(28): 7450–7455. doi: 10.1073/pnas.1702275114
- Park, J., Lee, S., Park, G., Cho, H., Choi, D., Umeda, M., Choi, Y., Hwang, D. & Hwang, I.**, 2021a. C YTO K ININ-RESPONSIVE G ROWTH REGULATOR regulates cell expansion and cytokinin-mediated cell cycle progression. *Plant Physiology* **186**(3): 1734–1746. doi: 10.1093/plphys/kiab180
- Park, Y., Lee, H., Ha, J., Kim, J.Y. & Park, C.**, 2017. COP 1 conveys warm temperature information to hypocotyl thermomorphogenesis. *New Phytologist* **215**(1): 269–280. doi: 10.1111/nph.14581
- Park, Y.-J., Kim, J.Y., Lee, J.-H., Han, S.-H. & Park, C.-M.**, 2021b. External and Internal Reshaping of Plant Thermomorphogenesis. *Trends in Plant Science* **26**(8): 810–821. doi: 10.1016/j.tplants.2021.01.002
- Park, Y.-J., Lee, H.-J., Gil, K.-E., Kim, J.Y., Lee, J.-H., Lee, H., Cho, H.-T., Vu, L.D., De Smet, I. & Park, C.-M.**, 2019. Developmental Programming of Theronastic Leaf Movement. *Plant Physiology* **180**(2): 1185–1197. doi: 10.1104/pp.19.00139
- Pascual, L.S., Segarra-Medina, C., Gómez-Cadenas, A., López-Climent, M.F., Vives-Peris, V. & Zandalinas, S.I.**, 2022. Climate change-associated multifactorial stress combination: A present challenge for our ecosystems. *Journal of Plant Physiology* **276**: 153764. doi: 10.1016/j.jplph.2022.153764
- Pastori, G.M. & Foyer, C.H.**, 2002. Common Components, Networks, and Pathways of Cross-Tolerance to Stress. The Central Role of "Redox" and Abscisic Acid-Mediated Controls. *Plant Physiology* **129**(2): 460–468. doi: 10.1104/pp.011021
- Patel, J., Khandwal, D., Choudhary, B., Ardesana, D., Jha, R.K., Tanna, B., Yadav, S., Mishra, A., Varshney, R.K. & Siddique, K.H.M.**, 2022. Differential Physio-Biochemical and Metabolic Responses of Peanut (*Arachis hypogaea* L.) under Multiple Abiotic Stress Conditions. *International Journal of Molecular Sciences* **23**(2): 660. doi: 10.3390/ijms23020660
- Pedersen, O., Perata, P. & Voeselek, L.A.C.J.**, 2017. Flooding and low oxygen responses in plants. *Functional Plant Biology* **44**(9): iii. doi: 10.1071/FPv44n9_FO
- Pederson, D.G.**, 1968. Environmental stress, heterozygote advantage and genotype-environment interaction in Arabidopsis. *Heredity* **23**(1): 127–138. doi: 10.1038/hdy.1968.11

- Peeters, A.J.M., Cox, M.C.H., Benschop, J.J., Vreeburg, R.A.M., Bou, J. & Voeselek, L.A.C.J.**, 2002. Submergence research using *Rumex palustris* as a model; looking back and going forward. *Journal of Experimental Botany* **53**(368): 391–398. doi: 10.1093/jexbot/53.368.391
- Peláez-Vico, M.Á., Tukuli, A., Singh, P., Mendoza-Cózatl, D.G., Joshi, T. & Mittler, R.**, 2023. Rapid systemic responses of *Arabidopsis* to waterlogging stress. *Plant Physiology* kiad433. doi: 10.1093/plphys/kiad433
- Peng, J., Li, Z., Wen, X., Li, W., Shi, H., Yang, L., Zhu, H. & Guo, H.**, 2014. Salt-Induced Stabilization of EIN3/EIL1 Confers Salinity Tolerance by Deterring ROS Accumulation in *Arabidopsis*. *PLoS Genetics* **10**(10): e1004664. doi: 10.1371/journal.pgen.1004664
- Peng, P., Li, R., Chen, Z.-H. & Wang, Y.**, 2022. Stomata at the crossroad of molecular interaction between biotic and abiotic stress responses in plants. *Frontiers in Plant Science* **13**: 1031891. doi: 10.3389/fpls.2022.1031891
- Perby, L.K., Richter, S., Weber, K., Hieber, A.J., Hess, N., Crocoll, C., Mogensen, H.K., Pribil, M., Burow, M., Nielsen, T.H. & Muströph, A.**, 2022. Cytosolic phosphofructokinases are important for sugar homeostasis in leaves of *Arabidopsis thaliana*. *Annals of Botany* **129**(1): 37–52. doi: 10.1093/aob/mcab122
- Perdomo, J.A., Conesa, M.Á., Medrano, H., Ribas-Carbó, M. & Galmés, J.**, 2015. Effects of long-term individual and combined water and temperature stress on the growth of rice, wheat and maize: relationship with morphological and physiological acclimation. *Physiologia Plantarum* **155**(2): 149–165. doi: 10.1111/ppl.12303
- Pereira, A.**, 2016. Plant Abiotic Stress Challenges from the Changing Environment. *Frontiers in Plant Science* **7**. doi: 10.3389/fpls.2016.01123
- Perincherry, L., Stepien, Ł. & Vasudevan, S.E.**, 2021. Cross-Tolerance and Autoimmunity as Missing Links in Abiotic and Biotic Stress Responses in Plants: A Perspective toward Secondary Metabolic Engineering. *International Journal of Molecular Sciences* **22**(21): 11945. doi: 10.3390/ijms222111945
- Perrella, G., Bäurle, I. & Van Zanten, M.**, 2022. Epigenetic regulation of thermomorphogenesis and heat stress tolerance. *New Phytologist* **234**(4): 1144–1160. doi: 10.1111/nph.17970
- Pirasteh-Anosheh, H., Saed-Moucheshi, A., Pakniyat, H. & Pessarakli, M.**, 2016. Stomatal responses to drought stress. In: P. Ahmad (ed.): *Water Stress and Crop Plants*. John Wiley & Sons, Ltd (Chichester, UK): pp. 24–40. doi: 10.1002/9781119054450.ch3
- Pollastrini, M., Desotgiu, R., Camin, F., Ziller, L., Gerosa, G., Marzuoli, R. & Bussotti, F.**, 2014. Severe drought events increase the sensitivity to ozone on poplar clones. *Environmental and Experimental Botany* **100**: 94–104. doi: 10.1016/j.envexpbot.2013.12.016
- Postiglione, A.E. & Muday, G.K.**, 2023. Abscisic acid increases hydrogen peroxide in mitochondria to facilitate stomatal closure. *Plant Physiology* **192**(1): 469–487. doi: 10.1093/plphys/kiac601
- Praat, M., De Smet, I. & Van Zanten, M.**, 2021. Protein kinase and phosphatase control of plant temperature responses. *Journal of Experimental Botany* erab345. doi: 10.1093/jxb/erab345
- Pradhan, G.P., Prasad, P.V.V., Fritz, A.K., Kirkham, M.B. & Gill, B.S.**, 2012. Effects of drought and high temperature stress on synthetic hexaploid wheat. *Functional Plant Biology* **39**(3): 190. doi: 10.1071/FP11245
- Prasad, P.V.V., Pisipati, S.R., Momčilović, I. & Ristic, Z.**, 2011. Independent and Combined Effects of High Temperature and Drought Stress During Grain Filling on Plant Yield and Chloroplast EF-Tu Expression in Spring Wheat: Effects of Temperature and Drought on Wheat Plants. *Journal of Agronomy and Crop Science* **197**(6): 430–441. doi: 10.1111/j.1439-037X.2011.00477.x
- Prasch, C.M. & Sonnewald, U.**, 2013. Simultaneous Application of Heat, Drought, and Virus to *Arabidopsis* Plants Reveals Significant Shifts in Signaling Networks. *Plant Physiology* **162**(4): 1849–1866. doi: 10.1104/pp.113.221044
- Prasch, C.M. & Sonnewald, U.**, 2015. Signaling events in plants: Stress factors in combination change the picture. *Environmental and Experimental Botany* **114**: 4–14. doi: 10.1016/j.envexpbot.2014.06.020
- Praveen, A., Dubey, S., Singh, S. & Sharma, V.K.**, 2023. Abiotic stress tolerance in plants: a fascinating action of defense mechanisms. *3 Biotech* **13**(3): 102. doi: 10.1007/s13205-023-03519-w
- Prigge, M.J., Greenham, K., Zhang, Y., Santner, A., Castillejo, C., Mutka, A.M., O'Malley, R.C., Ecker, J.R., Kunkel, B.N. & Estelle, M.**, 2016. The *Arabidopsis* Auxin Receptor F-Box Proteins AFB4 and AFB5 Are Required for Response to the Synthetic Auxin Picloram. *G3 Genes|Genomes|Genetics* **6**(5): 1383–1390. doi: 10.1534/g3.115.025585
- Proveniers, M.C.G. & Van Zanten, M.**, 2013. High temperature acclimation through PIF4 signaling. *Trends in Plant Science* **18**(2): 59–64. doi: 10.1016/j.tplants.2012.09.002
- Pshybytko, N.L., Kruk, J., Kabashnikova, L.F. & Strzalka, K.**, 2008. Function of plastoquinone in heat stress reactions of plants. *Biochimica et Biophysica Acta (BBA) - Bioenergetics* **1777**(11): 1393–1399. doi: 10.1016/j.bbabi.2008.08.005
- Qamer, Z., Chaudhary, M.T., Du, X., Hinze, L. & Azhar, M.T.**, 2021. Review of oxidative stress and antioxidative defense mechanisms in *Gossypium hirsutum* L. in response to extreme abiotic conditions. *Journal of Cotton Research* **4**(1): 9. doi: 10.1186/s42397-021-00086-4
- Qi, M., Liu, X., Li, Y., Song, H., Yin, Z., Zhang, F., He, Q., Xu, Z. & Zhou, G.**, 2021. Photosynthetic resistance and resilience under drought, flooding and rewatering in maize plants. *Photosynthesis Research* **148**(1–2): 1–15. doi: 10.1007/s11120-021-00825-3
- Quint, M., Delker, C., Franklin, K.A., Wigge, P.A., Halliday, K.J. & van Zanten, M.**, 2016. Molecular and genetic control of plant thermomorphogenesis. *Nature Plants* **2**(1): 15190. doi: 10.1038/nplants.2015.190
- Rahikainen, M., Pascual, J., Alegre, S., Durian, G. & Kangasjärvi, S.**, 2016. PP2A Phosphatase as a Regulator of ROS Signaling in Plants. *Antioxidants* **5**(1): 8. doi: 10.3390/antiox5010008
- Rajhi, I., Yamauchi, T., Takahashi, H., Nishiuchi, S., Shiono, K., Watanabe, R., Mliki, A., Nagamura, Y., Tsutsumi, N., Nishizawa, N.K. & Nakazono, M.**, 2011. Identification of genes expressed in maize root cortical cells during lysigenous aerenchyma formation using laser microdissection and microarray analyses. *New Phytologist* **190**(2): 351–368. doi: 10.1111/j.1469-8137.2010.03535.x
- Rakusová, H., Gallego-Bartolomé, J., Vanstraelen, M., Robert, H.S., Alabadi, D., Blázquez, M.A., Benková, E. & Friml, J.**, 2011. Polarization of PIN3-dependent auxin transport for hypocotyl gravitropic response in *Arabidopsis thaliana*: PIN3 polarization for hypocotyl gravitropism. *The Plant Journal* **67**(5): 817–826. doi: 10.1111/j.1365-313X.2011.04636.x
- Ramakrishnan, M., Zhang, Z., Mullasser, S., Kalendar, R., Ahmad, Z., Sharma, A., Liu, G., Zhou, M. & Wei, Q.**, 2022. Epigenetic stress memory: A new approach to study cold and heat stress responses in plants. *Frontiers in Plant Science* **13**: 1075279. doi: 10.3389/fpls.2022.1075279
- Ramegowda, V., Gill, U.S., Sivalingam, P.N., Gupta, A., Gupta, C., Govind, G., Nataraja, K.N., Pereira, A., Udayakumar, M., Mysore, K.S. & Senthil-Kumar, M.**, 2017. GBF3 transcription factor imparts drought tolerance in *Arabidopsis thaliana*. *Scientific Reports* **7**(1): 9148. doi: 10.1038/s41598-017-09542-1
- Rampey, R.A., Woodward, A.W., Hobbs, B.N., Tierney, M.P., Lahner, B., Salt, D.E. & Bartel, B.**, 2006. An *Arabidopsis* Basic Helix-Loop-Helix Leucine Zipper Protein Modulates Metal Homeostasis and Auxin Conjugate Responsiveness. *Genetics* **174**(4): 1841–1857. doi: 10.1534/genetics.106.061044
- Rankenberg, T., Geldhof, B., van Veen, H., Holsteens, K., Van de Poel, B. & Sasidharan, R.**, 2021. Age-Dependent Abiotic Stress Resilience in Plants. *Trends in Plant Science* **26**(7): 692–705. doi: 10.1016/j.tplants.2020.12.016

- Rao, M.J., Xu, Y., Tang, X., Huang, Y., Liu, J., Deng, X. & Xu, Q.**, 2020. CsCYT75B1, a Citrus CYTOCHROME P450 Gene, Is Involved in Accumulation of Antioxidant Flavonoids and Induces Drought Tolerance in Transgenic Arabidopsis. *Antioxidants* **9**(2): 161. doi: 10.3390/antiox9020161
- Raschke, A., Ibañez, C., Ullrich, K.K., Anwer, M.U., Becker, S., Glöckner, A., Trenner, J., Denk, K., Saal, B., Sun, X., Ni, M., Davis, S.J., Delker, C. & Quint, M.**, 2015. Natural variants of ELF3 affect thermomorphogenesis by transcriptionally modulating PIF4-dependent auxin response genes. *BMC Plant Biology* **15**(1): 197. doi: 10.1186/s12870-015-0566-6
- Rasmussen, S., Barah, P., Suarez-Rodriguez, M.C., Bressendorff, S., Friis, P., Costantino, P., Bones, A.M., Nielsen, H.B. & Mundy, J.**, 2013. Transcriptome Responses to Combinations of Stresses in Arabidopsis. *Plant Physiology* **161**(4): 1783–1794. doi: 10.1104/pp.112.210773
- Rasool, N.**, 2023. Role of Plant Hormones in Mitigating Abiotic Stress. In: *Abiotic Stress in Plants - Adaptations to Climate Change* [Working Title]. IntechOpen. doi: 10.5772/intechopen.109983
- Raymond, C., Matthews, T. & Horton, R.M.**, 2020. The emergence of heat and humidity too severe for human tolerance. *Science Advances* **6**(19): eaaw1838. doi: 10.1126/sciadv.aaw1838
- Reed, J.W., Nagpal, P., Bastow, R.M., Solomon, K.S., Dowson-Day, M.J., Elumalai, R.P. & Millar, A.J.**, 2000. Independent Action of ELF3 and phyB to Control Hypocotyl Elongation and Flowering Time. *Plant Physiology* **122**(4): 1149–1160. doi: 10.1104/pp.122.4.1149
- Regulation of chloroplast development during the greening process**, 2020. Umeå University (Umeå).
- Reinelt, L., Whitaker, J., Kazakou, E., Bonnal, L., Bastianelli, D., Bullock, J.M. & Ostle, N.J.**, 2023. Drought effects on root and shoot traits and their decomposability. *Functional Ecology* **37**(4): 1044–1054. doi: 10.1111/1365-2435.14261
- Rejeb, I., Pastor, V. & Mauch-Mani, B.**, 2014. Plant Responses to Simultaneous Biotic and Abiotic Stress: Molecular Mechanisms. *Plants* **3**(4): 458–475. doi: 10.3390/plants3040458
- Ren, H., Wu, X., Zhao, W., Wang, Y., Sun, D., Gao, K. & Tang, W.**, 2022. Heat Shock-Induced Accumulation of the Glycogen Synthase Kinase 3-Like Kinase BRASSINOSTEROID INSENSITIVE 2 Promotes Early Flowering but Reduces Thermotolerance in Arabidopsis. *Frontiers in Plant Science* **13**: 838062. doi: 10.3389/fpls.2022.838062
- Reyes, J.C., Muro-Pastor, M.I. & Florencio, F.J.**, 2004. The GATA Family of Transcription Factors in Arabidopsis and Rice. *Plant Physiology* **134**(4): 1718–1732. doi: 10.1104/pp.103.037788
- Richter, A.S., Nägele, T., Grimm, B., Kaufmann, K., Schroda, M., Leister, D. & Kleine, T.**, 2023. Retrograde signaling in plants: A critical review focusing on the GUN pathway and beyond. *Plant Communications* **4**(1): 100511. doi: 10.1016/j.xplc.2022.100511
- Richter, R., Bastakis, E. & Schwechheimer, C.**, 2013. Cross-Repressive Interactions between SOC1 and the GATAs GNC and GNL/CGA1 in the Control of Greening, Cold Tolerance, and Flowering Time in Arabidopsis. *Plant Physiology* **162**(4): 1992–2004. doi: 10.1104/pp.113.219238
- Rillig, M.C., Ryo, M., Lehmann, A., Aguilar-Trigueros, C.A., Buchert, S., Wulf, A., Iwasaki, A., Roy, J. & Yang, G.**, 2019. The role of multiple global change factors in driving soil functions and microbial biodiversity. *Science* **366**(6467): 886–890. doi: 10.1126/science.aay2832
- Rivero, R.M., Mestre, T.C., Mittler, R., Rubio, F., Garcia-Sanchez, F. & Martinez, V.**, 2014. The combined effect of salinity and heat reveals a specific physiological, biochemical and molecular response in tomato plants: Stress combination in tomato plants. *Plant, Cell & Environment* **37**(5): 1059–1073. doi: 10.1111/pce.12199
- Rivero, R.M., Mittler, R., Blumwald, E. & Zandalinas, S.I.**, 2022. Developing climate-resilient crops: improving plant tolerance to stress combination. *The Plant Journal: For Cell and Molecular Biology* **109**(2): 373–389. doi: 10.1111/tbj.15483
- Rizhsky, L., Liang, H. & Mittler, R.**, 2002. The Combined Effect of Drought Stress and Heat Shock on Gene Expression in Tobacco. *Plant Physiology* **130**(3): 1143–1151. doi: 10.1104/pp.006858
- Rizhsky, L., Liang, H., Shuman, J., Shulaev, V., Davletova, S. & Mittler, R.**, 2004. When Defense Pathways Collide. The Response of Arabidopsis to a Combination of Drought and Heat Stress. *Plant Physiology* **134**(4): 1683–1696. doi: 10.1104/pp.103.033431
- Roberts, M.R.**, 2007. Does GABA Act as a Signal in Plants? Hints from Molecular Studies: Hints from Molecular Studies. *Plant Signaling & Behavior* **2**(5): 408–409. doi: 10.4161/psb.2.5.4335
- Rossatto, T., Souza, G.M., do Amaral, M.N., Auler, P.A., Pérez-Alonso, M.-M., Pollmann, S. & Braga, E.J.B.**, 2023. Cross-stress memory: Salt priming at vegetative growth stages improves tolerance to drought stress during grain-filling in rice plants. *Environmental and Experimental Botany* **206**: 105187. doi: 10.1016/j.envexpbot.2022.105187
- Ruckle, M.E., DeMarco, S.M. & Larkin, R.M.**, 2008. Plastid Signals Remodel Light Signaling Networks and Are Essential for Efficient Chloroplast Biogenesis in Arabidopsis. *The Plant Cell* **19**(12): 3944–3960. doi: 10.1105/tpc.107.054312
- Saab, I.N., Sharp, R.E., Pritchard, J. & Voetberg, G.S.**, 1990. Increased Endogenous Abscisic Acid Maintains Primary Root Growth and Inhibits Shoot Growth of Maize Seedlings at Low Water Potentials. *Plant Physiology* **93**(4): 1329–1336. doi: 10.1104/pp.93.4.1329
- Saddhe, A.A., Manuka, R. & Penna, S.**, 2021. Plant sugars: Homeostasis and transport under abiotic stress in plants. *Physiologia Plantarum* **171**(4): 739–755. doi: 10.1111/ppl.13283
- Sah, S.K., Reddy, K.R. & Li, J.**, 2016. Abscisic Acid and Abiotic Stress Tolerance in Crop Plants. *Frontiers in Plant Science* **7**. doi: 10.3389/fpls.2016.00571
- Sami, F., Yusuf, M., Faizan, M., Faraz, A. & Hayat, S.**, 2016. Role of sugars under abiotic stress. *Plant Physiology and Biochemistry* **109**: 54–61. doi: 10.1016/j.plaphy.2016.09.005
- Samperna, S., Boari, A., Vurro, M., Salzano, A.M., Reveglia, P., Evidente, A., Gismondi, A., Canini, A., Scaloni, A. & Marra, M.**, 2021. Arabidopsis Defense against the Pathogenic Fungus *Drechslera gigantea* Is Dependent on the Integrity of the Unfolded Protein Response. *Biomolecules* **11**(2): 240. doi: 10.3390/biom11020240
- Sang, Q., Fan, L., Liu, T., Qiu, Y., Du, J., Mo, B., Chen, M. & Chen, X.**, 2023. MicroRNA156 conditions auxin sensitivity to enable growth plasticity in response to environmental changes in Arabidopsis. *Nature Communications* **14**(1): 1449. doi: 10.1038/s41467-023-36774-9
- Saren, S., Budhlakoti, N., Mishra, K.K., Bharad, S., Potdukhe, N.R., Tyagi, B.S. & Singh, G.P.**, 2023. Resilience to Terminal Drought, Heat, and Their Combination Stress in Wheat Genotypes. *Agronomy* **13**(3): 891. doi: 10.3390/agronomy13030891
- Sarwat, M. (ed.)**, 2017. *Stress signaling in plants*. Volume 2. Springer (New York, NY: Heidelberg): 350 pp.
- Sasidharan, R., Hartman, S., Liu, Z., Martopawiro, S., Sajeev, N., van Veen, H., Yeung, E. & Voeselek, L.A.C.J.**, 2018. Signal Dynamics and Interactions during Flooding Stress. *Plant Physiology* **176**(2): 1106–1117. doi: 10.1104/pp.17.01232
- Sasidharan, R. & Voeselek, L.A.C.J.**, 2015. Ethylene-Mediated Acclimations to Flooding Stress. *Plant Physiology* **169**(1): 3–12. doi: 10.1104/pp.15.00387
- Sato, H., Suzuki, T., Takahashi, F., Shinozaki, K. & Yamaguchi-Shinozaki, K.**, 2019. NF-YB2 and NF-YB3 Have Functionally Diverged and Differentially Induce Drought and Heat Stress-Specific Genes. *Plant Physiology* **180**(3): 1677–1690. doi: 10.1104/pp.19.00391
- Sawers, R.J.H., Sheehan, M.J. & Brutnell, T.P.**, 2005. Cereal phytochromes: targets of selection, targets for manipulation? *Trends in Plant Science* **10**(3): 138–143. doi: 10.1016/j.tplants.2005.01.004
- Sazegari, S., Niazi, A. & Ahmadi, F.S.**, 2015. A study on the regulatory network with promoter analysis for Arabidopsis DREB-genes. *Biomedical Informatics*.

- Scharf, K.-D., Berberich, T., Ebersberger, I. & Nover, L.**, 2012. The plant heat stress transcription factor (Hsf) family: Structure, function and evolution. *Biochimica et Biophysica Acta (BBA) - Gene Regulatory Mechanisms* **1819**(2): 104–119. doi: 10.1016/j.bbagr.2011.10.002
- Schiermeier, Q.**, 2018. Droughts, heatwaves and floods: How to tell when climate change is to blame. *Nature* **560**(7716): 20–22. doi: 10.1038/d41586-018-05849-9
- Schulz, E., Tohge, T., Winkler, J.B., Albert, A., Schäffner, A.R., Fernie, A.R., Zuther, E. & Hinch, D.K.**, 2021. Natural Variation among Arabidopsis Accessions in the Regulation of Flavonoid Metabolism and Stress Gene Expression by Combined UV Radiation and Cold. *Plant and Cell Physiology* **62**(3): 502–514. doi: 10.1093/pcp/pcab013
- Schwenkert, S., Fernie, A.R., Geigenberger, P., Leister, D., Möhlmann, T., Naranjo, B. & Neuhaus, H.E.**, 2022. Chloroplasts are key players to cope with light and temperature stress. *Trends in Plant Science* **27**(6): 577–587. doi: 10.1016/j.tplants.2021.12.004
- Segarra-Medina, C., Alseekh, S., Fernie, A.R., Rambla, J.L., Pérez-Clemente, R.M., Gómez-Cádenas, A. & Zandalinas, S.I.**, 2023. Abscisic acid promotes plant acclimation to the combination of salinity and high light stress. *Plant Physiology and Biochemistry* **203**: 108008. doi: 10.1016/j.plaphy.2023.108008
- Seleiman, M.F., Al-Suhaibani, N., Ali, N., Akmal, M., Alotaibi, M., Refay, Y., Dindaroglu, T., Abdul-Wajid, H.H. & Battaglia, M.L.**, 2021. Drought Stress Impacts on Plants and Different Approaches to Alleviate Its Adverse Effects. *Plants* **10**(2): 259. doi: 10.3390/plants10020259
- Seo, P.J. & Park, C.-M.**, 2011. Signaling linkage between environmental stress resistance and leaf senescence in Arabidopsis. *Plant Signaling & Behavior* **6**(10): 1564–1566. doi: 10.4161/psb.6.10.17003
- Sewelam, N., Brilhaus, D., Bräutigam, A., Alseekh, S., Fernie, A.R. & Maurino, V.G.**, 2020. Molecular plant responses to combined abiotic stresses put a spotlight on unknown and abundant genes. *Journal of Experimental Botany* **71**(16): 5098–5112. doi: 10.1093/jxb/eraa250
- Shaar-Moshe, L., Blumwald, E. & Peleg, Z.**, 2017. Unique Physiological and Transcriptional Shifts under Combinations of Salinity, Drought, and Heat. *Plant Physiology* **174**(1): 421–434. doi: 10.1104/pp.17.00030
- Shabbir, R., Singhal, R.K., Mishra, U.N., Chauhan, J., Javed, T., Hussain, S., Kumar, S., Anuragi, H., Lal, D. & Chen, P.**, 2022. Combined Abiotic Stresses: Challenges and Potential for Crop Improvement. *Agronomy* **12**(11): 2795. doi: 10.3390/agronomy12112795
- Shannon, P., Markiel, A., Ozier, O., Baliga, N.S., Wang, J.T., Ramage, D., Amin, N., Schwikowski, B. & Ideker, T.**, 2003. Cytoscape: A Software Environment for Integrated Models of Biomolecular Interaction Networks. *Genome Research* **13**(11): 2498–2504. doi: 10.1101/gr.1239303
- Shao, H., Wang, H. & Tang, X.**, 2015. NAC transcription factors in plant multiple abiotic stress responses: progress and prospects. *Frontiers in Plant Science* **6**. doi: 10.3389/fpls.2015.00902
- Shapulatov, U., Van Zanten, M., Van Hoogdalem, M., Meisenburg, M., Van Hall, A., Kappers, I., Fasano, C., Facella, P., Loh, C.C., Perrella, G. & Van Der Krol, A.**, 2023. The Mediator complex subunit MED25 interacts with HDA9 and PIF4 to regulate thermomorphogenesis. *Plant Physiology* **192**(1): 582–600. doi: 10.1093/plphys/kiac581
- Sharma, P., Jha, A.B., Dubey, R.S. & Pessarakli, M.**, 2012. Reactive Oxygen Species, Oxidative Damage, and Antioxidative Defense Mechanism in Plants under Stressful Conditions. *Journal of Botany* **2012**: 1–26. doi: 10.1155/2012/217037
- Sharp, R.E. & LeNoble, M.E.**, 2002. ABA, ethylene and the control of shoot and root growth under water stress. *Journal of Experimental Botany* **53**(366): 33–37. doi: 10.1093/jexbot/53.366.33
- Shates, T.M., Sun, P., Malmstrom, C.M., Dominguez, C. & Mauck, K.E.**, 2019. Addressing Research Needs in the Field of Plant Virus Ecology by Defining Knowledge Gaps and Developing Wild Dicot Study Systems. *Frontiers in Microbiology* **9**: 3305. doi: 10.3389/fmicb.2018.03305
- Shelp, B.J., Aghdam, M.S. & Flaherty, E.J.**, 2021. γ -Aminobutyrate (GABA) Regulated Plant Defense: Mechanisms and Opportunities. *Plants* **10**(9): 1939. doi: 10.3390/plants10091939
- Shriram, V., Kumar, V., Devarumath, R.M., Khare, T.S. & Wani, S.H.**, 2016. MicroRNAs As Potential Targets for Abiotic Stress Tolerance in Plants. *Frontiers in Plant Science* **7**. doi: 10.3389/fpls.2016.00817
- Singh, A., Pandey, A., Srivastava, A.K., Tran, L.-S.P. & Pandey, G.K.**, 2016. Plant protein phosphatases 2C: from genomic diversity to functional multiplicity and importance in stress management. *Critical Reviews in Biotechnology* **36**(6): 1023–1035. doi: 10.3109/07388551.2015.1083941
- Sinha, K.V., Das, S.S. & Sanan-Mishra, N.**, 2021a. Overexpression of a RNA silencing suppressor, B2 protein encoded by Flock House virus, in tobacco plants results in tolerance to salt stress. *Phytoparasitica* **49**(2): 299–316. doi: 10.1007/s12600-020-00847-y
- Sinha, R., Fritschi, F.B., Zandalinas, S.I. & Mittler, R.**, 2021b. The impact of stress combination on reproductive processes in crops. *Plant Science* **311**: 111007. doi: 10.1016/j.plantsci.2021.111007
- Sinha, R., Induri, S.P., Peláez-Vico, M.Á., Tukuli, A., Shostak, B., Zandalinas, S.I., Joshi, T., Fritschi, F.B. & Mittler, R.**, 2023a. The transcriptome of soybean reproductive tissues subjected to water deficit, heat stress, and a combination of water deficit and heat stress. *The Plant Journal* **tpj.16222**. doi: 10.1111/tpj.16222
- Sinha, R., Shostak, B., Induri, S.P., Sen, S., Zandalinas, S.I., Joshi, T., Fritschi, F.B. & Mittler, R.**, 2023b. Differential transpiration between pods and leaves during stress combination in soybean. *Plant Physiology* **192**(2): 753–766. doi: 10.1093/plphys/kiad114
- Sinha, R., Zandalinas, S.I., Fichman, Y., Sen, S., Zeng, S., Gómez-Cadenas, A., Joshi, T., Fritschi, F.B. & Mittler, R.**, 2022. Differential regulation of flower transpiration during abiotic stress in annual plants. *New Phytologist* **235**(2): 611–629. doi: 10.1111/nph.18162
- Skubacz, A., Daszkowska-Golec, A. & Szarejko, I.**, 2016. The Role and Regulation of ABI5 (ABA-Insensitive 5) in Plant Development, Abiotic Stress Responses and Phytohormone Crosstalk. *Frontiers in Plant Science* **7**. doi: 10.3389/fpls.2016.01884
- Smit, M.E., McGregor, S.R., Sun, H., Gough, C., Bågman, A.-M., Soyars, C.L., Kroon, J.T., Gaudinier, A., Williams, C.J., Yang, X., Nimchuk, Z.L., Weijers, D., Turner, S.R., Brady, S.M. & Etchells, J.P.**, 2020. A PXY-Mediated Transcriptional Network Integrates Signaling Mechanisms to Control Vascular Development in Arabidopsis. *The Plant Cell* **32**(2): 319–335. doi: 10.1105/tpc.19.00562
- Soltabayeva, A., Dauletova, N., Serik, S., Sandybek, M., Omondi, J.O., Kurmanbayeva, A. & Srivastava, S.**, 2022. Receptor-like Kinases (LRR-RLKs) in Response of Plants to Biotic and Abiotic Stresses. *Plants* **11**(19): 2660. doi: 10.3390/plants11192660
- Son, S. & Park, S.R.**, 2023. Plant translational reprogramming for stress resilience. *Frontiers in Plant Science* **14**: 1151587. doi: 10.3389/fpls.2023.1151587
- Song, X.-J. & Matsuoka, M.**, 2009. Bar the windows: an optimized strategy to survive drought and salt adversities. *Genes & Development* **23**(15): 1709–1713. doi: 10.1101/gad.1834509
- Song, Y., Feng, L., Alyafei, M.A.M., Jaleel, A. & Ren, M.**, 2021. Function of Chloroplasts in Plant Stress Responses. *International Journal of Molecular Sciences* **22**(24): 13464. doi: 10.3390/ijms222413464
- Song, Y., Yang, C., Gao, S., Zhang, W., Li, L. & Kuai, B.**, 2014. Age-Triggered and Dark-Induced Leaf Senescence Require the bHLH Transcription Factors PIF3, 4, and 5. *Molecular Plant* **7**(12): 1776–1787. doi: 10.1093/mp/ssu109

- Spannagl, M., Mayer, K., Durner, J., Haberer, G. & Fröhlich, A.**, 2011. Exploring the genomes: From Arabidopsis to crops. *Journal of Plant Physiology* **168**(1): 3–8. doi: 10.1016/j.jplph.2010.07.008
- Sreenivasulu, N., Harshavardhan, V.T., Govind, G., Seiler, C. & Kohli, A.**, 2012. Contrapuntal role of ABA: Does it mediate stress tolerance or plant growth retardation under long-term drought stress? *Gene* **506**(2): 265–273. doi: 10.1016/j.gene.2012.06.076
- Stamm, P., Ravindran, P., Mohanty, B., Tan, E.L., Yu, H. & Kumar, P.P.**, 2012. Insights into the molecular mechanism of RGL2-mediated inhibition of seed germination in Arabidopsis thaliana. *BMC Plant Biology* **12**(1): 179. doi: 10.1186/1471-2229-12-179
- Stott, P.**, 2016. How climate change affects extreme weather events. *Science* **352**(6293): 1517–1518. doi: 10.1126/science.aaf7271
- Strader, L., Weijers, D. & Wagner, D.**, 2022. Plant transcription factors — being in the right place with the right company. *Current Opinion in Plant Biology* **65**: 102136. doi: 10.1016/j.pbi.2021.102136
- Suh, J.Y. & Kim, W.T.**, 2015. Arabidopsis RING E3 ubiquitin ligase AtATL80 is negatively involved in phosphate mobilization and cold stress response in sufficient phosphate growth conditions. *Biochemical and Biophysical Research Communications* **463**(4): 793–799. doi: 10.1016/j.bbrc.2015.06.015
- Sun, C., Ali, K., Yan, K., Fiaz, S., Dormatey, R., Bi, Z. & Bai, J.**, 2021. Exploration of Epigenetics for Improvement of Drought and Other Stress Resistance in Crops: A Review. *Plants* **10**(6): 1226. doi: 10.3390/plants10061226
- Sun, J., Qi, L., Li, Y., Chu, J. & Li, C.**, 2012. PIF4-Mediated Activation of YUCCA8 Expression Integrates Temperature into the Auxin Pathway in Regulating Arabidopsis Hypocotyl Growth. *PLoS Genetics* **8**(3): e1002594. doi: 10.1371/journal.pgen.1002594
- Sun, J., Qi, L., Li, Y., Zhai, Q. & Li, C.**, 2013a. PIF4 and PIF5 Transcription Factors Link Blue Light and Auxin to Regulate the Phototropic Response in Arabidopsis. *The Plant Cell* **25**(6): 2102–2114. doi: 10.1105/tpc.113.112417
- Sun, L., Lu, S.-J., Zhang, S.-S., Zhou, S.-F., Sun, L. & Liu, J.-X.**, 2013b. The Lumen-Facing Domain Is Important for the Biological Function and Organelle-to-Organelle Movement of bZIP28 during ER Stress in Arabidopsis. *Molecular Plant* **6**(5): 1605–1615. doi: 10.1093/mp/sst059
- Sunkar, R., Li, Y.-F. & Jagadeeswaran, G.**, 2012. Functions of microRNAs in plant stress responses. *Trends in Plant Science* **17**(4): 196–203. doi: 10.1016/j.tplants.2012.01.010
- Susila, H., Nasim, Z. & Ahn, J.**, 2018. Ambient Temperature-Responsive Mechanisms Coordinate Regulation of Flowering Time. *International Journal of Molecular Sciences* **19**(10): 3196. doi: 10.3390/ijms19103196
- Sutanto, S.J., Vitolo, C., Di Napoli, C., D'Andrea, M. & Van Lanen, H.A.J.**, 2020. Heatwaves, droughts, and fires: Exploring compound and cascading dry hazards at the pan-European scale. *Environment International* **134**: 105276. doi: 10.1016/j.envint.2019.105276
- Suzuki, N.**, 2016. Hormone signaling pathways under stress combinations. *Plant Signaling & Behavior* **11**(11): e1247139. doi: 10.1080/15592324.2016.1247139
- Suzuki, N., Bassil, E., Hamilton, J.S., Inupakutika, M.A., Zandalinas, S.I., Tripathy, D., Luo, Y., Dion, E., Fukui, G., Kumazaki, A., Nakano, R., Rivero, R.M., Verbeck, G.F., Azad, R.K., Blumwald, E. & Mittler, R.**, 2016a. ABA Is Required for Plant Acclimation to a Combination of Salt and Heat Stress. *PLOS ONE* **11**(1): e0147625. doi: 10.1371/journal.pone.0147625
- Suzuki, N., Bassil, E., Hamilton, J.S., Inupakutika, M.A., Zandalinas, S.I., Tripathy, D., Luo, Y., Dion, E., Fukui, G., Kumazaki, A., Nakano, R., Rivero, R.M., Verbeck, G.F., Azad, R.K., Blumwald, E. & Mittler, R.**, 2016b. ABA Is Required for Plant Acclimation to a Combination of Salt and Heat Stress. *PLOS ONE* **11**(1): e0147625. doi: 10.1371/journal.pone.0147625

- Suzuki, N., Bassil, E., Hamilton, J.S., Inupakutika, M.A., Zandalinas, S.I., Tripathy, D., Luo, Y., Dion, E., Fukui, G., Kumazaki, A., Nakano, R., Rivero, R.M., Verbeck, G.F., Azad, R.K., Blumwald, E. & Mittler, R.**, 2016c. ABA Is Required for Plant Acclimation to a Combination of Salt and Heat Stress. *PLOS ONE* **11**(1): e0147625. doi: 10.1371/journal.pone.0147625
- Suzuki, N., Koussevitzky, S., Mittler, R. & Miller, G.**, 2012. ROS and redox signalling in the response of plants to abiotic stress: ROS and redox signalling in plants. *Plant, Cell & Environment* **35**(2): 259–270. doi: 10.1111/j.1365-3040.2011.02336.x
- Suzuki, N., Rivero, R.M., Shulaev, V., Blumwald, E. & Mittler, R.**, 2014. Abiotic and biotic stress combinations. *New Phytologist* **203**(1): 32–43. doi: 10.1111/nph.12797
- Suzuki, N., Rizhsky, L., Liang, H., Shuman, J., Shulaev, V. & Mittler, R.**, 2005. Enhanced Tolerance to Environmental Stress in Transgenic Plants Expressing the Transcriptional Coactivator Multiprotein Bridging Factor 1c. *Plant Physiology* **139**(3): 1313–1322. doi: 10.1104/pp.105.070110
- Swiezewska, E.**, 2004. Ubiquinone and Plastoquinone Metabolism in Plants. In: *Methods in Enzymology*. Elsevier: Vol. 378, pp. 124–131. doi: 10.1016/S0076-6879(04)78007-6
- Takenaka, S., Yamamoto, R. & Nakamura, C.**, 2018. Genetic diversity of submergence stress response in cytoplasm of the Triticum-Aegilops complex. *Scientific Reports* **8**(1): 16267. doi: 10.1038/s41598-018-34682-3
- Tamang, B.G., Li, S., Rajasundaram, D., Lamichhane, S. & Fukao, T.**, 2021. Overlapping and stress-specific transcriptomic and hormonal responses to flooding and drought in soybean. *The Plant Journal* **107**(1): 100–117. doi: 10.1111/tpj.15276
- Tarahi Tabrizi, S., Sawicki, A., Zhou, S., Luo, M. & Willows, R.D.**, 2016. GUN4-Protoporphyrin IX Is a Singlet Oxygen Generator with Consequences for Plastid Retrograde Signaling. *Journal of Biological Chemistry* **291**(17): 8978–8984. doi: 10.1074/jbc.C116.719989
- Tasset, C., Singh Yadav, A., Sureshkumar, S., Singh, R., Van Der Woude, L., Nekrasov, M., Tremethick, D., Van Zanten, M. & Balasubramanian, S.**, 2018. POWERDRESS-mediated histone deacetylation is essential for thermomorphogenesis in Arabidopsis thaliana. *PLOS Genetics* **14**(3): e1007280. doi: 10.1371/journal.pgen.1007280
- Tatematsu, K., Kumagai, S., Muto, H., Sato, A. & Watahiki, M.K.**, 2004. MASSUGU2 Encodes Aux / IAA19, an Auxin-Regulated Protein That Functions Together with the Transcriptional Activator NPH4 / ARF7 to Regulate Differential Growth Responses of Hypocotyl and Formation of Lateral Roots in Arabidopsis thaliana. **16**(February): 379–393. doi: 10.1105/tpc.018630.elusive.
- Tax, F.E. & Vernon, D.M.**, 2001. T-DNA-Associated Duplication/Translocations in Arabidopsis. Implications for Mutant Analysis and Functional Genomics. *Plant Physiology* **126**(4): 1527–1538. doi: 10.1104/pp.126.4.1527
- Tian, F., Hu, X.-L., Yao, T., Yang, X., Chen, J.-G., Lu, M.-Z. & Zhang, J.**, 2021. Recent Advances in the Roles of HSFs and HSPs in Heat Stress Response in Woody Plants. *Frontiers in Plant Science* **12**: 704905. doi: 10.3389/fpls.2021.704905
- Tissot, N., Robe, K., Gao, F., Grant-Grant, S., Boucherez, J., Bellegarde, F., Maghiaoui, A., Marcelin, R., Izquierdo, E., Benhamed, M., Martin, A., Vignols, F., Roschttardt, H., Gaymard, F., Briat, J. & Dubos, C.**, 2019. Transcriptional integration of the responses to iron availability in Arabidopsis by the bHLH factor ILR3. *New Phytologist* **223**(3): 1433–1446. doi: 10.1111/nph.15753
- Toulotte, J.M., Pantazopoulou, C.K., Sanclemente, M.A., Voeselek, L.A. & Sasidharan, R.**, 2022. Water stress resilient cereal crops: lessons from wild relatives. *Journal of Integrative Plant Biology* **13**: 13222. doi: 10.1111/jipb.13222
- Tricker, P.J., ElHabt, A., Schmidt, J. & Fleury, D.**, 2018. The physiological and genetic basis of combined drought and heat tolerance in wheat. *Journal of Experimental Botany* **69**(13): 3195–3210. doi: 10.1093/jxb/ery081

- Tripathy, K.P., Mukherjee, S., Mishra, A.K., Mann, M.E. & Williams, A.P.**, 2023. Climate change will accelerate the high-end risk of compound drought and heatwave events. *Proceedings of the National Academy of Sciences* **120**(28): e2219825120. doi: 10.1073/pnas.2219825120
- Tuteja, N.**, 2007a. Abscisic Acid and Abiotic Stress Signaling. *Plant Signaling & Behavior* **2**(3): 135–138. doi: 10.4161/psb.2.3.4156
- Tuteja, N.**, 2007b. Abscisic Acid and Abiotic Stress Signaling. *Plant Signaling & Behavior* **2**(3): 135–138. doi: 10.4161/psb.2.3.4156
- Van Der Woude, L., Piotrowski, M., Klaasse, G., Paulus, J.K., Krahn, D., Ninck, S., Kaschani, F., Kaiser, M., Novák, O., Ljung, K., Bulder, S., Van Verk, M., Snoek, B.L., Fiers, M., Martin, N.I., Van Der Hoorn, R.A.L., Robert, S., Smeekens, S. & Van Zanten, M.**, 2021. The chemical compound ‘Heatin’ stimulates hypocotyl elongation and interferes with the Arabidopsis NIT1-subfamily of nitrilases. *The Plant Journal* **106**(6): 1523–1540. doi: 10.1111/tpj.15250
- Van Der Woude, L.C., Perrella, G., Snoek, B.L., Van Hoogdalem, M., Novák, O., Van Verk, M.C., Van Kooten, H.N., Zorn, L.E., Tonckens, R., Dongus, J.A., Praat, M., Stouten, E.A., Proveniers, M.C.G., Vellutini, E., Patitaki, E., Shapulatov, U., Kohlen, W., Balasubramanian, S., Ljung, K., Van Der Krol, A.R., Smeekens, S., Kaiserli, E. & Van Zanten, M.**, 2019. HISTONE DEACETYLASE 9 stimulates auxin-dependent thermomorphogenesis in Arabidopsis thaliana by mediating H2A.Z depletion. *Proceedings of the National Academy of Sciences* **116**(50): 25343–25354. doi: 10.1073/pnas.1911694116
- Van Dooren, T.J.M., Silveira, A.B., Gilbault, E., Jiménez-Gómez, J.M., Martin, A., Bach, L., Tisné, S., Quadrana, L., Loudet, O. & Colot, V.**, 2020. Mild drought in the vegetative stage induces phenotypic, gene expression, and DNA methylation plasticity in Arabidopsis but no transgenerational effects. *Journal of Experimental Botany* **71**(12): 3588–3602. doi: 10.1093/jxb/eraa132
- Van Veen, H., Mustroph, A., Barding, G.A., Vergeer-van Eijk, M., Welschen-Evertman, R.A.M., Pedersen, O., Visser, E.J.W., Larive, C.K., Pierik, R., Bailey-Serres, J., Voeselek, L.A.C.J. & Sasidharan, R.**, 2013. Two Rumex Species from Contrasting Hydrological Niches Regulate Flooding Tolerance through Distinct Mechanisms. *The Plant Cell* **25**(11): 4691–4707. doi: 10.1105/tpc.113.119016
- Van Veen, H., Vashisht, D., Akman, M., Girke, T., Mustroph, A., Reinen, E., Hartman, S., Kooiker, M., Van Tienderen, P., Schranz, M.E., Bailey-Serres, J., Voeselek, L.A.C.J. & Sasidharan, R.**, 2016. Transcriptomes of eight Arabidopsis thaliana accessions reveal core conserved, genotype- and organ-specific responses to flooding stress. *Plant Physiology* pp.00472.2016. doi: 10.1104/pp.16.00472
- Van Wyk, S.G., Du Plessis, M., Cullis, C.A., Kunert, K.J. & Vorster, B.J.**, 2014. Cysteine protease and cystatin expression and activity during soybean nodule development and senescence. *BMC Plant Biology* **14**(1): 294. doi: 10.1186/s12870-014-0294-3
- Van Zanten, M., Bours, R., Pons, T.L. & Proveniers, M.C.G.**, 2013. Plant acclimation and adaptation to warm environments. In: K.A. Franklin & P.A. Wigge (eds.): *Temperature and Plant Development*. John Wiley & Sons, Inc (Oxford): pp. 49–78. doi: 10.1002/9781118308240.ch3
- Vashisht, D., Hesselink, A., Pierik, R., Ammerlaan, J.M.H., Bailey-Serres, J., Visser, E.J.W., Pedersen, O., Van Zanten, M., Vreugdenhil, D., Jamar, D.C.L., Voeselek, L.A.C.J. & Sasidharan, R.**, 2011. Natural variation of submergence tolerance among Arabidopsis thaliana accessions. *New Phytologist* **190**(2): 299–310. doi: 10.1111/j.1469-8137.2010.03552.x
- Veciana, N., Martín, G., Leivar, P. & Monte, E.**, 2022a. BBX16 mediates the repression of seedling photomorphogenesis downstream of the GUN1/GLK1 module during retrograde signalling. *New Phytologist* **234**(1): 93–106. doi: 10.1111/nph.17975
- Veciana, N., Martín, G., Leivar, P. & Monte, E.**, 2022b. BBX16 mediates the repression of seedling photomorphogenesis downstream of the GUN1/GLK1 module during retrograde signalling. *New Phytologist* **234**(1): 93–106. doi: 10.1111/nph.17975
- Verelst, W., Bertolini, E., De Bodt, S., Vandepoele, K., Demeulenaere, M., Enrico Pè, M. & Inzé, D.**, 2013. Molecular and Physiological Analysis of Growth-Limiting Drought Stress in Brachypodium distachyon Leaves. *Molecular Plant* **6**(2): 311–322. doi: 10.1093/mp/sss098
- Verhoeven, A., Kloth, K.J., Kupczok, A., Oymans, G.H., Damen, J., Rijnsburger, K., Jiang, Z., Deelen, C., Sasidharan, R., van Zanten, M. & van der Vlugt, R.A.A.**, 2023. Arabidopsis latent virus 1, a comovirus widely spread in Arabidopsis thaliana collections. *New Phytologist* **237**(4): 1146–1153. doi: 10.1111/nph.18466
- Verma, V., Ravindran, P. & Kumar, P.P.**, 2016. Plant hormone-mediated regulation of stress responses. *BMC Plant Biology* **16**(1): 86. doi: 10.1186/s12870-016-0771-y
- Violet-Chabrand, S. & Lawson, T.**, 2020. Thermography methods to assess stomatal behaviour in a dynamic environment. *Journal of Experimental Botany* **71**(7): 2329–2338. doi: 10.1093/jxb/erz573
- Vile, D., Pervent, M., Belluau, M., Vasseur, F., Bresson, J., Muller, B., Granier, C. & Simonneau, T.**, 2012. Arabidopsis growth under prolonged high temperature and water deficit: independent or interactive effects?: Plant responses to high temperature and water deficit. *Plant, Cell & Environment* **35**(4): 702–718. doi: 10.1111/j.1365-3040.2011.02445.x
- Villalba-Bermell, P., Marquez-Molins, J., Marques, M.-C., Hernandez-Azurdia, A.G., Corell-Sierra, J., Picó, B., Monforte, A.J., Elena, S.F. & Gomez, G.G.**, 2021. Combined Stress Conditions in Melon Induce Non-additive Effects in the Core miRNA Regulatory Network. *Frontiers in Plant Science* **12**: 769093. doi: 10.3389/fpls.2021.769093
- Vives-Peris, V., López-Climent, M.F., Pérez-Clemente, R.M. & Gómez-Cadenas, A.**, 2020. Root Involvement in Plant Responses to Adverse Environmental Conditions. *Agronomy* **10**(7): 942. doi: 10.3390/agronomy10070942
- Voeselek, L.A.C.J.**, 2003. Interactions Between Plant Hormones Regulate Submergence-induced Shoot Elongation in the Flooding-tolerant Dicot Rumex palustris. *Annals of Botany* **91**(2): 205–211. doi: 10.1093/aob/mcf116
- Voeselek, L.A.C.J. & Bailey-Serres, J.**, 2015. Flood adaptive traits and processes: an overview. *New Phytologist* **206**(1): 57–73. doi: 10.1111/nph.13209
- Volodarsky, D., Leviatan, N., Otcheretianski, A. & Fluhr, R.**, 2009. HORMONOMETER: A Tool for Discerning Transcript Signatures of Hormone Action in the Arabidopsis Transcriptome. *Plant Physiology* **150**(4): 1796–1805. doi: 10.1104/pp.109.138289
- Vu, L.D., Xu, X., Gevaert, K. & De Smet, I.**, 2019. Developmental Plasticity at High Temperature. *Plant Physiology* **181**(2): 399–411. doi: 10.1104/pp.19.00652
- Wahab, A., Abdi, G., Saleem, M.H., Ali, B., Ullah, S., Shah, W., Mumtaz, S., Yasin, G., Muresan, C.C. & Marc, R.A.**, 2022. Plants’ Physio-Biochemical and Phyto-Hormonal Responses to Alleviate the Adverse Effects of Drought Stress: A Comprehensive Review. *Plants* **11**(13): 1620. doi: 10.3390/plants11131620
- Waidmann, S., Sarkel, E. & Kleine-Vehn, J.**, 2020. Same same, but different: growth responses of primary and lateral roots. *Journal of Experimental Botany* **71**(8): 2397–2411. doi: 10.1093/jxb/eraa027
- Walter, J., Jentsch, A., Beierkuhnlein, C. & Kreyling, J.**, 2013. Ecological stress memory and cross stress tolerance in plants in the face of climate extremes. *Environmental and Experimental Botany* **94**: 3–8. doi: 10.1016/j.envexpbot.2012.02.009
- Wang, T., Huang, S., Zhang, A., Guo, P., Liu, Y., Xu, C., Cong, W., Liu, B. & Xu, Z.**, 2021. JM17–WRKY40 and HY5–ABI5 modules regulate the expression of ABA-responsive genes in Arabidopsis. *New Phytologist* **230**(2): 567–584. doi: 10.1111/nph.17177

- Wang, Y., Selinski, J., Mao, C., Zhu, Y., Berkowitz, O. & Whelan, J.**, 2020. Linking mitochondrial and chloroplast retrograde signalling in plants. *Philosophical Transactions of the Royal Society B: Biological Sciences* **375**(1801): 20190410. doi: 10.1098/rstb.2019.0410
- Wani, S.H., Kumar, V., Shriram, V. & Sah, S.K.**, 2016. Phytohormones and their metabolic engineering for abiotic stress tolerance in crop plants. *The Crop Journal* **4**(3): 162–176. doi: 10.1016/j.cj.2016.01.010
- Waters, M.T., Moylan, E.C. & Langdale, J.A.**, 2008. GLK transcription factors regulate chloroplast development in a cell-autonomous manner. 432–444. doi: 10.1111/j.1365-313X.2008.03616.x
- Waters, M.T., Wang, P., Korkaric, M., Capper, R.G., Saunders, N.J. & Langdale, J.A.**, 2009. GLK Transcription Factors Coordinate Expression of the Photosynthetic Apparatus in Arabidopsis. *The Plant Cell* **21**(4): 1109–1128. doi: 10.1105/tpc.108.065250
- Welchen, E., Canal, M.V., Gras, D.E. & Gonzalez, D.H.**, 2021. Cross-talk between mitochondrial function, growth, and stress signalling pathways in plants. *Journal of Experimental Botany* **72**(11): 4102–4118. doi: 10.1093/jxb/eraa608
- Wickham, H.**, 2009. ggplot2: Elegant Graphics for Data Analysis. Springer New York (New York, NY). doi: 10.1007/978-0-387-98141-3
- Winkel, A., Pedersen, O., Ella, E., Ismail, A.M. & Colmer, T.D.**, 2014. Gas film retention and underwater photosynthesis during field submergence of four contrasting rice genotypes. *Journal of Experimental Botany* **65**(12): 3225–3233. doi: 10.1093/jxb/eru166
- Wright, S.T.C. & Hiron, R.W.P.**, 1972. The Accumulation of Abscisic Acid in Plants During Wilting and Under Other Stress Conditions. In: D.J. Carr (ed.): *Plant Growth Substances 1970*. Springer Berlin Heidelberg (Berlin, Heidelberg): pp. 291–298. doi: 10.1007/978-3-642-65406-0_39
- Wu, G., Zhang, C., Chu, L.-Y. & Shao, H.-B.**, 2007. Responses of higher plants to abiotic stresses and agricultural sustainable development. *Journal of Plant Interactions* **2**(3): 135–147. doi: 10.1080/17429140701586357
- Wu, G.-Z., Chalvin, C., Hoelscher, M., Meyer, E.H., Wu, X.N. & Bock, R.**, 2018. Control of Retrograde Signaling by Rapid Turnover of GENOMES UNCOUPLED1. *Plant Physiology* **176**(3): 2472–2495. doi: 10.1104/pp.18.00009
- Xu, J., Hou, Q.-M., Khare, T., Verma, S.K. & Kumar, V.**, 2019. Exploring miRNAs for developing climate-resilient crops: A perspective review. *Science of The Total Environment* **653**: 91–104. doi: 10.1016/j.scitotenv.2018.10.340
- Xu, W., Jia, L., Shi, W., Liang, J., Zhou, F., Li, Q. & Zhang, J.**, 2013. Abscisic acid accumulation modulates auxin transport in the root tip to enhance proton secretion for maintaining root growth under moderate water stress. *New Phytologist* **197**(1): 139–150. doi: 10.1111/nph.12004
- Yamaguchi, N., Matsubara, S., Yoshimizu, K., Seki, M., Hamada, K., Kamitani, M., Kurita, Y., Nomura, Y., Nagashima, K., Inagaki, S., Suzuki, T., Gan, E.-S., To, T., Kakutani, T., Nagano, A.J., Satake, A. & Ito, T.**, 2021. H3K27me3 demethylases alter HSP22 and HSP17.6C expression in response to recurring heat in Arabidopsis. *Nature Communications* **12**(1): 3480. doi: 10.1038/s41467-021-23766-w
- Yamauchi, T., Shimamura, S., Nakazono, M. & Mochizuki, T.**, 2013. Aerenchyma formation in crop species: A review. *Field Crops Research* **152**: 8–16. doi: 10.1016/j.fcr.2012.12.008
- Yang, D.-H., Andersson, B., Aro, E.-M. & Ohad, I.**, 2001. The redox state of the plastoquinone pool controls the level of the light-harvesting chlorophyll a/b binding protein complex II (LHC II) during photoacclimation. *Photosynthesis Research* **68**(2): 163–174. doi: 10.1023/A:1011849919438
- Yang, S.-D., Seo, P.J., Yoon, H.-K. & Park, C.-M.**, 2011. The Arabidopsis NAC Transcription Factor VNI2 Integrates Abscisic Acid Signals into Leaf Senescence via the COR / RD Genes. *The Plant Cell* **23**(6): 2155–2168. doi: 10.1105/tpc.111.084913
- Yang, X., Wang, J., Mao, X., Li, C., Li, L., Xue, Y., He, L. & Jing, R.**, 2022a. A Locus Controlling Leaf Rolling Degree in Wheat under Drought Stress Identified by Bulk Segregant Analysis. *Plants* **11**(16): 2076. doi: 10.3390/plants11162076
- Yang, X., Zhu, X., Wei, J., Li, W., Wang, H., Xu, Y., Yang, Z., Xu, C. & Li, P.**, 2022b. Primary root response to combined drought and heat stress is regulated via salicylic acid metabolism in maize. *BMC Plant Biology* **22**(1): 417. doi: 10.1186/s12870-022-03805-4
- Yasir, T.A., Wasaya, A., Hussain, M., Ijaz, M., Farooq, M., Farooq, O., Nawaz, A. & Hu, Y.-G.**, 2019. Evaluation of physiological markers for assessing drought tolerance and yield potential in bread wheat. *Physiology and Molecular Biology of Plants* **25**(5): 1163–1174. doi: 10.1007/s12298-019-00694-0
- Yasuda, M., Ishikawa, A., Jikumaru, Y., Seki, M., Umezawa, T., Asami, T., Maruyama-Nakashita, A., Kudo, T., Shinozaki, K., Yoshida, S. & Nakashita, H.**, 2008. Antagonistic Interaction between Systemic Acquired Resistance and the Abscisic Acid-Mediated Abiotic Stress Response in Arabidopsis. *The Plant Cell* **20**(6): 1678–1692. doi: 10.1105/tpc.107.054296
- Ye, N., Wang, Y., Yu, H., Qin, Z., Zhang, J., Duan, M. & Liu, L.**, 2023. Abscisic Acid Enhances Trehalose Content via OsTPP3 to Improve Salt Tolerance in Rice Seedlings. *Plants* **12**(14): 2665. doi: 10.3390/plants12142665
- Yeung, E., Bailey-Serres, J. & Sasidharan, R.**, 2019. After The Deluge: Plant Revival Post-Flooding. *Trends in Plant Science* **24**(5): 443–454. doi: 10.1016/j.tplants.2019.02.007
- Yeung, E., van Veen, H., Vashisht, D., Sobral Paiva, A.L., Hummel, M., Rankenberg, T., Steffens, B., Steffen-Heins, A., Sauter, M., de Vries, M., Schuurink, R.C., Bazin, J., Bailey-Serres, J., Voeselek, L.A.C.J. & Sasidharan, R.**, 2018. A stress recovery signaling network for enhanced flooding tolerance in Arabidopsis thaliana. *Proceedings of the National Academy of Sciences* **115**(26). doi: 10.1073/pnas.1803841115
- Yeung, E.Y.-L.**, 2018. Molecular mechanisms mediating post-submergence recovery in Arabidopsis thaliana.
- Yong, B., Xie, H., Li, Z., Li, Y.-P., Zhang, Y., Nie, G., Zhang, X.-Q., Ma, X., Huang, L.-K., Yan, Y.-H. & Peng, Y.**, 2017. Exogenous Application of GABA Improves PEG-Induced Drought Tolerance Positively Associated with GABA-Shunt, Polyamines, and Proline Metabolism in White Clover. *Frontiers in Physiology* **8**: 1107. doi: 10.3389/fphys.2017.01107
- Yoo, C.Y., Han, S. & Chen, M.**, 2020. Nucleus-to-Plastid Phytochrome Signalling in Controlling Chloroplast Biogenesis. In: J.A. Roberts (ed.): *Annual Plant Reviews online*. Wiley: 1st ed., pp. 251–280. doi: 10.1002/9781119312994.apr0615
- Yoo, C.Y., Pasorek, E.K., Wang, H., Cao, J., Blaha, G.M., Weigel, D. & Chen, M.**, 2019. Phytochrome activates the plastid-encoded RNA polymerase for chloroplast biogenesis via nucleus-to-plastid signaling. *Nature Communications* **10**(1): 2629. doi: 10.1038/s41467-019-10518-0
- Yoon, Y., Seo, D.H., Shin, H., Kim, H.J., Kim, C.M. & Jang, G.**, 2020. The Role of Stress-Responsive Transcription Factors in Modulating Abiotic Stress Tolerance in Plants. *Agronomy* **10**(6): 788. doi: 10.3390/agronomy10060788
- Yoshida, Y., Sarmiento-Mañú, R., Yamori, W., Ponce, M.R., Micol, J.L. & Tsukaya, H.**, 2018. The Arabidopsis phyB-9 Mutant Has a Second-Site Mutation in the VENOSA4 Gene That Alters Chloroplast Size, Photosynthetic Traits, and Leaf Growth. *Plant Physiology* **178**(1): 3–6. doi: 10.1104/pp.18.00764
- Yu, W., Wang, L., Zhao, R., Sheng, J., Zhang, S., Li, R. & Shen, L.**, 2019. Knockout of SIMAPK3 enhances tolerance to heat stress involving ROS homeostasis in tomato plants. *BMC Plant Biology* **19**(1): 354. doi: 10.1186/s12870-019-1939-z

- Yu, X., Li, L., Li, L., Guo, M., Chory, J. & Yin, Y.**, 2008. Modulation of brassinosteroid-regulated gene expression by jumonji domain-containing proteins ELF6 and REF6 in Arabidopsis. *Proceedings of the National Academy of Sciences* **105**(21): 7618–7623. doi: 10.1073/pnas.0802254105
- Yuan, H., Zhao, L., Guo, W., Yu, Y., Tao, L., Zhang, L., Song, X., Huang, W., Cheng, L., Chen, J., Guan, F., Wu, G. & Li, H.**, 2019. Exogenous Application of Phytohormones Promotes Growth and Regulates Expression of Wood Formation-Related Genes in *Populus simonii* × *P. nigra*. *International Journal of Molecular Sciences* **20**(3): 792. doi: 10.3390/ijms20030792
- Yuan, L., Chen, M., Wang, L., Sasidharan, R., Voeselek, L.A.C.J. & Xiao, S.**, 2023a. Multi-stress resilience in plants recovering from submergence. *Plant Biotechnology Journal* **21**(3): 466–481. doi: 10.1111/pbi.13944
- Yuan, L., Chen, M., Wang, L., Sasidharan, R., Voeselek, L.A.C.J. & Xiao, S.**, 2023b. Multi-stress resilience in plants recovering from submergence. *Plant Biotechnology Journal* **21**(3): 466–481. doi: 10.1111/pbi.13944
- Zandalinas, S.I., Balfagón, D., Arbona, V. & Gómez-Cadenas, A.**, 2017a. Modulation of Antioxidant Defense System Is Associated with Combined Drought and Heat Stress Tolerance in Citrus. *Frontiers in Plant Science* **8**: 953. doi: 10.3389/fpls.2017.00953
- Zandalinas, S.I., Balfagón, D., Arbona, V., Gómez-Cadenas, A., Inupakutika, M.A. & Mittler, R.**, 2016a. ABA is required for the accumulation of APX1 and MBF1c during a combination of water deficit and heat stress. *Journal of Experimental Botany* **67**(18): 5381–5390. doi: 10.1093/jxb/erw299
- Zandalinas, S.I., Balfagón, D., Gómez-Cadenas, A. & Mittler, R.**, 2022a. Plant responses to climate change: metabolic changes under combined abiotic stresses. *Journal of Experimental Botany* **73**(11): 3339–3354. doi: 10.1093/jxb/erac073
- Zandalinas, S.I., Balfagón, D., Gómez-Cadenas, A. & Mittler, R.**, 2022b. Plant responses to climate change: metabolic changes under combined abiotic stresses. *Journal of Experimental Botany* **73**(11): 3339–3354. doi: 10.1093/jxb/erac073
- Zandalinas, S.I., Fichman, Y., Devireddy, A.R., Sengupta, S., Azad, R.K. & Mittler, R.**, 2020a. Systemic signaling during abiotic stress combination in plants. *Proceedings of the National Academy of Sciences* **117**(24): 13810–13820. doi: 10.1073/pnas.2005077117
- Zandalinas, S.I., Fritsch, F.B. & Mittler, R.**, 2020b. Signal transduction networks during stress combination. *Journal of Experimental Botany* **71**(5): 1734–1741. doi: 10.1093/jxb/erz486
- Zandalinas, S.I., Fritsch, F.B. & Mittler, R.**, 2021a. Global Warming, Climate Change, and Environmental Pollution: Recipe for a Multifactorial Stress Combination Disaster. *Trends in Plant Science* **26**(6): 588–599. doi: 10.1016/j.tplants.2021.02.011
- Zandalinas, S.I. & Mittler, R.**, 2022. Plant responses to multifactorial stress combination. *New Phytologist* **234**(4): 1161–1167. doi: 10.1111/nph.18087
- Zandalinas, S.I., Mittler, R., Balfagón, D., Arbona, V. & Gómez-Cadenas, A.**, 2018. Plant adaptations to the combination of drought and high temperatures. *Physiologia Plantarum* **162**(1): 2–12. doi: 10.1111/ppl.12540
- Zandalinas, S.I., Rivero, R.M., Martínez, V., Gómez-Cadenas, A. & Arbona, V.**, 2016b. Tolerance of citrus plants to the combination of high temperatures and drought is associated to the increase in transpiration modulated by a reduction in abscisic acid levels. *BMC Plant Biology* **16**(1): 105. doi: 10.1186/s12870-016-0791-7
- Zandalinas, S.I., Sales, C., Beltrán, J., Gómez-Cadenas, A. & Arbona, V.**, 2017b. Activation of Secondary Metabolism in Citrus Plants Is Associated to Sensitivity to Combined Drought and High Temperatures. *Frontiers in Plant Science* **7**. doi: 10.3389/fpls.2016.01954
- Zandalinas, S.I., Sengupta, S., Fritsch, F.B., Azad, R.K., Nechushtai, R. & Mittler, R.**, 2021b. The impact of multifactorial stress combination on plant growth and survival. *New Phytologist* **230**(3): 1034–1048. doi: 10.1111/nph.17232

- Zha, P., Jing, Y., Xu, G. & Lin, R.**, 2017. PICKLE chromatin-remodeling factor controls thermosensory hypocotyl growth of Arabidopsis. *Plant, Cell & Environment* **40**(10): 2426–2436. doi: 10.1111/pce.13049
- Zhang, H., Gannon, L., Hassall, K.L., Deery, M.J., Gibbs, D.J., Holdsworth, M.J., Van Der Hoorn, R.A.L., Lilley, K.S. & Theodoulou, F.L.**, 2018. N-terminomics reveals control of Arabidopsis seed storage proteins and proteases by the Arg/N-end rule pathway. *New Phytologist* **218**(3): 1106–1126. doi: 10.1111/nph.14909
- Zhang, H. & Sonnewald, U.**, 2017. Differences and commonalities of plant responses to single and combined stresses. *The Plant Journal* **90**(5): 839–855. doi: 10.1111/tpj.13557
- Zhang, H., Zhao, Y. & Zhu, J.-K.**, 2020a. Thriving under Stress: How Plants Balance Growth and the Stress Response. *Developmental Cell* **55**(5): 529–543. doi: 10.1016/j.devcel.2020.10.012
- Zhang, H., Zhu, J., Gong, Z. & Zhu, J.-K.**, 2022a. Abiotic stress responses in plants. *Nature Reviews Genetics* **23**(2): 104–119. doi: 10.1038/s41576-021-00413-0
- Zhang, H., Zhu, J., Gong, Z. & Zhu, J.-K.**, 2022b. Abiotic stress responses in plants. *Nature Reviews Genetics* **23**(2): 104–119. doi: 10.1038/s41576-021-00413-0
- Zhang, J., Jia, W., Yang, J. & Ismail, A.M.**, 2006. Role of ABA in integrating plant responses to drought and salt stresses. *Field Crops Research* **97**(1): 111–119. doi: 10.1016/j.fcr.2005.08.018
- Zhang, J., Vrieling, K., Klinkhamer, P.G.L. & Bezemer, T.M.**, 2021a. Exogenous application of plant defense hormones alters the effects of live soils on plant performance. *Basic and Applied Ecology* **56**: 144–155. doi: 10.1016/j.baae.2021.07.011
- Zhang, J. & Zhang, X.**, 1994. Can early wilting of old leaves account for much of the ABA accumulation in flooded pea plants? *Journal of Experimental Botany* **45**(9): 1335–1342. doi: 10.1093/jxb/45.9.1335
- Zhang, K., Sun, Y., Li, M. & Long, R.**, 2021b. CrUGT87A1, a UDP-sugar glycosyltransferase (UGTs) gene from *Carex rigescens*, increases salt tolerance by accumulating flavonoids for antioxidation in Arabidopsis thaliana. *Plant Physiology and Biochemistry* **159**: 28–36. doi: 10.1016/j.plaphy.2020.12.006
- Zhang, Q., Yuan, W., Wang, Q., Cao, Y., Xu, F., Dodd, I.C. & Xu, W.**, 2022c. ABA regulation of root growth during soil drying and recovery can involve auxin response. *Plant, Cell & Environment* **45**(3): 871–883. doi: 10.1111/pce.14137
- Zhang, Y., Li, Y., Hassan, M.J., Li, Z. & Peng, Y.**, 2020b. Indole-3-acetic acid improves drought tolerance of white clover via activating auxin, abscisic acid and jasmonic acid related genes and inhibiting senescence genes. *BMC Plant Biology* **20**(1): 150. doi: 10.1186/s12870-020-02354-y
- Zhang, Y., Luan, Q., Jiang, J. & Li, Y.**, 2021c. Prediction and Utilization of Malondialdehyde in Exotic Pine Under Drought Stress Using Near-Infrared Spectroscopy. *Frontiers in Plant Science* **12**: 735275. doi: 10.3389/fpls.2021.735275
- Zhang, Y., Zhang, A., Li, X. & Lu, C.**, 2020c. The Role of Chloroplast Gene Expression in Plant Responses to Environmental Stress. *International Journal of Molecular Sciences* **21**(17): 6082. doi: 10.3390/ijms21176082
- Zhao, F., Zhang, D., Zhao, Y., Wang, W., Yang, H., Tai, F., Li, C. & Hu, X.**, 2016a. The Difference of Physiological and Proteomic Changes in Maize Leaves Adaptation to Drought, Heat, and Combined Both Stresses. *Frontiers in Plant Science* **7**. doi: 10.3389/fpls.2016.01471
- Zhao, H., Nie, K., Zhou, H., Yan, X., Zhan, Q., Zheng, Y. & Song, C.**, 2020a. ABI5 modulates seed germination via feedback regulation of the expression of the PYR/PYL/RCAR ABA receptor genes. *New Phytologist* **228**(2): 596–608. doi: 10.1111/nph.16713
- Zhao, H., Wu, D., Kong, F., Lin, K., Zhang, H. & Li, G.**, 2017. The Arabidopsis thaliana Nuclear Factor Y Transcription Factors. *Frontiers in Plant Science* **07**. doi: 10.3389/fpls.2016.02045

- Zhao, J., Lu, Z., Wang, L. & Jin, B.**, 2020b. Plant Responses to Heat Stress: Physiology, Transcription, Noncoding RNAs, and Epigenetics. *International Journal of Molecular Sciences* **22**(1): 117. doi: 10.3390/ijms22010117
- Zhao, Q., Li, M., Jia, Z., Liu, F., Ma, H., Huang, Y. & Song, S.**, 2016b. AtMYB44 Positively Regulates the Enhanced Elongation of Primary Roots Induced by N⁻³-Oxo-Hexanoyl-Homoserine Lactone in *Arabidopsis thaliana*. *Molecular Plant-Microbe Interactions* **29**(10): 774–785. doi: 10.1094/MPMI-03-16-0063-R
- Zhao, S., Zhang, Q., Liu, M., Zhou, H., Ma, C. & Wang, P.**, 2021a. Regulation of Plant Responses to Salt Stress. *International Journal of Molecular Sciences* **22**(9): 4609. doi: 10.3390/ijms22094609
- Zhao, X., Huang, J. & Chory, J.**, 2019a. GUN1 interacts with MORF2 to regulate plastid RNA editing during retrograde signaling. *Proceedings of the National Academy of Sciences* **116**(20): 10162–10167. doi: 10.1073/pnas.1820426116
- Zhao, Y., Chan, Z., Gao, J., Xing, L., Cao, M., Yu, C., Hu, Y., You, J., Shi, H., Zhu, Y., Gong, Y., Mu, Z., Wang, H., Deng, X., Wang, P., Bressan, R.A. & Zhu, J.-K.**, 2016c. ABA receptor PYL9 promotes drought resistance and leaf senescence. *Proceedings of the National Academy of Sciences* **113**(7): 1949–1954. doi: 10.1073/pnas.1522840113
- Zhao, Y., Jiang, T., Li, L., Zhang, X., Yang, T., Liu, C., Chu, J. & Zheng, B.**, 2021b. The chromatin remodeling complex imitation of switch controls stamen filament elongation by promoting jasmonic acid biosynthesis in *Arabidopsis*. *Journal of Genetics and Genomics* **48**(2): 123–133. doi: 10.1016/j.jgg.2021.02.003
- Zhao, Y., Qiang, C., Wang, X., Chen, Y., Deng, J., Jiang, C., Sun, X., Chen, H., Li, J., Piao, W., Zhu, X., Zhang, Z., Zhang, H., Li, Z. & Li, J.**, 2019b. New alleles for chlorophyll content and stay-green traits revealed by a genome wide association study in rice (*Oryza sativa*). *Scientific Reports* **9**(1): 2541. doi: 10.1038/s41598-019-39280-5
- Zheng, Y., Wang, X., Cui, X., Wang, K., Wang, Y. & He, Y.**, 2023. Phytohormones regulate the abiotic stress: An overview of physiological, biochemical, and molecular responses in horticultural crops. *Frontiers in Plant Science* **13**: 1095363. doi: 10.3389/fpls.2022.1095363
- Zhou, R., Yu, X., Ottosen, C.-O., Rosenqvist, E., Zhao, L., Wang, Y., Yu, W., Zhao, T. & Wu, Z.**, 2017. Drought stress had a predominant effect over heat stress on three tomato cultivars subjected to combined stress. *BMC Plant Biology* **17**(1): 24. doi: 10.1186/s12870-017-0974-x
- Zhou, R., Yu, X., Ottosen, C.-O., Zhang, T., Wu, Z. & Zhao, T.**, 2020. Unique miRNAs and their targets in tomato leaf responding to combined drought and heat stress. *BMC Plant Biology* **20**(1): 107. doi: 10.1186/s12870-020-2313-x
- Zhou, Y., Zhou, B., Pache, L., Chang, M., Khodabakhshi, A.H., Tanaseichuk, O., Benner, C. & Chanda, S.K.**, 2019. Metascape provides a biologist-oriented resource for the analysis of systems-level datasets. *Nature Communications* **10**(1): 1523. doi: 10.1038/s41467-019-09234-6
- Zhu, J.-K.**, 2002. SALT AND DROUGHT STRESS SIGNAL TRANSDUCTION IN PLANTS. *Annual Review of Plant Biology* **53**(1): 247–273. doi: 10.1146/annurev.arplant.53.091401.143329
- Zhu, J.-K.**, 2016. Abiotic stress signaling and responses in plants. *Cell* **167**(2): 313–324. doi: 10.1016/j.cell.2016.08.029
- Zhu, L., Wen, W., Thorpe, M.R., Hocart, C.H. & Song, X.**, 2021a. Combining Heat Stress with Pre-Existing Drought Exacerbated the Effects on Chlorophyll Fluorescence Rise Kinetics in Four Contrasting Plant Species. *International Journal of Molecular Sciences* **22**(19): 10682. doi: 10.3390/ijms221910682
- Zhu, Q., Feng, Y., Xue, J., Chen, P., Zhang, A. & Yu, Y.**, 2023. Advances in Receptor-like Protein Kinases in Balancing Plant Growth and Stress Responses. *Plants* **12**(3): 427. doi: 10.3390/plants12030427
- Zhu, T., Fonseca De Lima, C.F. & De Smet, I.**, 2021b. The heat is on: how crop growth, development, and yield respond to high temperature. *Journal of Experimental Botany* erab308. doi: 10.1093/jxb/erab308
- Zhu, T., Van Zanten, M. & De Smet, I.**, 2022a. Wandering between hot and cold: temperature dose-dependent responses. *Trends in Plant Science* **27**(11): 1124–1133. doi: 10.1016/j.tplants.2022.06.001
- Zhu, T., Zou, L., Li, Y., Yao, X., Xu, F., Deng, X., Zhang, D. & Lin, H.**, 2018. Mitochondrial alternative oxidase-dependent autophagy involved in ethylene-mediated drought tolerance in *Solanum lycopersicum*. *Plant Biotechnology Journal* **16**(12): 2063–2076. doi: 10.1111/pbi.12939
- Zhu, Z., Wang, J., Li, C., Li, L., Mao, X., Hu, G., Wang, J., Chang, J. & Jing, R.**, 2022b. A transcription factor TaMYB5 modulates leaf rolling in wheat. *Frontiers in Plant Science* **13**: 897623. doi: 10.3389/fpls.2022.897623
- Zhuang, J., Wang, Y., Chi, Y., Zhou, L., Chen, J., Zhou, W., Song, J., Zhao, N. & Ding, J.**, 2020. Drought stress strengthens the link between chlorophyll fluorescence parameters and photosynthetic traits. *PeerJ* **8**: e10046. doi: 10.7717/peerj.10046
- Zhuang, Y., Wei, M., Ling, C., Liu, Y., Amin, A.K., Li, P., Li, P., Hu, X., Bao, H., Huo, H., Smalle, J. & Wang, S.**, 2021. EGY3 mediates chloroplastic ROS homeostasis and promotes retrograde signaling in response to salt stress in *Arabidopsis*. *Cell Reports* **36**(2): 109384. doi: 10.1016/j.celrep.2021.109384
- Ziemer, P.**, 2008. Die Bedeutung der GRAS-Proteine für die Entwicklung von Pflanzen untersucht am Modellorganismus *Arabidopsis thaliana*.
- Zioutopoulou, A., Patitaki, E., Xu, T. & Kaiserli, E.**, 2021. The Epigenetic Mechanisms Underlying Thermomorphogenesis and Heat Stress Responses in *Arabidopsis*. *Plants* **10**(11): 2439. doi: 10.3390/plants10112439
- Zou, C., Sun, K., Mackaluso, J.D., Seddon, A.E., Jin, R., Thomashow, M.F. & Shiu, S.-H.**, 2011. Cis-regulatory code of stress-responsive transcription in *Arabidopsis thaliana*. *Proceedings of the National Academy of Sciences* **108**(36): 14992–14997. doi: 10.1073/pnas.1103202108
- Zou, Y., Zhang, Y. & Testerink, C.**, 2022. Root dynamic growth strategies in response to salinity. *Plant, Cell & Environment* **45**(3): 695–704. doi: 10.1111/pce.14205
- Zubo, Y.O., Blakley, I.C., Franco-Zorrilla, J.M., Yamburenko, M.V., Solano, R., Kieber, J.J., Loraine, A.E. & Schaller, G.E.**, 2018. Coordination of Chloroplast Development through the Action of the GNC and GLK Transcription Factor Families. *Plant Physiology* **178**(1): 130–147. doi: 10.1104/pp.18.00414

Layman summary

Climate change is causing more frequent heat waves, droughts, and flooding events. These weather extremes are considered major threats to global food and feed production, which is already under pressure to keep up with the demand of the growing and more affluent human population. Therefore, improving the ability of plants to withstand these abiotic stresses is essential for ensuring food security.

Plants growing in the field cannot escape from harsh environmental conditions. To survive these stresses, plants must induce certain traits that allow better performance in these circumstances. This process is known as 'acclimation'. Acclimation responses are controlled by complex molecular signaling networks (e.g., changes in expression of many genes). In the past few decades, mechanisms underlying plant acclimation to diverse abiotic stresses have been extensively studied by researchers. However, abiotic stresses in nature often occur simultaneously or sequentially, rather than in isolation. For instance, high temperature often co-occurs with droughts, and droughts are followed by flooding events. Stress combinations often elicit distinct acclimation responses compared to those imposed by individual stresses. Our current understanding of how plants cope with combinatorial abiotic stresses is still scarce.

Abiotic stresses in agricultural settings are usually milder than those used in experimental laboratory studies. However, even subtle environmental shifts can prompt a multitude of effects in some sensitive plant species, including *Arabidopsis thaliana*, the most commonly used model species in plant research. Taken together, it is crucial to understand the acclimation strategies to mild combinatorial abiotic stresses.

The goal of this thesis was to uncover how *Arabidopsis* plants cope with the co-occurrence of abiotic stresses at a mild severity. My work focused on two stress combinations; i) simultaneously occurring high ambient temperature and drought and ii) flooding followed by drought. Both are relevant in nature and in an agricultural context and have already - and will further increase - in their frequency due to climate change. The knowledge obtained by my work can potentially contribute to the development of next-generation crops with enhanced resilience to multiple (combinatorial) abiotic stresses.

Chapter 2 describes *Arabidopsis* traits that respond to combined and sequential abiotic stresses. It was observed that stress combinations in general compound their effects on plant growth, development and physiology, compared to the corresponding individual stresses. This chapter also presents the experimental setup that is used for

investigating the underlying (molecular) basis of the observed traits in the subsequent chapters.

In Chapter 3 we measured global changes in gene expression using a transcriptomics approach, to potentially explain the observed differences between the responses to combinatorial and the corresponding single stresses. Combined or sequential stresses resulted in changes in the expression of different genes than observed under the corresponding individual stresses. These genes are likely responsible for specific biological processes relevant to combined stress responses, such as the communication between plastids and nucleus (i.e., retrograde signaling), and abscisic acid (ABA) signaling.

Of the identified candidate genes, transcription factors (TFs) that increased in their expression during combinatorial stresses were deemed the most interesting for further investigation. TFs are master regulators responsible for inducing and repressing transcription of downstream target genes. In Chapter 4 we analyzed the response of mutants of a selection of identified candidate TFs, under combined stress conditions. We uncovered important roles for some of these TFs in controlling typical plant traits that were relevant to plant growth, development, and survival under combinatorial stresses. Of all tested TFs, EARLY FLOWERING 6 (ELF6) and ARABIDOPSIS DOPSIS TOXICOS EN LEVADURA 80 (ATL80), together with the plant hormone ABA, are considered master regulators contributing to the acclimation responses to combined and/or sequential abiotic stresses.

Because the transcriptomics data pointed to the involvement of chloroplasts in the response to high temperatures, Chapter 5 zoomed in on the role of GOLDEN2-LIKE 2 (GLK2), a TF responsible for chloroplast development and the expression of photosynthesis-related genes encoded in the nucleus, under high-temperature conditions. Likely, GLK2 participates in negatively controlling *Arabidopsis* high-temperature responses, independent of a well-studied retrograde signaling pathway mediated by GENOMES UNCOUPLED 1 (GUN1). Yet, it is still ambiguous whether GLK2 regulates high-temperature responses through the manipulation of the phytohormone auxin, marking a direction for future exploration.

To summarize, the findings presented in this thesis provide novel insights into the strategies plants adopt to cope with combinatorial abiotic stresses that occur either simultaneously or sequentially, at a mild severity. My findings can contribute to the development of crops with enhanced resilience to multiple environmental stressors, which is increasingly important in the context of climate change.

Samenvatting

Door klimaatverandering komen hittegolven, periodes van droogte en overstromingen steeds vaker voor. Deze weersextremen vormen een grote bedreiging voor de wereldwijde voedsel- en voederproductie, die al onder druk staat om aan de vraag van de groeiende en welvarende wereldbevolking te voldoen. Daarom is het verbeteren van het vermogen van planten om abiotische stress te weerstaan essentieel om voedselzekerheid te kunnen garanderen.

Planten kunnen niet weglopen van stressvolle situaties. Om te kunnen overleven moeten planten bepaalde eigenschappen ontwikkelen om zich aan te passen. Dit proces staat bekend als 'acclimatisatie'. Acclimatisatieresponsen worden gecontroleerd door complexe moleculaire signaaltransductienetwerken (bijv. veranderingen in de expressie van vele genen). In de afgelopen decennia hebben onderzoekers de mechanismen die aan de basis liggen van acclimatisatie van planten uitgebreid bestudeerd. In de natuur komen abiotische stressfactoren echter vaak gelijktijdig of opeenvolgend voor, in plaats van geïsoleerd. Hoge temperaturen komen bijvoorbeeld vaak voor in combinatie met droogte en periodes van droogte worden regelmatig gevolgd door overstromingen. Een combinatie van stressen leidt vaak tot andere reacties van de plant dan wanneer de plant slechts één stress tegelijk ervaart. Ons huidige begrip van hoe planten omgaan met combinaties van abiotische stress is echter nog steeds beperkt.

In de landbouwcontext is de stress die planten ervaren meestal milder dan de stress die gebruikt wordt in experimentele laboratoriumstudies. Maar zelfs subtiele veranderingen in de omgeving kunnen een veelheid aan effecten teweegbrengen in sommige gevoelige plantensoorten, waaronder *Arabidopsis thaliana*, de meest gebruikte modelsoort in plantenonderzoek. Kortom, het is cruciaal om strategieën die planten gebruiken om aan te passen aan combinaties van milde abiotische stress te begrijpen.

Het doel van het onderzoek beschreven in dit proefschrift was om te ontdekken hoe *Arabidopsis* planten omgaan met combinaties van milde abiotische stress. Mijn werk richtte zich op twee stresscombinaties: i) gelijktijdig optredende hoge omgevingstemperatuur en droogte en ii) overstroming gevolgd door droogte. Beide zijn relevant in de natuur en in een landbouwcontext en komen vaker voor als gevolg van klimaatverandering. De kennis die door mijn werk is verkregen kan bijdragen aan de ontwikkeling van gewassen met een verbeterde weerbaarheid tegen meervoudige (combinatorische) abiotische stress.

Hoofdstuk 2 beschrijft hoe *Arabidopsis* planten reageren op combinaties van milde abiotische stress. Er wordt beschreven dat effecten op plantengroei, -ontwikkeling en

-fysiologie worden versterkt wanneer stressen zijn gecombineerd in vergelijking met de corresponderende individuele stressoren. Dit hoofdstuk presenteert ook de experimentele opzet die gebruikt is voor het onderzoeken van de onderliggende (moleculaire) basis van de waargenomen veranderingen in de plant in de volgende hoofdstukken.

In hoofdstuk 3 beschrijven we hoe we grootschalig genexpressie hebben gemeten met behulp van een transcriptomics-benadering, met als doel om de waargenomen verschillen in de reactie op gecombineerde en individuele stressoren te verklaren. Wanneer stressen werden gecombineerd traden er andere veranderingen in de expressie van genen op dan wanneer stressen individueel werden toegediend. Deze genen zijn waarschijnlijk verantwoordelijk voor specifieke biologische processen die relevant zijn voor gecombineerde stressresponsen, zoals de communicatie tussen plastiden en celkern (d.w.z. retrograde signalering) en de signalering van het plantenhormoon Abscisinezuur (ABA).

Transcriptiefactoren waarvan de expressie toenam tijdens gecombineerde stress werden het meest interessant geacht voor verder onderzoek. Transcriptiefactoren reguleren namelijk het aanzetten en onderdrukken van de expressie van andere genen en spelen dus een centrale rol in biologische processen. In hoofdstuk 4 analyseren we mutanten van een selectie van geïdentificeerde transcriptiefactoren onder gecombineerde stresscondities. We ontdekten dat sommige van deze transcriptiefactoren een belangrijke rol spelen in het controleren van groei, ontwikkeling en overleving van planten wanneer deze zijn blootgesteld aan gecombineerde stress. Van alle geteste transcriptiefactoren worden EARLY FLOWERING 6 (ELF6) en ARABIDOPSIS DOPSIS TOXICOS EN LEVADURA 80 (ATL80), samen met het plantenhormoon ABA, beschouwd als regulatoren die bijdragen aan de acclimatisatieresponsen op gecombineerde abiotische stress.

Omdat de transcriptomics gegevens wezen op de betrokkenheid van chloroplasten in de reactie van planten op hoge temperaturen, wordt in hoofdstuk 5 ingezoomd op de rol van de GOLDEN2-LIKE 2 (GLK2), een transcriptiefactor die verantwoordelijk is voor de ontwikkeling van chloroplasten en de expressie van fotosynthese-gerelateerde genen die gecodeerd zijn in de celkern wanneer de plant hoge temperatuur ervaart. Het is aannemelijk dat GLK2 responsen van *Arabidopsis* op hoge temperaturen onderdrukt, onafhankelijk van een goed bestudeerde retrograde signaaltransductieroute die onder invloed staat van GENOMES UNCOUPLED 1 (GUN1). Het is nog onduidelijk of GLK2 de reactie op hoge temperatuur stuurt via het fytohormoon auxine. Dit zal toekomstig onderzoek moeten uitwijzen.

摘要

气候变化正加剧着高温、干旱和洪涝灾害的频发。这些极端的气候灾害被认为是威胁全球粮食和饲料生产的主要因素，而目前来看粮食和饲料生产已然难以满足日益增长的人口所带来的超额需求。因此，提高植物抗逆能力对于保障粮食安全和产量至关重要。

野生植物没有办法逃避环境胁迫带给它们的负面影响。为了使自己能在逆境中存活，植物会不断地改变自身的表型，而这个过程即所谓的“适应性”。适应性反应由复杂的分子信号网络进行调控（例如一些基因表达水平的变化）。在过去的几十年里，研究人员已就调控植物适应各种非生物逆境胁迫的机制进行了深入研究。然而在自然界和野外条件下这些非生物胁迫往往同时或接连发生，而不是单一出现。比如高温胁迫经常与干旱共存，而干旱之后往往伴随洪涝的频发。这些多重逆境胁迫引发的植物适应性反应往往与单一胁迫所带来的不尽相同，而我们对于植物如何应对多重胁迫的理解却又少之又少。

一般发生在自然和野外环境下的非生物胁迫往往比实验研究中模拟的胁迫要温和许多。但即使是这样温和的胁迫也足以让一些对环境变化敏感的植物物种造成巨大影响，这其中就包括在植物学研究中最常用到的模型植物拟南芥(*Arabidopsis thaliana*)。总之，理解植物如何适应温和程度的非生物胁迫是非常重要的。

本篇论文的目的在于揭示拟南芥如何应对温和程度的多重非生物胁迫。本研究主要针对两种多重非生物胁迫进行研究：一，同时发生的高温和干旱的胁迫，二，洪涝之后接连出现干旱的胁迫。这两种情况在野外和农业种植中都很常见，并且由于气候变化，它们出现的频率已然在不断地增加。本研究所得结论可助力于开发能够抵御多重非生物胁迫的新型作物。

本文第二章阐述了拟南芥在同时和连续发生的非生物胁迫下的响应特征。与单一胁迫相比，多重胁迫通常会在植物生长、发育和生理学层面上产生更大的影响。本章还构建了适用于在后续章节进一步研究适应性反应的分子机制的实验体系。

在第三章中，我们使用转录组学方法研究了基因表达的整体变化，该研究能用以解释植物在响应多重胁迫和单一胁迫时的特征性差异。相较于单一胁迫，同时或连续发生的非生物胁迫会诱使一些特定基因的表达。这基因的表达会影响植物中某些特定生物学过程的进行，比如质体和核之间的信息交流（即逆向信号传导）以及脱落酸（ABA）信号传导。

在所筛选出的特定基因中，那些在多重胁迫中高度表达的转录因子(TFs)被认为是最值得进一步研究的对象。转录因子是负责调控下游目的基因转录的重要调节因子。在第四章中，我们研究了在多重胁迫条件下一些突变体（缺少目标转录因子表达的拟南芥植株）的适应性反应。我们发现一些转录因子在控制植物生长、发育和在多重胁迫下生存率等

方面起到重要作用。在所筛选和测试的转录因子中，EARLY FLOWERING 6 (ELF6) ARABIDOPSIS DOPSIS TOXICOS EN LEVADURA 80 (ATL80) 以及脱落酸被认为是对同时和/或连续发生的非生物胁迫的适应性反应起重要作用的因子。

由于转录组学的数据表明叶绿体参与了植物对高温的适应性反应，于是在第五章里，我们深入地探讨了GOLDEN2-LIKE 2 (GLK2) 在高温中起到的调控作用。GLK2 是一种植物转录因子，其负责调控叶绿体的发育以及调控细胞核所编码的光合作用相关基因的表达。GLK2 调控植物高温的适应性反应独立于由 GENOMES UNCOUPLED 1 (GUN1) 介导的逆向信号传导。然而，我们依然不清楚GLK2 是否通过调控生长素来调节高温适应性反应，而这意味着未来我们会在这一领域进行进一步的探索。

综上所述，本文对植物如何策略性地适应较为温和的多重非生物胁迫提供了研究和一些新的见解。我们的研究结论可帮助研发具有抵御不同环境胁迫能力的作物，而这在气候变化的大背景下显得尤为重要。

Acknowledgments

I still remember the day I arrived in Utrecht five years ago, feeling a bit worried as a complete freshman and not knowing if I was welcome or if I could handle everything by myself. I began with almost nothing - no plans for my life, no friends, and (almost) no furniture in my apartment. Now, I have friends and furniture but still no clear plans. Looking back, I see my growth - in the first year of my PhD, I used to call my parents and cried over the failure of my experiments, but later, I learnt to manage stress by setting the failures aside for a few days and enjoying coffee and spicy gossip with friends. So, first and foremost, I'd like to express gratitude to myself for making great progress and being still alive. Congratulations JZ, you survived your PhD, Arabidopsis Latent Virus 1 (ArLV1), coronavirus, and the phytotron drama while still being young and shiny. Of course, I appreciate those who provided me with companionship along the journey.

I'd like to thank my supervisors, Rashmi and Martijn. It's been a great time working with you both. Rashmi, you are such a professional and supportive supervisor. I sometimes made fun of you by calling you 'old', but what I really meant was that you are as patient and wise as the elderly. Martijn, thank you for being so helpful and supportive over the years! You always provided me with encouragement and informative (and quick) feedback. I would also like to express my gratitude to Rens and Sjef for their generous help and guidance throughout my PhD adventure.

I'd like to thank everyone in PSR and/or the flooding team for being amazing colleagues! Nora, thank you for offering me the opportunity to work with you! I'm excited to go on this new adventure! Moe, I admire your passion for work (which I lack), and I think that's what makes you a great scientist. Dorota, I was honestly impressed by the work you presented during your first work discussion. I believe you will make great contribution to the UU plant community. Ava, I couldn't have survived my PhD without your help! We've been working together for so long, and I'm very proud of you for making ArLV1 so impactful! Evelien, you are always the person I turned to when I needed help, thank you for always being patient and providing support! Melissa, your creativity and dedication to work are impressive. I believe you will soon get what you desire and deserve. Natalia, I will miss sitting next to you in O201! We understand each other because both of us have experienced the pain of phenotyping! Angelica, I miss going out for drinks and movies with you and the girls. I wish you all the best in your future career! Zeguang, I really appreciate your help and encouragement at the start of my PhD! Sjon, I still don't understand how you managed to defeat my six Pokemons with just one when we played the Pokémon game together. Justine, I am happy that you enjoyed the (non-spicy) hotpot dinner! It was fun to talk about life with you. Hans,

I appreciate your help in the RNA-seq analysis, and I wish you and Joe the best of luck in Groningen. Tom, I'm honored to witness your PhD defence as your paranymph. I really admire your intelligence and calmness. Myrthe, it is a pleasure to work with you on the collaboration project and also in the EPS PhD council. I enjoyed complaining about life with you during coffee time. Gyöngyi, I'm curious how much energy you have! You're a wonderful colleague who never hides true feelings and always shows kindness to everyone. Erbil, it's great to have you in PSR, and I wish you all the best with the rest of your PhD. Elmar, good luck with your PhD project with Gyöngyi! I am sure you will do an excellent job. Joy, I am excited to start working with you soon! Viktoria, thanks for your yummy cookies! It's so nice to have you as our officemate in O201. Osama, welcome to O201 and I hope you enjoy your stay in PSR!

Of the people in ECPD/PES, I'd want to first thank all the PIs: Ronald, Kaisa, Daan, and Andrés, thank you for providing invaluable suggestions and feedback during work discussions. Also, many thanks to my former officemates in Z309: Lisa, we should keep doing our bubble-tea gossip more often! Thanks for always being there when I was depressed and needed to talk. Sara, I miss sitting in Z309 with you and eating Haribo together. Thank you for being helpful all the time! Leo, congratulations on the amazing ggPlantmap! I still remember the days that we both suffered from lab work and the Dutch language course. Mariana, thank you for being my gym and gossiping buddy during COVID! I am so proud of you for your new position in Wageningen! Chrysa, we always consider you an (additional) officemate, I wish you and Giannis all the best in Greece! I would like to thank all of the PES/MPF technicians for their great assistance in the lab and phytotron: Diederik, Sara, Muthanna, Yorrit, Liao (nice to have you back in UU), Emilie, Tuğba, Ankie and Jolanda. Many thanks also to the current and former PhDs and postdocs: Pierre, Nicole, Sanne, Kyra, Gabriele, Viktoria, Siddhant, Rianne, Lucila, Martina, Jesse, Kasper, Valérie, Sarah, Yaron, and Putri! I'd like to particularly thank Alejandro for guiding me through the multi-stress project and providing valuable advice!

I want to thank all of the students who assisted me with my PhD project: Yihong, Romy, and Elias! I couldn't have accomplished my PhD without the help from all of you! I'd also like to thank all of the collaborators: René from Wageningen University & Research, and Ive and Xiangyu from Ghent University/VIB; it's a pleasure working with you all!

Next, I'd like to thank my wonderful Chinese friends in the Netherlands: Linge, Hao, Xin, Guan, and Guang. Linge, I'm lucky to start my PhD at the same time as you. I enjoy having lunch with you in the food court and complaining about life. Hao, we should definitely play Steam games together and have coffee more regularly. You have a

fantastic personality that is incredibly influential! Xin, you always took care of me like my older brother, I appreciate the companionship from you and Gert during the past five years. Guan and Guang, if I lived in Enkhuizen, I'd come to visit you every day and stay with Liya and Lisa. Thank you for always inviting me to dinner!

I'd like to give special thanks to my best friends, Shitao and Tong. Thank you for always being patient, tolerant, and encouraging. I know I'm not a very nice person to get along with, yet you never left me alone when I needed companionship. I also want to thank my parents for their support for all of the decisions I made, no matter how ridiculous they were. Dad, you are such a non-traditional Chinese father as you always tell me how much you love me. Mom, even though we sometimes do not understand each other, I know you love me more than all your luxurious bags. In my heart, you are the best parents in the world!

I also have a few words for my grandma who brought me up: it's been more than twelve years since you left, and I missed you much. I sometimes wondered why you never came into my dream. I think the answer is that you did not want to bother me as you always cared for my feelings and spoiled me when I was a child. Thank you, grandma, for everything you did for me.

Last but not least, I'd like to express my gratitude to Junfeng. As I always said, life is difficult. But my life would not be any better without you.

Curriculum Vitae

Zhang Jiang (蒋章) was born on August 27th, 1992 in Changchun, China. After graduating from High School Attached to Northeast Normal University (东北师范大学附属中学) in 2011, he moved to Jilin University (吉林大学) to pursue his bachelor's degree in biotechnology. In 2015, he finished his bachelor's study and started his MSc program at the same university. During his master's time, he investigated how environmental factors affect the accumulation of plant secondary metabolites, under the supervision of Prof. Xia Chen. After completing his MSc project, he came to the Netherlands for his PhD at Utrecht University in 2018. There he studied the mechanisms underlying plant responses to combined and sequential abiotic stresses under the supervision of Prof. Rashmi Sasidharan and Dr. Martijn van Zanten. The results of his PhD work are presented in this thesis.

List of publications

De Smet, I., Xu, X., Praat, M., Pizzio, G., **Jiang, Z.**, Driever, S., Wang, R., De Cotte, B.V., Villers, S., Gevaert, K., Leonhardt, N., Nelissen, H., Kinoshita, T., Vanneste, S., Rodriguez, P., Zanten, M.V., Vu, L., 2023. A conserved signaling axis integrates conflicting environmental drought and heat signals to control stomatal aperture in plants (Preprint). In Review (2023).

Verhoeven, A.; Kloth, K. J.; Kupczok, A.; Oymans, G. H.; Damen, J.; Rijnsburger, K.; **Jiang, Z.**; Deelen, C.; Sasidharan, R.; van Zanten, M.; van der Vlugt, R. A. A. Arabidopsis Latent Virus 1, a Comovirus Widely Spread in Arabidopsis Thaliana Collections. *New Phytologist* 2023, 237 (4), 1146–1153.

Morales, A.; de Boer, H. J.; Douma, J. C.; Elsen, S.; Engels, S.; Glimmerveen, T.; Sajeev, N.; Huber, M.; Luimes, M.; Luitjens, E.; Raatjes, K.; Hsieh, C.; Teapal, J.; Wildenbeest, T.; **Jiang, Z.**; Pareek, A.; Singla-Pareek, S.; Yin, X.; Evers, J.; Anten, N. P. R.; van Zanten, M.; Sasidharan, R. Effects of Sublethal Single, Simultaneous and Sequential Abiotic Stresses on Phenotypic Traits of Arabidopsis Thaliana. *AoB PLANTS* 2022, 14 (4), plac029.

Tang, M.; Zhao, W.; Xing, M.; Zhao, J.; **Jiang, Z.**; You, J.; Ni, B.; Ni, Y.; Liu, C.; Li, J.; Chen, X. Resource Allocation Strategies among Vegetative Growth, Sexual Reproduction, Asexual Reproduction and Defense during Growing Season of *Aconitum Kusnezoffii* Reichb. *The Plant Journal* 2021, 105 (4), 957–977.

